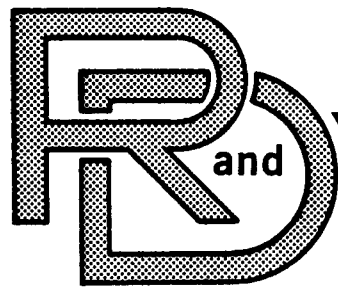


TECHNICAL LIBRARY
REFERENCE COPY

Q34

AD-A141018

2041



CENTER
LABORATORY
TECHNICAL REPORT

NO. 12912

ESTABLISHMENT OF A COMPUTER-AIDED DESIGN (CAD)/
COMPUTER-AIDED MANUFACTURING (CAM) PROCESS
FOR THE PRODUCTION OF COLD FORGED GEARS
Contract Number DAAE07-82-C-4063



January 1984

by David Kuhlmann, P. S. Raghupathi,
& Taylan Altan
Battelle Columbus Division
505 King Avenue
Columbus, Ohio 43201-2693

Approved for Public Release:
Distribution Unlimited.

20020722199

U.S. ARMY TANK-AUTOMOTIVE COMMAND
RESEARCH AND DEVELOPMENT CENTER
Warren, Michigan 48090

Reproduced From
Best Available Copy

AN 46423

NOTICES

This report is not to be construed as an official Department of the Army position.

Mention of any trade names or manufacturers in this report shall not be construed as an official endorsement or approval of such products or companies by the United States Government.

Destroy this report when it is no longer needed. Do not return it to the originator.

UNCLASSIFIED

SECURITY CLASSIFICATION OF THIS PAGE (When Data Entered)

REPORT DOCUMENTATION PAGE		READ INSTRUCTIONS BEFORE COMPLETING FORM
1. REPORT NUMBER 12912	2. GOVT ACCESSION NO.	3. RECIPIENT'S CATALOG NUMBER
4. TITLE (and Subtitle) Computer-Aided Design (CAD)/Computer-Aided Manufacturing (CAM) Process for the Production of Cold Forged Gears		5. TYPE OF REPORT & PERIOD COVERED Final Report - Phase I 11 Nov 82 - 10 Jan 84
		6. PERFORMING ORG. REPORT NUMBER
7. AUTHOR(s) DJ Kuhlmann, PS Raghupathi, T Altan		8. CONTRACT OR GRANT NUMBER(s) DAAE07-82-C-4063
9. PERFORMING ORGANIZATION NAME AND ADDRESS Battelle Columbus Laboratories 505 King Avenue Columbus, Ohio 43201		10. PROGRAM ELEMENT, PROJECT, TASK AREA & WORK UNIT NUMBERS Manufacturing Methods and Technology Project No. 4825005
11. CONTROLLING OFFICE NAME AND ADDRESS U. S. Army Tank-Automotive Command Attention: Mr. D. Ostberg, DRSTA-RCKM Warren, Michigan 48090		12. REPORT DATE January, 1984
		13. NUMBER OF PAGES
14. MONITORING AGENCY NAME & ADDRESS (if different from Controlling Office)		15. SECURITY CLASS. (of this report) Unclassified
		15a. DECLASSIFICATION/DOWNGRADING SCHEDULE
16. DISTRIBUTION STATEMENT (of this Report) Approved for Public Release, Distribution Unlimited		
17. DISTRIBUTION STATEMENT (of the abstract entered in Block 20, if different from Report)		
18. SUPPLEMENTARY NOTES		
19. KEY WORDS (Continue on reverse side if necessary and identify by block number) Computer Aided Design/Manufacturing (CAD/CAM), Spur and Helical Gears, Cold Forging, Computer Graphics, Gear Geometry, Finite Element Analysis, Slab Analysis, Forging, Extrusion, Die Design, Modelling Trials.		
20. ABSTRACT (Continue on reverse side if necessary and identify by block number) In Phase I of the program, computer-aided design techniques have been developed to design the dies for cold forging spur and helical gears. The geometry of the spur and helical gears has been obtained from the kinematics of the hobbing/shaper machines and cutters. Analysis of forging load was done using both slab and finite element methods. These computed loads were compared in modeling trials with lead as the model material using production tooling. The theoretical and experimental results compared well with each other.		

DD FORM 1 JAN 73 1473

EDITION OF 1 NOV 65 IS OBSOLETE

1

UNCLASSIFIED

SECURITY CLASSIFICATION OF THIS PAGE (When Data Entered)

The tool geometry was then corrected for elastic deformation due to forming and shrinkage effects due to interference fit of the die assembly. Provision has also been made in the computer program to modify the geometry for temperature differentials if warm or hot forming must be used in special cases.

Wire electrical discharge machining paths for manufacturing both the die and punch for spur gear forming and machine settings (hobbing or shaping) to cut the electrode for a helical gear die were then computed using the corrections described above. A computer program called GEARDI developed in this phase performs all of the above.

In Phase II of the project, dies designed using the computer program GEARDI will be manufactured and production trials will be conducted to validate the program.

PREFACE

This is the final report for the work carried out during Phase I of contract number DAAE07-82-C-4063 from August 11, 1982 through January 10, 1984. It is published for technical information only and does not necessarily represent the recommendations, conclusions, or approval of the United States Army. This contract with Battelle Columbus Division, Columbus, Ohio, was initiated under the project "Computer-Aided Design (CAD)/Computer-Aided Manufacturing (CAM) Process for the Production of Cold Forged Gears." It is being conducted under the direction of Mr. Donald Ostberg, DRSTA-RCKM of TACOM. Battelle's Columbus Division is the prime contractor on this program with Eaton Corporation of Cleveland, Ohio, as subcontractor.

At Battelle, Dr. Taylan Altan is the Program Manager, Dr. P. S. Raghupathi is the Principal Investigator, and Mr. David J. Kuhlmann is the project engineer. Other Battelle staff, namely Dr. S. I. Oh and Messrs. Jeff Ficke and Will Sunderland also contributed to the program as required. At Eaton, the Program Manager, Principal Investigator, and Project Engineer are Messrs. A. L. Sabroff, J. R. Douglas, and G. Horvat respectively. Other Eaton staff, namely Mr. R. Hoffman and others also contributed to the program as required.

THIS PAGE LEFT BLANK INTENTIONALLY

TABLE OF CONTENTS

Section	Page
1.0. INTRODUCTION	17
2.0. OBJECTIVES	17
3.0. CONCLUSIONS.	18
4.0. RECOMMENDATIONS.	19
4.1. <u>Technology Transfer</u>	19
4.2. <u>Phase II Effort</u>	19
5.0. DISCUSSION	20
5.1. <u>Background</u>	20
5.1.1. <u>Samanta Process</u>	20
5.1.2. Hydrostatic extrusion.	20
5.1.3. Hot Forging.	20
5.2. <u>Program Highlights</u>	20
5.2.1. <u>Application of CAD/CAM to Forging</u>	20
5.3. <u>Program Approach</u>	23
5.3.1. <u>Task 1</u>	23
5.3.2. <u>Task 2</u>	23
5.3.3. Development of the Interactive Computer Aided Design System	34
List of References	37
APPENDIX A. GENERATION OF GEAR TOOTH GEOMETRY FOR SPUR AND HELICAL GEARS.	A-1
APPENDIX B. STRESS ANALYSIS, ELASTIC DEFLECTION AND BULK SHRINKAGE.	B-1
APPENDIX C. SPUR GEAR FORGING LOAD ESTIMATION USING THE FINITE ELEMENT METHOD	C-1
APPENDIX D. RESULTS OF THE PROJECT AS APPLIED TO SAMPLE GEARS.	D-1
APPENDIX E. DESCRIPTION OF THE COMPUTER PROGRAM "GEARDI" (USER'S MANUAL).	E-1
APPENDIX F. STRUCTURE AND SUBROUTINES OF THE COMPUTER PROGRAM "GEARDI".	F-1
APPENDIX G. ANALYSIS OF METAL FLOW USING LEAD AS A MODEL MATERIAL.	G-1

TABLE OF CONTENTS (CONTINUED)

Section	Page
APPENDIX H. TOOL DESIGN CONCEPTS FOR FORMING SPUR AND HELICAL GEARS	H-1

LIST OF ILLUSTRATIONS

Figure	Title	Page
5-1.	Major Steps Common to CAD/CAM Methods Used for Forging Die Design and Manufacture.	22
5-2.	Design Process for Gear Forming Dies.	24
5-3.	Descriptive Computer Aided Design Procedure for Spur and Helical Gear Forming Dies	25
5-4.	Typical Summary Sheet for Gear Design	26
5-5.	Basic Geometry of a Hob and a Shaper Cutter	27
5-6.	Tooling Used for Model Radial Flow Trials	29
5-7.	Load-Stroke Curve from Model Radial Flow Trials	31
5-8.	Comparison of Loads Predicted During Radial Forging of Spur Gears Using Empirical Equations, FEM Analysis, and Modeling Study.	32
5-9.	Flowchart of the GEARDI System.	35
A-1.	Hobbing Machine	A-4
A-2.	Shaper Cutter Machine	A-4
A-3.	Geometry of a Basic Hob	A-6
A-4.	Chip Loads Cut by Successive Hob Teeth.	A-6
A-5.	Complete Generating Action of the Hob	A-6
A-6.	How Different Hob Flutes Form the Gear Tooth.	A-7
A-7.	Geometry of a Shaper Cutter	A-7
A-8.	Shaper Cutter and Work Piece.	A-8
A-9.	Generating Action of Shaper Cutter.	A-8

LIST OF ILLUSTRATIONS (CONTINUED)

Figure	Title	Page
A-10.	Work Gear in Crossed-Axes Mesh with Rotary Shaving Cutter Mounted Above	A-8
A-11.	Gear Terminology.	A-9
A-12.	Tip Relief and Tip Chamfer on a Gear Tooth.	A-9
A-13.	Undercut Produced by a Protuberance Hob and the Basic Protuberance Hob Tooth Form	A-11
A-14.	Geometric Parameters of an Involute	A-11
A-15.	Determination of Tooth Profile from Basic Gear Parameters.	A-13
A-16.	Tip Chamfer on a Spur Gear Tooth.	A-13
A-17.	Tip Relief on a Spur Gear Tooth	A-14
A-18.	Fillet Form of Rounded Corner of Hob Tooth.	A-14
A-19.	Detailed Geometry of Hob with Rounded Corner.	A-16
A-20.	Geometry of a Protuberance Hob.	A-16
A-21.	Defining a Single Point on a Trochoid Generated by a Specific Point on the Hob Profile	A-18
A-22.	Hob Producing Undercut.	A-18
A-23.	Geometric Parameters Used for Shaper Cutter Equation.	A-19
A-24.	Geometry of Full-Rounded Shaper Cutter Tooth.	A-19
A-25.	Geometry of Bottom and Top Land Sections on a Spur Gear Tooth	A-21
B-1.	Typical Tool Setup for Extruding Spur or Helical Gears	B-5
B-2.	Frictional Forces in the Extrusion of Spur and Helical Gears	B-6
B-3.	Typical Tool Setup for Forging Spur or Helical Gears.	B-8

LIST OF ILLUSTRATIONS (CONTINUED)

Figure	Title	Page
B-4.	a) Configuration of a Triangular Groove, and b) Assumed State of Stress	B-9
B-5.	Schematics of the Metal Flow in a Rectangular Cavity Prior to Corner Filling	B-10
B-6.	Configuration of a Spur Gear Tooth Prior to Corner Filling	B-11
B-7.	Schematic of the Metal Flow During Corner Filling . .	B-13
B-8.	Finite Element Mesh used to Estimate Elastic Deflection of a Spur Gear Die	B-15
B-9.	Thick Shell Model of a Spur Gear Die.	B-16
B-10.	Coaxial Cylinder Heat Transfer Model of Spur/Helical Gear Tooling.	B-19
B-11.	Die Under Internal and External Pressure.	B-21
B-12.	Stress Distribution in Die Under a) External, and b) Internal Pressures	B-21
B-13.	Change of Outer Radius of the Insert and Inner Radius of the Outer Ring Due to Shrink Fitting	B-22
B-14.	Stress Distributions in a Shrink-Fit Die Assembly . .	B-23
C-1.	Assumed Initial Workpiece-die Configuration at the Gear Tooth Corner	C-4
C-2.	Initial Mesh Used for Metal Flow Simulation in Gear Cavity.	C-7
C-3.	Schematics of the Metal Flow During Corner Filling. . .	C-8
C-4.	Flow Stress Behavior for Perfectly Plastic Material (Solid Line) and Nearly Perfectly Plastic Material (Dashed Line).	C-11
C-5.	Finite Element Metal Flow Simulation Steps for Gear Tooth Corner Filling.	C-12

LIST OF ILLUSTRATIONS (CONTINUED)

Figure	Title	Page
C-6.	Inner Die Radial Pressure vs. Contact Length of Workpiece on the Gear Top Land.	C-13
D-1.	Helical Gear Example; Title and Generation Method Specification	D-4
D-2.	Helical Gear Example; Geometry Input.	D-5
D-3.	Helical Gear Example; Data Echo	D-6
D-4.	Helical Gear Example; Tooth Profile Display	D-7
D-5.	Helical Gear Example; Entire Gear Display	D-9
D-6.	Helical Gear Example; Input of Forming Data	D-10
D-7.	Helical Gear Example; Forming Data Echo and Initial Solution.	D-11
D-8.	Helical Gear Example; Changing of Forming Parameters. .D-12	
D-9.	Helical Gear Example; Forming Data Echo and Results of Second Analysis.	D-13
D-10.	Helical Gear Example; Original and Corrected Geometry Display	D-14
D-11.	Helical Gear Example; Fillet Alter Option During New Cutter Generation	D-16
D-12.	Helical Gear Example; Display of Corrected and New Cutter Geometry	D-17
D-13.	Helical Gear Example; EDM File Options.	D-18
D-14.	Spur Gear Example; Title and Generation Method Specification	D-19
D-15.	Spur Gear Example; Geometry Input	D-20
D-16.	Spur Gear Example; Data Echo and Data Change Sequence .D-21	
D-17.	Spur Gear Example; Check Data Option.	D-23
D-18.	Spur Gear Example; Drawing of Tooth Profile	D-24

LIST OF ILLUSTRATIONS (CONTINUED)

Figure	Title	Page
D-19.	Spur Gear Example; Entire Gear Form Using No Clearance on the Mating Gear.	D-25
D-20.	Spur Gear Example; Display of Original and Corrected Tooth Geometries.	D-26
D-21.	Spur Gear Example; Specification of a New Cutting Tool.	D-27
D-22.	Spur Gear Example; Initial Fillet Alteration Sequence.	D-28
D-23.	Spur Gear Example; Corrected (Original) Geometry and New Cutter Geometry	D-29
D-24.	Spur Gear Example; Data Check During New Cutter Creation.	D-30
D-25.	Spur Gear Example; Second Alteration of Fillet Geometry.	D-31
D-26.	Spur Gear Example; Second Display of New Cutter Geometry.	D-32
D-27.	Spur Gear Example; EDM Options.	D-33
D-28.	Spur Gear Example; Geometry Input Via Pre-Existing File.	D-34
D-29.	Spur Gear Example; Display of Gear Tooth with Altered Fillet.	D-36
D-30.	Spur Gear Example; Entire Gear with Altered Fillet.	D-37
D-31.	Spur Gear Example; Input of Forming Parameters.	D-38
D-32.	Spur Gear Example; Echo of Forming Data and First Analysis.	D-39
D-33.	Spur Gear Example; Altering of the Percent Fill	D-40
D-34.	Spur Gear Example; Results of the Second Forging Analysis.	D-41

LIST OF ILLUSTRATIONS (CONTINUED)

Figure	Title	Page
D-35.	Spur Gear Example; Display of Original and Corrected Tooth Profiles.D-42
D-36.	Spur Gear Example; Path of Wire EDM of Forging Die. . .	.D-43
D-37.	Spur Gear Example; Path for Wire EDM of Forging PunchD-44
D-38.	Spur Gear Example; Comparison of Original and Altered Gear Tooth ProfilesD-45
E-1.	Flowchart of the GEARDI Computer Program.	E-4
E-2.	Sample Data File.	E-9
E-3.	Protuberance Hob DimensionsE-10
E-4.	Altered Gear Tooth Fillet Geometry.E-11
E-5.	a) 0.0% and b) 50% Filling of Gear Tooth CavityE-13
E-6.	Die Angle SpecificationE-14
F-1.	Control Structure Flowchart for the GEARDI Program. . .	F-4
G-1.	Extrusion Setup Used for Preparing Lead Specimens . . .	G-5
G-2.	Top and Section View of Die Used for Spur Gear Modeling Studies.	G-6
G-3.	Top and Side View of Punch and Counter Punch Used for Spur Gear Modeling Studies.	G-7
G-4.	Friction Factor Determination for Various Lubricants Applied to Lead Rings and Forged at Room Temperature. .	G-10
G-5.	Tooling for Radial Flow Trials.G-12
G-6.	Typical Load vs. Stroke Curve as Generated from a Radial Flow Trial with the Model Material Lead.G-13
G-7.	Side View of Radial Flow Trial Specimen Numbers 101 Through 109 (PbO + oil lubricant; specimen No. 103 not shown).G-15

LIST OF ILLUSTRATIONS (CONTINUED)

Figure	Title	Page
G-8.	Side View of Radial Flow Trial Specimen Numbers 110 Through 117 (no lubricant).G-16
G-9.	Isometric View of Radial Flow Trial Specimen Numbers 101 Through 109 (PbO + oil lubricant; specimen No. 103 not shown).G-17
G-10.	Isometric View of Radial Flow Trial Specimen Numbers 110 Through 117 (no lubricant).G-18
G-11.	Bottom View of Radial Flow Trial Specimen Numbers 101 Through 109 (PbO + oil lubricant; specimen No. 103 not shown).G-19
G-12.	Bottom View of Radial Flow Trial Specimen Numbers 110 Through 117 (no lubricant).G-20
G-13.	Typical Flow Stress Curve for Lead Using Ring Test Data and the Computer Program RINGFSG-22
G-14.	Comparison of FEM and GEARDI Results for Corner Filling of the Tip of a Single Gear ToothG-25
G-15.	Production Scale Tooling Setup; Moving Punch.G-27
G-16.	Production Scale Tooling; Stationary Punch, Moving Counter PunchG-28
G-17.	Typical Load-stroke Curve for Production Scale Simulation.G-30
G-18.	Production Scale Simulation Specimen Numbers 201 and 202G-31
G-19.	Production Scale Simulation Specimen Numbers 203 and 204G-32
G-20.	Production Scale Simulation Specimen Numbers 205 and 206G-33
G-21.	Production Scale Simulation Specimen Numbers 207 and 209G-34
G-22.	Production Scale Simulation Specimen Numbers 210 and 211G-35

LIST OF ILLUSTRATIONS (CONTINUED)

Figure	Title	Page
G-23.	Production Scale Simulation Specimen Numbers 212 and 213G-36
G-24.	Geometry of Partially and Completely Formed Spur Gears from Production Scale Simulation.G-38
G-25.	Variations in Gear Dimensions with Respect to Moving Punch Position.G-40
G-26.	Variations in Gear Dimensions with Respect to Moving Counter Punch Position (punch is inverted and stationary)G-41
H-1.	Schematic of a Spline Rolling Operation with Racks (ROTO-FLO proces)	H-8
H-2.	Planetary Rolling - GROB Process.	H-9
H-3.	Schematic Representation of the Oscillating Rolling Method.H-10
H-4.	Suggested Tool Design for Cold Forging of Spur Gears. .H-11	
H-5.	Double-action Tooling for Forging of Spur GearsH-13	
H-6.	Typical Tool Setup for Extruding Helical Gears.H-14	
H-7.	Extrusion Process for Helical Gears Using a Streamlined DieH-15

LIST OF TABLES

Table	Title	Page
B-1.	Variation in Radial Displacement with Different Inner Radius Values.	B-17
G-1.	Results of Lubrication Trials Using Lead Ring Specimens.	G-9
G-2.	Incremental Radial Flow Study Trials Using Thin Billets.	G-14
G-3.	Ratio of Radial Pressure to Flow Stress for Various Radial Flow Test Specimens	G-23
G-4.	Variation in Punch Pressure to Flow Stress Ratio with Increasing Percent Fill as Computed by the GEARDI Program.	G-24
G-5.	Production Scale Simulation Forging Data	G-29
G-6.	Dimensions of Forged and Partially Forged Lead Spur Gears.	G-39
H-1.	Summary of Major Forming Methods for Manufacturing Splines and Gears.	H-4

THIS PAGE LEFT BLANK INTENTIONALLY

1.0. INTRODUCTION

This report covers the work performed in Phase I of the contract No. DAAE07-82-C-4063 with Battelle as the prime contractor and Eaton Corporation as the subcontractor. This project was initiated under the Manufacturing Methods and Technology Program. The purpose of the project is to develop a general purpose Computer-Aided Design/Manufacturing (CAD/CAM) technique for producing cold forged spur and helical gears.

In recent years, there has been considerable efforts directed at reducing the material and production costs associated with the manufacturing of precision parts. Metalforming processes, namely cold extrusion, precision forging, warm forging and some powder metal (P/M) forming methods are being widely used in many high technology industries to manufacture various parts whose functional surfaces can be finish-formed without requiring further machining.

In general, gear manufacturing processes are highly specialized due to the complex geometry and high accuracy requirements of the gear teeth. Precision forming methods for gears have been successfully used for a few types of spur gears. These forming methods offer considerable advantages such as a reduction in machining (material and energy losses) and an increase in fatigue life. To establish precision forming as an economical production technique requires the capability to design and manufacture dies with precise and reproducible dimensions with long life and acceptable cost.

The traditional method of die design and manufacture employs information developed by extensive experience and trial and error. Each new gear design requires a new and costly die development program which makes the precision forming process economically less attractive. Therefore, in this project, methods were developed to apply existing advances in CAD/CAM technology (finite element, metal forming and heat transfer analysis) to gear forming die design and manufacture. This approach benefits from the capability of the computer in computation time and information storage, reduces trial and error, and represents a general method applicable to the family of spur and helical gears.

2.0. OBJECTIVES

The overall objective of this program is to develop a general purpose CAD/CAM technique for producing precision-forging and

extrusion dies for the family of spur and helical gears. Using dies made by this process, gears can be precision formed from wrought billets or powder metal (P/M) preforms. The specific objectives of this program are to:

- optimize the design and the manufacturing of dies used in precision-gear forming by CAD/CAM techniques,
- reduce the cost of die and process development for precision forming of spur and helical gears of different sizes and modules by CAD/CAM techniques,
- make the CAD/CAM system flexible, making it (1) useful for the family of spur and helical gears and (2) easily introduced into production by forge shops.

This report covers the details of Phase I only. In developing the present CAD/CAM system for Phase I the system was made user oriented. The user does not need to know computer programming. However, some training is probably necessary to operate the system effectively. The user should be an engineer with gear/forging/extrusion experience so that engineering judgements can be made during the operation of the CAD system. The present CAD system will be upgraded and corrected after the discrepancies between the predicted and measured values have been determined in Phase II.

3.0. CONCLUSIONS

The developed CAD/CAM system, named GEARDI, produces reliable results when applied to the analysis of the forging and extrusion of spur and helical gears. Each of the specific objectives of this program have been met as follows:

- the computer program GEARDI allows the user to interactively design optimum spur and helical gear forming dies. This has been achieved by programming the necessary gear profile geometry and metal forming equations in a variable format to allow the user to design dies for specific applications.
- Modeling studies with lead as the model material, using a spur gear forging die, have been performed and have given a better understanding of the metal flow in the forming process. The loads predicted by the program GEARDI have been compared with those measured in model experiments, using lead as forging material. This comparison showed that the computer predictions were in good agreement with measured load values. Thus, model studies established the credibility of the computer program. This allows the GEARDI

program user to conduct prototype forming analyses within the computer and reduce the cost of die and process development.

- Current gear manufacturing terminology is used in the GEARDI program which makes it easy to use. The method of defining the gear geometry in the program is based on the conventional gear manufacturing methods of hobbing and shaper cutting, thus making it easy to introduce into production.

The program has powerful application possibilities, not only in the area of metal forming but also, with its ability to design hobs and shaper cutters and to modify the fillet to a non-trochoidal shape, in the area of gear and gear train design.

4.0. RECOMMENDATIONS

4.1. Technology Transfer

The results of the project should be provided to all interested U.S. companies. Thus, the probability of implementing the project results for producing forged or extruded spur and helical gears will be enhanced.

The prime contractor, Battelle, worked closely with the subcontractor, Eaton Corporation, who is already forging spur gears on a production basis. Some of the project results will be used by Eaton for precision forging or extrusion of spur and/or helical gears. In addition, several other companies have indicated interest in the results of this project. An effort should be made to contact as many gear manufacturing companies as possible in order to generate interest in the results of the project. At the completion of the Phase II effort, the possibility of starting a user's group for the GEARDI program should be considered. As the sponsor of the user's group, Battelle could provide technical support for the program and also make revisions and additions to the program as suggested by member companies.

4.2. Phase II Effort

During the upcoming Phase II effort, representative spur and helical gears will be formed using dies designed by the GEARDI program. During this phase, the true capabilities of the program should be evaluated. A comprehensive test procedure should be begun to completely analyze the gears produced by the computer-aided designed dies. This will enable a quantitative comparison between the formed gears and machined gears.

5.0. DISCUSSION

5.1. Background

Precision forging of spur gears has been documented on many occasions. Several studies have investigated the effects of temperature and tool loads on the gear tooth geometry (1,2)*. Corrections to the forging die in these instances amounted to either an increase or decrease in the root diameter, outside diameter or the module. There has been no effort to determine the geometry of a conventional hob and shaper cutter which will cut the corrected geometry.

5.1.1. Samanta Process. The extrusion of spur gears has been outlined by Samanta (3). The main application of this process has been the production of automobile starter pinions. As such, the gear has not been made to the close tolerances and high finish characteristic of transmission and axle gears of a similar size. However, the process does greatly reduce the manufacturing time compared to the operations it replaces.

5.1.2. Hydrostatic extrusion. Helical gears have been produced by hydrostatic extrusion (4). This approach requires the extrusion of long billets to achieve necessary production rates and, as such, poses several economical problems which must be solved in order to make this forming method successful. The results of this program have not been utilized for manufacturing gears on a production basis.

5.1.3. Hot Forging. Eaton Corporation, the subcontractor in the present program, has developed a process for hot forging spur gears to near net tolerances. The gears produced by this method must be finish machined after forging but significant material savings have been achieved.

5.2. Program Highlights

5.2.1. Application of CAD/CAM to Forging. In recent years, CAD/CAM techniques have been applied to die design and manufacture for forging rib-web aircraft structural parts (5), track shoes for military vehicles (6), and precision turbine and compressor blades (7). The experience gained in all of these applications indicates that a certain methodology is necessary for CAD/CAM of dies for precision and/or near net shape forming. This approach is also applicable, with appropriate modifications, to precision forming

*Numbers in parentheses refer to references at the end of the report.

of spur and helical gears. As illustrated in Figure 5-1, the inputs to the CAD/CAM method are;

- the geometry of the part to be formed,
- data on billet material under forming conditions, billet and die temperatures, and rate and amount of deformation,
- friction coefficient to quantify the friction shear stress at the material and die interface,
- forming conditions, (temperatures, deformation rates, suggested number of forming operations).

With these input data, a preliminary design of the finish forming die can be made and flash dimensions can be estimated. Next, stresses necessary to finish form the part and temperatures in the forming dies are calculated. The temperature calculations take into account the heat generated due to deformation, friction and the heat transfer during the contact between the hot, formed part and cooler dies. The elastic die deflections due to temperatures and stresses can be estimated and used to predict the small corrections necessary on the finish die geometry. The knowledge of the forming stresses also allow the prediction of forming load and energy. The estimation of die geometry corrections is necessary for obtaining close tolerance-formed parts and for machining the finish dies to exact dimensions. The corrected finish die geometry is used to estimate the necessary volume distribution in the preform or blocker stage.

The ultimate design of the preform or blocker die requires a metal flow simulation - a computerized definition of metal distribution at each instant during forging. This simulation is mathematically complex and can only be performed for relatively simple forgings like blade airfoils or cylindrical forgings. In more complex applications, preform or (blocker) design can be determined by a computerized use of experience-based formulas. After the preform (blocker) design is completed, the dies or electrodes for this forging operation are manufactured by numerical control, as it is the preferred case for finish forging dies.

This overall procedure, described above and illustrated in Figure 5-1, was applied to CAD/CAM spur and helical gear forming with the following modifications;

- NC machining of the gear forging dies (finish and preform) is not economical because it requires (1) a 5-axis NC machine and (2) considerable machining time to generate the complex surface of each individual gear tooth.

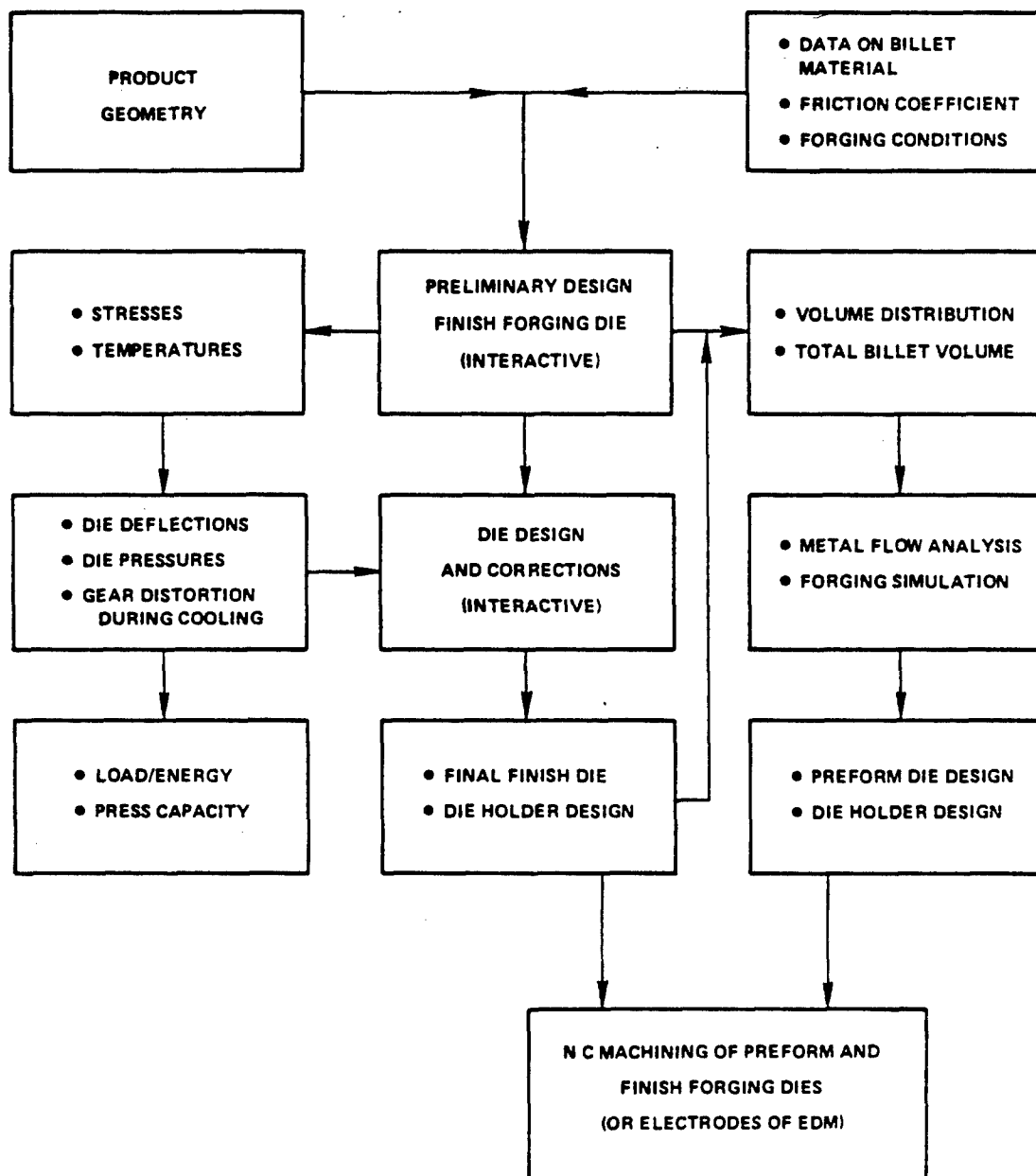


FIGURE 5-1. Major Steps Common to CAD/CAM Methods Used for Forging Die Design and Manufacture

- The preform dies for gear forging can be designed as indicated in Figure 5-2. However, the experience gained by companies' precision forging spur gears indicates that the manufacture of a preforming die is not necessary as all of the required material movement can be done in one finish forging die.

5.3. Program Approach

In Phase I, the CAD of forging and extrusion dies has been carried out. All of the Phase I work was conducted at Battelle with some input from Eaton Corporation. A simplified flow diagram for the computer-aided design and manufacturing of forging and extrusion dies for spur and helical gears is shown in Figure 5-2. This outline is very similar to that used in other CAD/CAM forming programs, as seen in Figure 1. Descriptive computer-aided design procedures for the dies are given in Figure 5-3.

Following the outline of Figures 5-2 and 5-3, Phase I of the present project was divided into:

- Task 1. - Transformation of Dimensional Data into Computer-Compatible Digital Data
- Task 2. - Computer Aided Design (CAD) of Forming Dies
- Task 3. - Development of an Interactive CAD System

5.3.1. Task 1. The objective of this task was to describe spur and helical gear geometry in digital form for use in the computer. The gear tooth geometry was generated by simulating in the computer the motions of both hob and shaper cutter cutting machines. These two machines were selected since the majority of gears produced by conventional cutting methods are either hobbled or cut using a shaper cutter (8). For defining the tooth geometry, standard equations were used to simulate the gear cutting process (9-13). The derivations of these equations are given in Appendix A. These equations are included in the computer program GEARDI, which was developed under Task 3.

To define the tooth geometry, certain gear and/or tool parameters had to be specified. Some additional data pertaining to the mating gear was also required in certain instances. All the data required for the computations was obtained from the so-called "summary sheet" developed by gear designers (Figure 5-4) and also the geometry of the cutting tool (Figure 5-5). With these data, the equations given in Appendix A were used to calculate the x and y coordinates of the points describing the gear tooth profile.

5.3.2. Task 2. The geometry of the forming die is different from

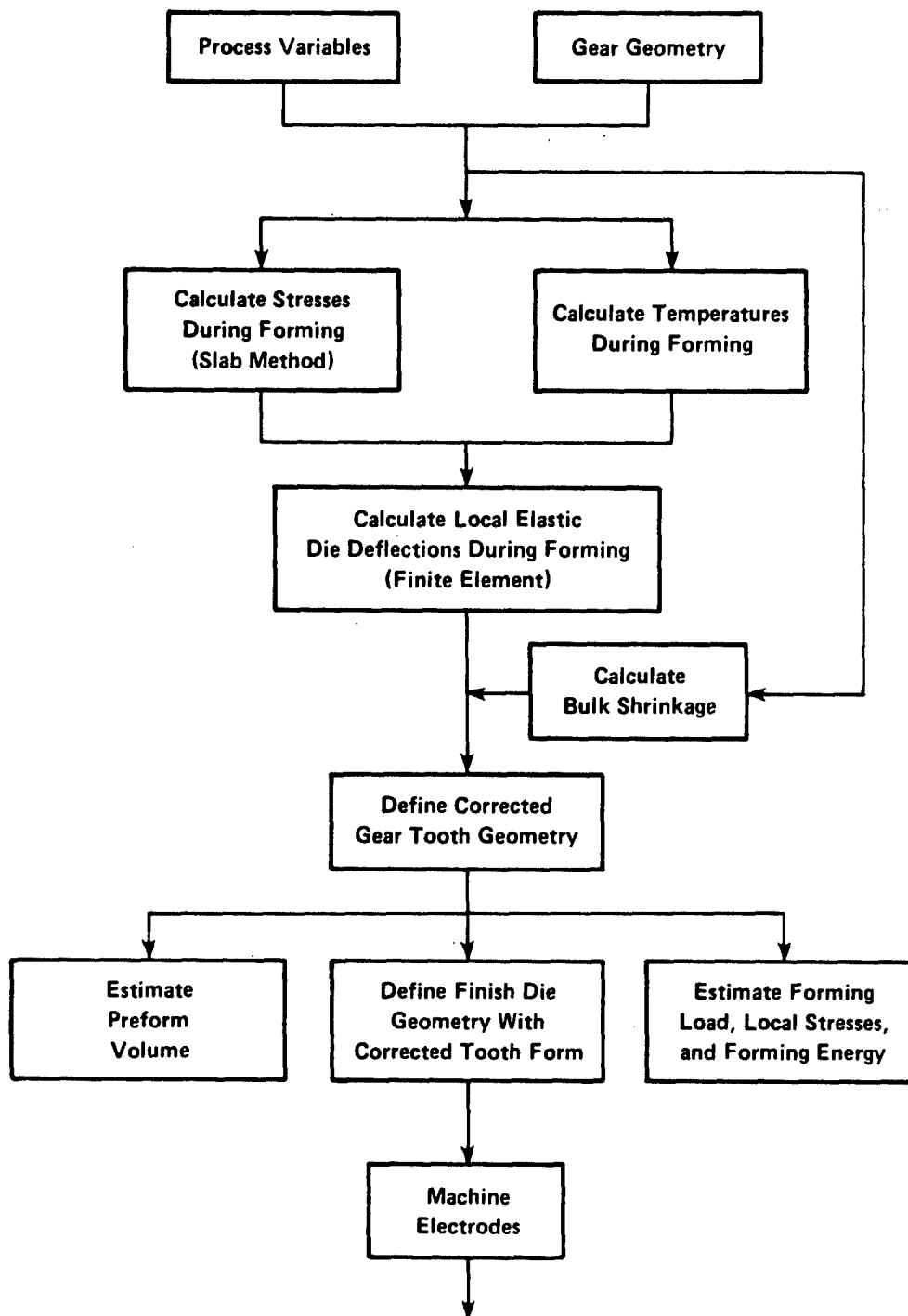


FIGURE 5-2. Design Process for Gear Forming Dies

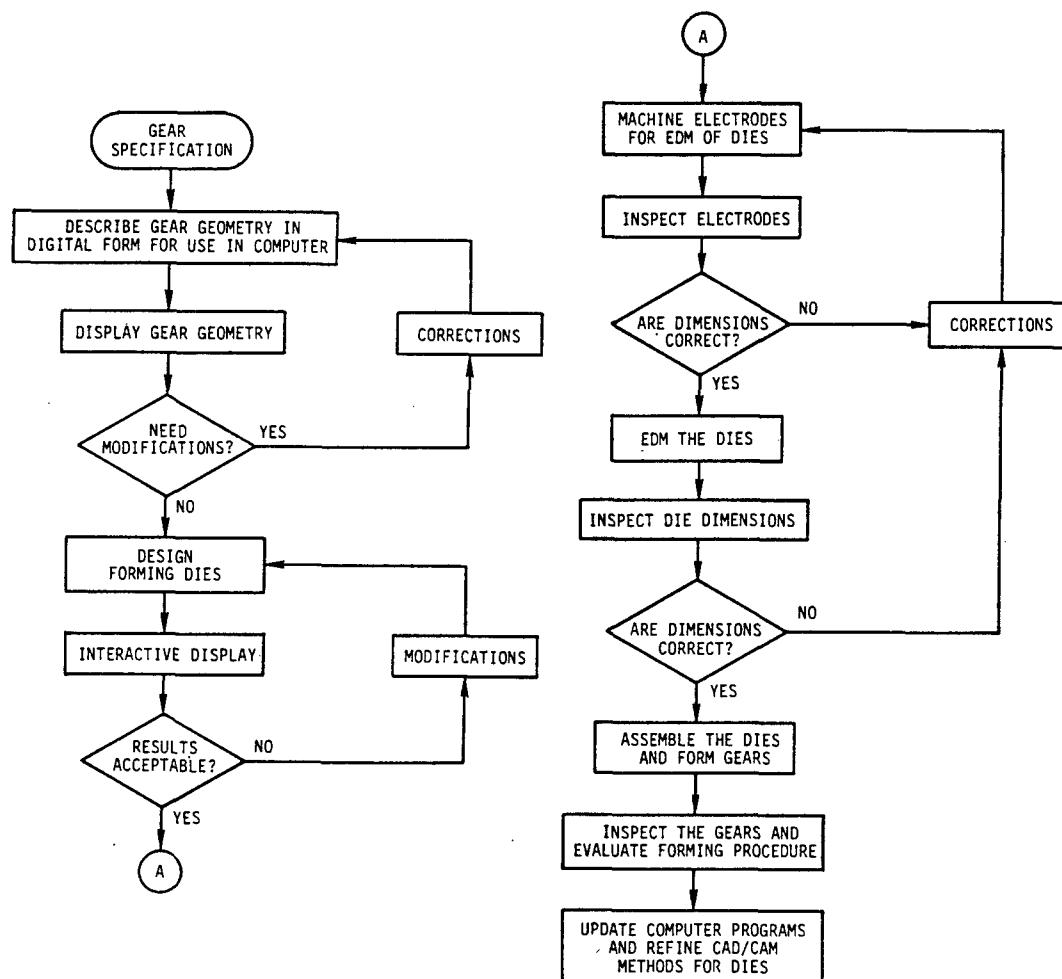


FIGURE 5-3. Descriptive Computer Aided Design Procedure for Spur and Helical Gear Forming Dies

DRAWING INFORMATION FOR:			
A DRIVEN COUNTER SHAFT			
	ENGLISH (INCH)	METRIC (MM)	
IDENTIFICATION NUMBER	81.0220	81.0220	
SET NUMBER	810.0123	810.0123	
NUMBER OF TEETH	32.	32.	
NORMAL DIAMETRAL PITCH (MODULE)	10.0000	2.540	
NORMAL PRESSURE ANGLE	19.0000	19.000	
HELIX ANGLE	31.5739	31.574	
HAND OF HELIX	LEFT		
LEAD	19.2000	487.680	
TRANSVERSE DIAMETRAL PITCH (MODULE)	8.5197	2.981	
TRANSVERSE PRESSURE ANGLE	22.0064	22.006	
MAXIMUM OUTER DIAMETER	4.079	103.60	
MINIMUM OUTER DIAMETER	4.069	103.35	
MAXIMUM TIP CHAMFER DIAMETER	4.049	102.84	
MINIMUM TIP CHAMFER DIAMETER	4.039	102.59	
THEORETICAL PITCH DIAMETER	3.7560	95.402	
MINIMUM ROOT DIAMETER	3.511	89.18	
BALL/PIN DIAMETER FOR (MOP)	0.2160	5.486	
MAX. MEAS. OVER PINS (MOP)	4.1716	105.958	
MIN. MEAS. OVER PINS (MOP)	4.1681	105.870	
MIN. CALIPER MEAS. (4) TEETH	1.1056	28.082	
MAX. CALIPER MEAS. (4) TEETH	1.1071	28.121	
MEAN FACE WIDTH	0.875	22.23	
MIN. NORM TOPLAND (MAX. O.D. W/O CHAM)	0.029	0.74	
MIN. THEO. NORM. CIRC. TOOTH THICKNESS	0.1626	4.130	
TOOTH THICKNESS @ HALF OF WHOLE DEPTH	0.1764	4.481	
CASE DEPTH023/.033	0.59/0.83	
MAX. PITCH DIAMETER RUNOUT (TIR)	0.0025	0.063	
	ROLL ANG. =====	RADIUS =====	RADIUS =====
051 @ MAX. OUTER RADIUS	34.95	2.0395	51.803
DATA @ MAX. END OF ACTIVE PROFILE	33.99	2.0245	51.422
===== @ MAX. HIGH CONTACT POINT	30.30	1.9697	50.030
@ OPER. PITCH POINT	25.02	1.9000	48.260
@ MIN. LOW CONTACT POINT	22.42	1.8697	47.491
@ MIN. START OF ACTIVE PROFILE	17.45	1.8202	46.233
@ START OF INVOLUTE CHECK	16.72	1.8138	46.070
@ BASE RADIUS	0.00	1.7412	44.226
061 MAX. LEAD VARIATION		0.0004	0.010
DATA MAX. LEAD RANGE		0.0008	0.020
===== CROWNING IN MIDDLE 80% OF TOOTH00000/.00050	.000/.012
071 MAX. RUNOUT (T.I.R.)		0.0025	0.063
DATA MAX. TOOTH TO TOOTH COMPOSITE VAR.		0.0008	0.020
===== MAX. TOTAL COMPOSITE VARIATION		0.0032	0.081
MAX. PITCH VARIATION		0.0004	0.010
MAX. PITCH RANGE		0.0029	0.073

FIGURE 5-4. Typical Summary Sheet for Gear Design

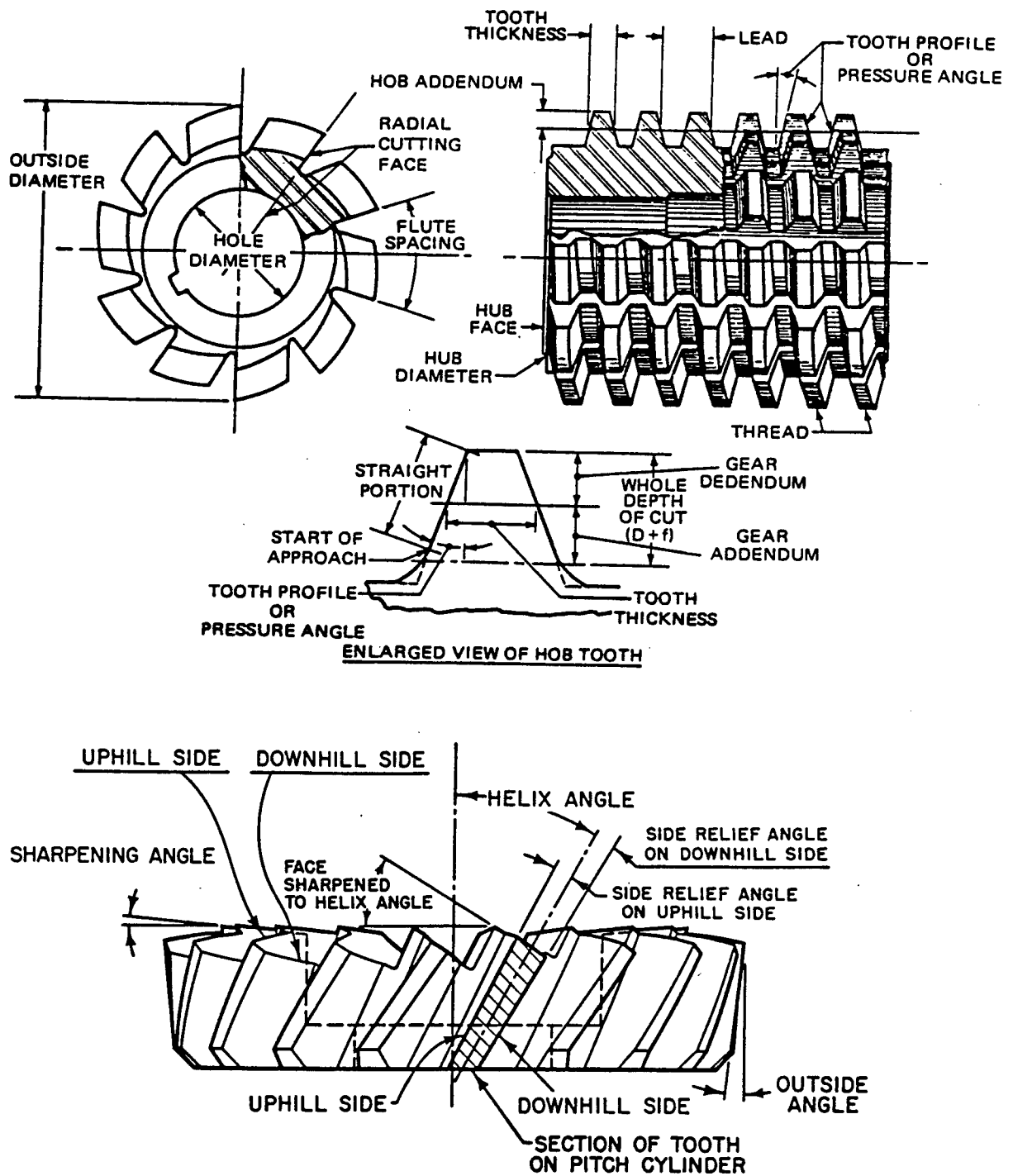


FIGURE 5-5. Basic Geometry of a Hob and a Shaper Cutter (11,16)

that of the formed gear because:

- A shrink fit is normally used to hold the die in the die holder causing a contraction of the die surfaces.
- The dies may be heated prior to forming and then further by the hot billet during forming. This makes the die insert expand.
- During forming, the die surface deforms elastically due to forming stresses.
- Prior to forming, the billet may be heated and formed at a high temperature. Due to unequal coefficients of thermal expansion of the die and billet materials, the die and the billet expand or shrink in unequal amounts.
- After forming, the gear shrinks during cooling from forming temperature to room temperature.

To get accuracy in the formed gears, each of the geometrical variations listed above were estimated and the die geometry corrected accordingly. For this purpose, the present task was conducted in various subtasks, as discussed below.

5.3.2.1. Calculation of the stress distribution and forging load. To determine the elastic deflection of the forming dies, stresses acting on the die during the forming processes had to be known. This stress analysis was necessary to obtain not only the elastic deflection, but also to calculate the forming pressure and load. The stresses in the gear tooth cavity during forming were calculated for extrusion using the slab method. For forging, an analysis for estimating the load in a flashless forging process was used to determine the punch pressure and punch force. The method takes into account the amount of die filling desired. Die filling is a three-dimensional concept and relates to both the amount of material movement into the corners of the gear tooth tip and the amount of radial flow at any given axial position in the gear.

As with the gear geometry, parametric information was required to adequately define the forming process. Additionally, a Finite Element Method (FEM) analysis, applicable to metalforming (14), was done to determine the required tool pressures to achieve adequate die filling in the tip corners of the gear teeth for the forging process. The details of these two methods of calculation are given in Appendices B and C respectively. A modeling study was also conducted to simulate the gear tooth filling process during forging and is described fully in Appendix G. Figure 5-6 shows the tooling used in the modeling study. The tooling consisted of a die

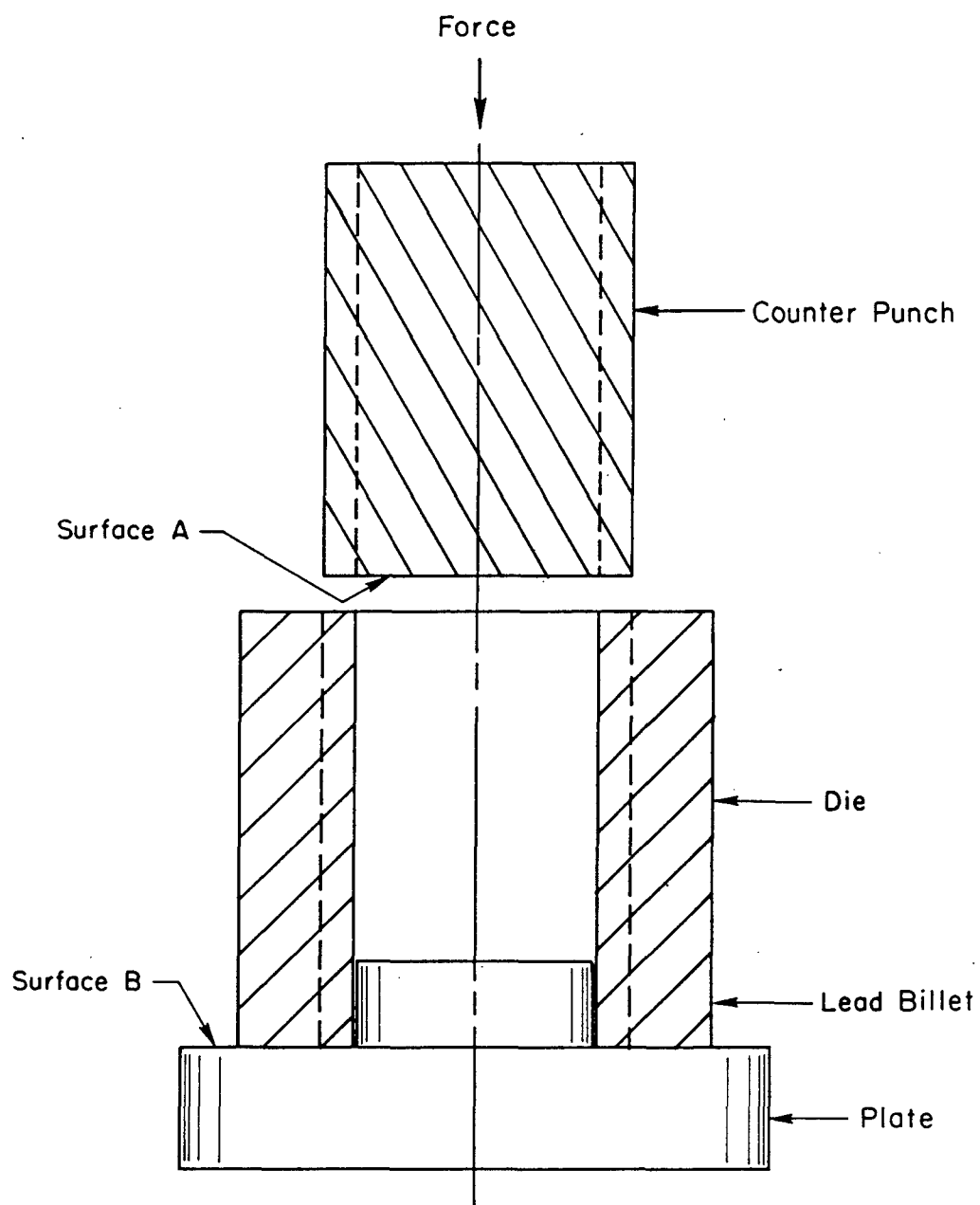


FIGURE 5-6. Tooling Used for Model Radial Flow Trials

cavity in the shape of a gear, a mating punch, and a flat bottom die. For each specimen deformed, a load-stroke curve (Figure 5-7) was recorded. Figure 5-8 shows a comparison of the results of the empirical, FEM, and modeling analyses.

There is close agreement between the computed and measured values of the punch pressure. As a part of the modeling study, a production scale simulation was also conducted using production type tooling. These experiments gave detailed information on the way in which the gear tooth cavity is filled when the configuration of the tooling is varied.

5.3.2.2. Estimation of elastic die deflections due to mechanical loading. The deformations resulting from the forging load are generally elastic if a proper die material with appropriate mechanical properties is selected. Using the forging pressure obtained from the flashless forging equations, as described in Appendix B, the elastic deflection of the die due to loading was computed using a finite element code at Battelle called NSYMFT. A preliminary simple calculation showed that the order of magnitude of this correction was quite small. This point was also highlighted in a recent publication on a spiral bevel gear forging project (15). The elastic deformation due to mechanical loading was calculated using NSYMFT and agreed closely with the results of the simple calculation.

It was decided that the corrections due to the elastic deformation of the die under mechanical loading could be adequately computed using a simple calculation and a FEM analysis did not need to be carried out for each new die design.

5.3.2.3. Estimation of the bulk shrinkage due to temperatures and shrink fit assembly. The first major component of bulk shrinkage is due to temperatures. The temperature of the die increases during the forming due to heat transfer from the heated billet. The following are the outcome of the thermal interaction between the die and the billet;

- The dimensions of the billet increase as it is heated from room temperature to the forming temperature. The dimensions of the billet change further during the forming operation during (a) temperature increases because of heat generation due to plastic deformation and (b) temperature drop because of heat loss from the billet to the dies. The change in temperature of the billet is not constant over the entire cross section, but varies depending on the local deformations and heat transfer.
- After forming, the formed gear is cooled in a sand-graphite medium to room temperature. During this period, the

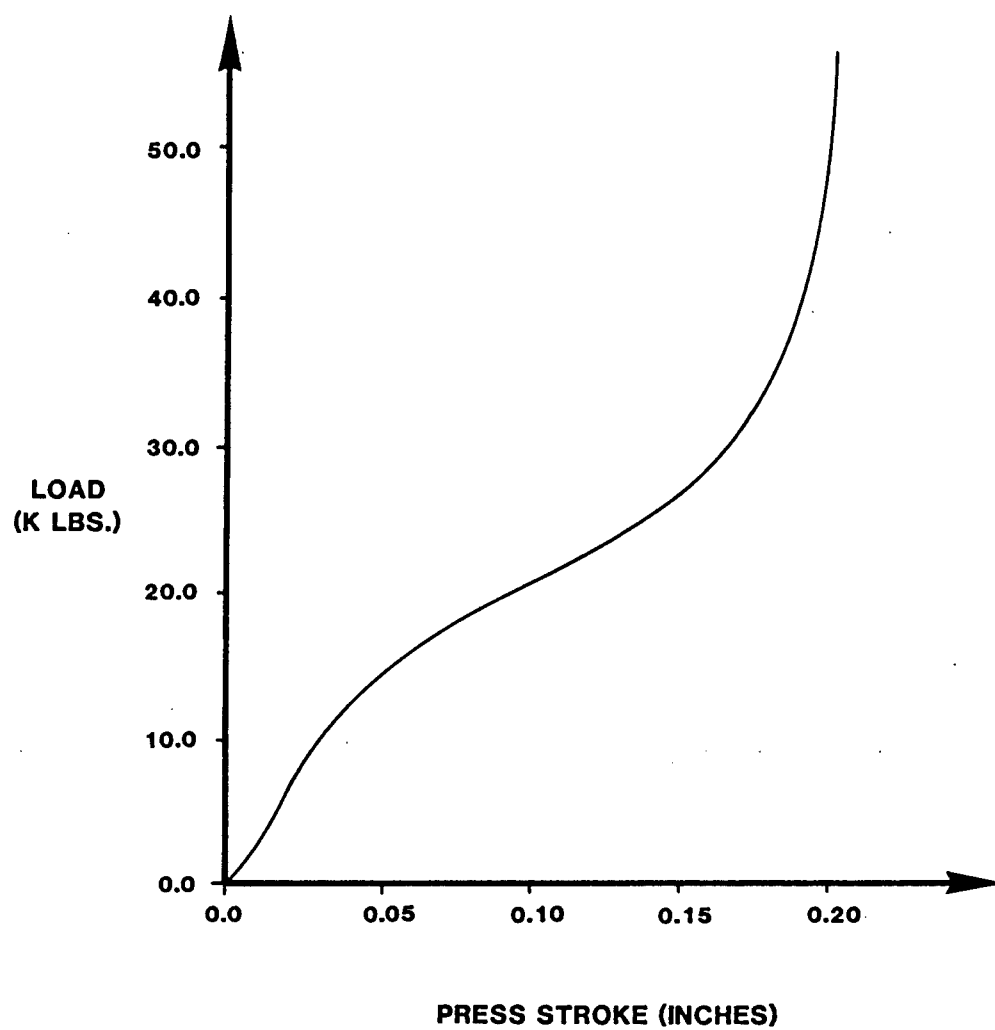


FIGURE 5-7. Load-Stroke Curve from Model Radial Flow Trials

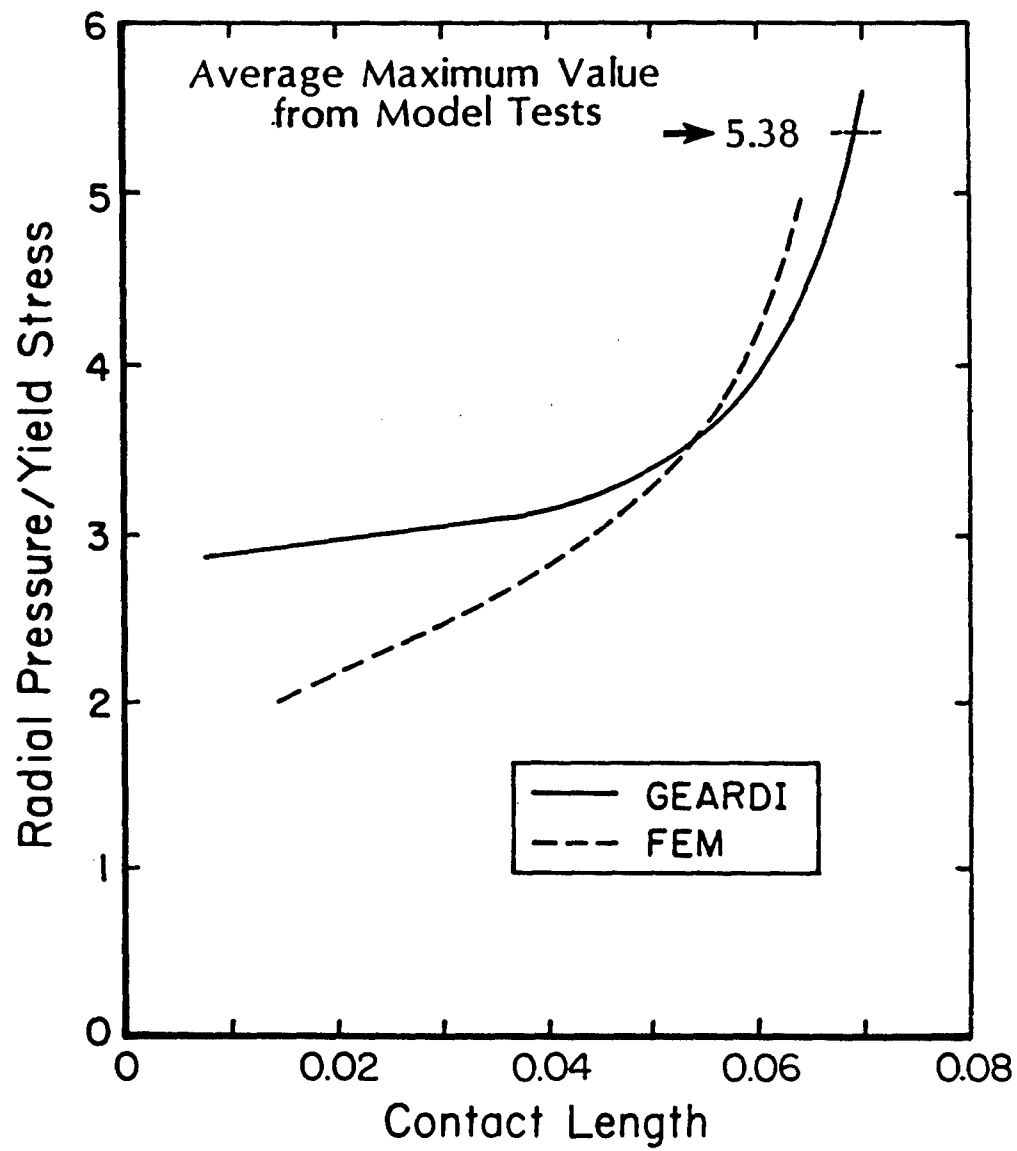


FIGURE 5-8. Comparison of Loads Predicted During Radial Forging of Spur Gears Using Empirical Equations, FEM Analysis, and Modeling Study

magnitude of the gear dimensions decreases.

Based on the results of a similar heat transfer problem in a related spiral bevel gear forging program, it was determined that a simple heat transfer analysis based on average temperatures would be fully adequate for estimating the die corrections in the present project. The die and the gear tooth cavities must be larger than the nominal room temperature size of the formed gear and gear tooth.

The second aspect of bulk shrinkage is the change of inner die dimensions due to shrink-fitting of the die assembly. These were compensated for to achieve the desired dimensions on the finished gear or pinion. A simple solution based on thick circular cylinders under internal pressure was used to compute the changes on the inner diameter of the die assembly. The details of this computation are given in Appendix B.

5.3.2.4. Modification of the gear tooth geometry. In this task the results of the die correction analyses were used to alter the coordinates of the gear tooth profile to achieve the die geometry. Helical gear dies must be made by using a solid electrode but spur gears die can be cut using either a solid electrode or a wide EDM process. In either case, a corrected set of gear tooth profile coordinates is needed. This new set of coordinates was computed by applying a correction factor to the radius vector from the center of the gear to each point on the gear tooth profile. The correction in the radial direction is given by;

$$\Delta r = C_r * r \quad (4)$$

where;

$$C_r = C_T + C_D + S_{Sr},$$

C_T = average correction for temperature shrinkage,

C_D = average correction for elastic deflection,

C_{Sr} = average correction for shrink fitting.

In addition to using the above correction factors to determine the new set of gear tooth profile coordinates, a correction was made to compensate for the amount of "overburn" which will occur during the EDM process. Overburn refers to the fact that there is a zone around the edge of the electrode or wire which is burned away from the EDM workpiece due to the size of the electric arc. Thus, for the die electrode, the coordinates were moved radially inward to accomodate the overburn.

When forming helical gears, the three-dimensional nature of the die requires that the die be cut using a helical electrode. This electrode will have a tooth geometry different from the formed gear as previously mentioned. To cut this electrode on a conventional hob or shaper cutter machine requires the generation of new hob or shaper cutter dimensions, different from the dimensions used to cut the gear.

5.3.3. Development of the Interactive Computer Aided Design System. This final task involved the creation of a graphics oriented CAD program named GEARDI which enables the user to design spur and helical gears, predict tooling loads, pressures, and deformations for forming the gears, and define the information required to manufacture tooling using the method of Electrical Discharge Machining (EDM). All of the mathematical analyses, given in Appendices A (Generation of Gear Tooth Geometry for Spur and Helical Gears), B (Stress Analysis, Elastic Deflection and Bulk Shrinkage), C (Spur Gear Forging Load Estimation Using the Finite Element Method), and G (Analysis of Metal Flow Using Lead as a Model Material) were included in the program. All of the subroutines of GEARDI were written in standard VAX FORTRAN.

To facilitate the understanding of the programming steps, the listing of the program includes a generous number of "COMMENT" statements. The structure of the overall GEARDI system is shown in Figure 5-9. Appendix D (Results of the Project as Applied to Sample Gears) gives a detailed description of how the computer program can be used to solve typical design problems. A user's manual is included in Appendix E and a list of all subroutines used in the program is contained in Appendix F.

THIS PAGE LEFT BLANK INTENTIONALLY

LIST OF REFERENCES

- (1) Kato, I., Nishiguchi, M., and Fukuyasu, T., "Design of Precision Forging (Spur Gear)," Sumitomo Metal Industries Ltd., Japan, 1981.
- (2) Abdel-Rahman, A., R., O., and Dean, T., A., "The Quality of Hot Forged Spur Gear Forms, Parts I and II," Int. J., Mach. Tool Des. Res., Vol 21, No. 2., Pergamon Press Ltd., Great Britain, 1981, pp. 109-141.
- (3) Stickels, C., A., and Samanta, S., K., "Cold Forming in Gear Manufacture," Metals Engineering Quarterly, November, 1974.
- (4) Hornmark, N., Hilsson, J., O., H., and Mills, C., P., Metal Forming, August, 1970, p. 227.
- (5) Akgerman, N., Subramanian, T., L., and Altan, T., "CAD/CAM as Applied to Closed-Die Forging," SME Paper MS-75-516, presented at the CAD/CAM III Conference in Chicago, February 13, 1975.
- (6) Billhardt, C., F., Akgerman, N., and Altan, T., "CAD/CAM for Closed-Die Forging of Track Shoes and Links," SME Paper MS-76-739, October, 1976.
- (7) Akgerman, N., and Altan, T., "Application of CAD/CAM in Forging Turbine and Compressor Blades," ASME paper 75-GT-42, published in ASME Trans., Journal of Engineering for Power, 98, Series A., No. 2, April, 1976, p. 290.
- (8) Newman, J. Richard, "Gear Manufacturing Methods and Machines, A Review of Modern Practices," Proceedings of the National Conference on Power Transmission, Vol. 5, Fifth Annual Meeting.
- (9) Buckingham, E., Analytical Mechanics of Gears, Dover Publications, Inc., New York, 1949.
- (10) Dudley, Darle W., Gear Handbook, 1st Ed., McGraw-Hill Book Co., New York, 1962.
- (11) Modern Methods of Gear Manufacture, 4th Ed., National Broach and Machine Division/Lear Siegler, Inc., Publication, Detroit, MI, 1972.
- (12) Shigley, J., E., Kinematic Analysis of Mechanisms, 2nd Ed., McGraw-Hill Book Co., New York, 1969.

- (13) Spotts, M. F., Design of Machine Elements, 5th Ed., Prentice-Hall, Inc., Englewood Cliffs, NJ, 1978.
- (14) Oh, S., I., Lahoti, G., D., and Altan, T., "ALPID - A General Purpose FEM Program for Metal Forming," submitted to NAMRC IX.
- (15) Mages, W., "Advantageous Application of Recent Metal Forming Processes for Manufacture of Gear and Drive Components" (in German) VDI Report 332, 1979, p. 97-106.
- (16) "Know Your Shaper Cutters," Illinois/Eclipse publication, Chicago, 1977.

APPENDIX A

GENERATION OF GEAR TOOTH GEOMETRY FOR SPUR AND HELICAL GEARS

THIS PAGE LEFT BLANK INTENTIONALLY

1.0. INTRODUCTION

There are several methods for manufacturing spur and helical gears using some form of cutting tool. These include the form-cutting processes of milling, broaching and shear cutting and the generating methods of hobbing and shaper cutting. Cost, flexibility, speed and accuracy are all factors affecting the manufacturing process chosen for a particular application and are the main reasons why hobbing and shaper cutting are the most common gear manufacturing methods (Figures A-1 and A-2). Gear teeth are used to provide a non-slip drive when power or motion is to be transmitted from one shaft to another. When the additional requirement that the motion of power shall be transmitted smoothly is imposed, the size and shape of the teeth become critical. In the case of spur and helical gears, the curves used are almost exclusively those of the involute family (2)*.

This appendix deals with the shape and proportions of involute spur and helical gear teeth and the calculation of the coordinates which define the tooth profile. These calculations are based on hob and shaper cutter generating methods. The basic geometry of the gears is presented along with several useful modifications to the standard tooth profiles.

2.0. MANUFACTURING METHODS

2.1. Hobbing

Hobbing is one of the most economical and versatile methods of generating spur and helical gear teeth using a cutting tool. One hob of a given pitch will cut the teeth of all involute spur and helical gears of the same normal pitch and pressure angle including all numbers of teeth and helix angles. The size of the teeth and the size of the work are limited only by the capacity of the hobbing machine on which the part is to be cut (Figure A-1) (2). The generation of a gear tooth is a continuous indexing process in which both the cutting tool and the workpiece rotate in a constant relationship while the hob is being fed into the work. As the hob is fed across the work once, all the teeth in the work are completely formed.

The hob is basically a worm which has been fluted and has form-

*Numbers in parentheses refer to references at the end of the appendix.

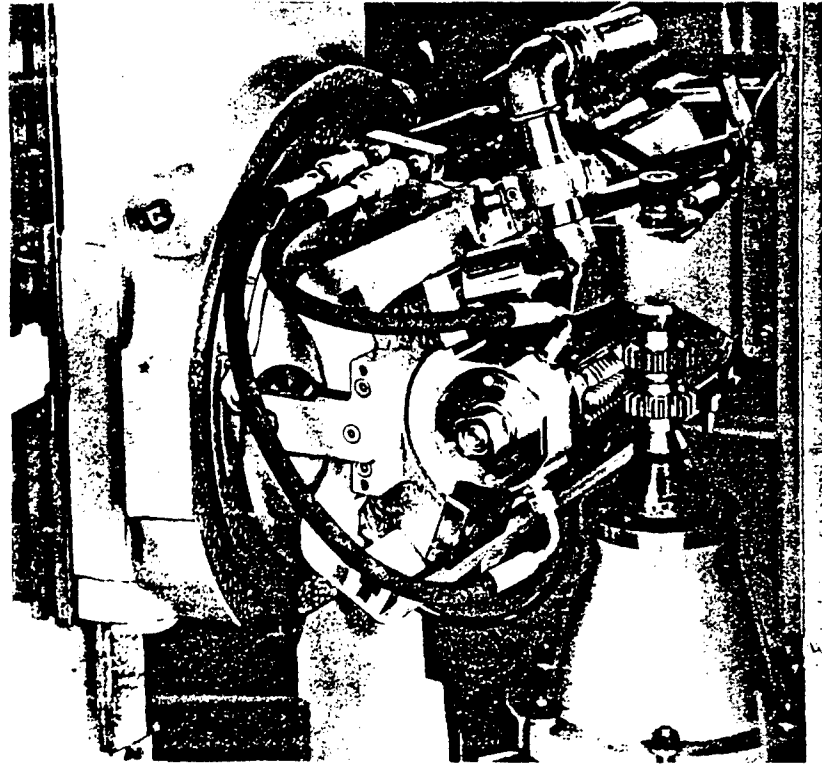


FIGURE A-1. Hobbing Machine (1)

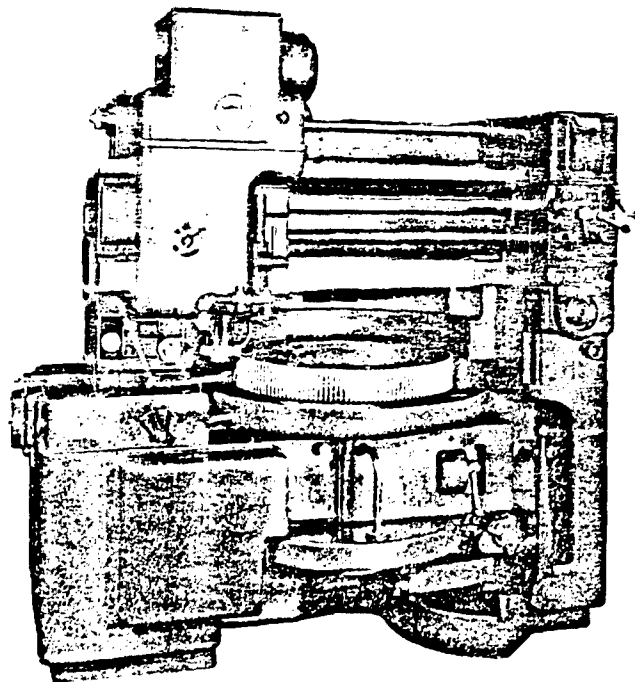


FIGURE A-2. Shaper Cutter Machine (2)

relieved teeth. The flutes provide the cutting edges. Each tooth is relieved radially to form clearance behind the cutting edge, allowing the faces of the teeth to be sharpened while retaining the original tooth profile (Figure A-3). Figures A-4, A-5, and A-6 are schematic diagrams showing the relationship between the hob and the gear.

2.2. Shaping

Like hobbing, gear shaping is a generating process. The tool used is a "pinion"-type tool (Figure A-7) as opposed to the "worm"-like tool used in hobbing. Cutting gears with shaper cutters is a planing or shaping process involving a reciprocating motion of the tool with chips removed only on one direction of the stroke. This is the principal upon which the gear shaper operates, as indicated in Figure A-8. The shape produced by the shaper cutter is shown in Figure A-9. In the tooth space to the right of the illustration are shown the successive positions taken by the cutter tooth as it "rolls" into the tooth space.

2.3. Shaving

Rotary gear shaving is a production process for gear finishing that uses a high-speed steel, hardened and ground, ultra-precision shaving cutter. The cutter looks like a helical gear. It has gashes in the flanks of the teeth that act as the cutting edges. The cutter is meshed with the gear in a crossed-axes relationship (Figure A-10), and rotated in both directions during the work cycle while the center distance is being reduced in small controlled steps. Simultaneously the work is traversed back and forth across the width of the cutter. Excellent surface finish is achieved with gear shaving. A value of 25- μ is the normal finish achieved with production gear shaving. The shaving process exhibits advantages in the ability to modify the tooth form. A crowned or tapered tooth form and minute modifications in the involute profile can be provided by shaving.

3.0. GEOMETRY OF SPUR GEAR TEETH

Figure A-11 shows the basic geometry of a spur gear tooth with the following definitions.

- addendum - the radial distance between the top land and the pitch circle
- backlash - the amount by which the width of a tooth space exceeds the thickness of the engaging tooth on the pitch circles

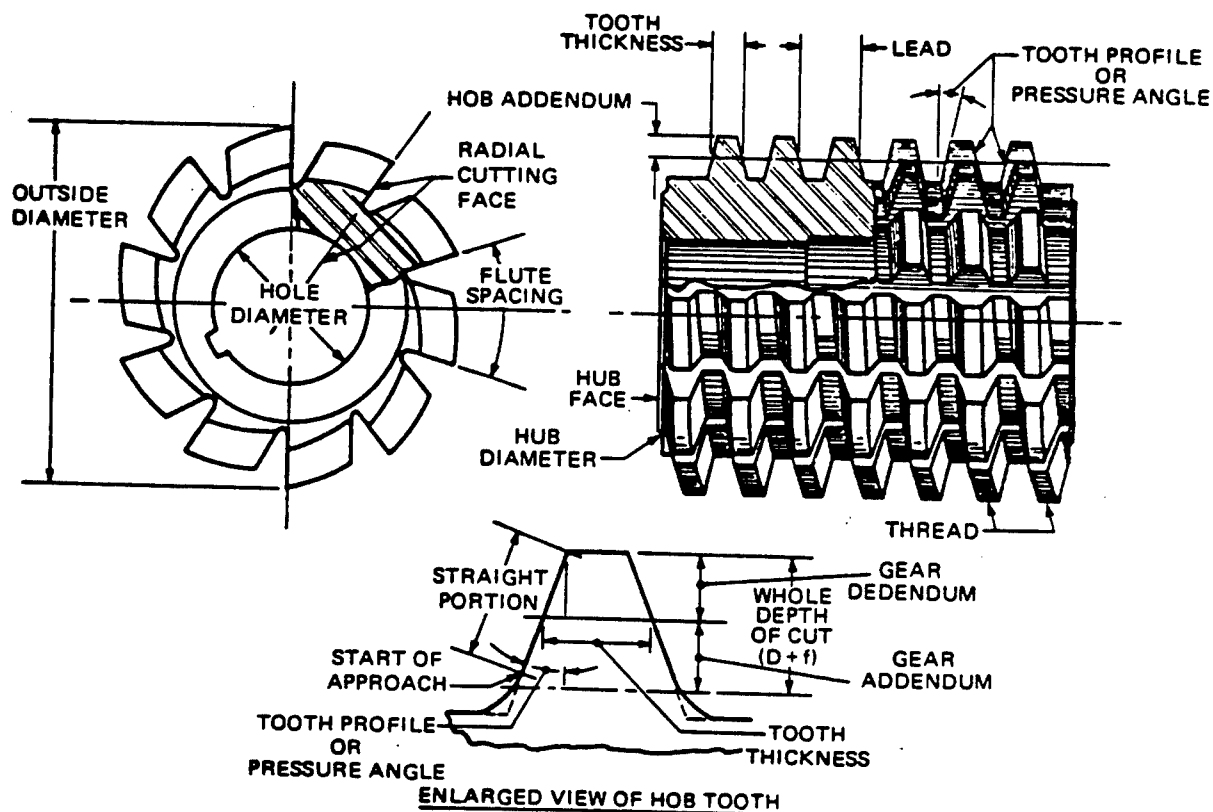


FIGURE A-3. Geometry of a Basic Hob (1)

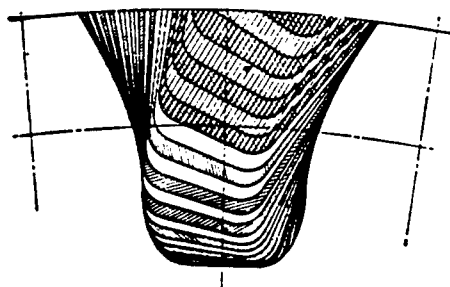


FIGURE A-4. Chip Loads Cut by Successive Hob Teeth (2)

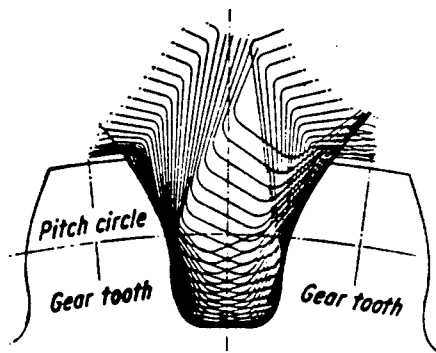


FIGURE A-5. Complete Generating Action of the Hob (2)

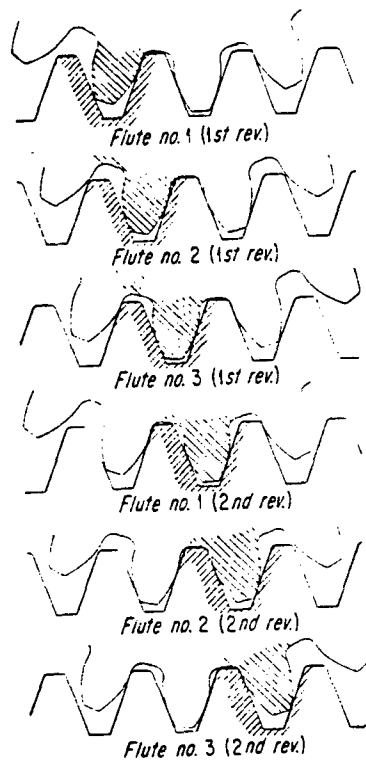


FIGURE A-6. How Different Hob Flutes Form the Gear Tooth (4)

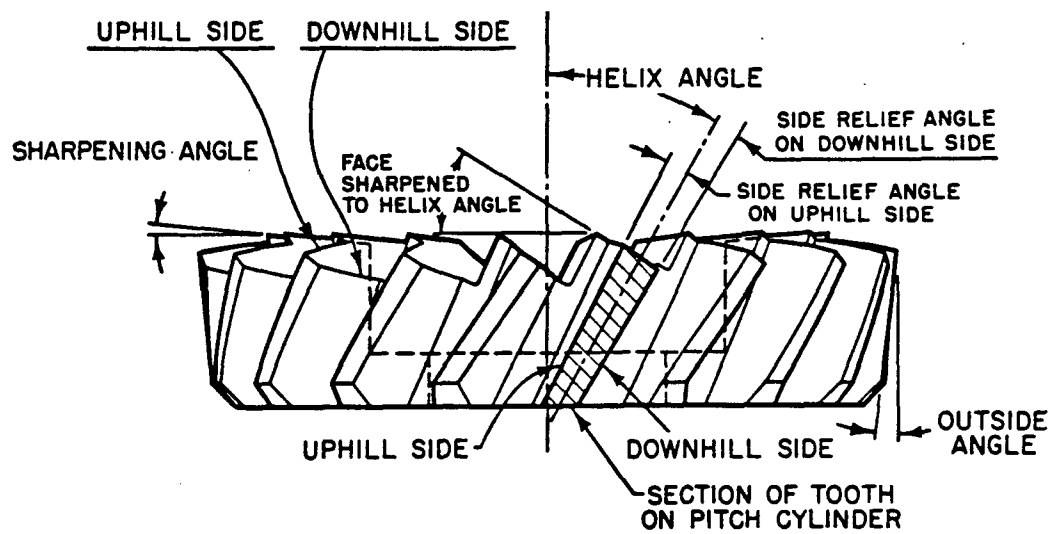


FIGURE A-7. Geometry of a Shaper Cutter (5)

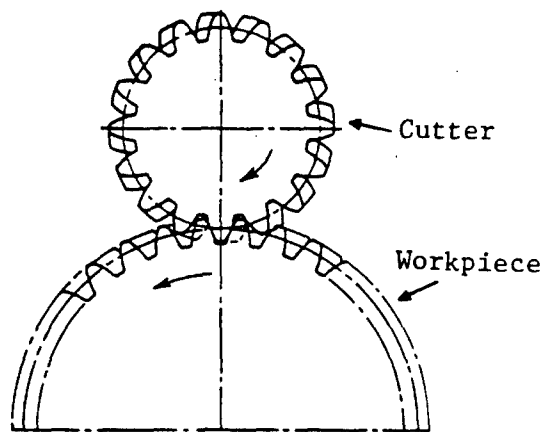


FIGURE A-8. Shaper Cutter and Work Piece (2)

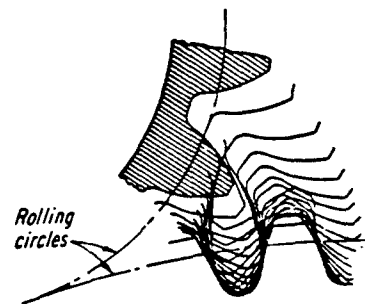


FIGURE A-9. Generating Action of Shaper Cutter (2)

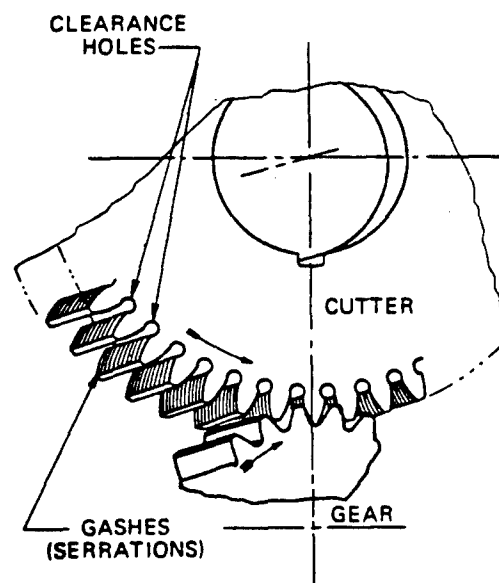


FIGURE A-10. Work Gear in Crossed-Axes Mesh with Rotary Shaving Cutter Mounted Above (1)

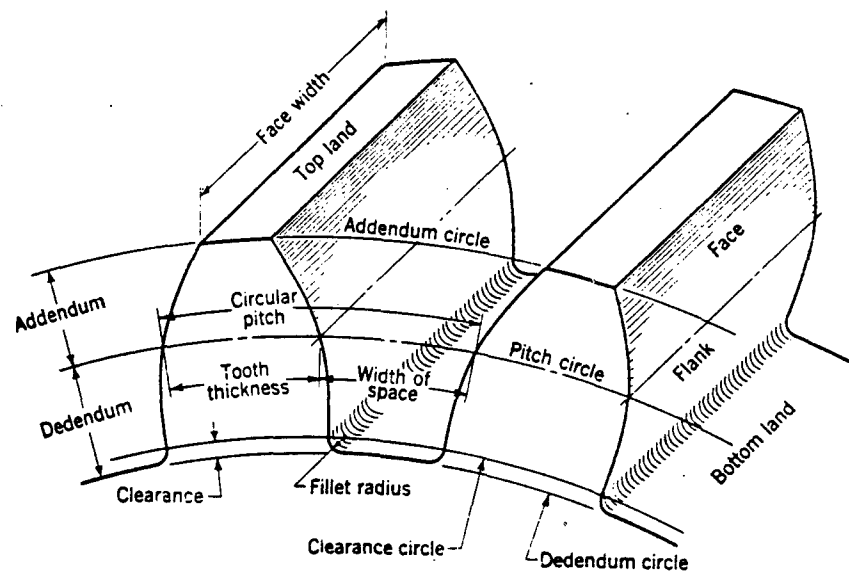


FIGURE A-11. Gear Terminology (3)

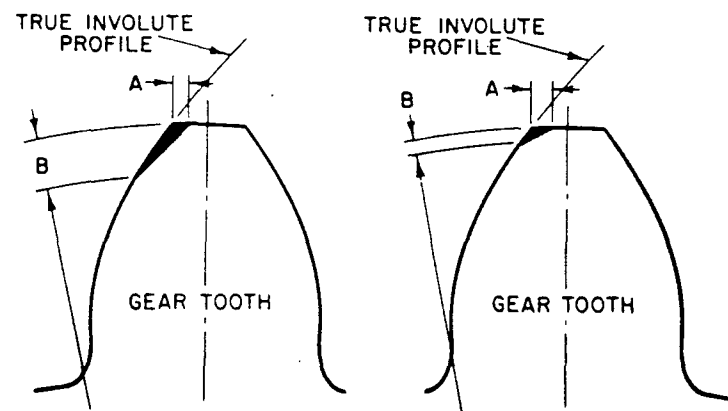


FIGURE A-12. Tip Relief and Tip Chamfer on a Gear Tooth (5)

- circular pitch - the distance, measured on the pitch circle, from a point on one tooth to a corresponding point on an adjacent tooth
- clearance - the amount by which the dedendum of a gear exceeds the addendum of its mating gear
- dedendum - the radial distance from the bottom land to the pitch circle
- diametral pitch - number of teeth on the gear per inch of pitch diameter
- pitch diameter - diameter of the theoretical pitch circle which is tangent to the corresponding pitch circle on a mating gear

There are two commonly used tooth profile modifications used to improve the performance of spur and helical gears; tip relief and tip chamfer. The methods of specifying these parameters are shown in Figure A-12. There are many different situations in which spur or helical gears may be designed based on hobbing and shaper cutting. Most spur and helical gear tooth profiles can be designed using one or more of the following: 1) hob generation, grounded corner, 2) pseudo-hob generation, rounded corner (hob designed to cut a given gear), 3) hob generation, tip protuberance (Figure A-13), 4) shaper generation, sharp corner, 5) shaper generation, full-rounded tip, and 6) mating gear plus operating conditions.

4.0. DETERMINATION OF GEAR GEOMETRY FOR SPUR GEARS

The following discussion describes the procedures used to compute the spur gear tooth coordinates and the equations employed in these procedures. These equations also apply to helical gears by taking into account the helix angle or twist of the gear.

The spur gear tooth profile may be divided into four sections; bottom land, fillet, involute, and top land. The rectangular coordinates of the fillet-involute region are computed from the polar coordinates using equations found in reference (2). The gear tooth profile equations are summarized below.

4.1. Involute

The involute equations remain the same for all generation methods. Referring to Figure A-14, for the involute, for each value of θ there is a unique value for r ;

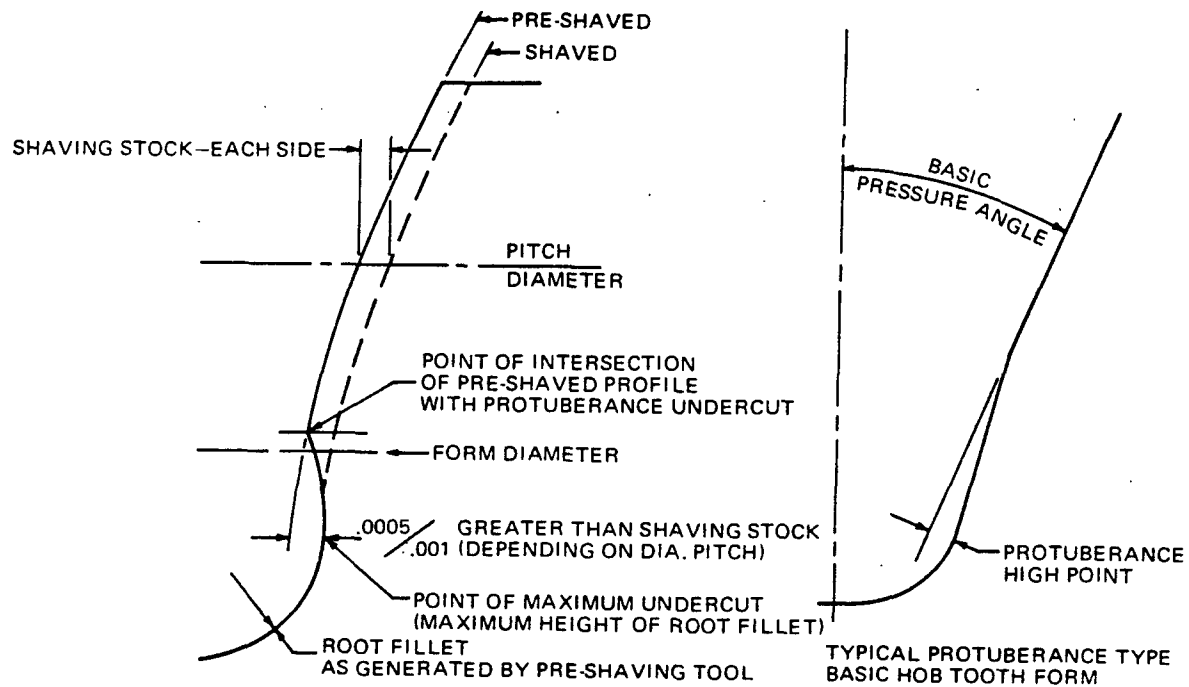


FIGURE A-13. Undercut Produced by a Protuberance Hob and the Basic Protuberance Hob Tooth Form (3)

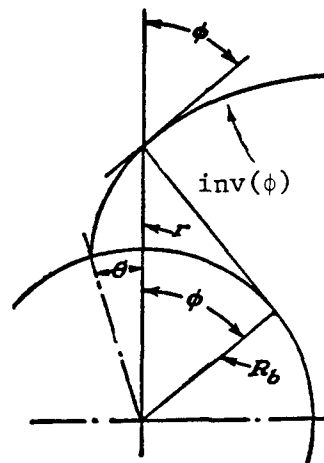


FIGURE A-14. Geometric Parameters of an Involute (symbols explained in text) (4)

$$\theta = \tan(\phi) - \phi = \text{inv}(\phi) , \quad (\text{A-1})$$

$$r = R_b / \cos(\phi) , \quad (\text{A-2})$$

where;

- θ = the involute angle measured from the point where the gear tooth profile intersects the base circle,
- ϕ = the pressure angle at any radius,
- $\text{inv}(\phi)$ = the involute function of ϕ ,
- r = any radius to a point on the tooth profile,
- R_b = the base radius of the gear

Note that the angle θ is measured from the radial line passing through the beginning of the involute curve on the base circle. The profile coordinates are computed using a rectangular coordinate system with the x-axis passing through the center of the tooth space. The polar angle, θ'' (Figure A-15), defining each profile point is measured from this center line, where;

- θ'' = any angle from the tooth space center line to a point on the gear tooth profile,
- H = half-width of entire tooth, in radians,
- T = any arc tooth thickness in the involute region, in units of length.
- T_p = the arc tooth thickness at the pitch radius,
- R_p = pitch radius,
- ϕ_p = pressure angle at the pitch radius,
- p = circular pitch,
- N_G = number of teeth on gear.

In cases where there is a chamfer on the tooth tip (see Figure A-16), the involute coordinates are computed until the radius reaches the depth at which the chamfer is to start. Referring to Figure A-16;

- T_{tc} = arc tooth thickness of gear at tip when tip, chamfer exists,
- T_t = arc tooth thickness at tip without tip chamfer
- t_c = arc length of tip chamfer,
- Δr_c = radial depth of tip chamfer.

Tip relief (Figure A-17) is another situation in which the involute is altered. In this case a new base circle is computed to be used in Equation (A-2). This new base circle is calculated to give the desired tooth tip thickness as specified by;

$$T_{tr} = T_t - t_r , \quad (\text{A-3})$$

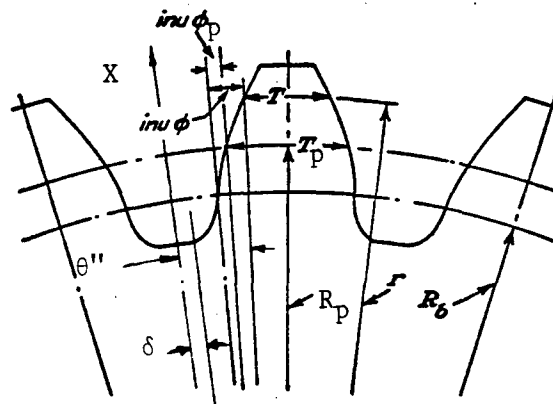


FIGURE A-15. Determination of Tooth Profile from Basic Gear Parameters (symbols explained in text) (4)

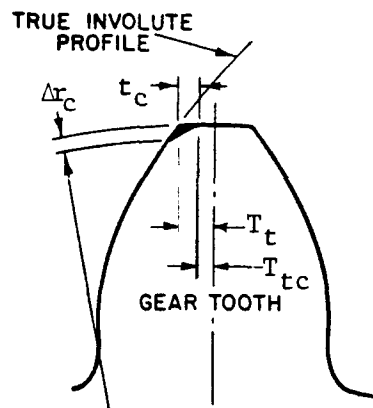


FIGURE A-16. Tip Chamfer on a Spur Gear Tooth (symbols explained in text) (5)

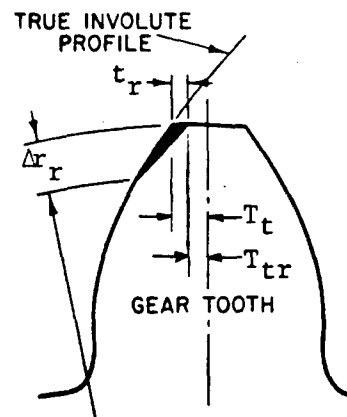


FIGURE A-17. Tip Relief on a Spur Gear Tooth (symbols explained in text) (5)

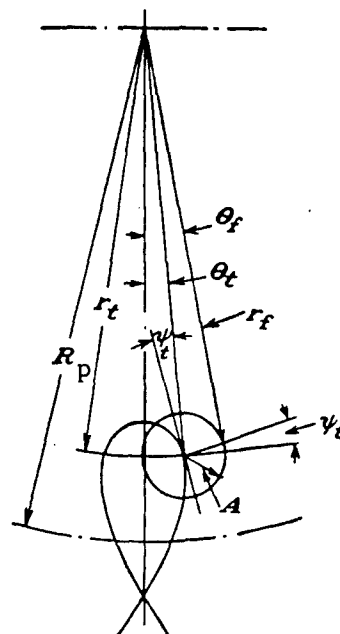


FIGURE A-18. Fillet Form of Rounded Corner of Hob Tooth (symbols explained in text) (4)

where;

T_{tr} = arc tooth thickness of gear at tip when tip relief exists,
 T_t = arc tooth thickness at tip without tip relief,
 t_r = arc length of tip relief,
 Δr_r = radial depth of tip relief.

4.2. Fillet

The shape of the gear tooth fillet is the only part of the tooth profile which is process dependent. In each case, a curve known as a trochoid is generated by the corner of the cutting tool at the tip.

When using a hob with a rounded corner (Figure A-19), the fillet shape (Figure A-18) is generated from the envelope of circular curves created by the trochoidal path of the center of the rounded corner. The x and y coordinates of any point on the tooth fillet are given by;

$$x = r_f \cdot \sin(\theta'') , \quad (A-4)$$

$$y = r_f \cdot \cos(\theta'') , \quad (A-5)$$

$$\theta'' = d + \theta_f , \quad (A-6)$$

where;

r_f = any radius to fillet.
 B = distance from center line of hob tooth to center of rounded corner on a hob,
 b = distance from pitch line of hob to center of rounded corner on hob,
 A = radius of rounded corner of hob tooth,
 d = angle between center line of gear-tooth space and origin of trochoid,
 θ_t = angle of trochoid in reference to trochoid origin,
 r_t = any radius of trochoid,
 ψ_t = angle between tangent to trochoid and radius vector,
 r_f = any radius to fillet,
 θ_f = angle of fillet in reference to trochoidal origin,
 x = abscissa of any point on the tooth profile,
 y = ordinate of any point on the tooth profile.

Sometimes a hob cutting tool with a protuberance tip (Figure A-20) is used in order to produce undercut for finishing purposes. The

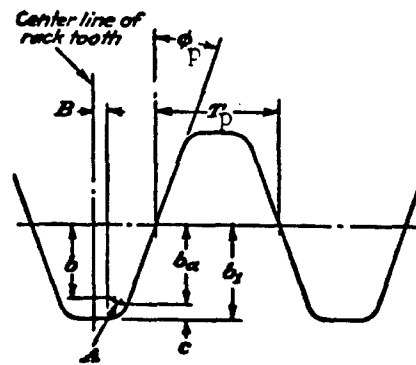


FIGURE A-19. Detailed Geometry of Hob with Rounded Corner (b_1 = hob addendum; c = clearance; rest of symbols explained in text) (4)

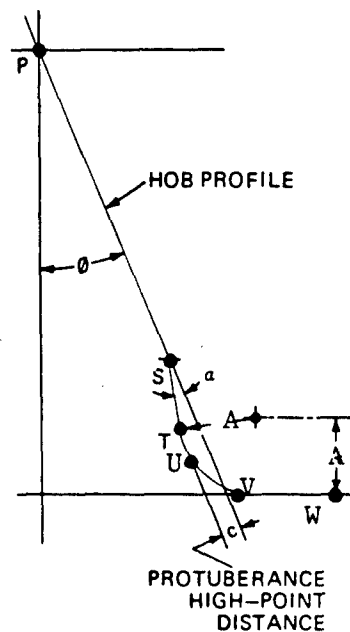


FIGURE A-20. Geometry of a Protuberance Hob (W = point on center line of hob at tip; V = beginning of rounded corner; U = end of rounded corner and beginning of parallel land length; T = end of parallel land length; S = point where straight line form of hob resumes; α = protuberance angle; P = pitch point) (1)

equations used to define the fillet are the same as for when using a round cornered hob except that now (refer to Figures A-21, A-18 and A-19);

$$b = y_t , \quad (A-6)$$

$$d = x_t/R_p , \quad (A-7)$$

$$\theta_f = \theta_t , \quad (A-8)$$

$$r_f = r_t , \quad (A-9)$$

where;

y_t = distance from pitch line of protuberance hob to candidate cutting point on hob (variable),

x_t = distance from center line of protuberance hob to candidate cutting point on hob (variable).

For all generation methods, the junction between the fillet and involute is computed the same and is defined as the intersection of the trochoid and involute curves, where;

R_{tf} = radius to top of fillet where fillet joins involute,

b_a = distance from pitch line of hob to point of tangency of rounded corner with straight-line form.

In cases where undercut is present, (Figure A-22) there are two possible intersection points and care must be taken to locate the correct point.

For the shaper generation methods when the tip is not fully rounded, an approach similar to that used for hob generation methods is used to compute the fillet coordinates. Referring to Figures A-23 and A-24;

e_1 = angle of rotation of gear (see ϵ in Figure A-23),

R_c = pitch radius of shaper cutter,

e_c = angle of rotation of shaper cutter (see ϵ in Figure A-23),

C = center distance between axis of gear and shaper cutter,

R_{oc} = outside radius of shaper cutter,

N_c = number of teeth in shaper cutter,

T_c = arc tooth thickness of shaper cutter at pitch radius,

ϕ_{oc} = pressure angle at tip of shaper cutter tooth.

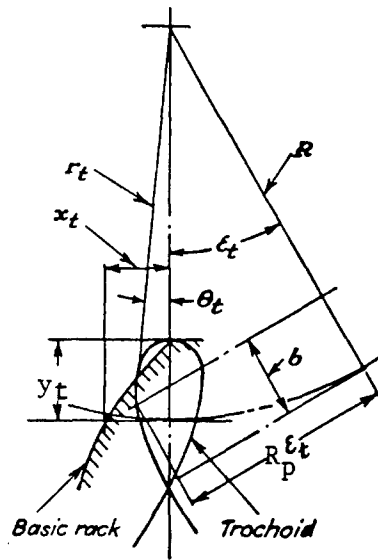


FIGURE A-21. Defining a Single Point on a Trochoid Generated by a Specific Point on the Hob Profile (ϵ_t = roll angle; rest of symbols explained in text) (4)

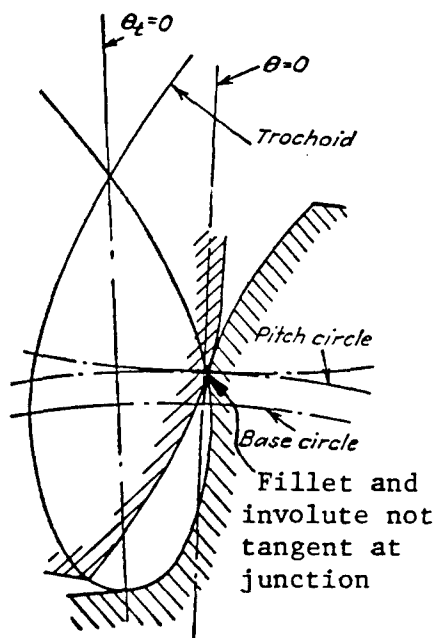


FIGURE A-22. Hob Producing Undercut (4)

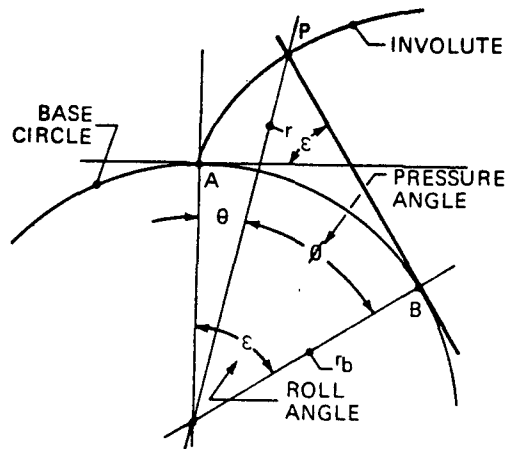


FIGURE A-23. Geometric Parameters Used for Shaper Cutter Equation (1)

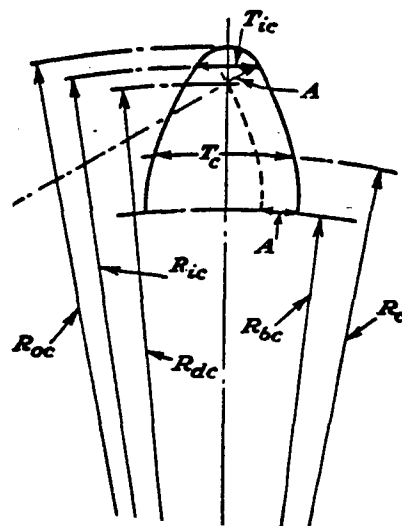


FIGURE A-24. Geometry of Full-Rounded Shaper Cutter Tooth (symbols explained in text) (4)

R_{bc} = base radius of shaper cutter.

The final case involves the use of a shaper cutter with a full rounded tip. The program is structured so as to compute an approximate value for the radius of the rounding (see Figure A-24). The following quantities are used to compute the fillet coordinates;

ϕ_{ic} = pressure angle at radius to top of involute on shaper cutter,

R_{ic} = radius to top of involute profile on shaper cutter,

T_{ic} = arc tooth thickness of shaper cutter at top of involute,

ϕ_{dc} = pressure angle at radius to center of rounding on shaper cutter,

R_{dc} = radius to center of rounding on shaper cutter,

4.3. Bottom Land

The bottom land of each gear tooth is a portion of a circle, the root circle. For half of a gear tooth this circle will extend from the tooth space center line to the point where the fillet begins. The rectangular coordinates are solved for by varying the polar angle from zero to the angle at the start of the fillet and using the following equations;

$$x = R_b \cdot \sin(\theta'') , \quad (A-10)$$

$$y = R_b \cdot \cos(\theta'') . \quad (A-11)$$

4.4. Top Land

The procedure for determining the coordinates of the top land is similar to that used in solving for the bottom land coordinates. The angle measured from the tooth space centerline is varied from θ_{ti}'' to θ_{max}'' and the outside radius is used in the polar equations (refer to Figure A-25);

$$x = R_o \cdot \sin(\theta'') , \quad (A-12)$$

$$y = R_o \cdot \cos(\theta'') , \quad (A-13)$$

where;

R_o = outside radius of gear,

θ_{ti}'' = angle from tooth space center line to top of involute on gear.

θ_{max}'' = maximum angle from tooth space center line to center of gear tooth.

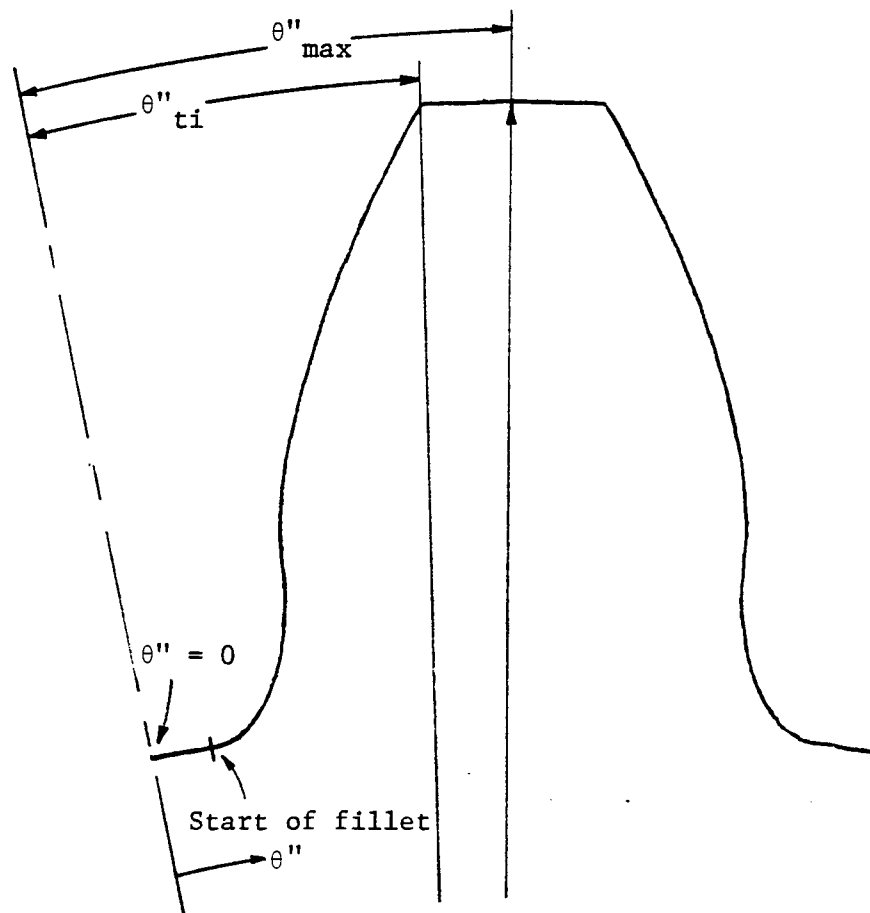


FIGURE A-25. Geometry of Bottom and Top Land Sections on a Spur Gear Tooth (symbols explained in text)

5.0. DETERMINATION OF GEAR GEOMETRY FOR HELICAL GEARS

The profile of a helical gear is defined in exactly the same way as a spur gear except that an additional parameter, the helix angle, must be specified. The helix angle is defined such that:

$$\tan(\psi) = (2 \cdot \pi \cdot R)/L , \quad (A-14)$$

where;

ψ = helix angle,

R = pitch radius of the helical gear,

L = helical lead (axial advance of a screw thread in one 360 degree turn).

LIST OF REFERENCES

- (1) Modern Methods of Gear Manufacture, National Broach Machine Division/ Lear Siegler, Inc. publication, Fourth Ed., Detroit, 1972.
- (2) Dudley, D.W., Gear Handbook, McGraw-Hill, New York, 1962.
- (3) Shigley, J.E., Kinematic Analysis of Mechanisms, McGraw-Hill, New York, 1969.
- (4) Buckingham, Earle, Analytical Mechanics of Gears, Dover Publications, Inc., New York, 1949.
- (5) "Know Your Shaper Cutters," Illinois/Eclipse publication, Chicago, 1977.

THIS PAGE LEFT BLANK INTENTIONALLY

APPENDIX B

STRESS ANALYSIS, ELASTIC DEFLECTION AND BULK SHRINKAGE

THIS PAGE LEFT BLANK INTENTIONALLY

1.0. INTRODUCTION

During forming at any temperature, dies are subjected to mechanical loading accompanied by fatigue loading (alternating mechanical stresses) and the associated elastic deflection. At elevated temperatures, the dies are also subjected to a) thermal stresses, and b) fatigue stresses due to alternating temperatures in the die. The die dimensions must be corrected to compensate for the elastic deflection due to mechanical stresses and the bulk shrinkage due to temperature differentials. The determination of the elastic deflections of the die requires knowledge of the stresses acting on the die during the forming process. A stress analysis will not only calculate the elastic deflections but will also calculate the forming load and energy. Bulk shrinkage of the dies can be obtained by determining the average increase in temperature of the die.

The changes caused on the die inner surfaces due to reinforcement rings (shrink fit assembly) can be initially neglected for the design especially at higher temperatures as the order of magnitude of these changes will be comparatively small. Any changes necessary for these can be included into the machining allowance.

2.0 STRESS ANALYSIS

The most widely used technique to analyze stresses in forming processes is the "slab method" (1)*. Spur and helical gears may either be extruded or forged (the latter with more difficulty in the case of helical gears). Hence, there are two entirely separate cases which must be considered in the stress analysis. The stress in the tooth cavity during extrusion will be analyzed by the slab method suggested in reference 1. The forging stress will also be analyzed by the slab method (2). The problems of cavity filling in the forging process will be considered as a flashless forging process and a method used in reference 3 will be used to predict the required loads for various degrees of tooth filling.

2.1. Extrusion Process

In the extrusion process, a sawn or sheared billet is used. The billet is annealed, surface treated (phosphate coating) and lubricated (soap, graphite or molybdenum disulfide) for the cold

*Numbers in parentheses refer to references at the end of the appendix.

extrusion process. For warm extrusion, the billet may be coated with a lubricant (graphite or molybdenum disulfide) and heated by induction under protective atmosphere to the desired extrusion temperature. A schematic of the extrusion process is shown in Figure B-1. At the end of the extrusion process, the part can either be ejected or a push-through extrusion principle can be used.

2.1.1. Total Punch Force Computation. The force required to extrude a spur or helical gear is given by the following equation;

$$F_p = F_{id} + F_{sh} + F_f, \quad (B-1)$$

where;

F_p = total punch force,
 F_{id} = ideal deformation force,
 F_{sh} = force due to shearing of the material at the entry and exit of the die,
 F_f = friction force along the die walls and the punch

2.1.2. Breakdown of Friction Force. Figure B-2 shows the geometry for the case of hollow forward extrusion using a stepped punch. In this figure, the friction has been broken down into five (5) components;

F_1 = friction on the container wall,
 F_2 = friction on the die shoulder,
 F_3 = friction on the die wall in the land zone,
 F_4 = friction on the mandrel wall in the deformation zone,
 F_5 = friction on the mandrel in the die land.

The total friction force F_f , is made up of the sum of friction forces F_1 through F_5 .

2.1.3. Punch Pressure Computation. Once the total punch force has been determined, the punch pressure must be computed;

$$P_p = F_p / A_o, \quad (B-2)$$

where;

P_p = punch pressure.
 A_o = cross sectional area of the gear.

2.1.4. Radial Pressure Computation.

$$P_{r_{max}} = P_p - \sigma_{f0}. \quad (B-3)$$

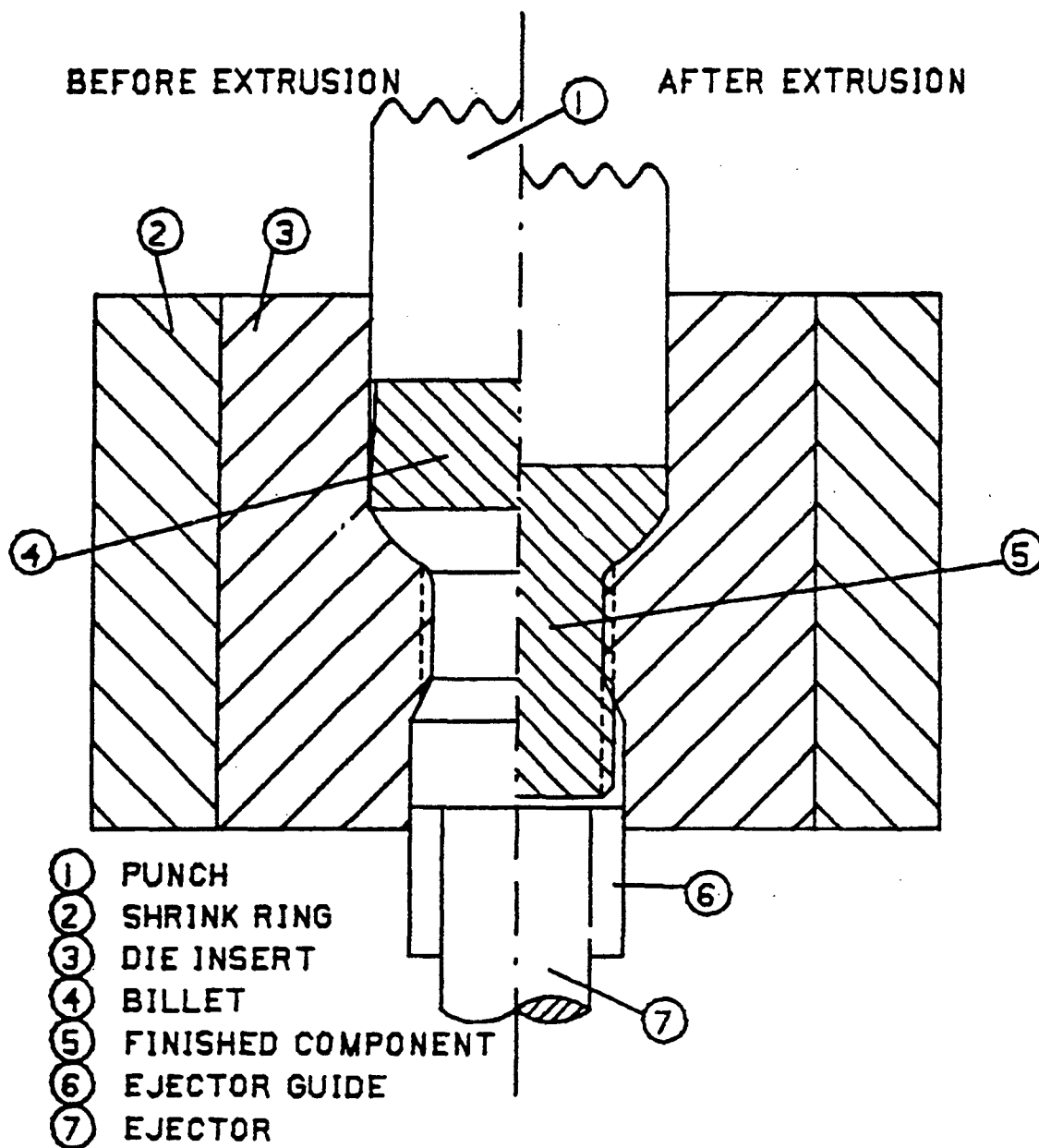


FIGURE B-1. Typical Tool Setup for Extruding Spur or Helical Gears

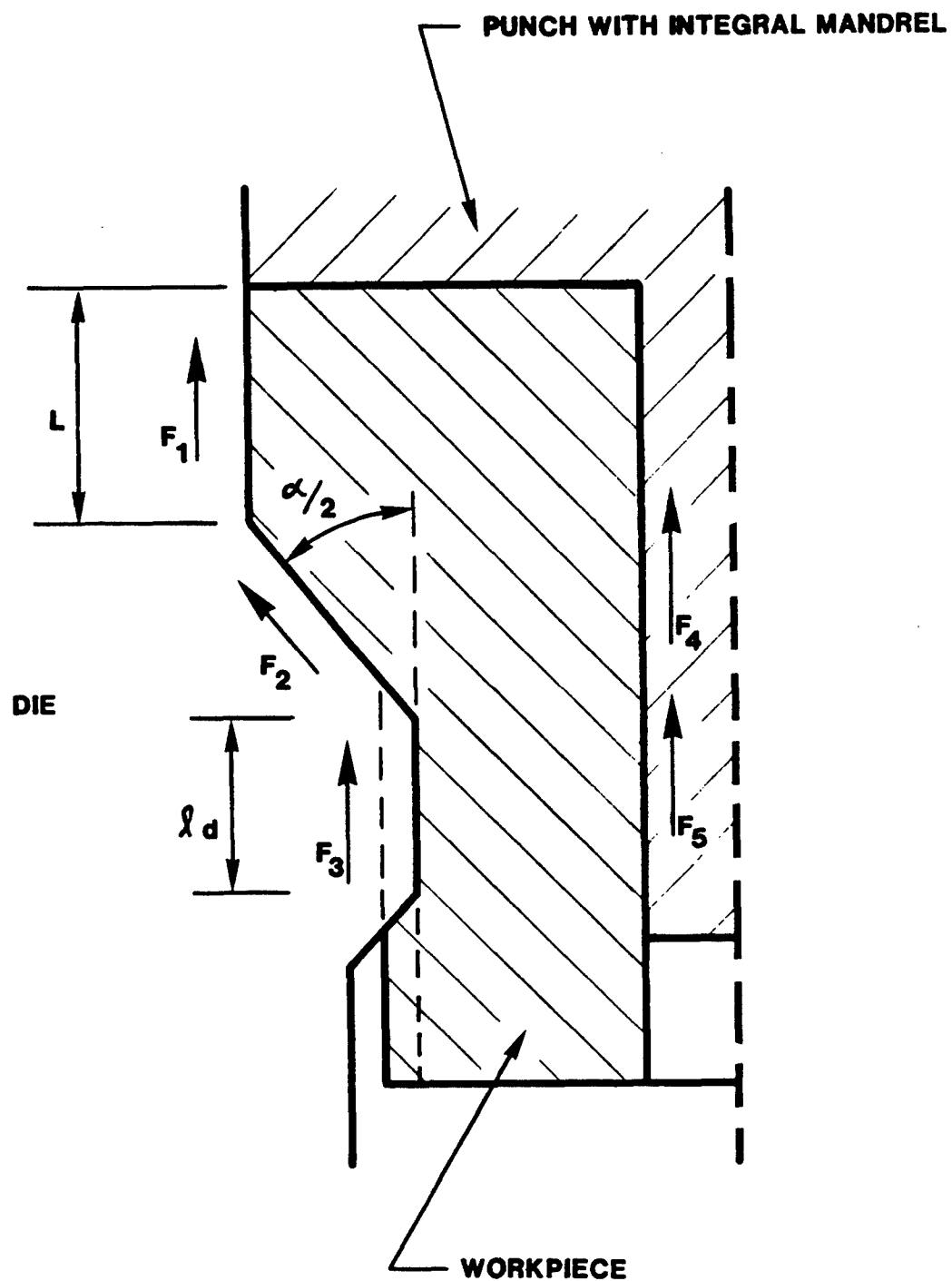


FIGURE B-2. Frictional Forces in the Extrusion of Spur and Helical Gears (symbols explained in text)

This maximum radial pressure is used to calculate the radial and tangential deflections of the die and permits the determination of the corrected tooth geometry for the extrusion die.

2.2. Forging Process

In the process of forging helical or spur gears, the billet diameter is slightly smaller than the root diameter of the gear. Figure B-3 shows the schematics of a possible forging operation. In this process, the material is extruded into the die radially. However, to avoid confusion between this radial or lateral extrusion process and the forward extrusion process mentioned earlier, this process has been termed a forging process. The billet is placed into the container and by the action of the punch or both the punch and counterpunches, the material is forced into the die cavity. In such a process, two regions of metal flow must be analyzed as described below.

The first region of plastic flow involves the movement of material into the tooth cavity until the outermost die surface is just touched by the material. This region has been analyzed using the slab method. This condition is called "zero corner fill" and is the minimum acceptable condition for the finished part. The second region uses equations developed in reference 3 and assumes an initial condition of "zero corner fill" and then proceeds to compute the required punch force to achieve various degrees of corner filling.

2.2.1. Region 1.

2.2.1.1. Average pressure for the case of sticking and sliding friction. For the purpose of stress calculations using the slab method, a configuration of the gear tooth as shown in Figure B-4a is used. Assuming the state of stress shown in Figure B-4b for the triangular groove, the average pressure for the case of sticking and sliding friction can be determined. Figure 4a does not resemble a gear in the area near the tooth tip which necessitates finding some way to model this area. Figure B-5 shows such a model (10). However, the actual shape of the gear tooth and material is a combination of Figures B-4 and B-5, one interpretation of which is shown in Figure B-6. The punch pressure can be represented as follows;

$$P_p = p + \sigma_{f0} , \quad (B-4)$$

where p is the average radial pressure for the case of sticking and sliding friction.

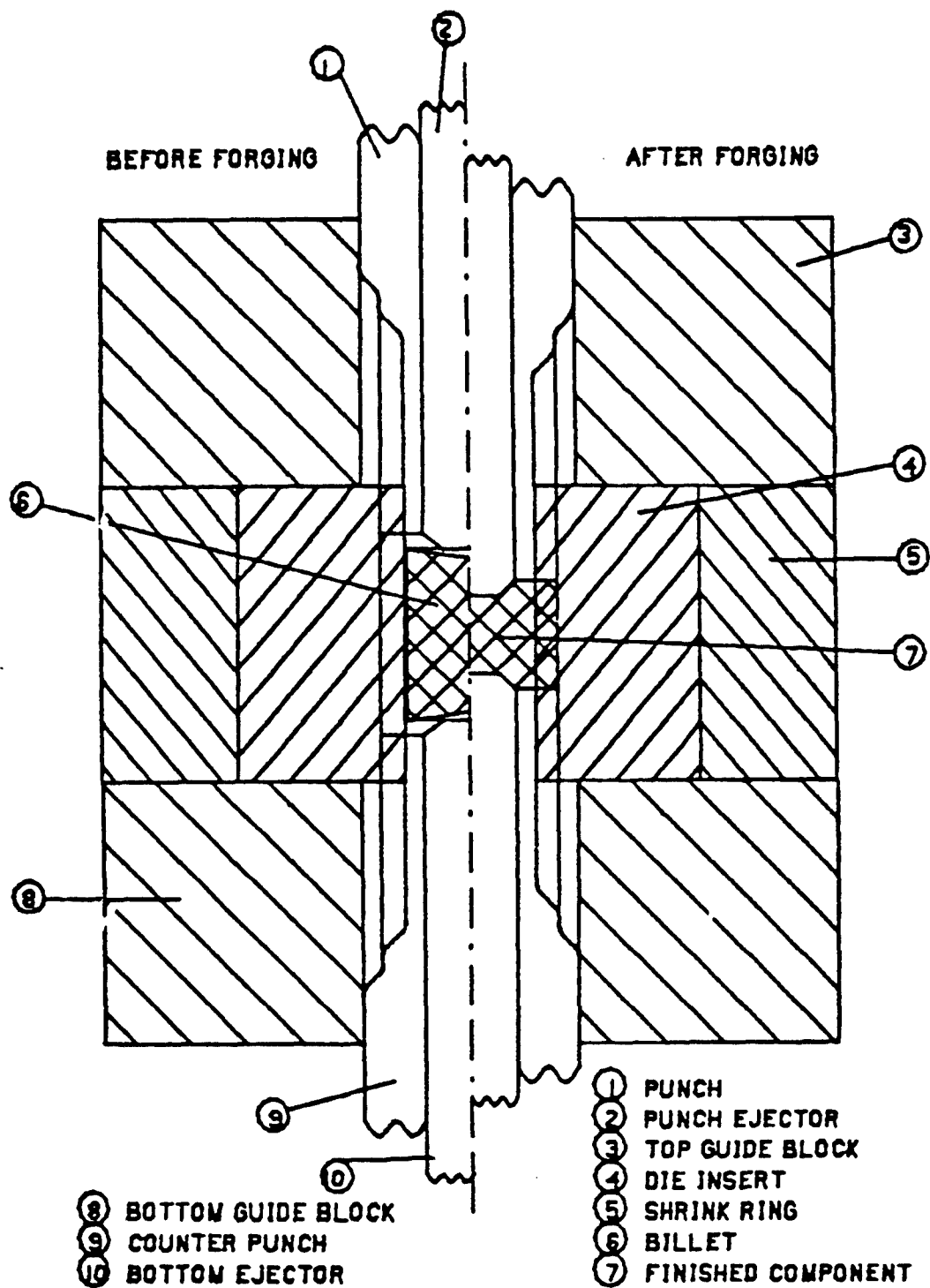


FIGURE B-3. Typical Tool Setup for Forging Spur or Helical Gears

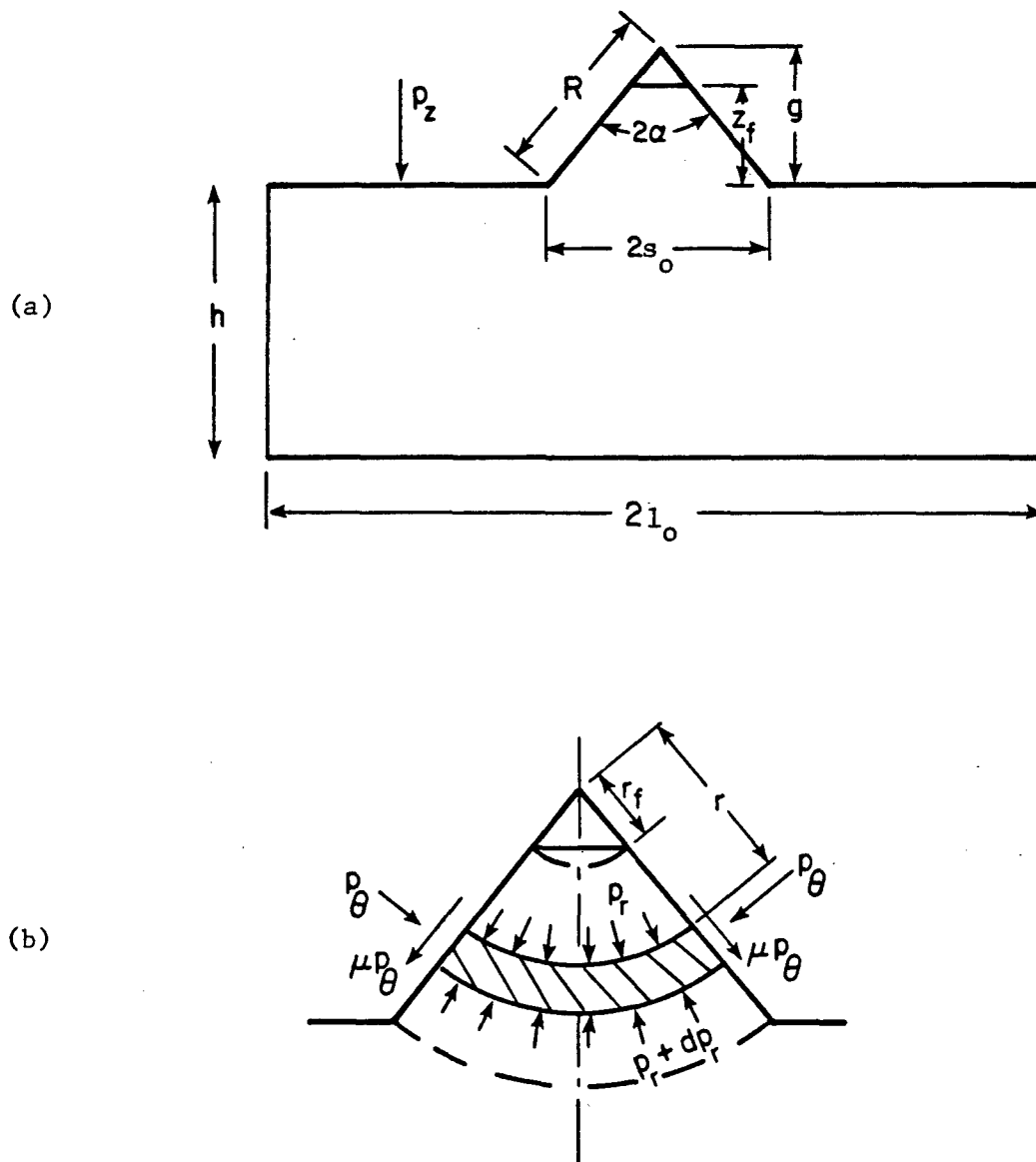


FIGURE B-4. a) Configuration of a Triangular Groove, and b) Assumed State of Stress

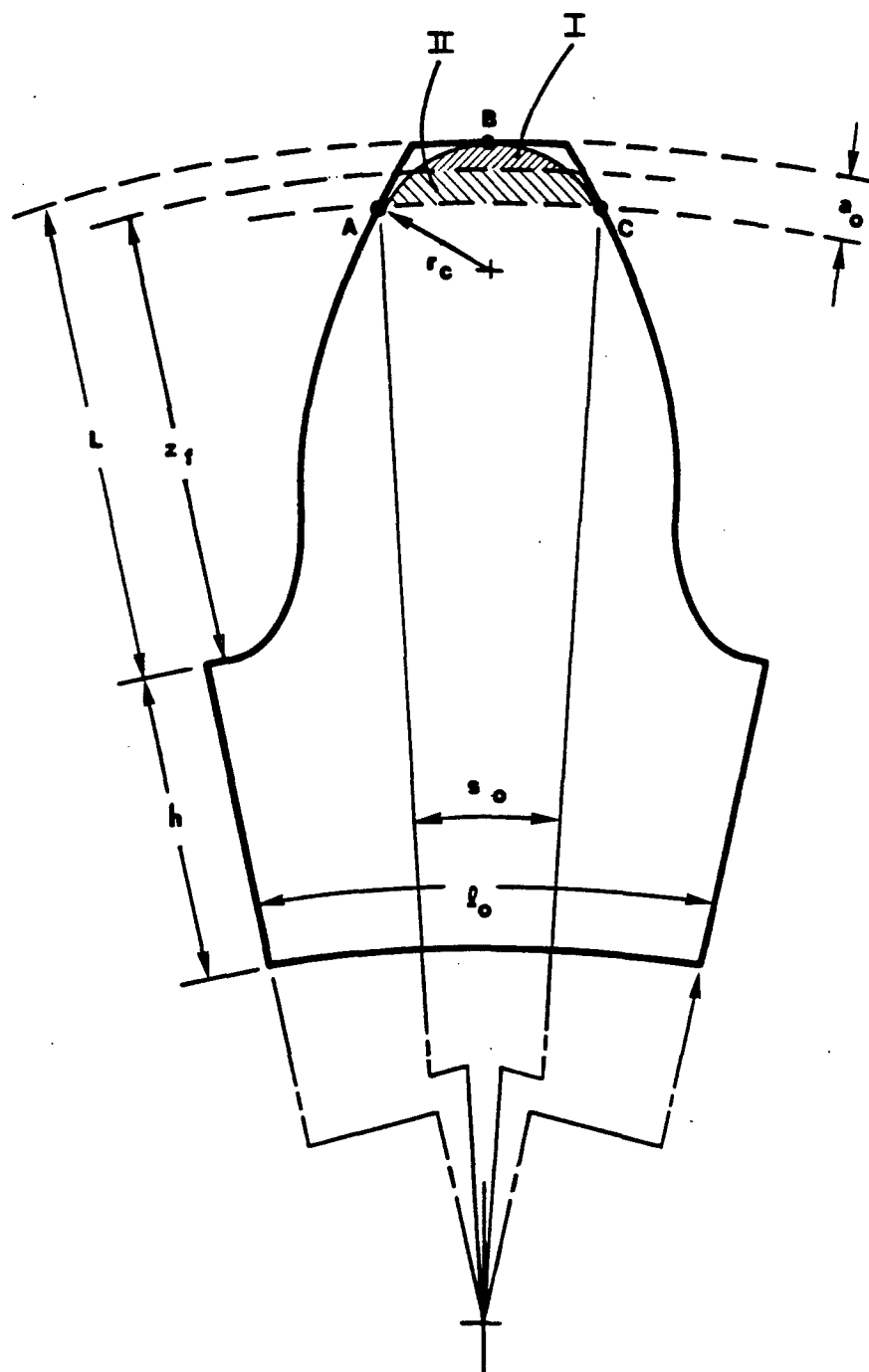


FIGURE B-6. Configuration of a Spur Gear Tooth Prior to Corner Filling (symbols explained in text)

2.2.2. Region 2

2.2.2.1. Background. When forging spur and helical gears, the most difficult area in which to achieve proper filling is at the corner of each tooth tip. If a model, such as the one described in the previous section is used, the value of a may be sufficiently small for the proper mechanical function of the gear. However, if a is too large, then more material will need to flow into the tip corners in order to produce a properly functioning gear. This will require an additional punch force. The previous analysis does not give a methodology to compute the additional forces required for any desired corner filling.

2.2.2.2. Definition of the final material position. For this analysis, an initial position for the material will be assumed to be the same as suggested in Figure B-6. Any further movement of the top punch will flatten out the top and the corner filling process will begin, as shown in Figure B-7. This is analogous to an upsetting process where the material at the tooth tip is forced into the corners. The area which will be upset and fill the corner can be calculated using formulas found in reference 8. To obtain the maximum radial pressure on the die wall, this pressure must be "transferred" back to the inner radius of the billet. Once the maximum radial pressure has been determined, Equation (B-4) may be used to calculate the maximum punch pressure.

In Appendix G, the computed values for a given tooth geometry have been analyzed. The finite element formulation used in this project for computing the forces required to fill the corners has been compared with both the formulations in this appendix. The most appropriate method has been utilized in the computer program.

3.0 ELASTIC DEFLECTION OF TOOL

The tools (dies) deform under forming load. The deformations are generally elastic if a proper die material with appropriate mechanical properties is selected. Using the radial pressure obtained from the previous stress analysis, the elastic deflection of the die, due to loading, can be computed using a finite element code available at Battelle (6). A preliminary simple calculation with the average value of mechanical stresses showed that the order of magnitude of this correction is very small. To determine if the additional accuracy of the FEM analysis would be desirable, a simple finite element elastic analysis using a program available at Battelle was conducted.

3.1. Finite Element Analysis

The finite element method computed the loads and displacements of

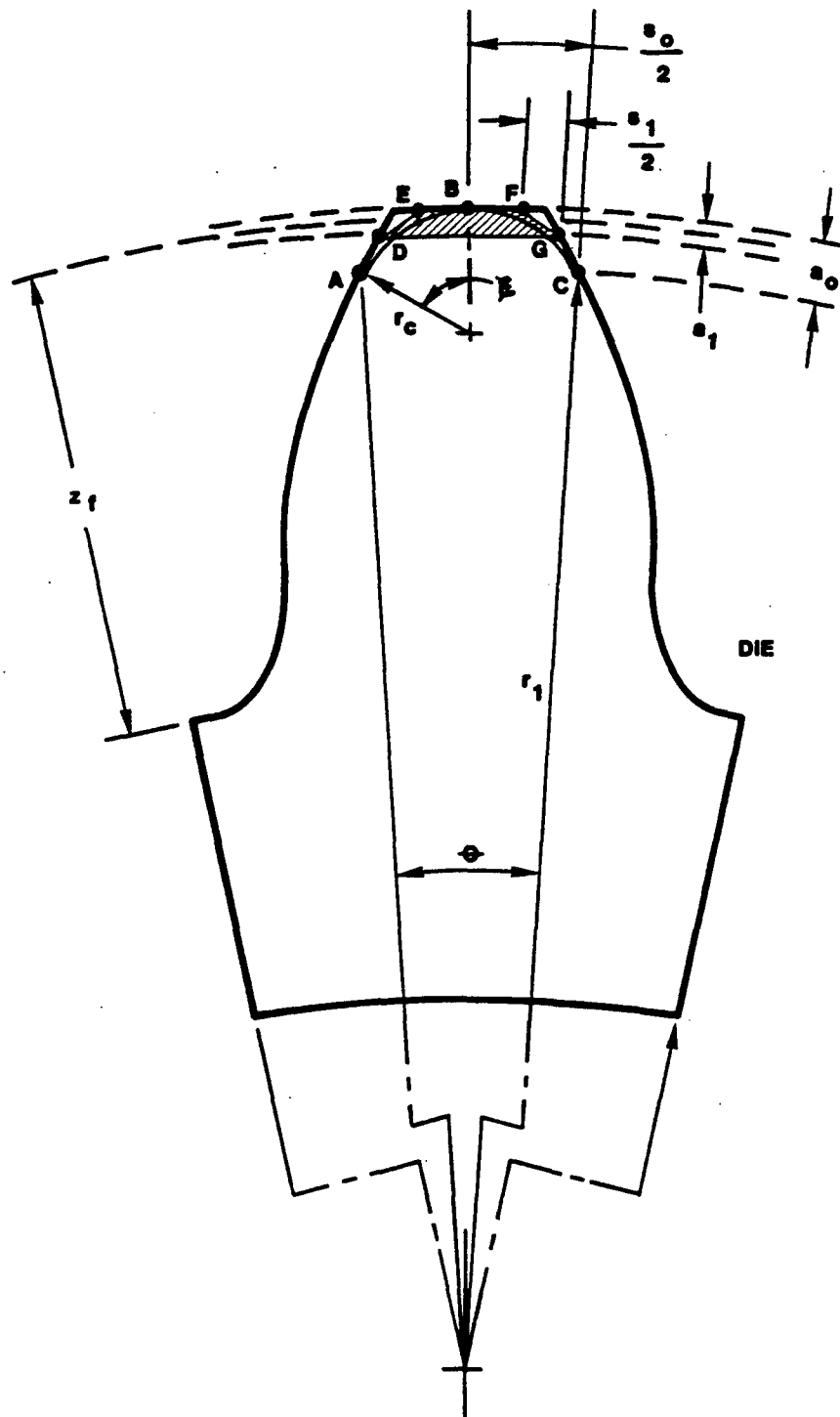


FIGURE B-7. Schematic of the Metal Flow During Corner Filling (symbols explained in text)

each of 57 nodes in an 11 element mesh. The mesh used is shown in Figure B-8.

3.2. Simplified Analysis

The elastic deformation due to mechanical loading, using a simplified approach, proceeds as follows. Using the previous forming stress analysis for a particular spur gear, the radial and tangential stresses at node 14 can be determined using an elastic thick shell model (11) for the die (see Figure B-9). The effect of this elastic deformation is to increase the cavity of the die. Hence, the die thickness should be made bigger (die cavity smaller) to compensate for the elastic deflection due to mechanical stresses. Table B-1 lists the radial displacement of three nodes on the die, nodes 1, 10, and 14, for different values of the inner radius using the simple thick cylinder approach. The gear die does not represent a true cylinder. The inner radius of an equivalent cylinder would lie somewhere between the root radius and the outside radius of the gear.

3.3. Comparison of FEM and Simple Analysis

Referring to Table B-1, when $a = 1.18$ (the pitch radius), the deflection computed using the simple approach came to within eight percent of the FEM results. Thus, it seems reasonable to choose the inner radius of the die to be equal to the pitch radius of the gear. This would allow the much simpler, less time-consuming and less costly thick-walled cylinder equations for calculating the elastic die deflections rather than doing a detailed FEM analysis. The errors introduced in the die design by using the simplified approach will be much smaller than the manufacturing tolerances on the die.

4.0. BULK SHRINKAGE DUE TO TEMPERATURES

If spur and helical gears are hot/warm formed, the temperature of the die will increase during the forming operation due to heat transfer from the heated billet. The following are the outcome of the thermal interaction between the die and the billet:

- The dimension of the billet increases as it is heated from room temperature to the forming temperature. The dimension of the billet changes further during the forming operation due to (a) temperature increases because of heat generation due to plastic deformation, and (b) temperature drop because of heat loss from the billet to the dies. The change in temperature of the billet is not constant over the entire cross section, but varies depending on the local deformation and heat transfer.

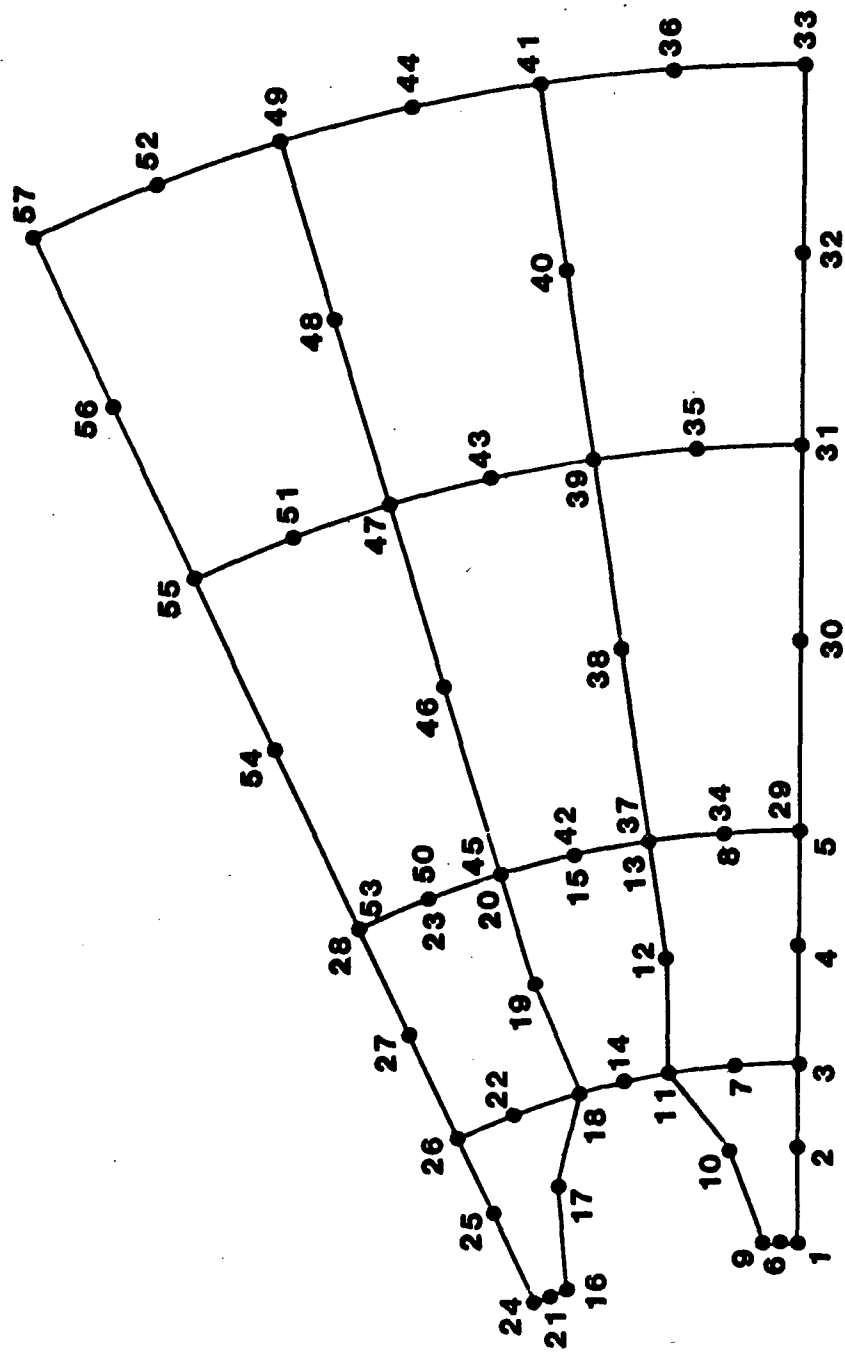


FIGURE B-8. Finite Element Mesh used to Estimate Elastic Deflection of a Spur Gear Die

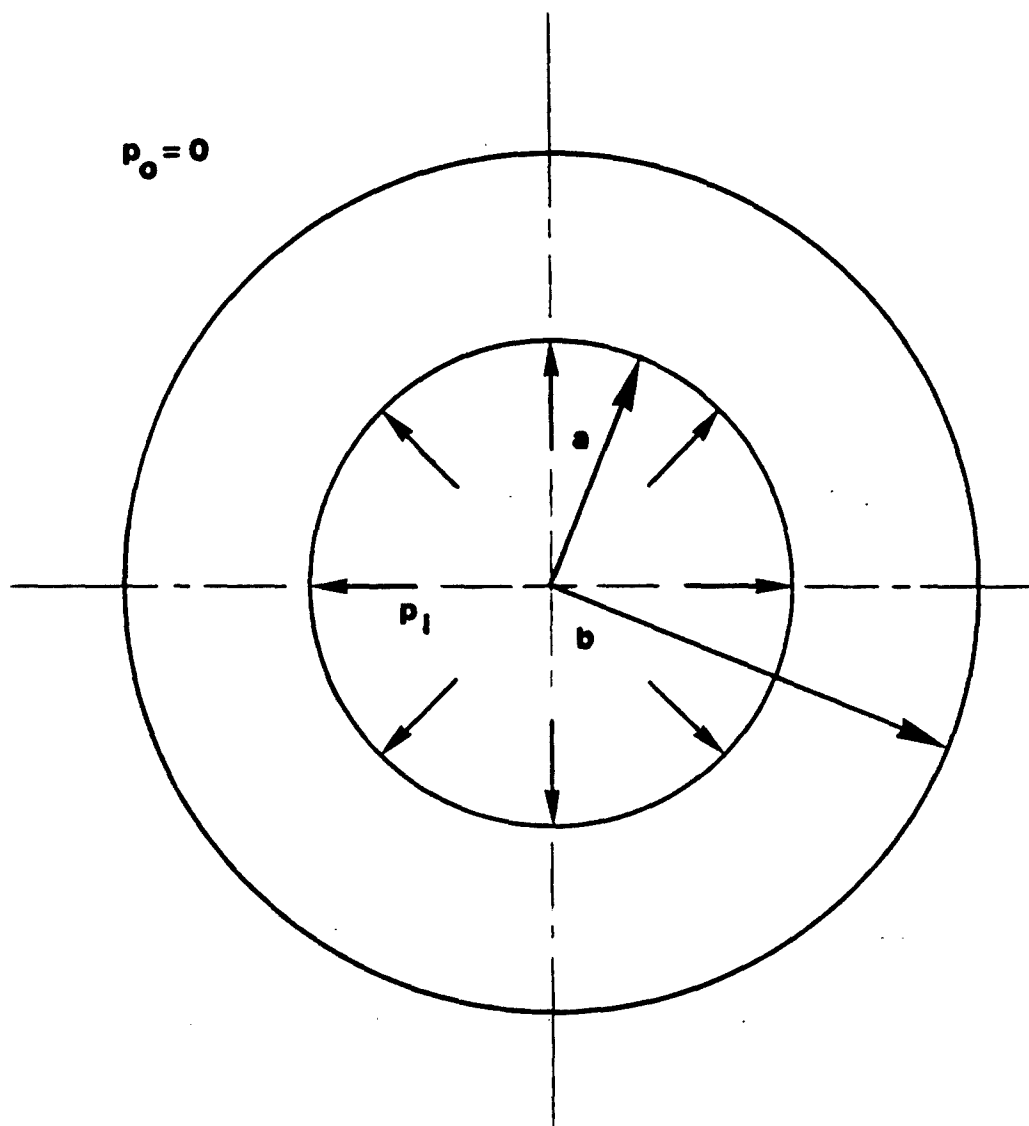
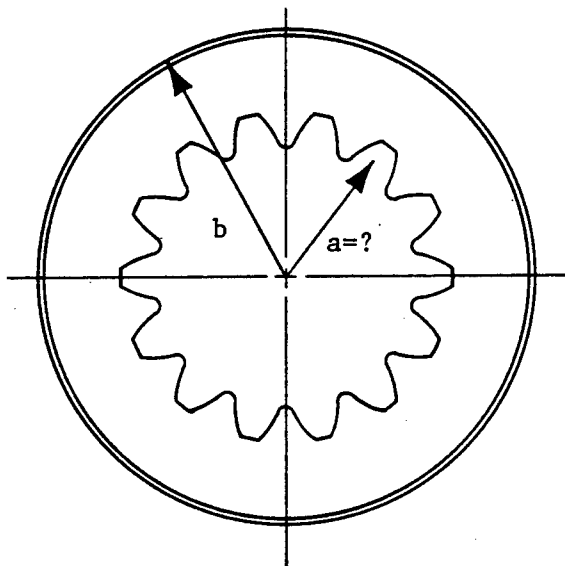


FIGURE B-9. Thick Shell Model of a Spur Gear Die (a = inner radius; b = outer radius; p_i = inside pressure; p_o = outside pressure)

TABLE B-1. Variation in Radial Displacement with Different Inner Radius Values ($b = 1.72$)

	a	u_1	u_{10}	u_{14}
Thick Cylinder Approach	1.01	2.69×10^{-3}	2.44×10^{-3}	2.29×10^{-3}
	1.18	--	11.12×10^{-3}	3.18×10^{-3}
	1.32	--	--	6.23×10^{-3}
	FEM	4.11×10^{-3}	3.81×10^{-3}	3.47×10^{-3}



- After forming, the formed gear may be cooled in a sand-graphite bath to room temperature. During this period, the magnitude of the gear dimensions decreases.

A heat transfer analysis during forming and subsequent cooling must be done to compensate for the changes in the gear dimensions. The temperature distribution during the forming cycle can be determined using the finite differencing technique. Using a computer program developed for this, the temperatures at the various parts of the die and the billet could be determined. From these values, the individual contraction/expansion of the various points in the billet and die could be computed. In the present approach however, an average change of die and billet temperature is computed from the heat transfer analysis - correction for the temperature changes is, therefore, uniform for all points in the billet and die. The reasons for making this approximation are:

- The forging cycle is very short (a few milliseconds). During this time, the gear is also restricted from expanding by the die and causes additional elastic deflection of the press frame. Hence, variations in temperature changes cannot be compensated for exactly.
- Some machining may have to be done on the gear tooth (based on the available technology to produce dies with the required surface finish and accuracy). Machining allowance also will take care of some of the errors introduced in the chosen approach.

The die cavity should be made larger to accommodate the higher temperature billet and the heated die.

4.1. Temperature Effects on the Die

The steady state temperature of the die during forming has been estimated using a one-dimensional, coaxial cylinder heat transfer analysis (12). Figure B-10 shows the heat transfer model of the die assembly and an electrical analog used in this analysis to compute the bulk shrinkage of the formed gear due to temperature effects.

4.2. Ambient Temperature Effects

Another important aspect of the effect of temperature on the die design is the cooling of the forged/extruded gear from forming temperature to ambient temperature. Due to differential cooling of the gear at various sections, distortion of the gear tooth could result. No special correction factors have been assumed for distortions. Controlled cooling procedures (cooling in a sand-

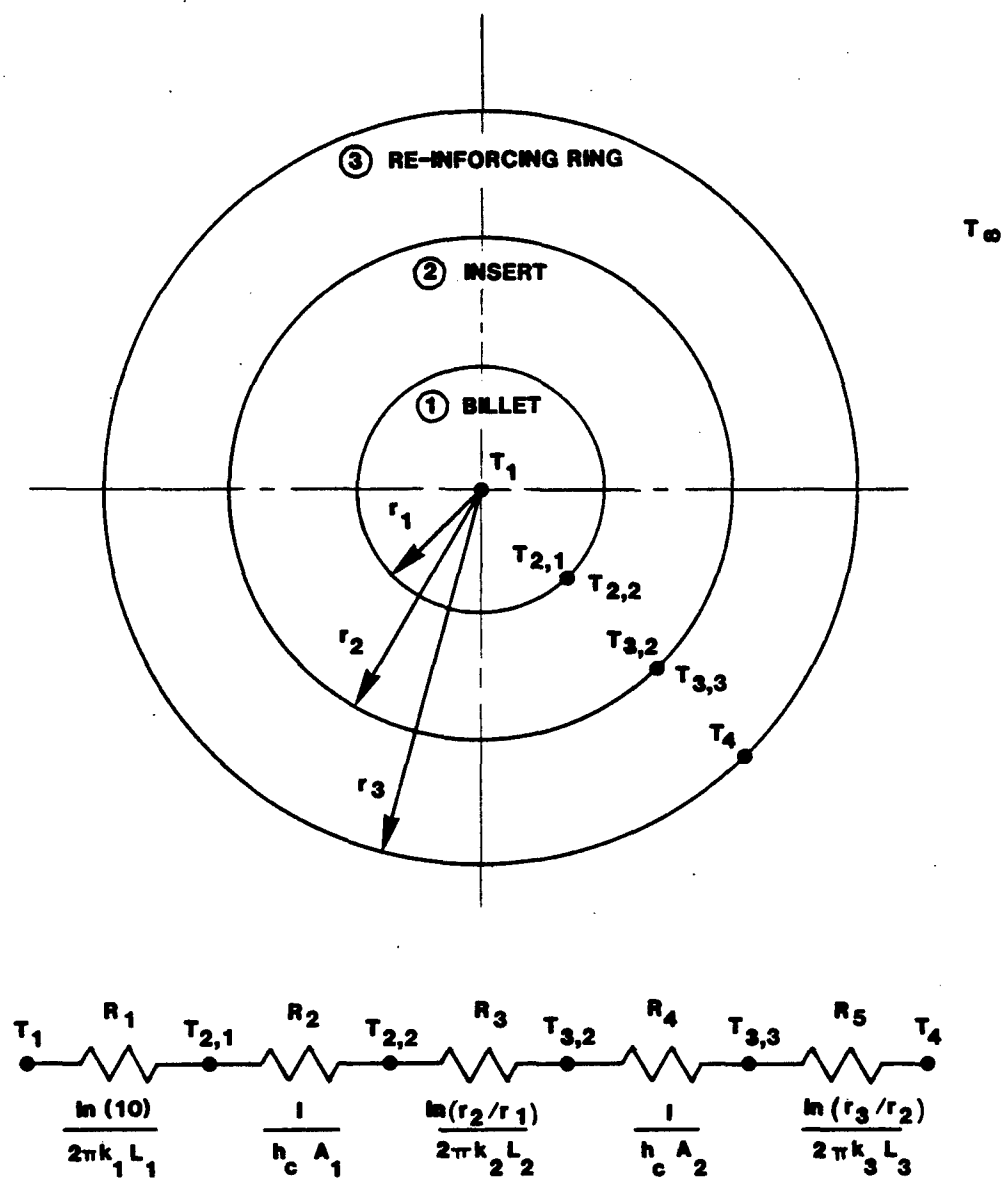


FIGURE B-10. Coaxial Cylinder Heat Transfer Model of Spur/Helical Gear Tooling (symbols explained in text)

graphite mixture for example) will be used during trials.

5.0 BULK SHRINKAGE DUE TO SHRINK FIT ASSEMBLY

The second aspect of bulk shrinkage is the change of inner die dimensions due to shrink-fitting of the die assembly. These should also be compensated for to achieve the desired dimensions on the finished gear. A simple solution based on thick circular cylinders under internal pressure has been used to compute the changes on the inner diameter of the die assembly.

5.1. Definition of the State of Stress

Figure B-11 shows a model of the tool assembly used to compute the amount of shrinkage in the gear insert due to the interference fit. The stress distributions in the die under external and internal pressures are shown in Figure B-12. Since the ends of the die are free, a plane stress condition can be assumed. During shrink fitting, the inner radius of the outer ring increases by u_2 and the outer radius of the insert decreases by u_1 (refer to Figure B-13). In order to model the interference fit, it was assumed that the inner cylinder was subject to an external pressure p^* and the outer cylinder to an internal pressure of p^* . This interference pressure p^* will cause a change, u_a , at the inner radius of the insert. A quantitative stress distribution due to shrink fitting is shown in Figure B-14.

The quantity, $\sigma_\theta - \sigma_r$ at the inner radius of the insert is critical for no yielding of the insert due to internal pressure. This criterion is widely used to design such assemblies; the interference radius, the outer ring, outer radius and the interference are computed using the strength properties of the inner and outer ring materials and the internal pressure to be transmitted. Some of the interference may be lost due to machining tolerances on the inner and outer ring common radii. With the known value of this interference, the change in the insert inner radius can be computed and used in correcting the die geometry.

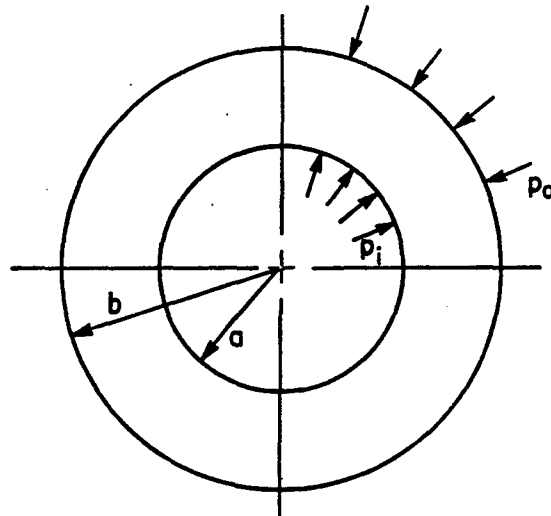


FIGURE B-11. Die Under Internal and External Pressure (symbols explained in text)

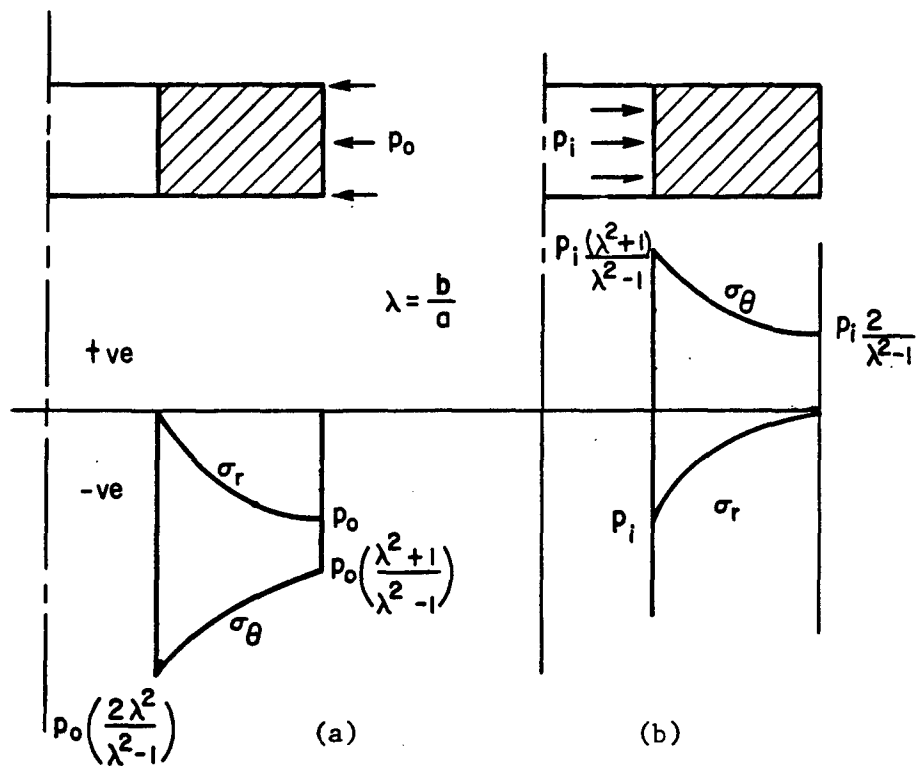


FIGURE B-12. Stress Distribution in Die Under a) External, and b) Internal Pressures (symbols explained in text)

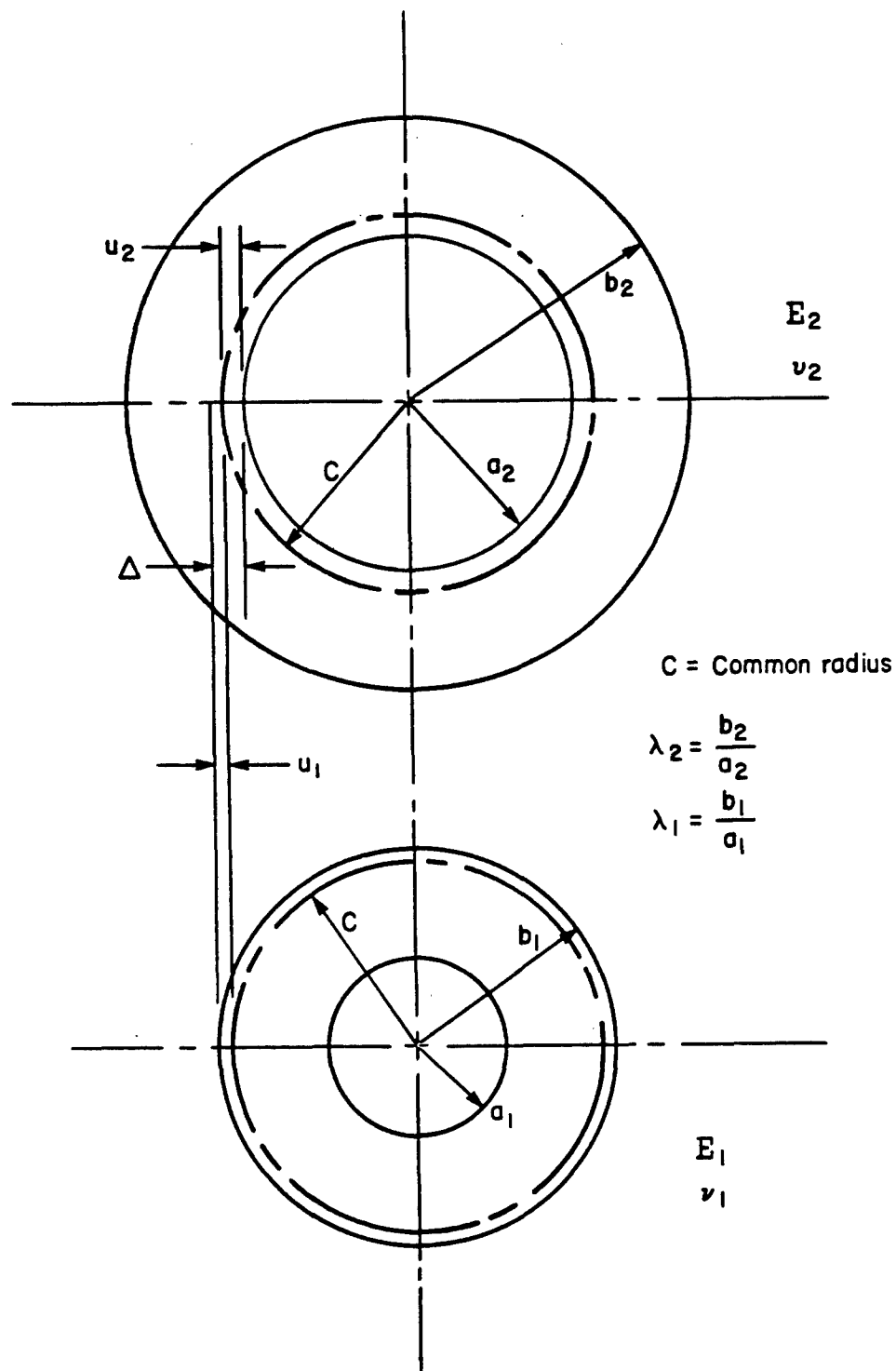


FIGURE B-13. Change of Outer Radius of the Insert and Inner Radius of the Outer Ring Due to Shrink Fitting (symbols explained in text)

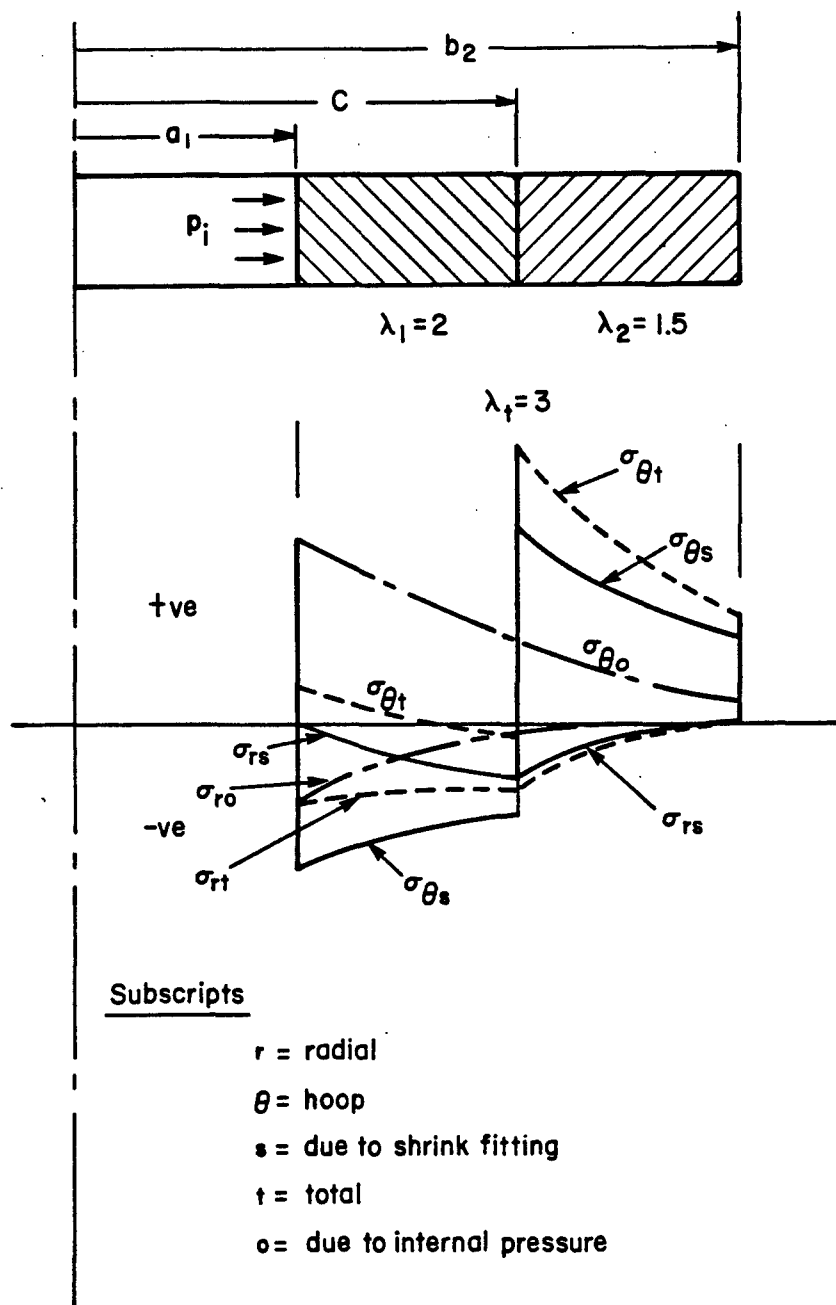


FIGURE B-14. Stress Distributions in a Shrink-Fit Die Assembly (symbols explained in text)

THIS PAGE LEFT BLANK INTENTIONALLY

LIST OF REFERENCES

- (1) Lange, K., Text Book of Metal Forming (in German), Vol. 1, Springer Verlag, 1973.
- (2) Thomsen, E. G., Yang, C. T., and Kobayashi, S., Mechanics of Plastic Deformation in Metal Processing, The MacMillan Company, New York, 1965.
- (3) Johne, P., "Flashless Closed Die Forging in Dies Without Provision for Excess Material Flow" (in German), Doctoral Dissertation, Technical University of Hanover, 1969.
- (4) Oh, S. I., Lahoti, G. D., and Altan, T., "Application of a Rigid-Plastic Finite Element Method to Some Metal Forming Operations," to be published in ASM Journal.
- (5) "Flow Stress of Steel-Iron for Material 40 NiMoCr (En 25)" (in German), VDEh Research Institute, 12 pages.
- (6) Karima, M. and Lahoti, G. D., Unpublished Study, Battelle Memorial Institute, 1981.
- (7) Mages, W., "Advantageous Application of Recent Metal Forming Processes for Gear and Drive Manufacture" (in German), VDI-Reports 332, 1979, pp. 97-106.
- (8) Bronstein, I. N. and Somendjajew, K. A., Handbook of Mathematics (in German), BSB B. G. Teubner Verlagsgesellschaft, Leipzig, East Germany, 1969.
- (9) Charmouard, A., Closed Die Forging (in French), Vol. 1, Dunod, Paris, 1964.
- (10) Raghupathi, P. S., Unpublished Study, Battelle Memorial Institute, 1982.
- (11) Boresi, A. P. et. al., Advanced Mechanics of Materials, 3rd ed., University of Illinois, Urbana-Champaign, Illinois, 1978.
- (12) Holman, J. P., Heat Transfer, McGraw-Hill Book Company, New York, 1976.

THIS PAGE LEFT BLANK INTENTIONALLY

APPENDIX C

SPUR GEAR FORGING LOAD ESTIMATION USING THE FINITE ELEMENT METHOD

THIS PAGE LEFT BLANK INTENTIONALLY

1.0. INTRODUCTION*

In precision spur gear forging, the teeth forming operation is performed so that no finish machining on the teeth is required after forming. An accurate estimation of forging load is important because of the large loads required to fill the gear tooth cavity, which could cause machine over-loading, extensive die wear, and premature die failure. In particular, the filling of the gear tooth tip corner is critical because of functional requirements of the gear and because the maximum loading occurs at this stage.

2.0. METHOD OF ANALYSIS

2.1. Geometry

Metal flow and loading after the workpiece touches the gear top land and during the tooth tip corner filling were simulated using ALPID (1), a rigid-viscoplastic FEM program. Figure C-1 shows the assumed initial gear tooth configuration. Previous studies have been conducted to investigate the workpiece profile before this stage for dies similar to the spur gear tooth cavity (2). This provided an approximation for the workpiece initial geometry. Although this forging operation is three-dimensional in nature, the simulation used a two-dimensional model and assumed that the forging operation could be approximated by a plane strain process. The simulation continued until the workpiece had completely filled the die cavity. The method used in the present study is based on a rigid-viscoplastic formulation. It is an extension of the rigid-plastic finite element method, developed by Lee and Kobayashi (3).

The details of the present method are discussed in earlier publications by Oh, Rebelo, and Kobayashi (4) and by Oh (5).

2.2. Model Material

A rigid-viscoplastic material is an idealization of an actual material, by neglecting the elastic response. The material shows the dependence of flow stress on strain rate in addition to the total strain and temperature. It can sustain a finite load without

*Work described in this Appendix was conducted at Battelle under the direction of Mr. Jeff Ficke.

Numbers in parentheses refer to references at the end of the appendix

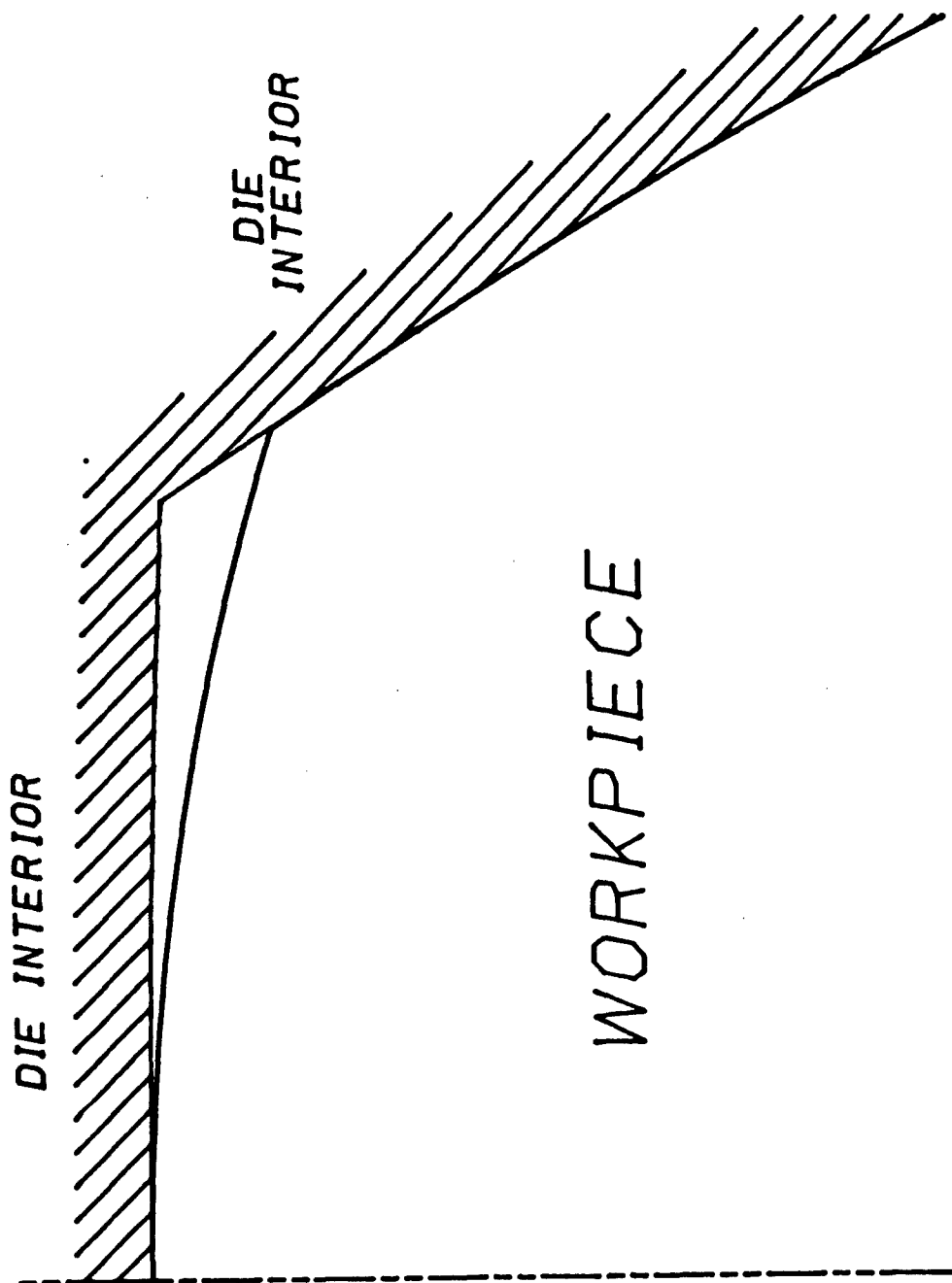


FIGURE C-1. Assumed Initial Workpiece-die Configuration at the Gear Tooth Corner

deformation. The rigid-viscoplastic material was introduced in this study for analytical convenience. It simplifies the solution process with a less demanding computational procedure. Moreover, the idealization offers excellent solution accuracies due to the negligible effects of elastic response at large strains in the actual material.

2.2. Mathematics

2.2.1. Constitutive Equation. The constitutive equation during forming is represented by;

$$\sigma_{ij} = \frac{2}{3} \cdot \frac{\bar{\sigma}}{\dot{\bar{\epsilon}}} \cdot \dot{\epsilon}_{ij} , \quad (C-1)$$

where;

σ_{ij} = deviatoric stress component,
 $\dot{\epsilon}_{ij} = 1/2 * (V_{i,j} + V_{m,i})$; strain rate component,
 V = velocity component,
 $\dot{}$ = differentiation,
 $\bar{\sigma}$ = effective stress,
 $\dot{\bar{\epsilon}}$ = effective strain rate.

2.2.2. Effective Stress. The effective stress, $\bar{\sigma}$, in general, is a function of total strain and strain rate and is expressed as;

$$\bar{\sigma} = \bar{\sigma}(\bar{\epsilon}, \dot{\bar{\epsilon}}, T) , \quad (C-2)$$

where;

$\bar{\epsilon}$ = effective strain,
 T = temperature.

In the case of rigid-plastic formulation, $\bar{\sigma}$ becomes a function of the total effective strain only.

2.2.3. Variational Principle Functional. The variational principle functional for the rigid-viscoplastic material can be written as;

$$\Phi = \int E(\dot{\bar{\epsilon}}) \cdot dv - \int \underline{F} \cdot \underline{V}^* \cdot dS + \int \frac{1}{2} \cdot K \cdot (\dot{\epsilon}_{kk})^2 \cdot dv , \quad (C-3)$$

where;

$E(\dot{\bar{\epsilon}})$ = work function; (integral of the effective stress with respect to the effective strain rate),
 v = volume,
 F = force,
 V = velocity,
 S = surface,

K = large positive constant which penalizes the
dilation strain rate component,
 $\dot{\epsilon}_{kk}$ = dilation strain rate component.

It can readily be shown that the mean stress is $\sigma_m = K \cdot \dot{\epsilon}_{kk}$. The above functional reduces to that of a rigid-plastic material if $\bar{\sigma}$ is a function of $\bar{\epsilon}$ only.

2.2.4. Velocity Solution. The velocity solution obtained by minimizing Equation (C-3) is the instantaneous solution. The geometry of the workpiece and the strain values can be updated by;

$$\begin{aligned} X_I^{(m)} &= X_I^{(m-1)} + \dot{U}_I^{(m)} \cdot \Delta t, \\ \bar{\epsilon}_J^{(m)} &= \bar{\epsilon}_J^{(m+1)} + \dot{\bar{\epsilon}}^{(m)} \cdot \Delta t, \end{aligned} \quad (C-4)$$

where;

X_I = coordinate of the I-th node,
 \dot{U}_I = velocity of the I-th node,
 $\bar{\epsilon}_J$ = effective strain at the J-th element
 Δt = time increment during which the deformation can be approximated as linear.

2.3. Solution Procedure for a Spur Gear Tooth Forging Process

2.3.1. Problem Statement. The spur gear simulated had 14 teeth with a diametral pitch of 5.921. The gear outside diameter and inside diameter were 2.634 in. (66.9 mm) and 1.375 in. (34.925 mm), respectively.

2.3.2. Modeling of the Gear Tooth. Due to symmetry and in order to reduce computational costs, only one-half of one gear tooth was considered for the simulation. The die cavity and initial FEM mesh are shown in Figure C-2. The gear tooth die profile was approximated by a series of 15 points on the involute profile. These points ranged from the gear top land to the dedendum with the highest concentration on the large curvature regions. The points were connected using straight line segments to complete the outer die definition.

2.3.3. Initial Configuration. As shown in Figure C-2, the simulation started from the point when the upper profile of the workpiece just contacted the top land of the gear. Metal flow from a tubular preform to this stage was not simulated, so the workpiece shape before this stage was approximated using empirical formulas (2).

2.3.4. Empirical Model. The model for the empirical representation of the tooth geometry is shown in Figure C-3. This

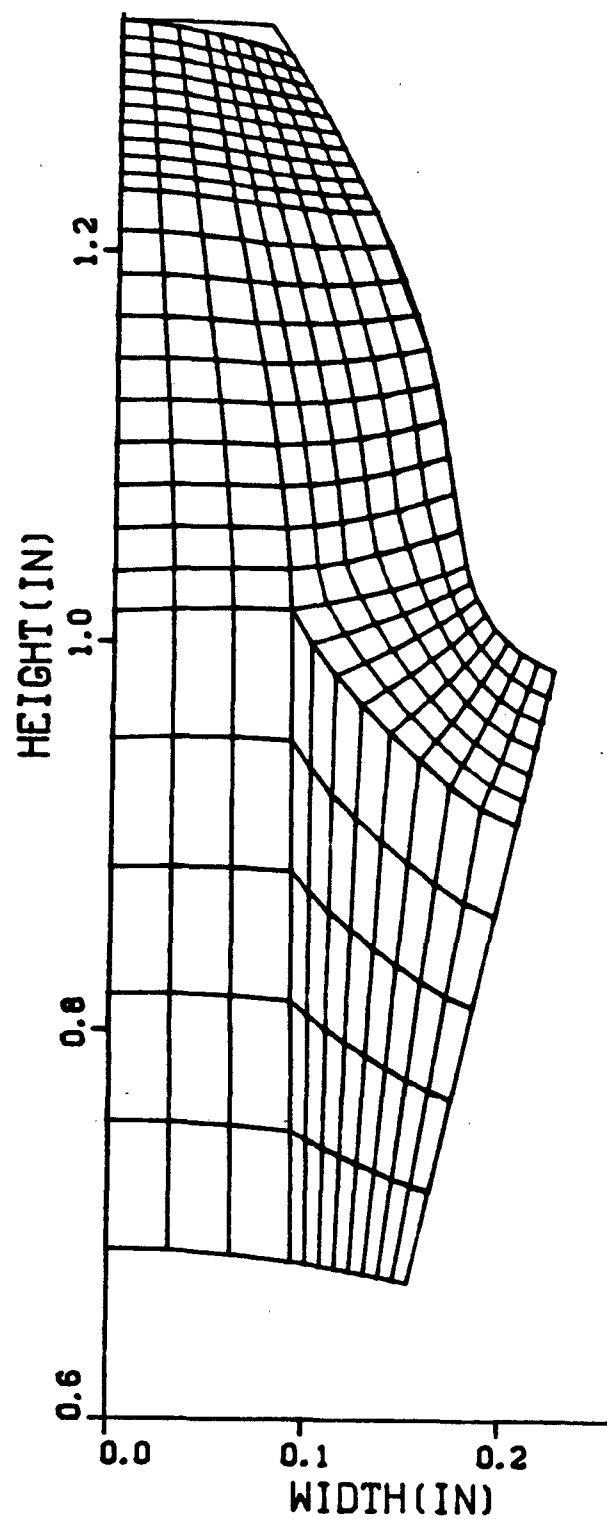


FIGURE C-2. Initial Mesh Used for Metal Flow Simulation in Gear Cavity

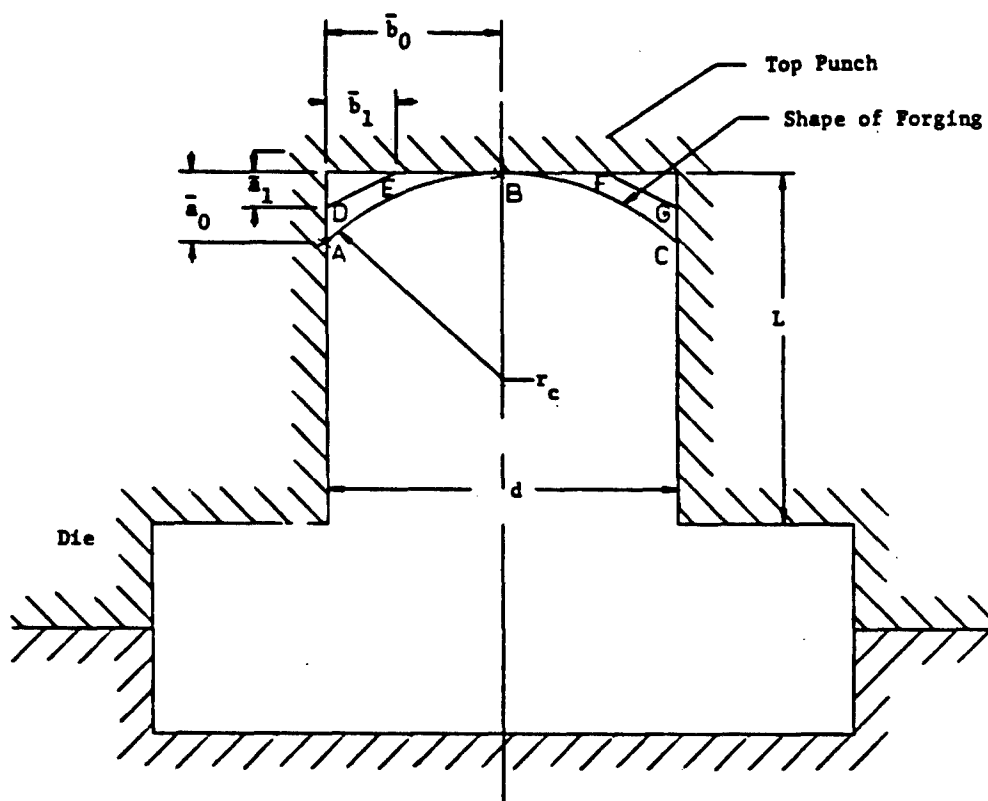


FIGURE C-3. Schematics of the Metal Flow During Corner Filling

simplified model assumes a constant wall thickness and represents the initial profile in terms of two parameters; A_0 and R_c . A_0 represents the difference between material flow along the central axis and the die surface. Hence, the value of A_0 is dependent on metal flow parameters such as friction and temperature. A_0 was selected for the simulation using the following equation;

$$A_0 = k \cdot d, \quad (C-5)$$

where;

$$\begin{aligned} d &= \text{tooth thickness,} \\ k &= 0.067 \text{ to } 0.1. \end{aligned}$$

The constant k depends on the friction factor. For low frictional conditions, the lower constant (0.067) is used, while for high frictional conditions the higher value (0.10) applies. The value of k ranges between the two extremes depending on the friction factor selected. R_c represents the radius of a particle sphere passing through the die surfaces a distance A_0 from the top land and contacting the top land at the center of the tooth tip. In terms of A_0 and d , defined above, the equation for R_c is given by;

$$R_c = (d^2/4 + A_0^2)/(2 \cdot A_0). \quad (C-6)$$

Since the spur gear tooth thickness is not constant, the process of solving for the values of A_0 and R_c is iterative. Using the thickness as the convergence variable, a friction shear factor of $m = 0.08$, and, because of the low frictional constant, k equal to 0.067, the solution converged to the initial workpiece profile geometry of;

$$\begin{aligned} A_0 &= 0.01072 \text{ in.}, \\ R_c &= 0.322 \text{ in.} \end{aligned}$$

2.3.5. Mesh Generation. The finite element mesh was generated (using an automatic mesh generator) with a large concentration of elements in the regions that were anticipated to come into contact with the outer die cavity. It can be seen in Figure C-3 that the element spacing was the smallest near the unfilled corner. This provided for proper representation of the tight corner radius. Displacement boundary conditions were placed on the left and right straight edges of the mesh to prevent material movement over these axes of symmetry.

2.3.6. Material Representation. The simulation was carried out using a nearly perfectly plastic material flow stress representation as follows;

$$\bar{\sigma} = 1 \cdot \epsilon^{0.03}. \quad (C-7)$$

A plot of this flow stress curve compared to a perfectly plastic representation is shown in Figure C-4. This flow stress behavior was selected over the perfectly plastic representation because it provided a smoother flow stress curve which aided in the solution convergence while introducing only a small error into the material representation.

2.3.7. Inner Die Modeling. The inner die radial pressure was simulated by providing the 12 nodal points along the inner diameter with a unit velocity boundary condition in the radial direction. The magnitude of the nodal velocity does not affect the simulation results because it was assumed that the material was highly rate-insensitive.

3.0. RESULTS AND DISCUSSIONS

The simulation was carried out until all free nodal points defining the unfilled corner contacted the gear tooth die cavity. This was accomplished in a step-by-step manner in which the step size was controlled so that the solution was updated each time a new node contacted the die cavity. The solution was completed in seven steps with a total inner die nodal point movement of 0.003 inch in the radial direction.

3.1. Grid Distortion Plots

Grid distortion plots generated for simulation steps 0, 2, 4, and 6 are shown in Figure C-5. There was a small amount of grid distortion during the final filling process. Also, at this stage of the forming process, a very small movement of the inner die caused a relatively large amount of metal flow into the unfilled corner.

3.2. Load Estimation

The load estimation for the corner filling of the gear tooth was predicted by the simulation. The load values predicted by ALPID are "normalized" loads because the material flow stress representation was assumed to be nearly perfectly plastic. This load can be considered as the actual load divided by the material yield stress at the appropriate location on the flow stress curve. The radial pressure predicted by ALPID, which is the load divided by the inner surface area, is plotted in Figure C-6. The inner die surface area, assuming a unit thickness, is equal to the inner die arc length. The radial pressure is plotted against the contact length of workpiece material with the gear top land, measured from the tooth centerline. In addition to the load and metal flow characteristics predicted by ALPID, the program also predicted

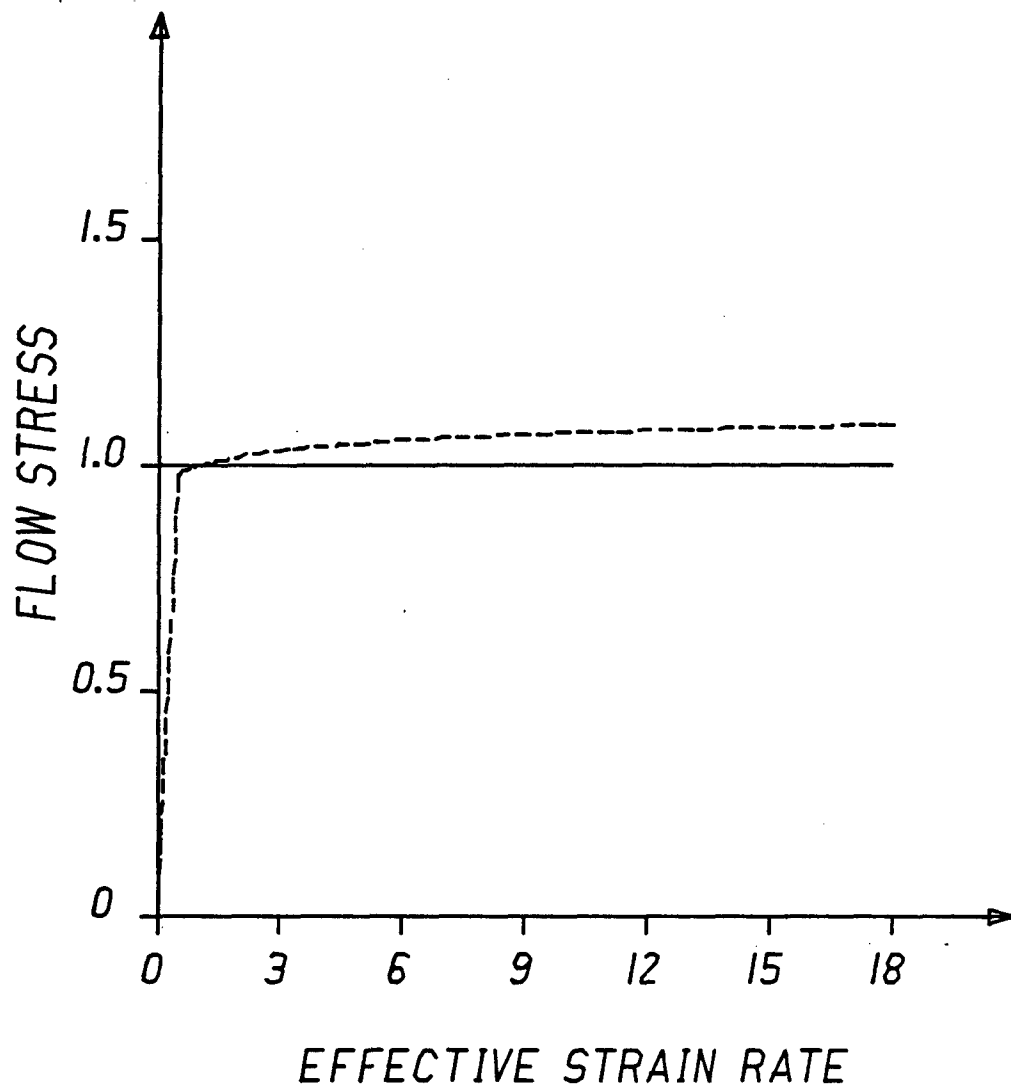
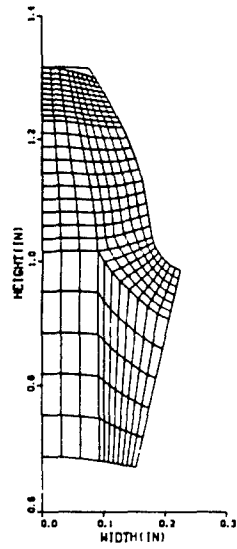
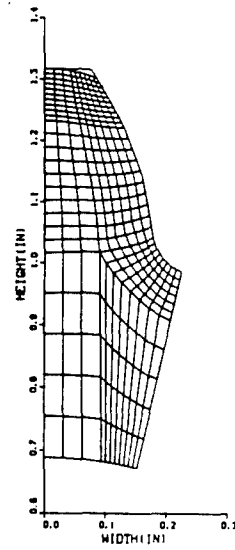


FIGURE C-4. Flow Stress Behavior for Perfectly Plastic Material (Solid Line) and Nearly Perfectly Plastic Material (Dashed Line)

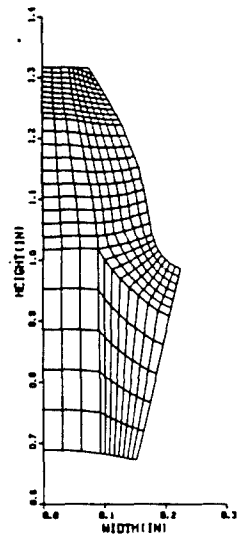
GEAR TOOTH FILLING STEP #0



GEAR CORNER FILLING STEP #2



GEAR CORNER FILLING STEP #4



GEAR CORNER FILLING STEP #6

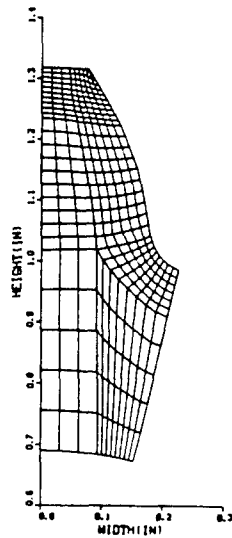


FIGURE C-5. Finite Element Metal Flow Simulation Steps for Gear Tooth Corner Filling

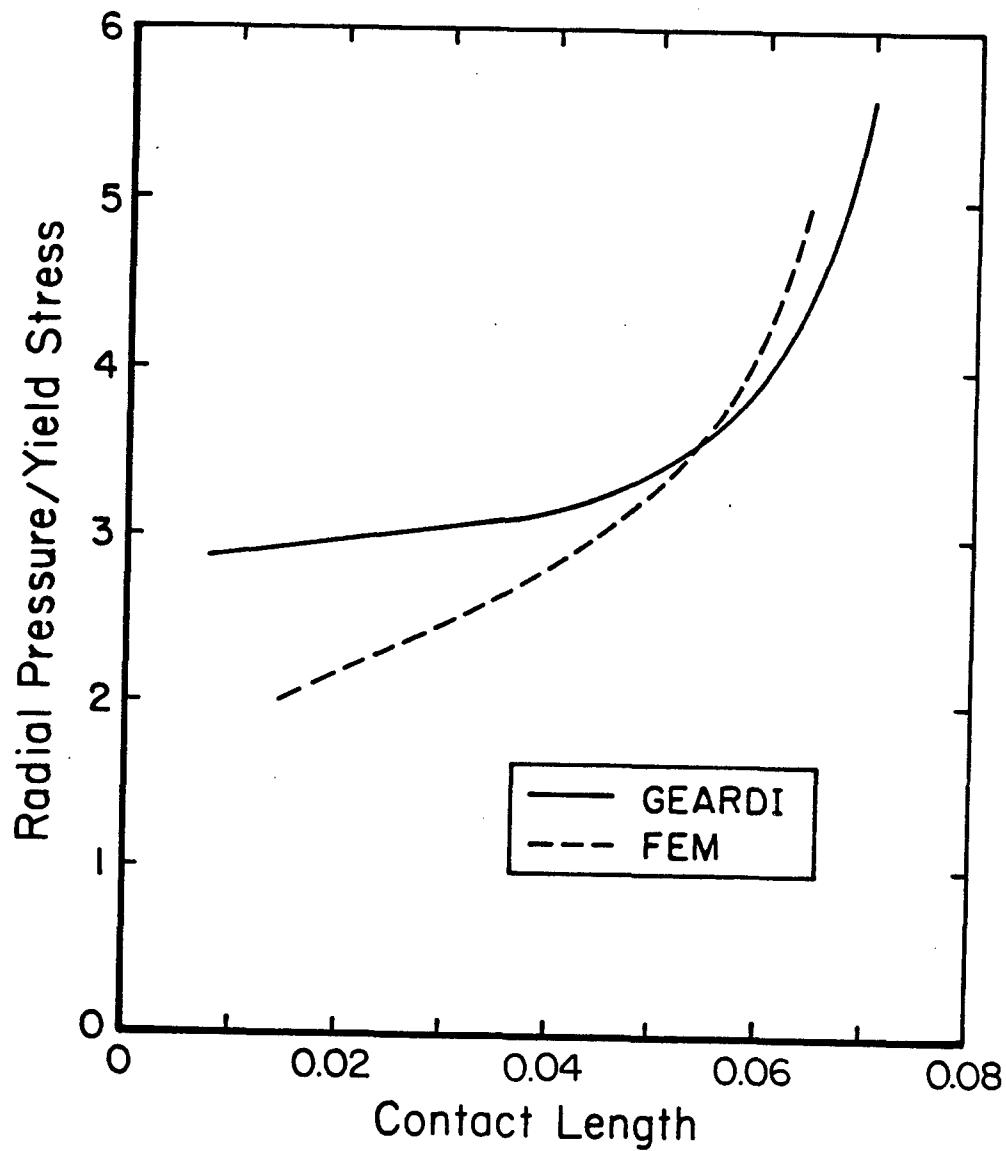


FIGURE C-6. Inner Die Radial Pressure vs. Contact Length of Workpiece on the Gear Top Land

local information about stress, strain, and velocity distribution. The effective strain rate values averaged between 5 and 10 1/sec. Using this average value, the maximum error entered into the calculations because of the smoothing of the flow stress curve was estimated at between 5 and 7 percent. This is compared with the perfectly plastic material behavior ($\bar{\sigma} = 1.0$).

4.0. CONCLUSIONS

The spur gear tooth corner filling simulation has been analyzed. Using empirical relationships to approximate workpiece shape and profile before the material contacted the gear top land, metal flow was simulated by FEM until the material had filled the die cavity. The analysis showed that with a small displacement of the inner radius (three-one-thousands of an inch in the radial direction), the gear tooth corner filled.

Metal flow was limited because of the small amount of material movement that was required. Excluding the material close to the tooth corner being filled, the finite element grid did not distort extensively.

The inner die pressure required to fill the gear predicted by ALPID was computed by assuming a 2-D plane strain deformation condition. Hence, the load and pressure values predicted are the radial pressure required to deform the gear assuming the pressure is in the transverse plane of the gear.

LIST OF REFERENCES

- (1) Oh, S. I., Lahoti, G. D., and Altan, T., "ALPID - A General Purpose FEM Program for Metal Forming," Proc. of NAMRC-IX, May 1981, State College, PA, p. 83.
- (2) Johne, P., "Flashless Closed Die Forging in Dies Without Provision for Excess Material Flow" (in German), Doctoral Dissertation, Technical University of Hannover, 1969.
- (3) Lee, C. H. and Kobayashi, S., "New Solutions to Rigid-Plastic Deformation Problems Using a Matrix Method," Trans. ASME, J. of Engr. for Ind., Vol. 95, 1973, p. 865.
- (4) Oh, S. I., Rebelo, N., and Kobayashi, S., "Finite Element Formulation for the Analysis of Plastic Deformation of Rate-Sensitive Materials for Metals Forming," Metal Forming Plasticity, IUTAM Symposium, Tutzing, Germany, 1978, p. 273.
- (5) Oh, S. I., "Finite Element Analysis of Metal Forming Problems with Arbitrarily Shaped Dies," Int. J. of Mech. Sci., 24, p. 479.
- (6) Oh, S. I., "Finite Element Analysis of Metal Forming Problems with Arbitrarily Shaped Dies," Int. J. of Mech. Sci., Vol. 17, p. 293, 1982.

THIS PAGE LEFT BLANK INTENTIONALLY

APPENDIX D

RESULTS OF THE PROJECT AS APPLIED TO SAMPLE GEARS

THIS PAGE LEFT BLANK INTENTIONALLY

1.0. INTRODUCTION

The computer-aided design/computer-aided manufacturing (CAD/CAM) software developed for this project is contained in the GEARDI program. The program can be used to design a wide variety of spur and helical gears and the tools needed to extrude or forge them. To demonstrate the full range of capabilities of this program, a step by step procedure which was used to design a sample helical gear extrusion die and a spur gear forging die and punch will be explained in detail. Figures are included wherever a new page is displayed on the computer terminal screen.

2.0. HELICAL GEAR EXAMPLE PROBLEM STATEMENT

This particular example deals with the design of an extrusion die for the manufacturing of a helical gear which is cut on a gear hobbing machine. The only information available was the original gear drawing. The particular hob which was used to cut the gear was not known nor were any of the hob dimensions known. The gear material was AISI-1016 with an annual production requirement of 20,000 parts. The only forming equipment available was a 500 ton mechanical press which had a maximum stroke of 10.0 inches and a maximum speed of 50 strokes per minute.

2.1. Program Execution

The first step in solving this design problem using the GEARDI was to type "RUN GEARDI" after logging on to the computer.

2.1.2. Geometry Input. Next, the program required that the user enter the known geometrical parameters. Figure D-1 shows the appearance of the first page of the design session at the computer terminal. The gear tooth generation method had to be chosen from among six options as described in Appendix A. The user now had to input all of the gear geometrical parameters as requested by the program (Figure D-2). Upon completion of the data input, the user was allowed to check any of the previously entered data and change it as necessary. When the data was being checked, the screen was cleared and all of the gear geometrical parameters were re-displayed on the screen for reference during the change routine (Figure D-3).

2.1.3. Tooth drawing. On the next page of the program, the gear tooth profile was drawn in both the transverse and normal planes with the transverse plane always having the widest of the two profiles (Figure D-4).

PROGRAM GEARDI - DESIGN OF SPUR/HELICAL GEAR FORGING DIES	
<pre> FILE INPUT(Y/N). N INPUT TITLE (50 MAX): HELICAL GEAR EXAMPLE DATA INPUT: SPECIFY GEAR TOOTH GENERATION METHOD 1. HOB GENERATION, ROUNDED CORNER 2. PSEUDO-HOB GENERATION, ROUNDED CORNER 3. HOB GENERATION, TIP PROTUBERANCE 4. SHAPER GENERATION, SHARP CORNER 5. SHAPER GENERATION, FULL-ROUNDED TIP 6. MATING GEAR PLUS OPERATING CONDITIONS SELECT: 2 </pre>	1

FIGURE D-1. Helical Gear Example; Title and Generation Method Specification

PROGRAM GEARDI - DESIGN OF SPUR/HELICAL GEAR FORGING DIES	
HELICAL GEAR EXAMPLE	
PSEUDO-HOB GENERATION, ROUNDED CORNER	

NUMBER OF GEAR TEETH	- 18
GEAR TRV DIAMETRAL PITCH	- 6
HELIX ANGLE	- 15.672
OUTSIDE DIAMETER OF GEAR (D)	- 3.333
GEAR TRV PRESSURE ANGLE (D)	- 20.705
GEAR DEPENDUM (D)	- 208
GEAR TRV TOOTH THICK (D)	- .262
DESIRE TIP RELIEF(Y/N), N	
DESIRE CHAMFER(Y/N), N	
DESIRE SHAVING STOCK(Y/N), N	
MEASURING PIN DIAM. (D)	- 0.275
CHECK DATA(Y/N), Y	

FIGURE D-2. Helical Gear Example; Geometry Input

PROGRAM GEARDI - DESIGN OF SPUR/HELICAL GEAR FORGING DIES		
HELICAL GEAR EXAMPLE		
PSEUDO-HOB GENERATION - ROUND CORNER		
	TRANSVERSE	NORMAL
1. NUMBER OF GEAR TEETH	18	
2. GEAR DIAMETRAL PITCH	6.00000	6.23167
3. HELIX ANGLE	15.67200	
4. OUTSIDE DIAMETER OF GEAR	3.33300	
5. GEAR PRESSURE ANGLE	20.70500	19.99730
6. PSEUDO-HOB TOOTH CRMR RAD		0.05000
7. GEAR ADDENDUM	0.16650	0.16650
8. GEAR DEDENDUM	0.20800	0.20800
9. GEAR TOOTH THICKNESS	0.26200	0.25226
10. TIP RELIEF DEPTH	0.00000	0.00000
11. TIP RELIEF ARC-LENGTH	0.00000	0.00000
12. CHAMFER DEPTH	0.00000	0.00000
13. CHAMFER ARC-LENGTH	0.00000	0.00000
14. SHAVING STOCK	0.00000	
15. MEASURING PIN DIAMETER	0.27500	
GEAR PITCH RADIUS	1.50000	
GEAR ROOT RADIUS	1.29200	
GEAR BASE RADIUS	1.40312	
GEAR CIRCULAR PITCH	0.48978	0.47374
GEAR TOOTH THICKNESS	0.52360	0.50413
TIP TOOTH THICKNESS	0.26200	0.25226
MEASUREMENT OVER PINS	0.11000	0.10591
GEAR AXIAL AREA (NO HOLE)	3.37641	
HELICAL LEAD	0.00000	
AXIAL PITCH	33.59272	
GEAR EQUIV NO. OF TEETH	1.86626	
	20.16656	
***WARNING - UNDERCUT CONDITION EXISTS**		
ANY DATA INCORRECTLY/W/3: N		

FIGURE D-3. Helical Gear Example; Data Echo

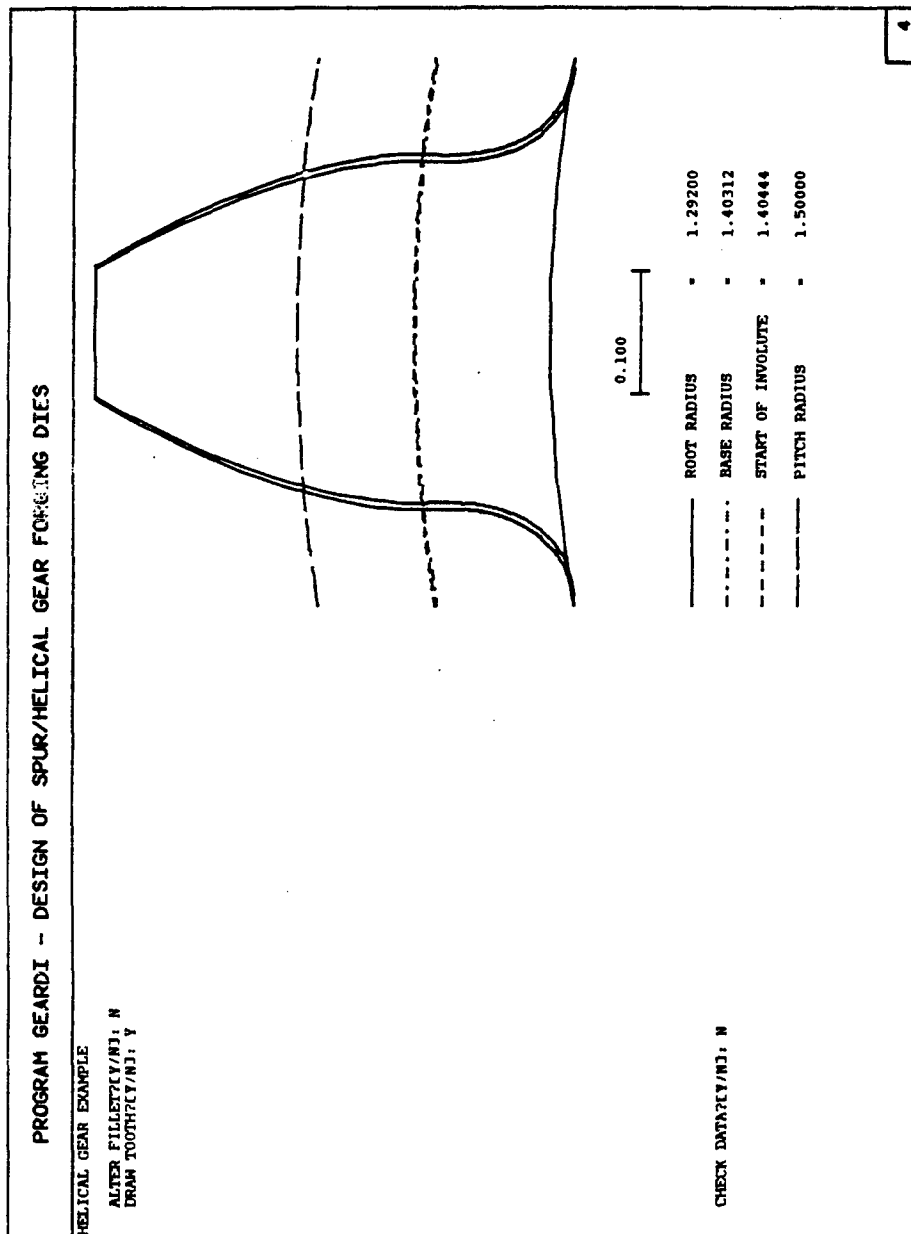


FIGURE D-4. Helical Gear Example; Tooth Profile Display

2.1.4. Gear drawing. The following program page (Figure D-5) shows the entire gear (user requested) which allowed for an additional visual check of the gear geometry. At this point, the user could have decided to eliminate the forming analysis in which the forces, loads, and deflections in forging or extrusion tooling would be calculated. In this example, the user decided to conduct a forming analysis.

2.1.5. Forming parameter inputs. The forming analysis parameters for the cold extrusion process were typed into the program as shown in Figure D-6.

2.1.6. Checking of forming parameters. The next program page (Figure D-7) re-displayed the forming parameters and the assigned default values. At the completion of the forming analysis, four values were displayed:

- the maximum limiting value for the flow stress of the selected material (based on room temperature),
- the ratio of the punch pressure to the maximum flow stress for the defined process,
- the maximum punch pressure, and
- the punch force.

Remembering that the available forming equipment consists of a 500 ton mechanical press, the user decided to make a change in the forming parameters since the computed punch force of 559 tons exceeded the press capacity.

2.1.7. Change of parameters. On the next program page, as shown in Figure D-8, the user selected the third forming parameter to be changed in an effort to lower the required tonnage for extrusion of the chosen gear.

2.1.8. Display of new gear forming parameters. Figure D-9 shows the new gear forming parameters as displayed by the program along with the results of the forming analysis conducted using the new values. These results indicated that the punch force of 443 tons was within the limits of the available mechanical press.

2.2. Output Display.

2.2.1. Original and corrected geometries. Proceeding from the forming analysis, the computer displayed the gear geometrical parameters and also the original gear tooth profile along with the corrected geometry based on the deflections computed in the forming analysis (Figure D-10).

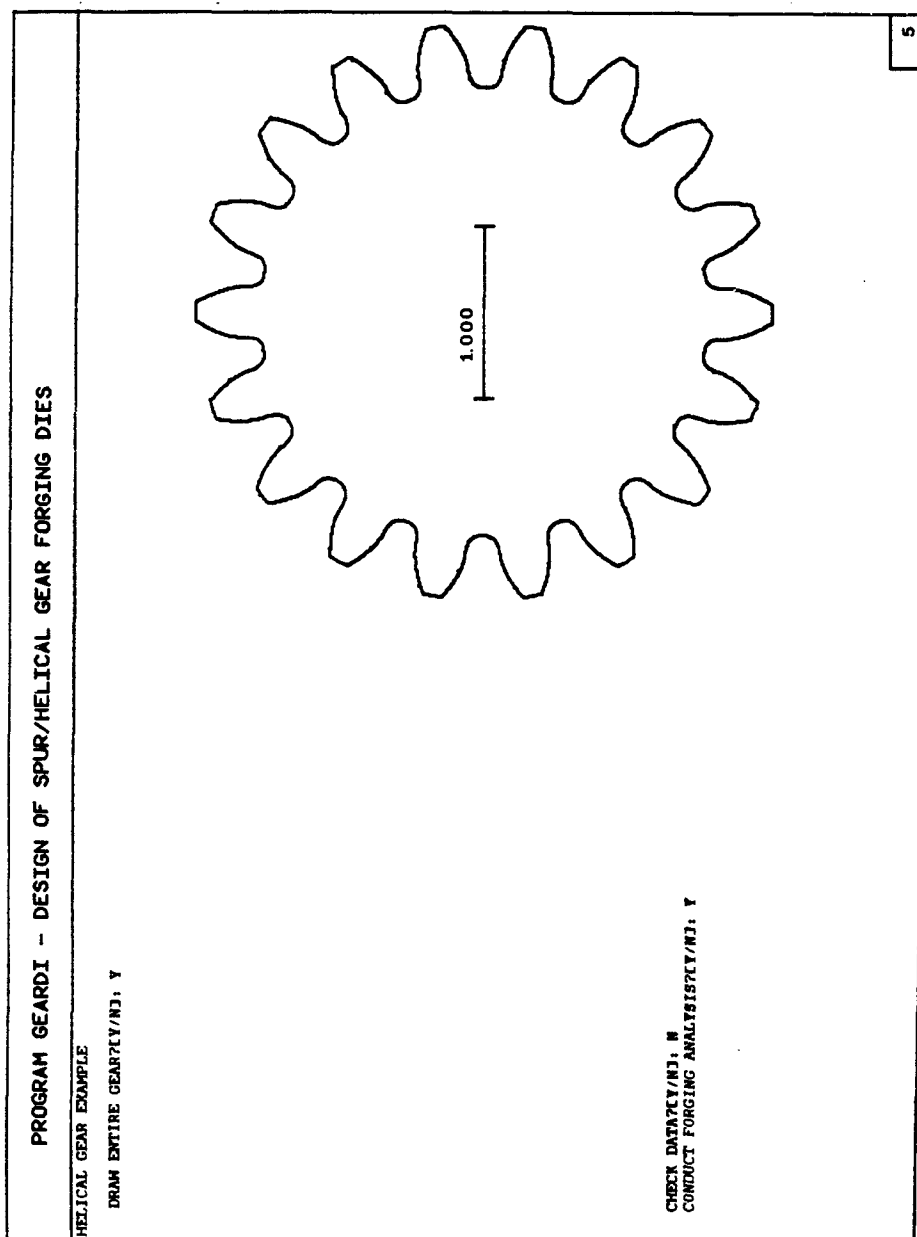


FIGURE D-5. Helical Gear Example; Entire Gear Display

PROGRAM GEARDI - DESIGN OF SPUR/HELICAL GEAR FORGING DIES	
HELICAL GEAR EXAMPLE	
STRESS CALCULATIONS; DATA INPUT	
FORGING OR EXTRUSION? (F/E), E	
COLD VS. WARM FORGING? (C/H), C	
DIE ANGLE (DEGREES)	= 50.
BILLET OUTSIDE DIAMETER (DI)	= 3.4
BILLET INSIDE DIAMETER	= 0.
FINISHED GEAR THICKNESS	= 1.4
FRICTION FACTOR (DI)	
PERCENT FILL DESIRED (DI)	
INITIAL YIELD STR (KSI) (DI)	
GEAR MATERIAL (EE, AS1016.DAT)	= AS1016.DAT
SHRINK FIT INTERFERENCE	= 0.0035

FIGURE D-6. Helical Gear Example; Input of Forming Data

PROGRAM GEARDI - DESIGN OF SPUR/HELICAL GEAR FORGING DIES	
HELICAL GEAR EXAMPLE	
STRESS CALCULATIONS: DATA CHECK	
1. COLD EXTRUSION/DIE ANGLE	= 50.00000
2. BILLET OUTSIDE DIAMETER	= 3.40000
3. BILLET INSIDE DIAMETER	= 0.00000
4. FINISHED GEAR THICKNESS	= 1.40000
5. FRICTION FACTOR	= 0.08000
6. INITIAL YLD STR (KSI)	= 0.00000
7. PERCENT FILE DESIRED	= 100.00000
8. GEAR MATERIAL	AS1016
9. SHRINK FIT INTERFERENCE	= 0.00350
INCORRECT DATA NO. (0-END):	
WARNING: INITIAL YIELD STRESS MUST BE < 20.56985	
PUNCH PRESSURE/AVE FLOW STRESS	= 1.48648
PUNCH PRESSURE (KSI)	= 123.44141
PUNCH FORCE (TONS)	= 560
CHANGE ANY FORMING PARAMETERS(Y/N): Y	

7

FIGURE D-7. Helical Gear Example; Forming Data Echo and Initial Solution

PROGRAM GEARDI - DESIGN OF SPUR/HELICAL GEAR FORGING DIES	
HELICAL GEAR EXAMPLE	
STRESS CALCULATIONS: DATA CHECK	
1. COLD EXTRUSION/DIE ANGLE	50.00000
2. BILLET OUTSIDE DIAMETER	3.40000
3. BILLET INSIDE DIAMETER	0.00000
4. FINISHED GEAR THICKNESS	1.40000
5. FRICTION FACTOR	0.08000
6. INITIAL YLD STR (KSI)	20.56985
7. PERCENT FILE DESIRED	100.00000
8. GEAR MATERIAL	AS1016
9. SHRINK FIT INTERFERENCE	0.00350
INCORRECT DATA NO. [0-END]: 3	
BILLET INSIDE DIAMETER	
INCORRECT DATA NO. [0-END]: 1.700	

FIGURE D-8. Helical Gear Example; Changing of Forming Parameters

PROGRAM GEARDI - DESIGN OF SPUR/HELICAL GEAR FORGING DIES	
HELICAL GEAR EXAMPLE	
STRESS CALCULATIONS: DATA CHECK	
1. COLD EXTRUSION/DIE ANGLE	= 50.00000
2. BILLET OUTSIDE DIAMETER	= 3.40000
3. BILLET INSIDE DIAMETER	= 1.70000
4. FINISHED GEAR THICKNESS	= 1.40000
5. FRICTION FACTOR	= 0.08000
6. INITIAL YLD STR (KSI)	= 20.56985
7. PERCENT FLE DESIRED	= 100.00000
8. GEAR MATERIAL	AS1016
9. SHRINK FIT INTERFERENCE	= 0.00350
INCORRECT DATA NO. 10-ENDDJ:	
WARNING: INITIAL YIELD STRESS MUST BE (20.56985	
PUNCH PRESSURE/AVE FLOW STRESS	= 1.57181
PUNCH PRESSURE (KSI)	= 130.52751
PUNCH FORCE (TONS)	= 444
CHANGE ANY FORMING PARAMETERS/INJ: N	
CHANGE PRODUCTION PERIOD/INJ: N	

FIGURE D-9. Helical Gear Example; Forming Data Echo and Results of Second Analysis

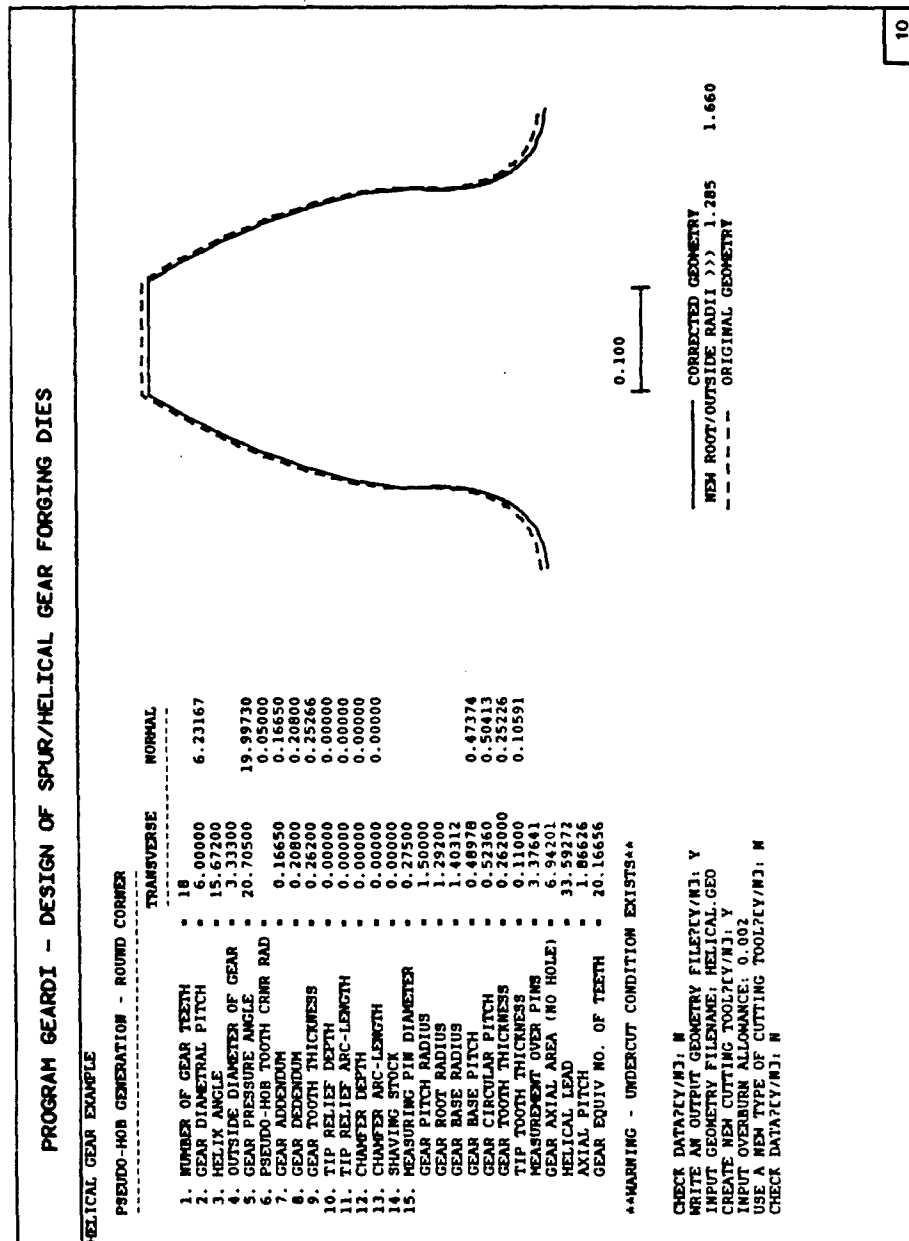


FIGURE D-10. Helical Gear Example; Original and Corrected Geometry Display

2.2.2. Fillet altering. Figure D-11 shows that the user was permitted to alter the fillet of the gear cut by the new cutting tool but this option was not chosen.

2.2.3. Display of corrected geometry and the geometry created by the new cutting tool. Both the corrected and new cutter geometries were displayed on the screen as shown in Figure D-12. The geometrical parameters printed to the left of the drawing corresponded to the new cutter and the gear generated by the new cutter. The location and magnitude of the maximum radial error was also displayed.

2.2.4. Creation of Electrical Discharge Machining (EDM) files. On the last program page for this example (Figure D-13) the user could have had the program write two data files which contain cartesian coordinates describing the entire circumferential geometry of the corrected die geometry and the geometry of a corresponding punch (to be used to burn the die and punch using the method of EDM). This option is explored completely in the following example.

3.0. SPUR GEAR EXAMPLE PROBLEM STATEMENT

The second example in this appendix deals with the design of a forging die for manufacturing a spur gear. The gear geometry was available from a blueprint but the design had not been used before. Hence, it was somewhat arbitrary as to whether a hob or shaper cutter generation method should have been used to cut the gear in a conventional manufacturing operation. The particular application in which this gear was to operate was known, as were the dimensions of the mating gear and the configuration of the two gears in relation to each other. So, the forging die was designed based on generation method number 6, mating gear/ operating conditions. Annual production requirements were not known but the type of forming equipment to be used was a 1,600 ton hydraulic press.

3.1. Spur Gear Example Program Results

3.1.1. Program Initialization. As in the first example and in all cases, the first step in any solution process is to specify the input geometry format (Figure D-14).

3.1.2. Geometry Input. Figure D-15 shows the process by which the gear geometry was entered for this case.

3.1.3. Checking of Data. The geometrical parameters previously input, were re-displayed as shown in Figure D-16. The clearance

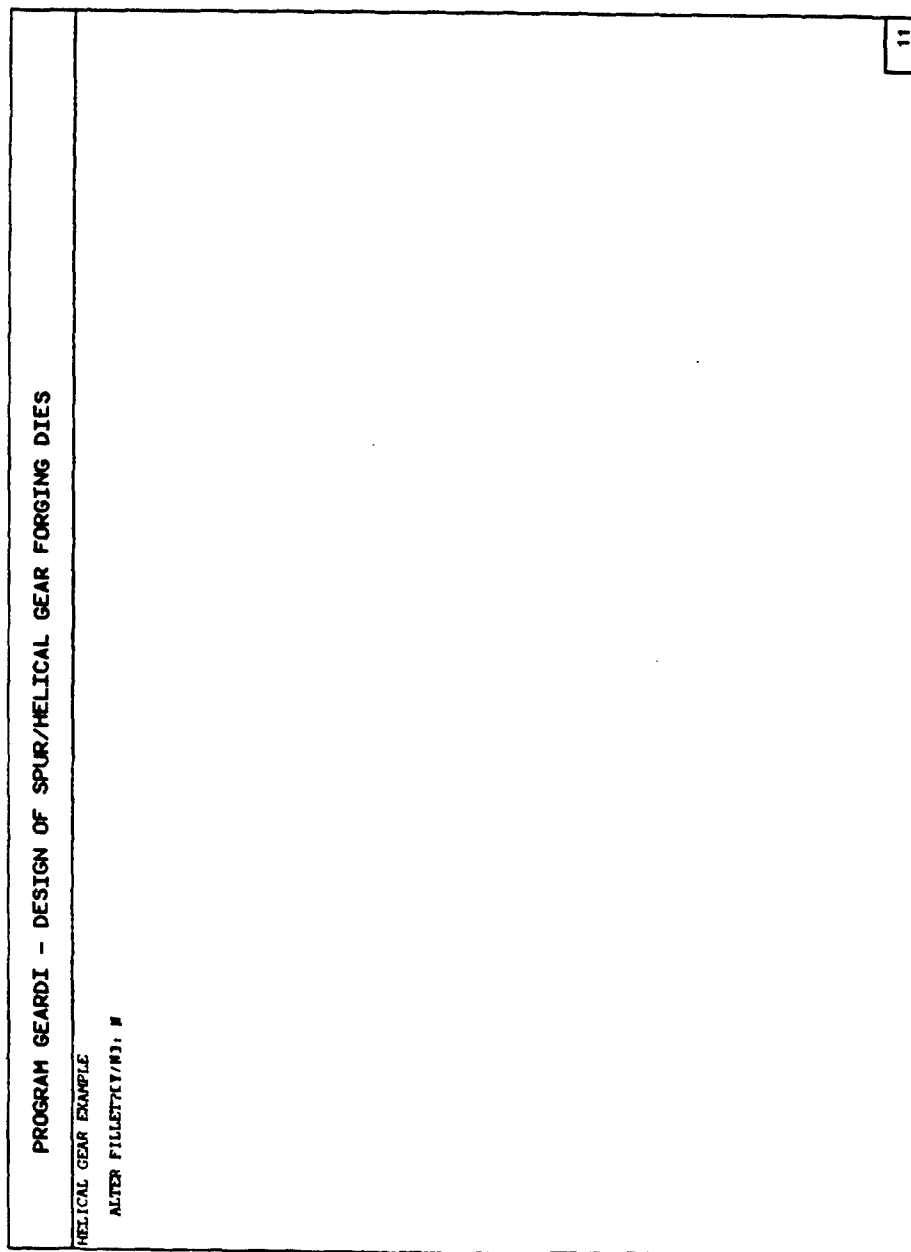


FIGURE D-11. Helical Gear Example; Fillet Alter Option During New Cutter Generation

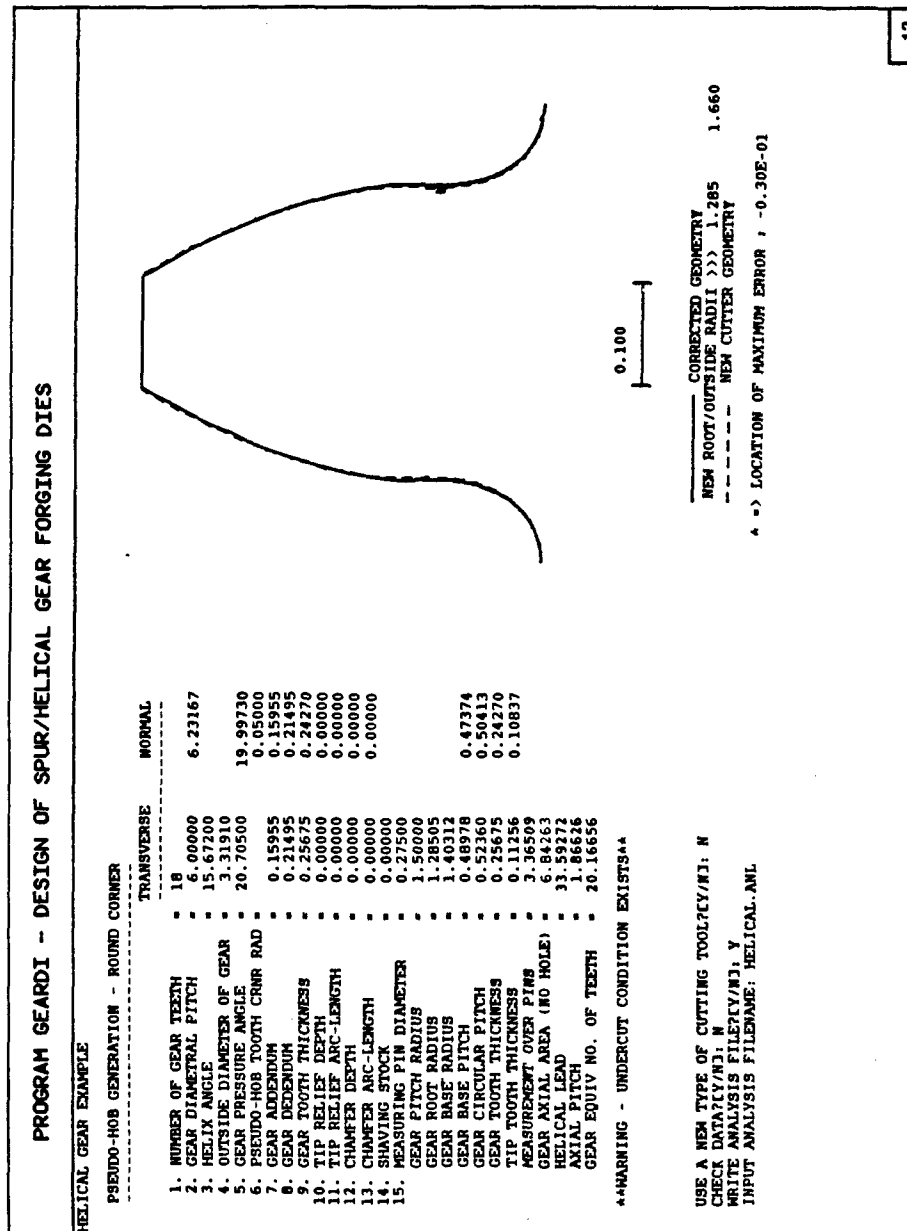


FIGURE D-12. Helical Gear Example; Display of Corrected and New Cutter Geometry

PROGRAM GEARDI - DESIGN OF SPUR/HELICAL GEAR FORGING DIES	<div data-bbox="419 446 447 1694">HELICAL GEAR EXAMPLE</div> <div data-bbox="447 446 1255 1694"> <p data-bbox="447 1388 497 1668">WRITE DIE EDM FILE7KV/N3; M WRITE PUNCH EDM FILE7LV/N3; M</p> </div>
---	--

13

FIGURE D-13. Helical Gear Example; EDM File Options

PROGRAM GEARDI - DESIGN OF SPUR/HELICAL GEAR FORGING DIES	
<pre> FILE INPUT(Y/N): N INPUT TITLE (50 MAX): SPUR GEAR EXAMPLE DATA INPUT: SPECIFY GEAR TOOTH GENERATION METHOD 1. ROB GENERATION, ROUNDED CORNER 2. PSEUDO-HOB GENERATION, ROUNDED CORNER 3. ROB GENERATION, TIP PROTRUSANCE 4. SHAPER GENERATION, SHARP CORNER 5. SHAPER GENERATION, FULL-ROUNDED TIP 6. MATING GEAR PLUS OPERATING CONDITIONS SELECT: 6 </pre>	1

FIGURE D-14. Spur Gear Example; Title and Generation Method Specification

PROGRAM GEARDI - DESIGN OF SPUR/HELICAL GEAR FORGING DIES	
SPUR GEAR EXAMPLE	
GIVEN MATING GEAR-OPERATING CONDITIONS ----- NUMBER OF GEAR TEETH * 15 NUMBER OF PINION TEETH * 16 TRANSVERSE DIAMETRAL PITCH * 5. HELIX ANGLE TRANSVERSE PRESSURE ANGLE (DJ) * 27.5 OUTSIDE DIAMETER OF GEAR (DJ) * 3.2 OUTSIDE DIAMETER OF PINN (DJ) * 3.5 AMOUNT OF BACKLASH (DJ) * 0.05 PINN TRV TOOTH THICK (DJ) * 0.31416 GEAR-PINION CENTER DIST. (DJ) * 3.1 DESIRE TIP RELIEF (Y/NJ): N DESIRE CHAMFER (Y/NJ): N DESIRE SHAVING STOCK (Y/NJ): N * 0.0 CLEARANCE (DJ) * 0.35 MEASURING PIN DIAMETER (DJ) CHECK DATA (Y/NJ): Y	
2	

FIGURE D-15. Spur Gear Example; Geometry Input

PROGRAM GEARDI - DESIGN OF SPUR/HELICAL GEAR FORGING DIES

SPUR GEAR EXAMPLE

GIVEN MATING GEAR-OPERATING CONDITIONS

INCORRECT DATA NO. [0-END]: 16
 CLEARANCE = 0.0
 INCORRECT DATA NO. [0-END]:

	TRANSVERSE	NORMAL
1. NUMBER OF GEAR TEETH	15	
2. NUMBER OF PINION TEETH	16	
3. GEAR DIAMETRAL PITCH	5.00000	5.00000
4. HELIX ANGLE	0.00000	
5. GEAR PRESSURE ANGLE	27.50000	27.50000
6. OUTSIDE DIAMETER OF GEAR	3.20000	
7. OUTSIDE DIAMETER OF PINN	3.50000	
8. AMOUNT OF BACKLASH	0.05000	
9. PINN TOOTH THICKNESS	0.31416	0.31416
10. GEAR-PINION CNTR DISTANCE	3.10000	
11. TIP RELIEF DEPTH	0.00000	0.00000
12. TIP RELIEF ARC-LENGTH	0.00000	0.00000
13. CHAMFER DEPTH	0.00000	0.00000
14. CHAMFER ARC-LENGTH	0.00000	0.00000
15. SHAVING STOCK	0.00000	
16. CLEARANCE	0.07000	
17. MEASURING PIN DIAMETER	0.35000	
GEAR PITCH RADIUS	1.50000	
GEAR ROOT RADIUS	1.28000	
GEAR BASE RADIUS	1.33052	0.55733
GEAR CIRCULAR PITCH	0.55733	0.62832
GEAR TOOTH THICKNESS	0.62832	0.26416
TIP TOOTH THICKNESS	0.26416	0.15874
MEASUREMENT OVER PINS	0.15874	
GEAR AXIAL AREA (NO HOLE)	3.39066	
	0.00000	

HARMING - UNDERCUT CONDITION EXISTS

ANY DATA INCORRECT?Y/N: Y

FIGURE D-16. Spur Gear Example; Data Echo and Data Change Sequence

was set to zero during the change sequence as shown in Figure D-16.

3.1.4. Geometry Check. On the next page of the program session, the user was once again asked if any data was to be changed and the user responded "N" (Figure D-17).

3.1.5. Altering of Fillet. At this point, the user was able to alter the fillet (Figure D-18) but this was not pursued. The gear tooth profile was then drawn in the transverse plane.

3.1.6. Drawing of Gear. As shown in Figure D-19 the entire gear was drawn.

3.1.7. Display of Corrected Geometry. The corrected geometry, which in this case was identical to the original geometry since no forming analysis was done, was displayed as shown in Figure D-20 along with the original geometry. A geometry file was specified which was read back into the program in the next step (see Figure D-21 and paragraph 3.1.13). The user chose to create a new cutting tool and also chose to use a new type of cutting tool. Figure D-21 shows the program sequence for specifying the FORM1.DAT data file as the new cutter geometry.

3.1.8. Altering of Fillet. In this example, the user initially used the default values for each of the four fillet altering parameters, as shown in Figure D-22.

3.1.9. Display of Original and New Fillet Geometries. Figure D-23 shows the new fillet geometry along with the geometry of the original fillet.

3.1.10. Checking of New Cutter Parameters. The new cutter parameters were displayed for checking by the user as shown in Figure D-24.

3.1.11. Display of New Fillet Parameters and Corresponding Geometry. Figure D-25 shows the new fillet parameters entered by the user. The geometry generated by this altered cutter was displayed (Figure D-26) along with the corrected geometry. An analysis file was written at the end of this program page.

3.1.12. Creation of Electrical Discharge Machining (EDM) Files. The next option available to the user was to create EDM files (Figure D-27) to cut the geometry generated by the new cutter. However, since no forming analysis had been done, this geometry was not correct. The program had to be run again using the new geometry and the altered fillet.

3.1.13. Input of Previously Created Data File. Figure D-28 shows

PROGRAM GEARDI - DESIGN OF SPUR/HELICAL GEAR FORGING DIES	
SPUR GEAR EXAMPLE	
CHECK DATA? Y/N: N	

FIGURE D-17. Spur Gear Example; Check Data Option

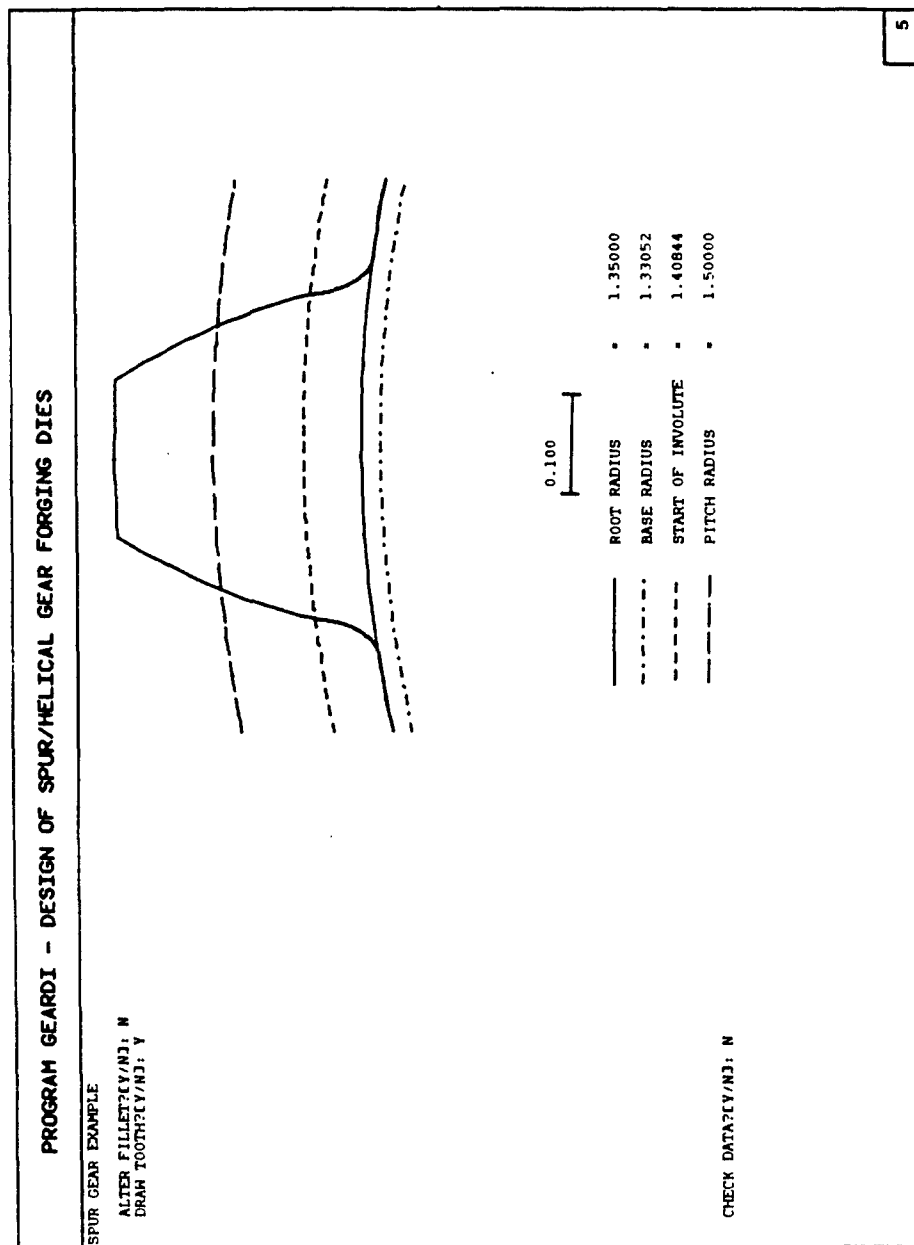


FIGURE D-18. Spur Gear Example; Drawing of Tooth Profile (path of mating gear)

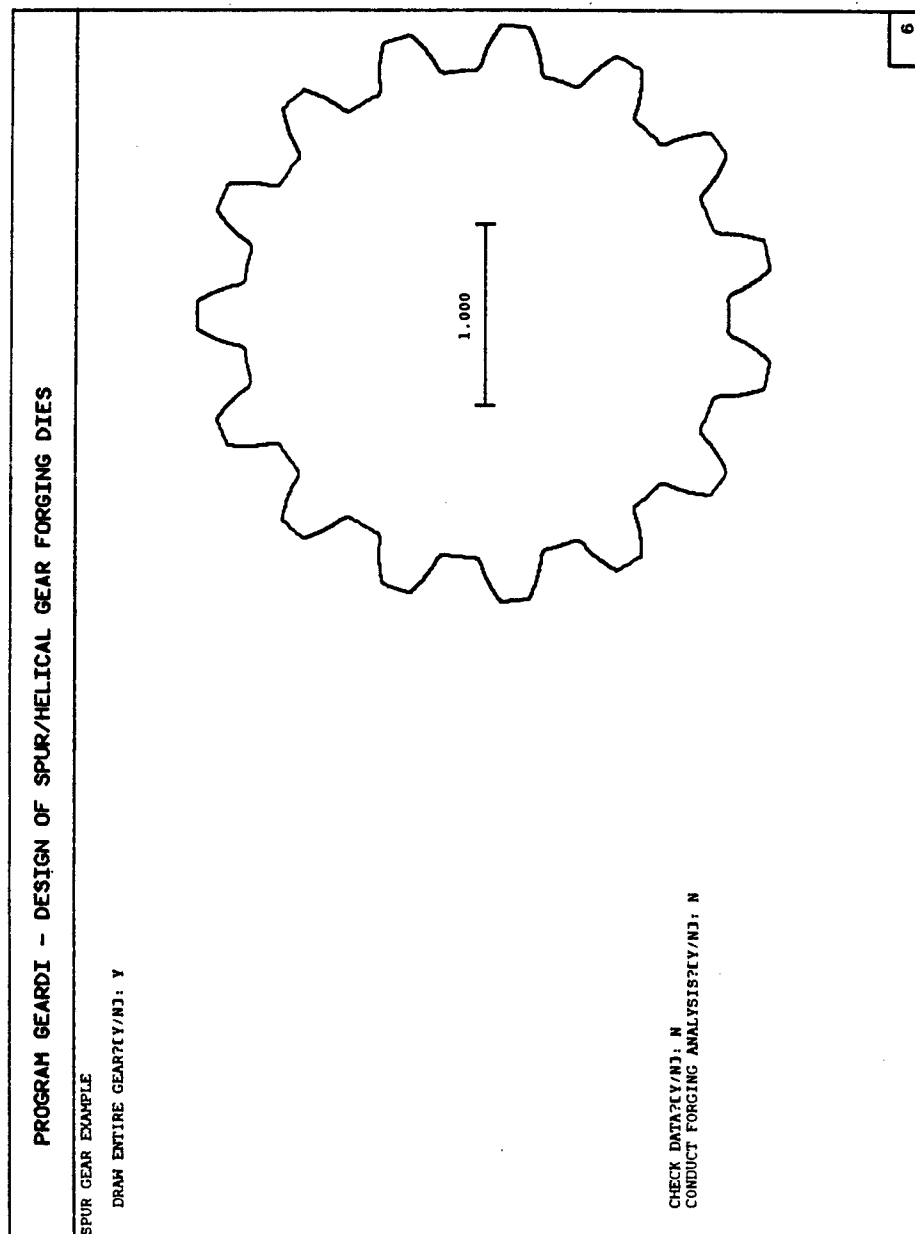


FIGURE D-19. Spur Gear Example; Entire Gear Form Using No Clearance on the Mating Gear

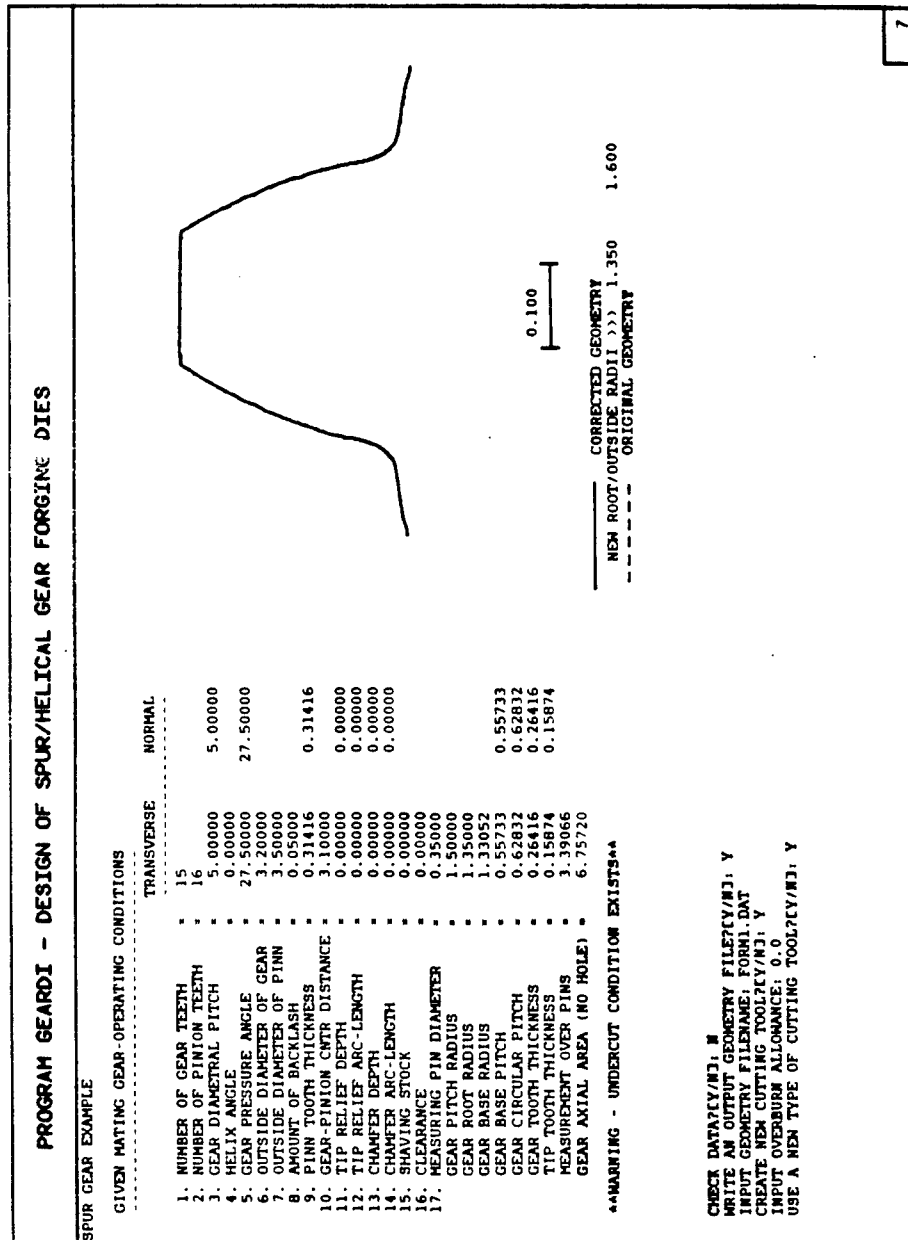


FIGURE D-20. Spur Gear Example; Display of Original and Corrected Tooth Geometries

PROGRAM GEARDI - DESIGN OF SPUR/HELICAL GEAR FORGING DIES	
SPUR GEAR EXAMPLE	<div> <div>FILE INPUT?/N1: Y</div> <div>INPUT GEOMETRY FILENAME: FORM1.DAT</div> <div>CHECK DATA?/N1: N</div> </div>

FIGURE D-21. Spur Gear Example; Specification of a New Cutting Tool

PROGRAM GEARDI - DESIGN OF SPUR/HELICAL GEAR FORGING DIES	
SPUR GEAR EXAMPLE	<p>ALTER FILLET(Y/N): Y</p> <p>ELLIPSE TRANSVERSE AXIS LENGTH (0.00000):</p> <p>ELLIPSE RADIAL AXIS LENGTH (0.00000):</p> <p>ELLIPSE OFFSET ANGLE (0.00000):</p> <p>CENTER LOCATION ABOVE OR BELOW (A/B): A</p>
9	

FIGURE D-22. Spur Gear Example; Initial Fillet Alteration Sequence

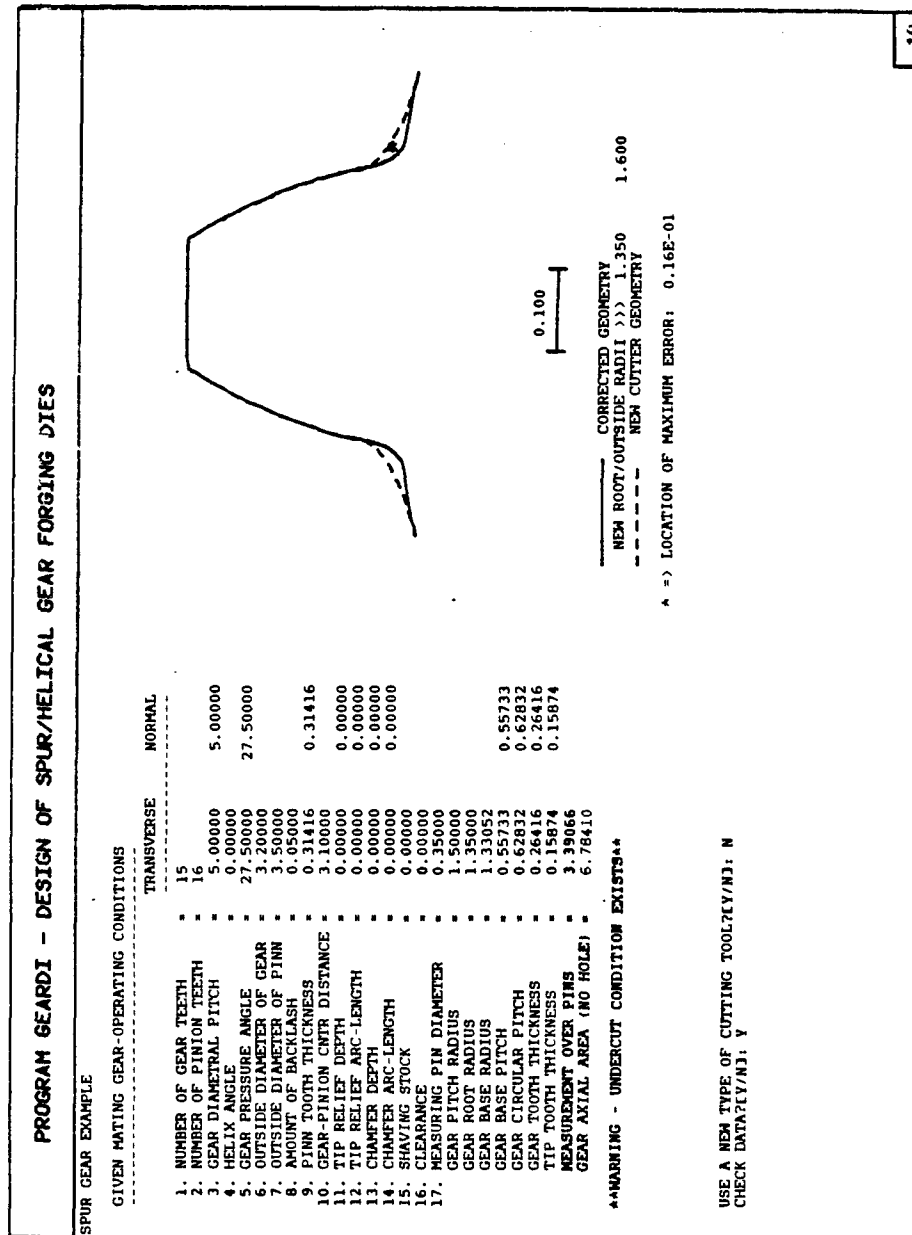


FIGURE D-23. Spur Gear Example; Corrected (Original) Geometry and New Cutter Geometry

PROGRAM GEARDI - DESIGN OF SPUR/HELICAL GEAR FORGING DIES

SPUR GEAR EXAMPLE

GIVEN MATING GEAR-OPERATING CONDITIONS

TRANSVERSE

NORMAL

INCORRECT DATA NO. [0-END]:

1. NUMBER OF GEAR TEETH - 15

2. NUMBER OF PINION TEETH - 16

3. GEAR DIAMETRAL PITCH - 5.00000

4. HELIX ANGLE - 0.00000

5. GEAR PRESSURE ANGLE - 27.50000

6. OUTSIDE DIAMETER OF GEAR - 3.50000

7. OUTSIDE DIAMETER OF PINN - 3.50000

8. AMOUNT OF BACKLASH - 0.00000

9. PINN TOOTH THICKNESS - 0.31416

10. GEAR-PINION CNTR DISTANCE - 3.1416

11. TIP RELIEF DEPTH - 0.00000

12. TIP RELIEF ARC-LENGTH - 0.00000

13. CHAMFER DEPTH - 0.00000

14. CHAMFER ARC-LENGTH - 0.00000

15. CHAMFER STOCK - 0.00000

16. MEASURING PIN DIAMETER - 0.00000

17. GEAR PITCH RADIUS - 1.50000

18. GEAR ROOT RADIUS - 1.35000

19. GEAR BASE RADIUS - 1.3052

20. GEAR CIRCULAR PITCH - 0.55733

21. GEAR TOOTH THICKNESS - 0.62832

22. TIP TOOTH THICKNESS - 0.26416

23. MEASUREMENT OVER PINS - 0.15874

24. GEAR AXIAL AREA (NO HOLE) - 3.39066

25. GEAR AXIAL AREA (NO HOLE) - 6.78410

11

WARNING - UNDERCUT CONDITION EXISTS
 ANY DATA INCORRECT(Y/N): Y

FIGURE D-24. Spur Gear Example; Data Check During New Cutter Creation

D-30

PROGRAM GEARDI - DESIGN OF SPUR/HELICAL GEAR FORGING DIES	
SPUR GEAR EXAMPLE	<div> <div>12</div> </div>
<p> ALTER FILLET? (Y/N): Y ELLIPSE TRANSVERSE AXIS LENGTH (0.13193): .15 ELLIPSE RADIAL AXIS LENGTH (0.05225): .2 ELLIPSE OFFSET ANGLE (0.00000): CENTER LOCATION ABOVE OR BELOW (A/B): A </p>	

FIGURE D-25. Spur Gear Example; Second Alteration of Fillet Geometry

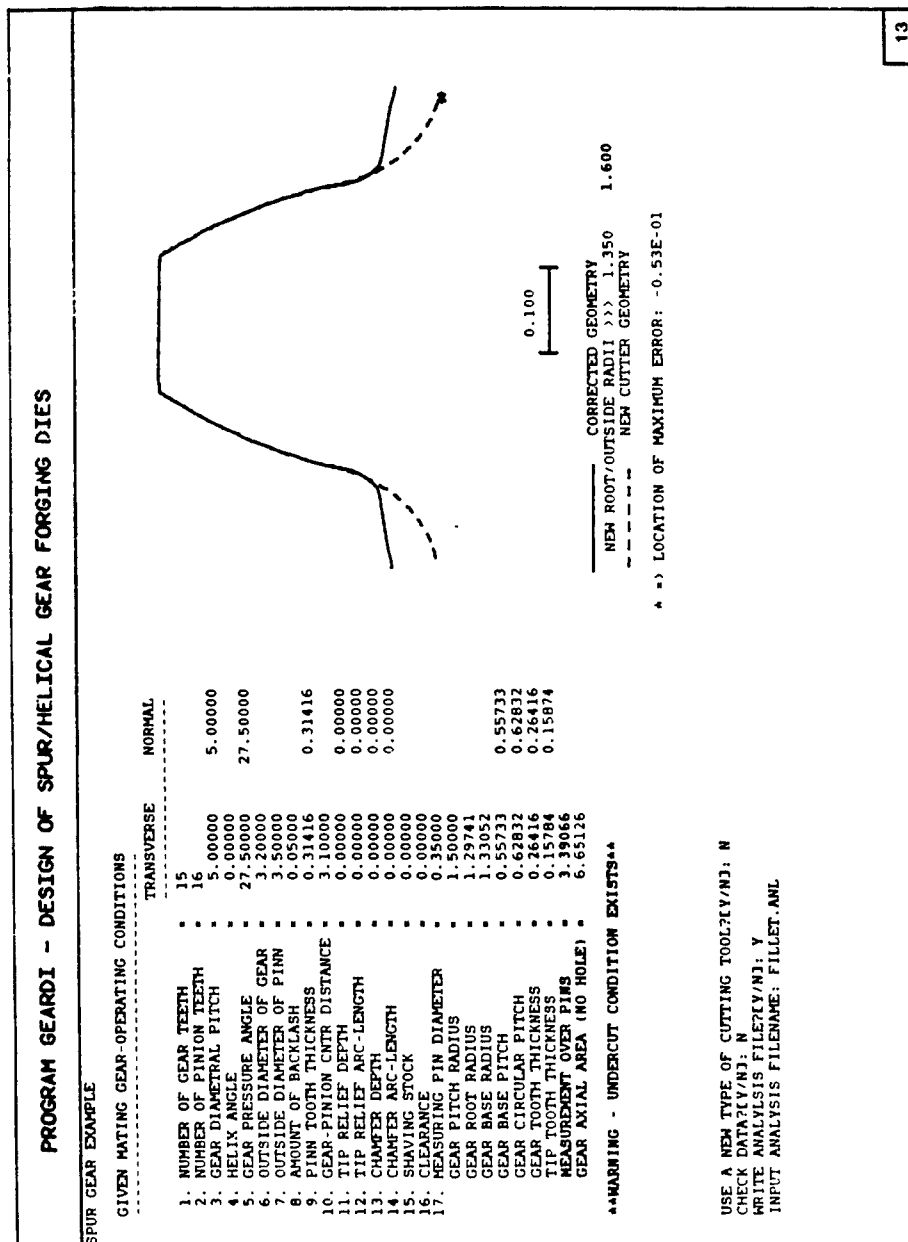


FIGURE D-26. Spur Gear Example; Second Display of New Cutter Geometry

PROGRAM GEARDI - DESIGN OF SPUR/HELICAL GEAR FORGING DIES	
SPUR GEAR EXAMPLE	
WRITE DIE EDM FILETY/NJ: N WRITE PUNCH EDM FILETY/NJ: N	

14

FIGURE D-27. Spur Gear Example; EDM Options

PROGRAM GEARDI - DESIGN OF SPUR/HELICAL GEAR FORGING DIES	
FILE INPUT?/N1: Y INPUT GEOMETRY FILENAME: FORM1.DAT CHECK DATA?/N1: N	1

FIGURE D-28. Spur Gear Example; Geometry Input Via Pre-Existing File

the sequence by which the user specified the name of the previously created data file (see paragraph 3.1.7).

3.1.14. Altering of Fillet. The fillet was altered in exactly the same fashion as in Figure D-25. The tooth was displayed (Figure D-29) just to make sure that the correct tooth form was in the memory of the program.

3.1.15. Drawing of Gear. In Figure D-30, the entire gear with the altered fillet was drawn. At this time, the user indicated that a forging analysis was to be conducted.

3.1.16. Input of Forming Parameters. Prior to the forming analysis, the user had to enter all of the forming parameters as shown in Figure D-31.

3.1.17. Results of Forming Analysis. On the next program page (Figure D-32), the forming parameters were echoed. In this example, the punch pressure was computed to be approximately 193 KSI. The user decided that the punch pressure could be slightly larger, so the choice was made to alter the forming parameters in an effort to improve the final forging geometry.

3.1.18. Changing of Forming Parameters. Figure D-33 shows the next page of the program session and the way in which the percent fill desired in the process was altered.

3.1.19. Results of New Forming Analysis. The new set of forming parameters along with the results of the second forging analysis were displayed on the terminal screen (Figure D-34).

3.1.20. Display of Corrected Tooth Profile. The next program page (Figure D-35) displayed all of the geometrical parameters relating to the design gear and the original and corrected tooth profiles.

3.1.21. Creation of Electrical Discharge Machining (EDM) Files. In Figure D-36, the user chose to have an EDM file created for manufacturing the forging die. On the same program page, the user chose to have an EDM file created for the forging punch (Figure D-37).

3.1.22. Comparison of Original Gear and Gear with Altered Fillet. Figure D-38 shows a comparison of the original gear and the gear with the altered fillet. Notice that the altered profile seems to extend into the tooth space. However, when the geometry was specified (Figure D-15), no clearance was given. The tooth form drawn in Figure D-18 was really the path of the mating gear which, as seen in Figure D-26, does not interfere with the altered fillet. The solid line of Figure D-38 shows the original gear

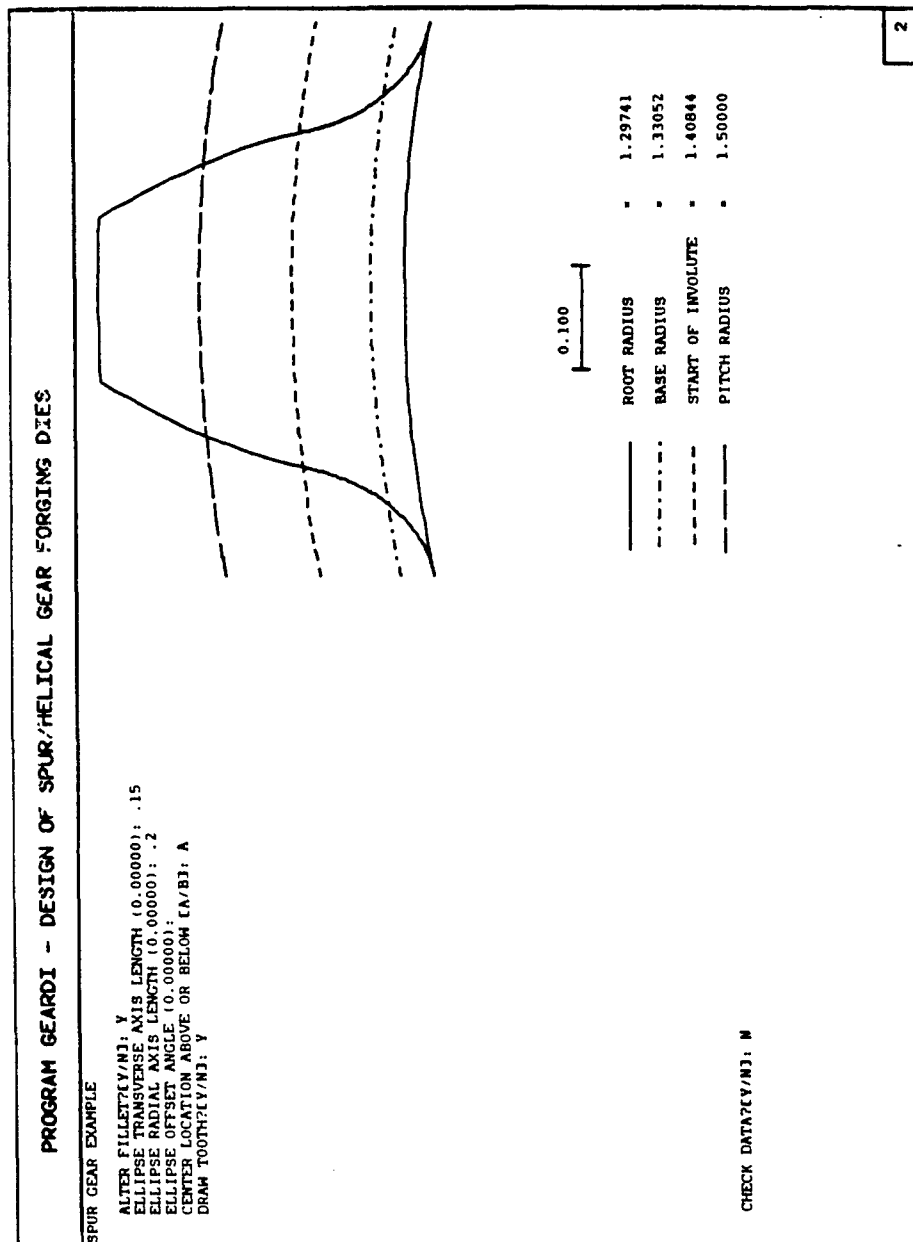


FIGURE D-29. Spur Gear Example; Display of Gear Tooth with Altered Fillet

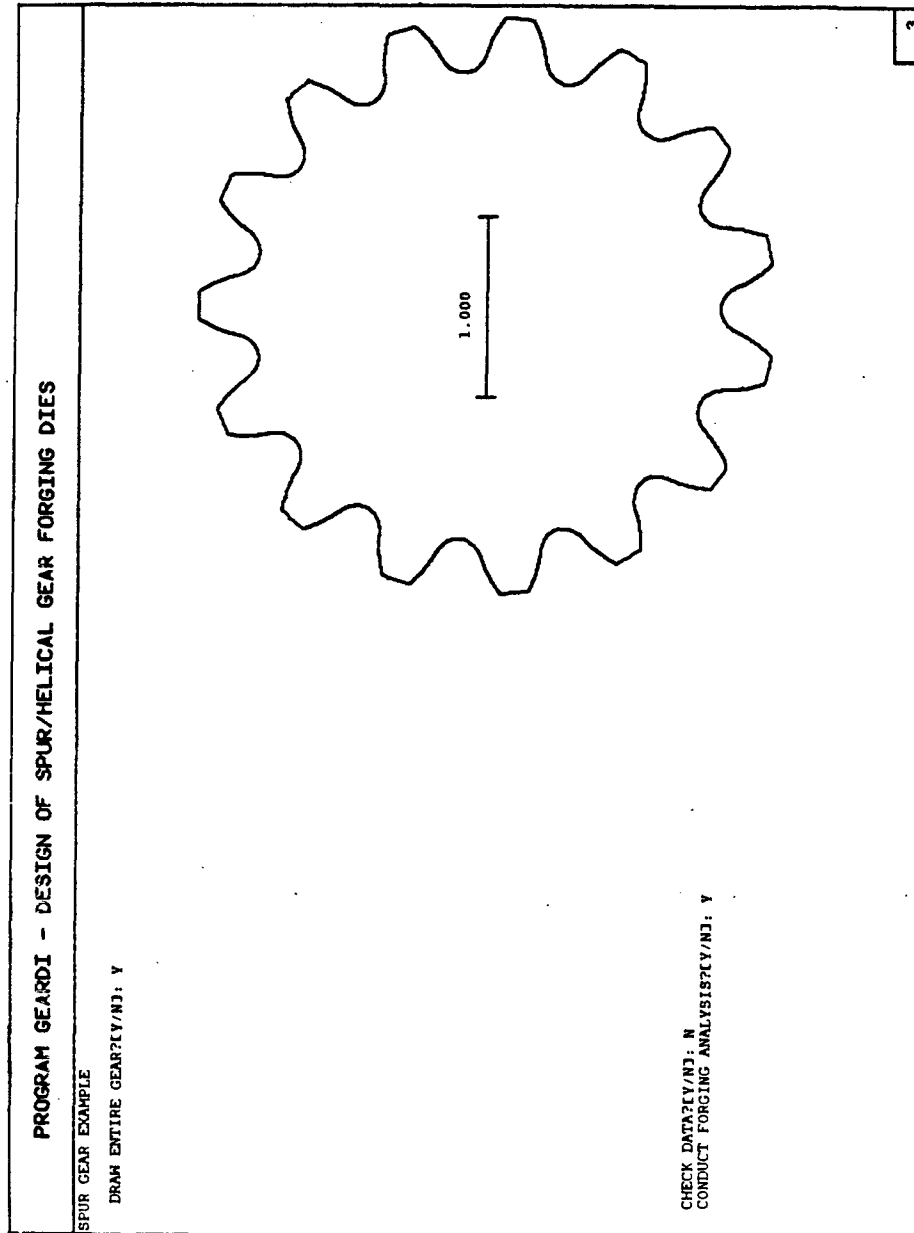


FIGURE D-30. Spur Gear Example; Entire Gear with Altered Fillet

PROGRAM GEARDI - DESIGN OF SPUR/HELICAL GEAR FORGING DIES	
SPUR GEAR EXAMPLE	
STRESS CALCULATIONS; DATA INPUT	
FORGING OR EXTRUSION? (F/E): F	
COLD VS. WARM FORGING? (C/H): C	
BILLET OUTSIDE DIAMETER (D)	
BILLET INSIDE DIAMETER	
FINISHED GEAR THICKNESS	2.1
FRICTION FACTOR (D)	
PERCENT FILL DESIRED (D)	50.
INITIAL YIELD STR (KSI) (D)	
GEAR MATERIAL (EG: A51016.DAT)	AS8620.DAT
SHRINK FIT INTERFERENCE	0.0035

FIGURE D-31. Spur Gear Example; Input of Forming Parameters

PROGRAM GEARDI - DESIGN OF SPUR/HELICAL GEAR FORGING DIES	
SPUR GEAR EXAMPLE	
STRESS CALCULATIONS: DATA CHECK	
1. COLD FORGING	= 2.69600
2. BILLET OUTSIDE DIAMETER	= 0.00000
3. BILLET INSIDE DIAMETER	= 2.10000
4. FINISHED GEAR THICKNESS	= 0.08000
5. FRICTION FACTOR	= 0.00000
6. INITIAL YLD STR (KSI)	= 50.00000
7. PERCENT FILE DESIRED	= AS8620
8. GEAR MATERIAL	= 0.00350
9. SHRINK FIT INTERFERENCE	= 0.00350
INCORRECT DATA NO. [0-END]:	
WARNING: INITIAL YIELD STRESS MUST BE < 18.94939	
PUNCH PRESSURE/AVE FLOW STRESS	= 3.98827
PUNCH PRESSURE (KSI)	= 195.84258
PUNCH FORCE (TONS)	= 651
CHANGE ANY FORMING PARAMETERS(Y/N): Y	

FIGURE D-32. Spur Gear Example; Echo of Forming Data and First Analysis

PROGRAM GEARDI - DESIGN OF SPUR/HELICAL GEAR FORGING DIES

SPUR GEAR EXAMPLE

STRESS CALCULATIONS, DATA CHECK

1. COLD FORGING

2. BILLET OUTSIDE DIAMETER

3. BILLET INSIDE DIAMETER

4. FINISHED GEAR THICKNESS

5. FRICTION FACTOR

6. INITIAL YLD STR (KSI)

7. PERCENT FILL DESIRED

8. GEAR MATERIAL

9. SHRINK FIT INTERFERENCE

2.69600

0.00000

2.10000

0.80000

18.94939

50.00000

AS8620

0.00350

INCORRECT DATA NO. (0-END): 7

PERCENT FILL DESIRED (D)

INCORRECT DATA NO. (0-END):

80.

6

FIGURE D-33. Spur Gear Example; Altering of the Percent Fill

PROGRAM GEARDI - DESIGN OF SPUR/HELICAL GEAR FORGING DIES	
SPUR GEAR EXAMPLE	
STRESS CALCULATIONS: DATA CHECK	

1. COLD FORGING	= 2.69600
2. BILLET OUTSIDE DIAMETER	= 0.00000
3. BILLET INSIDE DIAMETER	= 2.10000
4. FINISHED GEAR THICKNESS	= 0.08000
5. FRICTION FACTOR	= 18.94939
6. INITIAL YLD STR (KSI)	= 80.00000
7. PERCENT FILE DESIRED	= AS8620
8. GEAR MATERIAL	= 0.00350
9. SHRINK FIT INTERFERENCE	
INCORRECT DATA NO. [0-END]:	
WARNING: INITIAL YIELD STRESS MUST BE < 18.94939	
PUNCH PRESSURE/AVE FLOW STRESS	= 5.06873
PUNCH PRESSURE (KSI)	= 277.44318
PUNCH FORCE (TONS)	= 922
CHANGE ANY FORMING PARAMETERS?Y/N: N	
CHANGE PRODUCTION METHOD?Y/N: N	

FIGURE D-34. Spur Gear Example; Results of the Second Forging Analysis

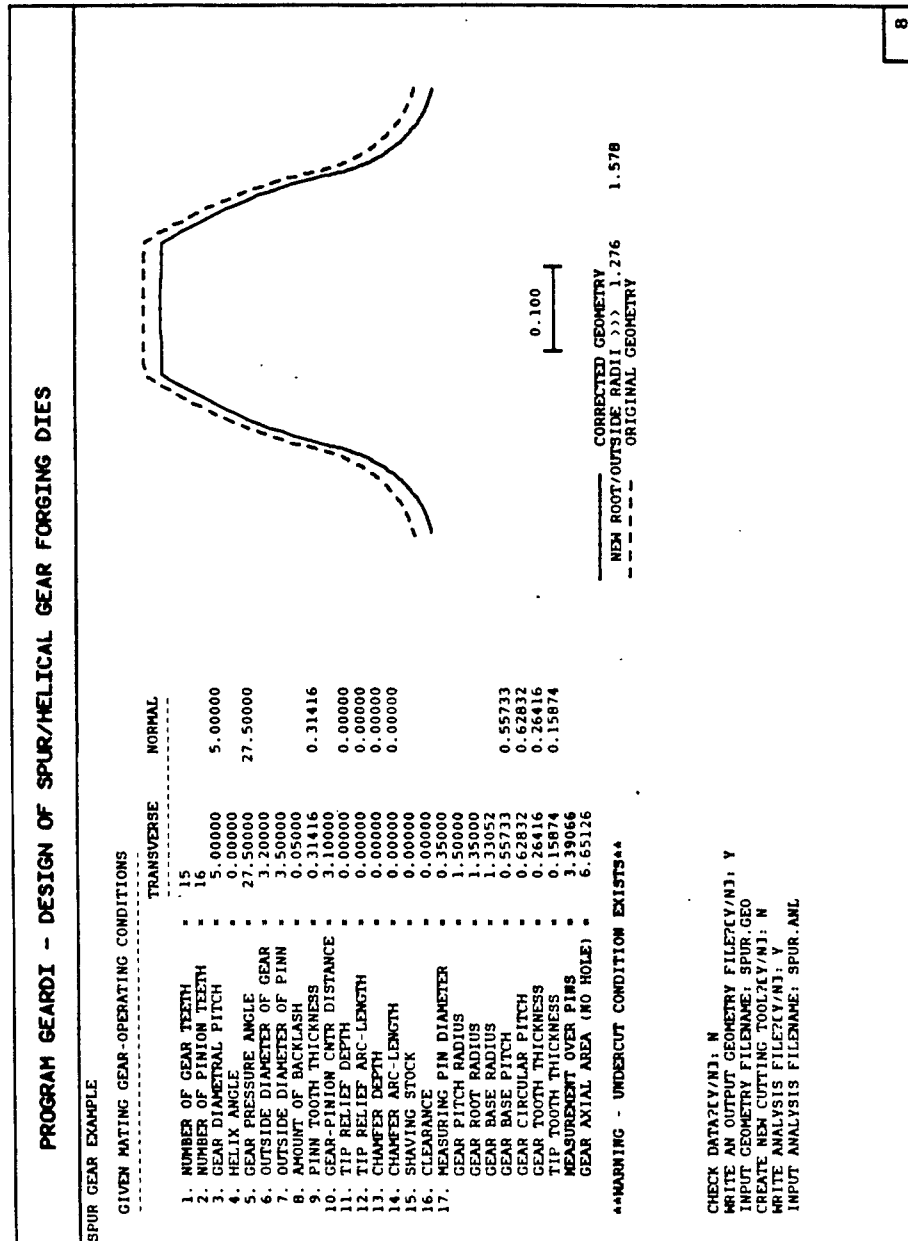


FIGURE D-35. Spur Gear Example; Display of Original and Corrected Tooth Profiles

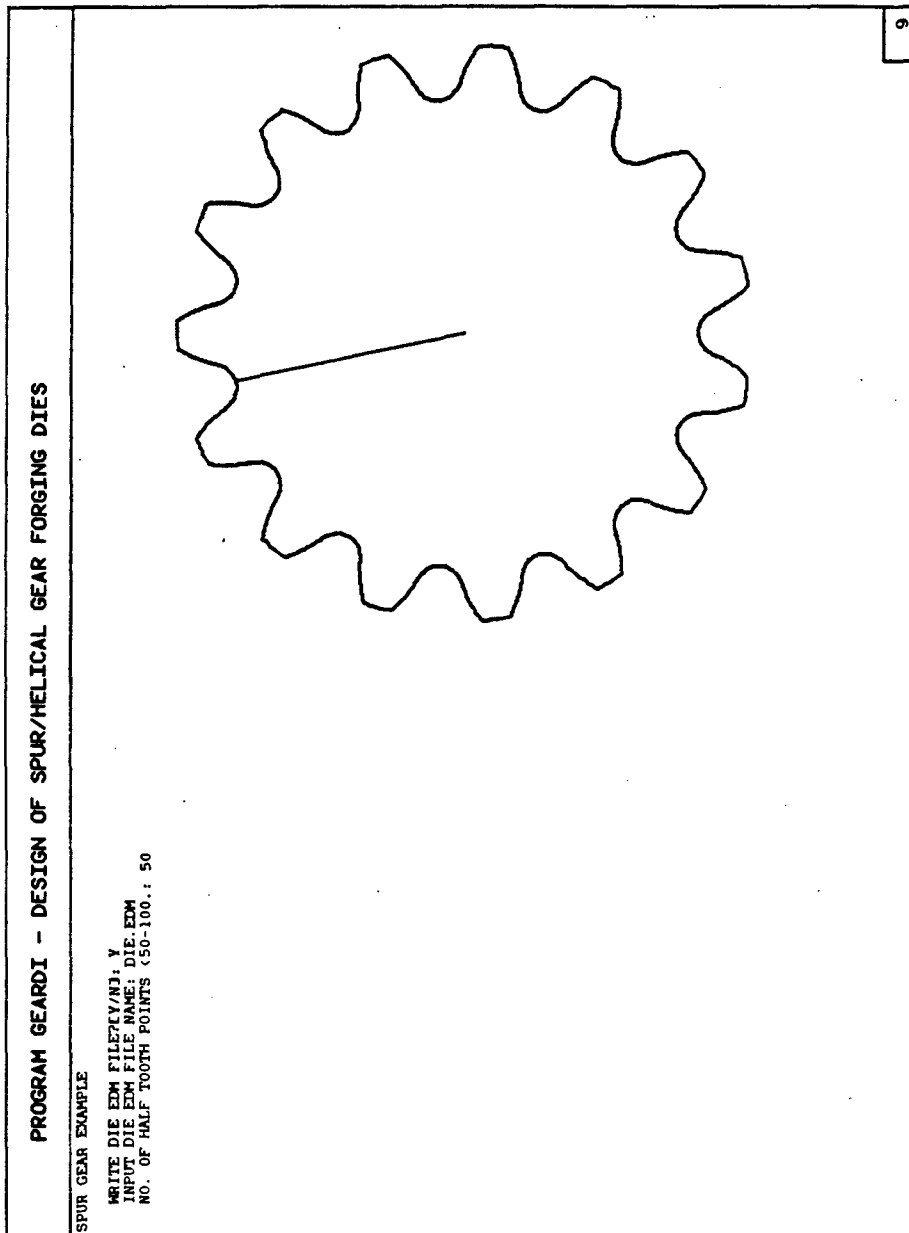


FIGURE D-36. Spur Gear Example; Path of Wire EDM of Forging Die

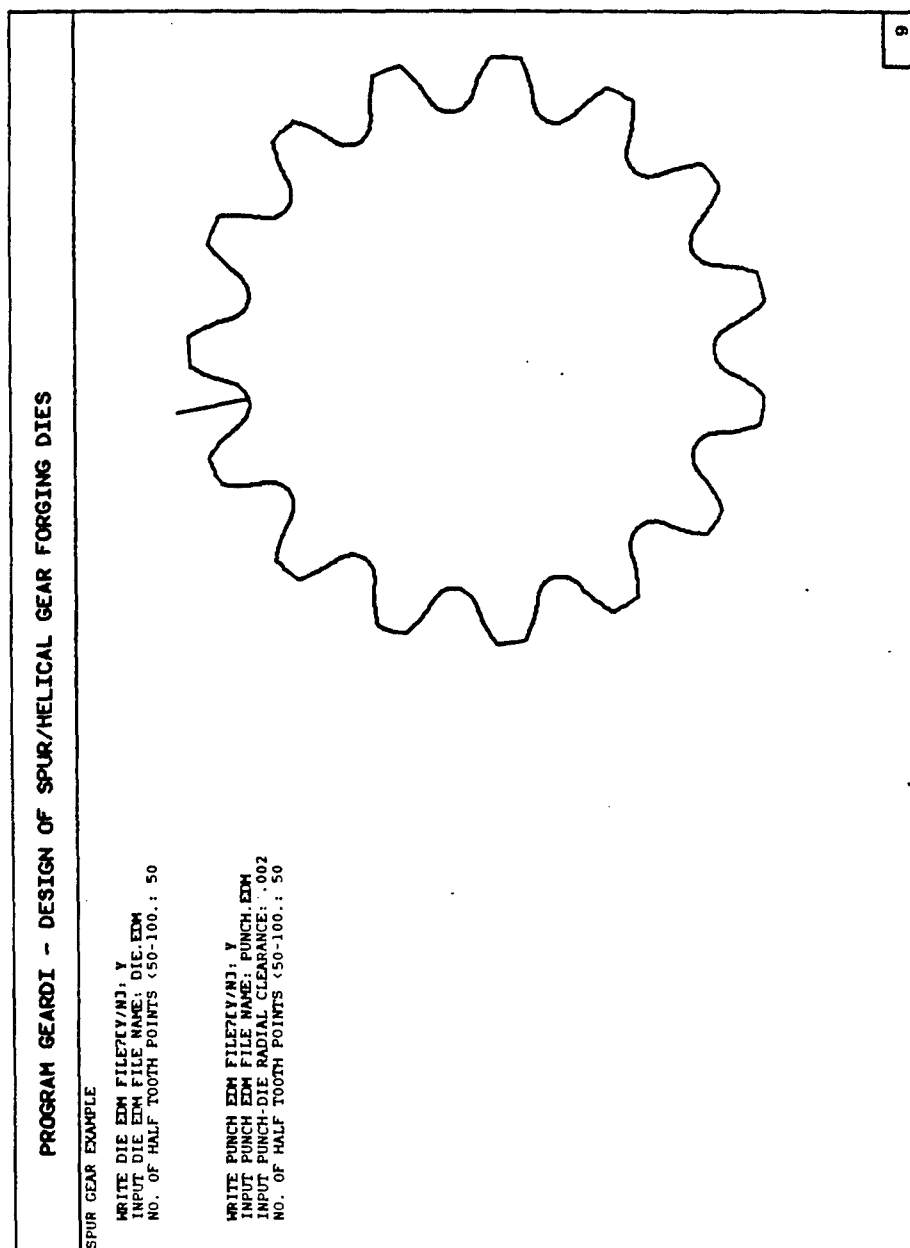
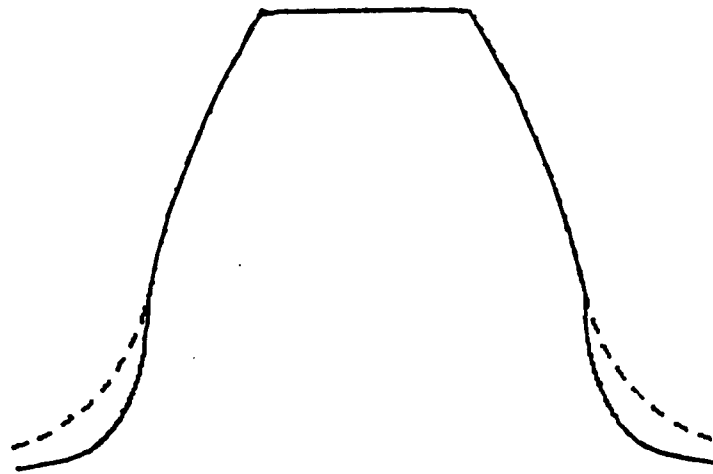


FIGURE D-37. Spur Gear Example; Path for Wire EDM of Forging Punch



———— Original Tooth Geometry
----- Altered Tooth Geometry

FIGURE D-38. Spur Gear Example; Comparison of Original and Altered Gear Tooth Profiles

geometry plus clearance.

4.0. SUMMARY

The above two examples show many of the capabilities of the GEARDI program which enable the metalforming and also the design engineer to solve a wide variety of gear production and application problems. The program was written in segmented form with each distinct computation process included in a specific region of the program. Thus, as more options are desired, they can be readily incorporated into the program. The potential number of applications for the GEARDI program are limited only by the abilities of the user.

APPENDIX E

DESCRIPTION OF THE COMPUTER PROGRAM "GEARDI" (USERS MANUAL)

THIS PAGE LEFT BLANK INTENTIONALLY

1.0. INTRODUCTION

A computer program named GEARDI, was developed to:

- define the exact tooth form of a spur or helical gear,
- compute the forming load required to produce the current gear design,
- compute the coordinates of the corrected gear geometry necessary for machining the Electrical Discharge Machining (EDM) electrodes by taking into account the change in the die geometry due to temperature differentials, load stresses, and shrink fitting, and,
- determine the specifications of a tool which will cut the altered tooth geometry on a conventional hobbing or shaper cutter machine.

The flowchart of the GEARDI program is shown in Figure E-1. This appendix describes the options available in the computer program. The use of this program with some examples is summarized in Appendix D.

2.0. TOOTH GEOMETRY

For the purpose of defining the tooth geometry, equations have been described using standard spur and helical gear tooth parameters. These equations have been presented in detail in Appendix A. To define the tooth geometry using these equations, a list of standard gear parameters must be supplied to the program by the user. This list of parameters is shown in Figure E-2. In the case when the user chooses to define the cut gear based on a protuberance hob cutting tool, extra hob parameters must be keyed in to the program; protuberance distance, parallel land length, and protuberance angle (Figure E-3). Normally, a hob or shaper cutter will cut a fillet in the shape of a trochoid. However, the GEARDI program has the capability of altering the fillet to an elliptical shape, as defined in Figure E-4.

Using the supplied input data for the generation of the tooth geometry, the interactive computer program GEARDI computes the x and y coordinates of the points describing the profile of the gear tooth. After computation, GEARDI displays the profile of a single gear tooth on the interactive graphics terminal. The display shows the locations and values of the major radii on the gear. The

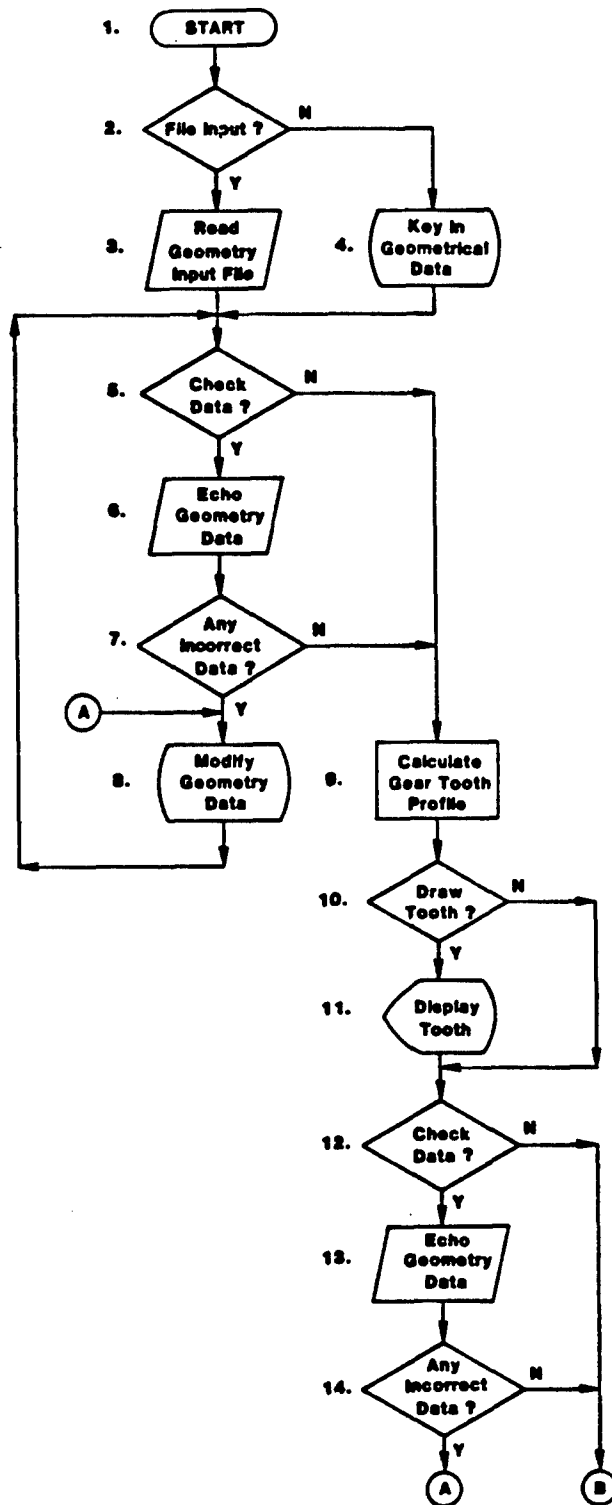


FIGURE E-1a. Flowchart of the GEARDI Computer Program

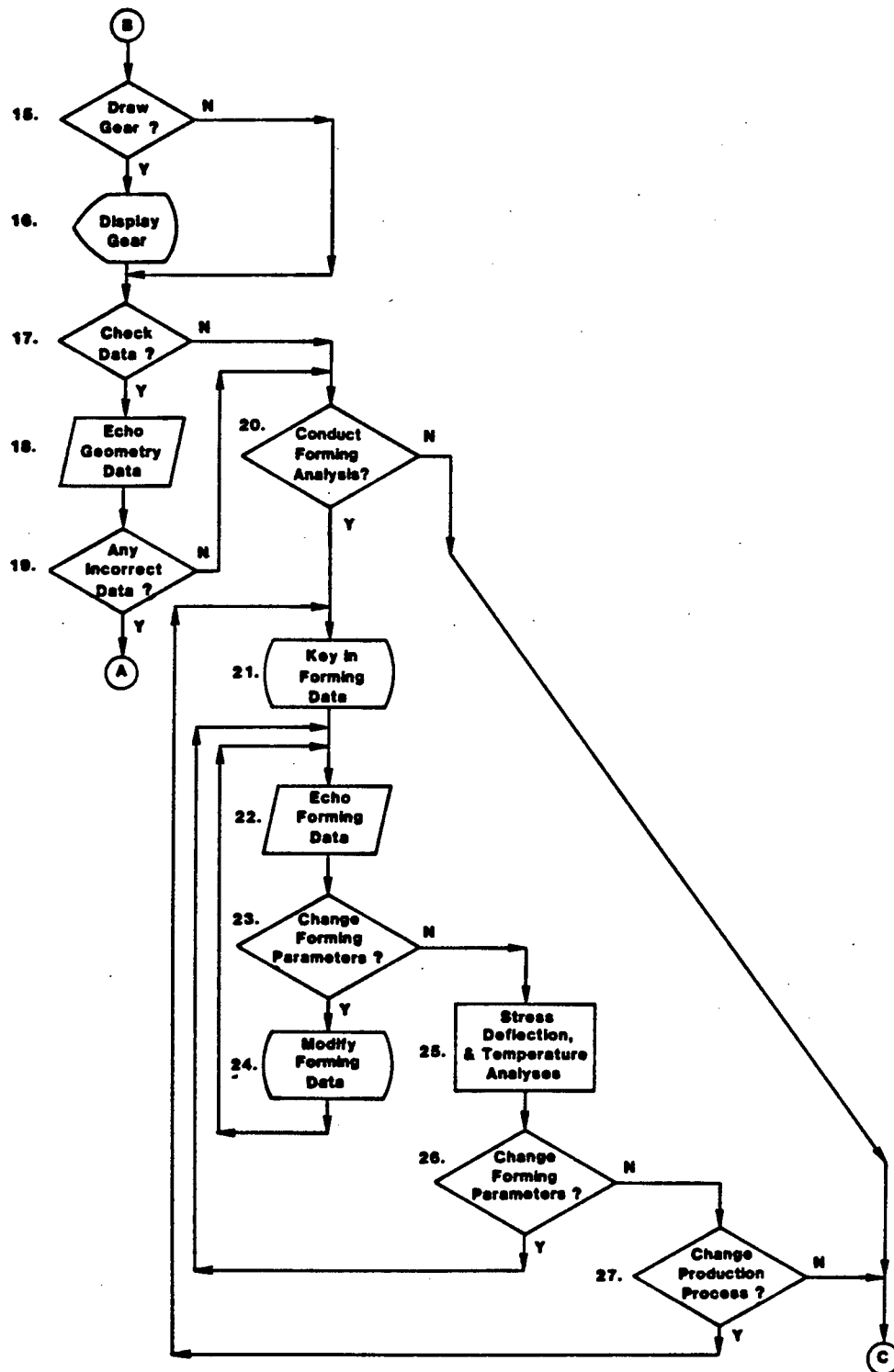


FIGURE E-1b. Flowchart of the GEARDI Computer Program (continued)

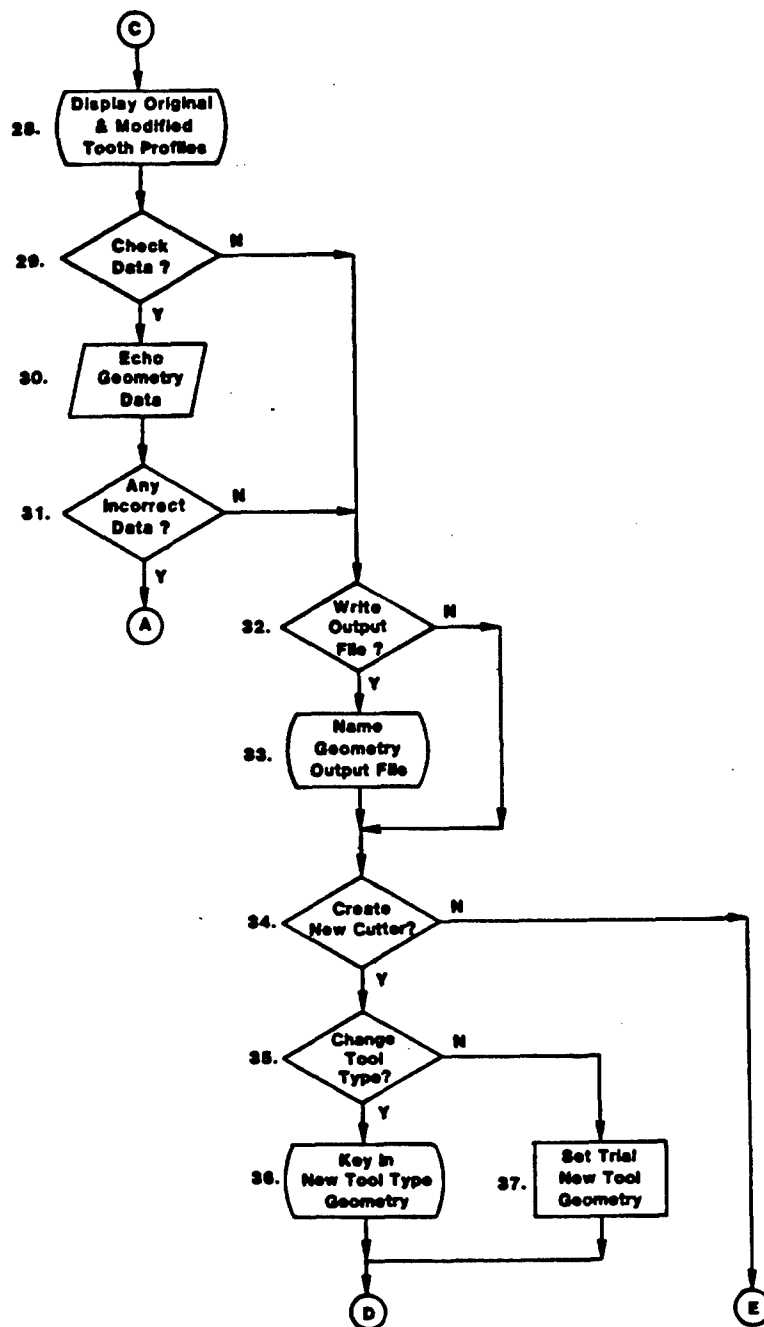


FIGURE E-1c. Flowchart of the GEARDI Computer Program (continued)

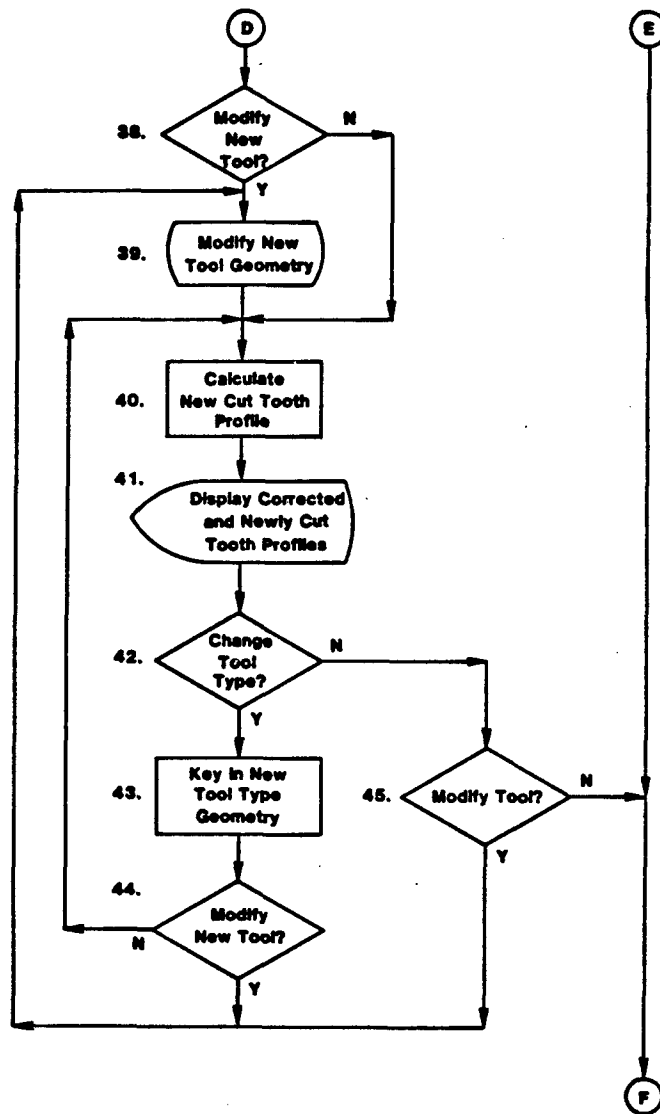


FIGURE E-1d. Flowchart of the GEARDI Computer Program (continued)

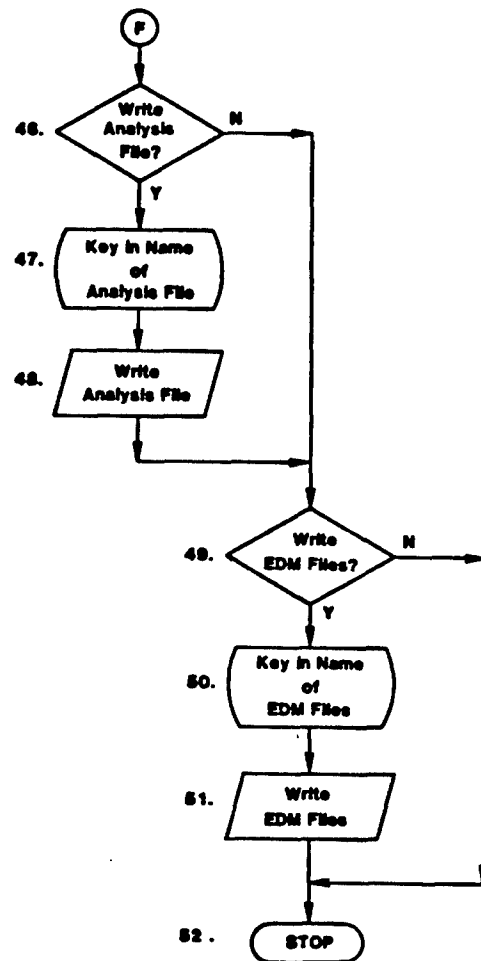


FIGURE E-1e. Flowchart of the GEARDI Computer Program (continued)

HELICAL GEAR EXAMPLE	
GENERATION METHOD	2
NUMBER OF GEAR TEETH	18
NUMBER OF PINION TEETH	0
TRANSVERSE DIAMETRAL PITCH	6.00000
NORMAL DIAMETRAL PITCH	6.23166
HELIX ANGLE	15.67182
GEAR OUTSIDE DIAMETER	3.33333
PINION OUTSIDE DIAMETER	0.00000
TRANSVERSE PRESSURE ANGLE	27.50000
NORMAL PRESSURE ANGLE	26.62071
GEAR TRANSVERSE TOOTH THICKNESS	0.26180
GEAR NORMAL TOOTH THICKNESS	0.25207
HOB/PINION TRANSVERSE TOOTH THICKNESS	0.26180
HOB/PINION NORMAL TOOTH THICKNESS	0.25207
GEAR ADDENDUM	0.16667
GEAR DEDENDUM	0.20833
HOB/PINION ADDENDUM	0.20833
HOB/PINION DEDENDUM	0.16667
HOB TOOTH CORNER RADIUS	0.03000
HOB PROTUBERANCE DISTANCE	0.00000
HOB PROTUBERANCE ANGLE	0.00000
HOB PROTUBERANCE PARALLEL LAND LENGTH	0.00000
SHAVING STOCK	0.00000
GEAR-PINION CENTER DISTANCE	0.00000
GEAR-PINION BACKLASH	0.00000
GEAR-PINION CLEARANCE	0.00000
GEAR TIP RELIEF DEPTH	0.00000
GEAR TIP RELIEF ARC	0.00000
TIP RELIEF FLAG	0
GEAR TIP CHAMFER DEPTH	0.01667
GEAR TIP CHAMFER ARC	0.01370
ALTERED FILLET MAJOR AXIS	0.00000
ALTERED FILLET MINOR AXIS	0.00000
ALTERED FILLET OFFSET ANGLE	0.00000
ALTERED FILLET CENTER LOCATION	0
GEAR ROOT RADIUS	1.29167
GEAR PITCH RADIUS	1.50000
GEAR OUTSIDE RADIUS	1.66667
GEAR TRANSVERSE CIRCULAR PITCH	0.52360
GEAR NORMAL CIRCULAR PITCH	0.50413
GEAR BASE RADIUS	1.33052
GEAR TIP TOOTH THICKNESS	0.03854
UNDERCUT FLAG	0
GEAR OUTSIDE DIAMETER DEFAULT FLAG	1
GEAR TRANSVERSE BASE PITCH	0.46444
GEAR NORMAL BASE PITCH	0.45069
GEAR LEAD	33.59313
EQUIVALENT NUMBER OF TEETH	20.16651
GEAR AXIAL PITCH	1.86629
MEASURING PIN DIAMETER	0.27500
GEAR OVER PINS DIMENSION	3.38109
GEAR BETWEEN PINS DIMENSION	2.62448
EXTRUSION	2
DIE ANGLE	50.00000
COLD	1
BILLET OUTSIDE DIAMETER	3.40000
BILLET INSIDE DIAMETER	1.56500
BILLET THICKNESS	1.48320
FINISHED GEAR THICKNESS	2.10000
FRICTION FACTOR	0.08000
PERCENT FILL	100.00000
MATERIAL YIELD STRENGTH (KSI)	20.56985
AS1016.DAT	
INTERFERENCE SHRINK FIT	0.00350
COLD EQUATION COEFFICIENT	104.80000
COLD EQUATION EXPONENT	0.26200

FIGURE E-2. Sample Data File

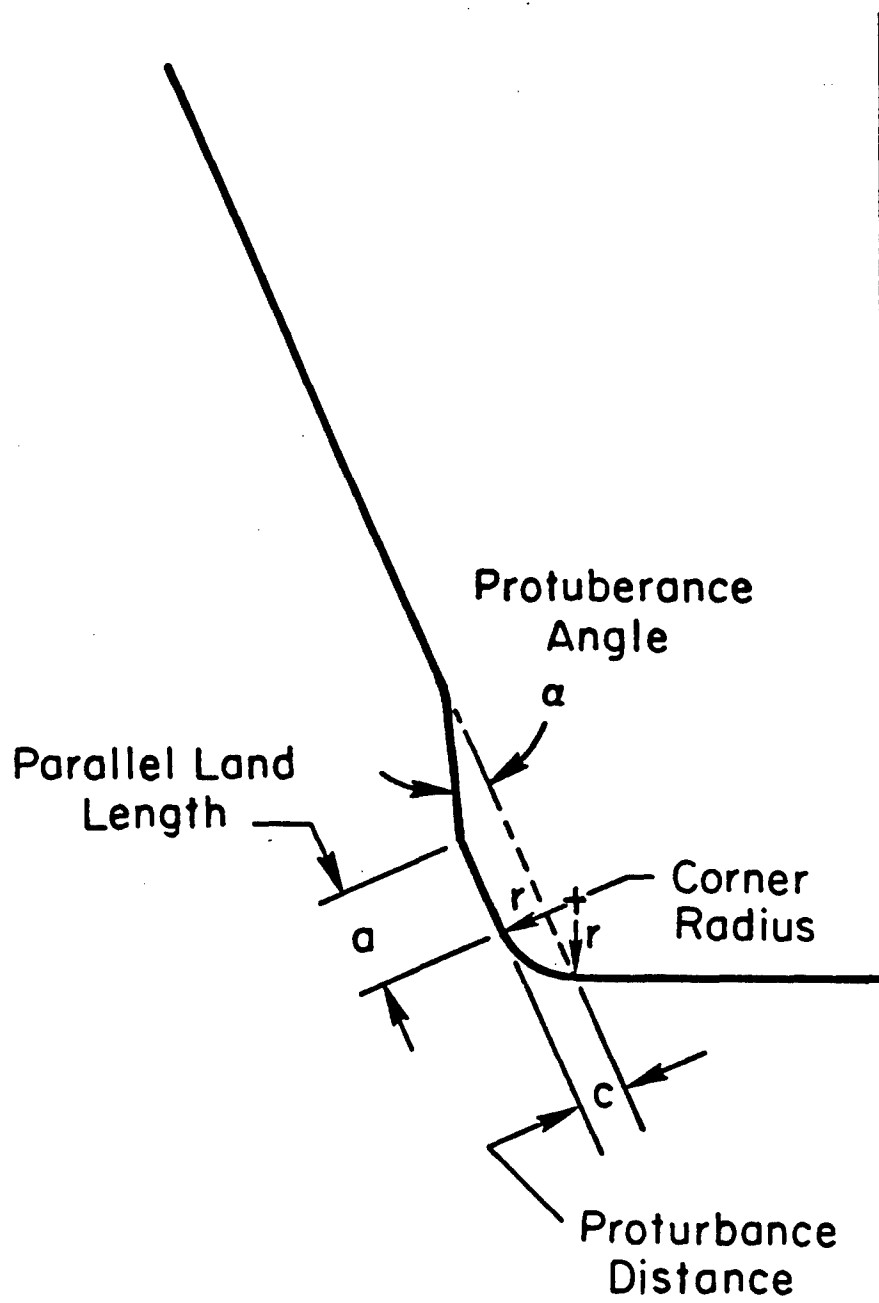


FIGURE E-3. Protuberance Hob Dimensions

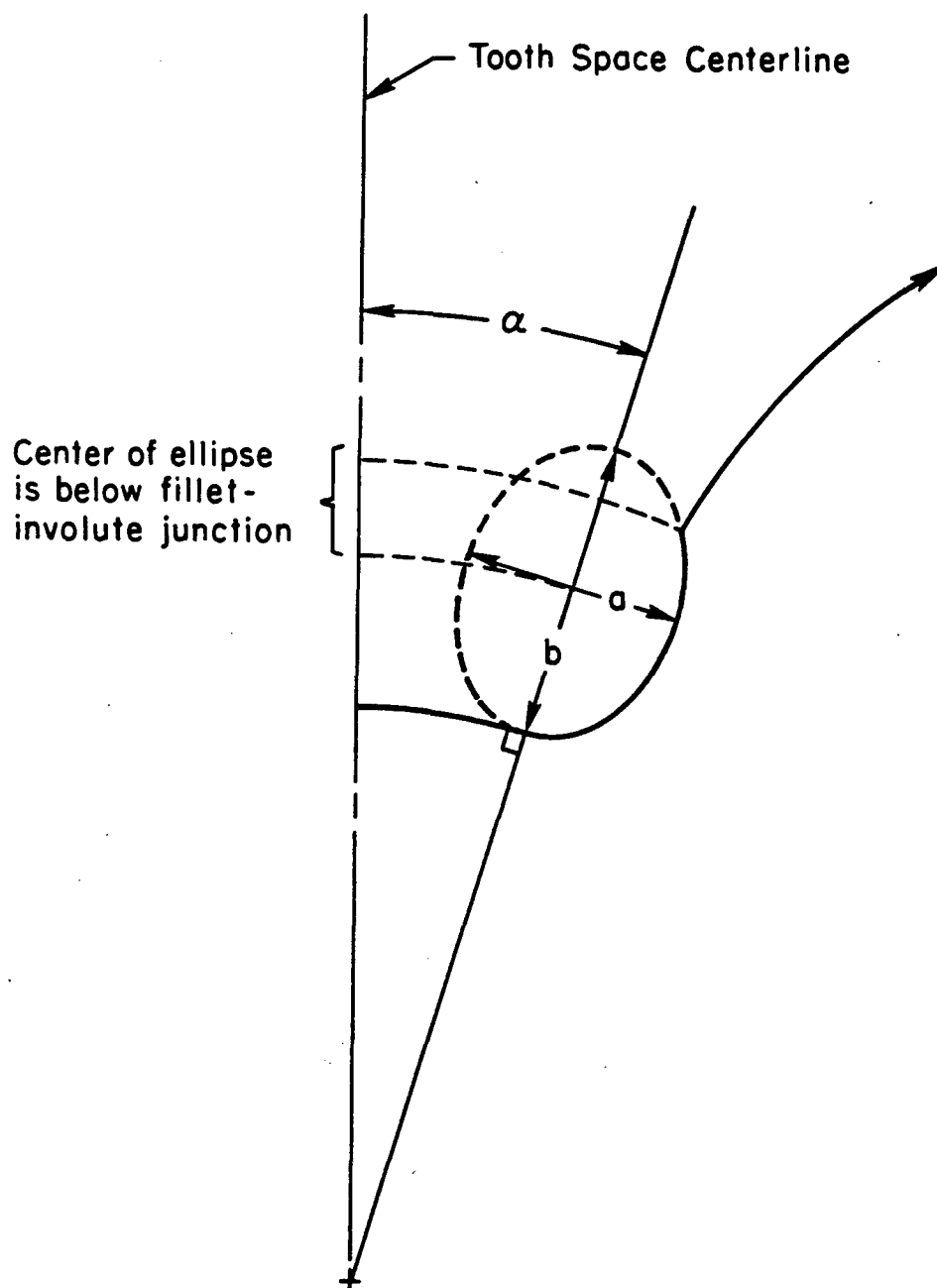


FIGURE E-4. Altered Gear Tooth Fillet Geometry (a = transverse axis; b = radial axis; α = offset angle)

program then draws the entire gear for visual checking.

3.0. FORMING LOADS

After the geometry for the gear has been defined, the user may choose to compute the load required for successful forming of the designed gear. Prior to this computation, the user must supply the program with various forming parameters. One of these manufacturing parameters is percent fill. The amount of filling is computed as a percentage of the length along the tooth tip of the die where the material has not yet come in contact. Figure E-5a shows a gear tooth cavity with zero percent fill and Figure E-5b shows a gear tooth cavity with 50 percent fill. Another manufacturing parameter defined by the user is the die angle (extrusion analysis only). The die angle is measured as shown in Figure E-6. The program computes the required punch pressure, punch force, and the ratio of the punch pressure to the maximum flow stress.

4.0. DIE CORRECTIONS

In the third stage, the program GEARDI calculates the change in the dimensions of the gear due to (a) the elastic deflection of the die during forming, (b) the shrink or press fitting of the die insert into the reinforcing ring, and (c) the change in the size of the die due to temperature effects if a warm forming process has been specified. No additional parameters must be specified at this point which have not already been defined in the previous sections of the program. After the die corrections have been calculated, the program displays the profile of a single gear tooth in both its original form and its corrected form.

5.0. NEW CUTTER/OUTPUT FILES

In the final stage of the program, the user is able to experiment with a variety of hobs and shaper cutters to see which one will cut the corrected tooth geometry most accurately. All of the design parameters used previously in the geometrical definition of the gear are also used in this section. The program automatically determines the maximum amount of radial error between the corrected tooth geometry and the geometry cut by the newly designed gear cutting tool. An added advantage of this section of the program is that it can be used to design hobs and shaper cutters if the user has previously chosen to omit the forming analysis. In this case, the corrected geometry is the true finished tooth geometry.

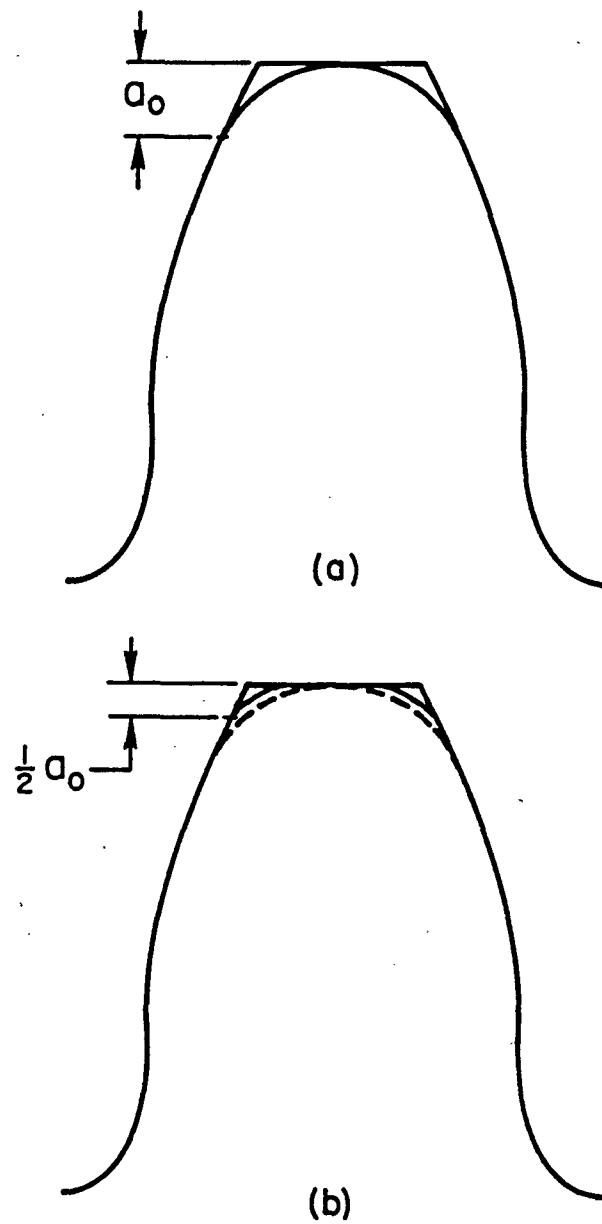
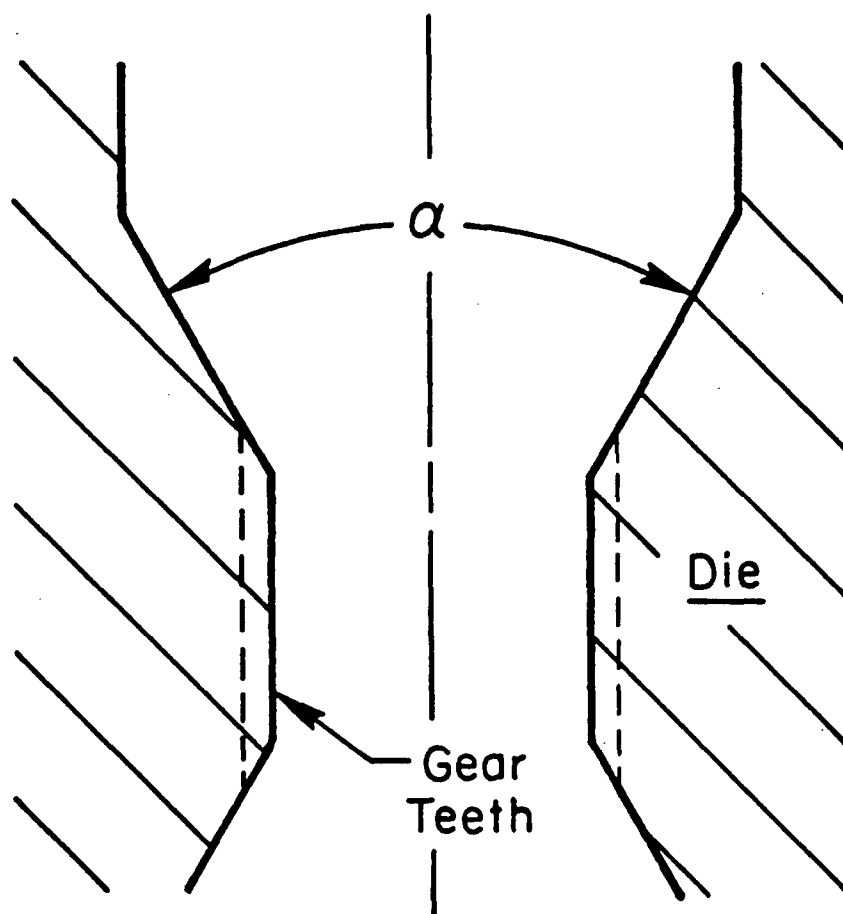


FIGURE E-5. a) 0.0% and b) 50% Filling of Gear Tooth Cavity



α = Die Angle

FIGURE E-6. Die Angle Specification

After the new cutting tool has been designed, the user may create an output file containing all the geometrical and forming input parameters, the results of the forming analysis, the new cutter specifications, and a list of coordinates for use in EDMing of the forging punch and/or the forging and extrusion dies to be used to form the gear.

In its present form, GEARDI can be run on both a Digital Equipment Corporation PDP-11/44 (RT-11 operating system) or a VAX 11/780 (VMS operating system). Also required is the PLOT10 TCS graphics software package from Tektronix, Inc. The source code is approximately 7500 lines long (counting comment lines) and the program can be used in the interactive mode only.

THIS PAGE LEFT BLANK INTENTIONALLY

APPENDIX F

STRUCTURE AND SUBROUTINES OF THE COMPUTER PROGRAM

"GEARDI"

THIS PAGE LEFT BLANK INTENTIONALLY

1.0. INTRODUCTION

The computer program GEARDI and its use are described in Appendix E. Following is a description of the program structure and the various subroutines. All subroutines were written in standard VAX (Digital Equipment Corporation VAX 11/780 computer) FORTRAN. The listing of the program includes a large number of comment statements. Thus, the programmer can follow the details of GEARDI by utilizing the information given in the present appendix together with:

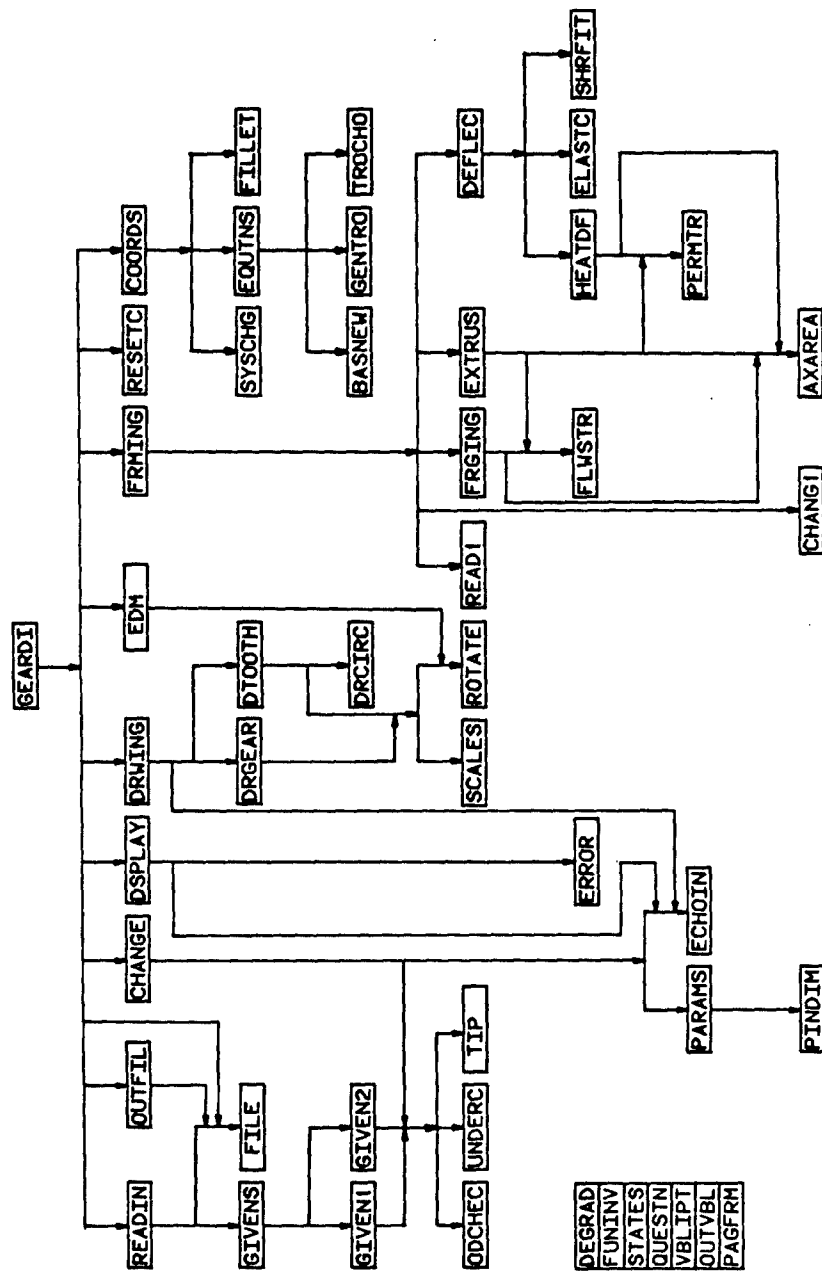
- Appendix A - Generation of Gear Tooth Geometry for Spur and Helical Gears,
- Appendix B - Stress Analysis, Elastic Deflection and Bulk Shrinkage.

2.0. PROGRAM STRUCTURE

The structure of the program GEARDI is shown in Figure F-1. The main program and all the subroutines of Figure F-1 are described below.

2.1. PLOT10 Subroutines

- ANCHO - outputs an ASCII character to terminal
- ANMODE - prepares terminal for alpha-numeric output
- CHRSIZ - sets character size on terminal
- DASHA - draws dashed lines in absolute user coordinates
- DRAWA - draws using absolute user coordinates
- DRAWR - draws using relative user coordinates
- DRWREL - draws using relative screen coordinates
- DSHREL - draws dashed lines in relative screen coordinates
- HOME - returns cursor to home position
- MOVABS - moves cursor in absolute screen coordinates
- MOVEA - moves cursor in absolute user coordinates



F-1. Control Structure Flowchart for the GEARDI Program

- MOVREL - moves cursor in relative screen coordinates
- NEWPAG - clears terminal screen
- SWINDO - dimensions terminal in screen coordinates
- TSEND - dumps contents of graphics buffer to terminal
- VWINDO - dimensions terminal in user coordinates

2.2. FORTRAN Subroutines

- ASSIGN - opens an auxiliary file for input or output
- CLOSE - closes an auxiliary file being used for data I/O

2.3. PROGRAM Subroutines

- AXAREA - calculates axial area of a gear
- BASNEW - computes involute base radius
- CHANG1 - allows change of forming parameters
- CHANGE - allows modification of input geometry
- COORDS - manages profile determining equations
- DEFLEC - manages die deflection equations
- DEGRAD - converts angle measure between degrees and radians
- DRCIRC - draws a portion of a circle
- DRGEAR - draws an entire gear
- DRWING - manages drawing of gear profile and whole gear
- DSPLAY - displays original and corrected tooth geometries
- DT00TH - draws a single gear tooth
- ECHOIN - re-prints (echos) gear input geometry
- EDM - creates output files for electrical discharge machining (EDM)
- ELASTC - computes elastic deflections in die due to forming loads

- EQUENS - contains all gear profile equations
- ERROR - computes error associated with a new cutter
- EXTRUS - computes maximum radial extrusion pressure
- FILE - geometry I/O using an external file
- FILLET - enables altering of gear tooth fillet
- FLWSTR - returns flow stress of a given material
- FRGING - computes maximum radial forging pressure
- FRMING - manages stress computation routines
- FUNINV - computes involute function of a given angle
- GEARDI - main program which calls all other subroutines
- GENTRO - generates candidate trochoid cutting points
- GIVEN1 - reads user supplied hob geometry data
- GIVEN2 - reads user supplied shaper cutter geometry data
- GIVENS - manages GIVEN1 and GIVEN2
- HEATDF - computes die deflections due to temperature
- ODCHEC - checks for compatible gear O.D. and tooth thickness
- UTFIL - writes an analysis output file
- UTFVL - outputs a variable to terminal
- PAGFRM - clears terminal; draws and numbers a new page
- PARAMS - computes extra gear parameters
- PERMTR - computes perimeter of a gear
- PINDIM - computes over pins dimensions of a gear
- QUESTN - presents a question to terminal
- READ1 - reads in user specified forming parameters

- READIN - manages input of gear geometry
- RESETC - resets gear geometry for a new cutting tool
- ROTATE - rotates a pair of coordinates through a given angle
- SCALES - computes size of scale line for a given drawing
- SHRFIT - computes die deflections due to shrink fitting
- STATES - presents a statement to terminal
- SYSCHG - normalizes gear geometry
- TIP - computes gear tip tooth thickness
- TROCHO - determines cutting point of a protuberance hob
- UNDERC - checks for an undercut condition in gear fillet
- VBLIPT - reads a variable

THIS PAGE LEFT BLANK INTENTIONALLY

APPENDIX G

ANALYSIS OF METAL FLOW USING LEAD AS A MODEL MATERIAL

THIS PAGE LEFT BLANK INTENTIONALLY

1.0. INTRODUCTION

Forging and extrusion are two of the more important processes that can be used for manufacturing spur and helical gears. In both cases, the production rates can vary between 10 and 20 parts per minute in an automated system. The load-stroke curves for such processes do not generally give any detailed information on how the material flows during the forming operation. Information which may be useful to the die designer includes;

- at what load does the material begin to flow;
- where does the material first begin to flow;
- in which direction does the material move;
- in what order are the various areas of the part filled; and
- which areas of the part are the most difficult to fill?

To answer these and similar questions requires knowledge of the relationships between material properties, friction conditions, and process mechanics. However, the extent of such knowledge at the present time makes an exact theoretical analysis of practical forming operations difficult (1)*. A powerful tool in forming process development is the use of highly deformable model materials to simulate real forming operations. This appendix deals with the simulation of the material flow in a spur gear forging die. The study was divided into three tasks. Task I involved a series of ring tests to determine the best lubricant to use. The second task studied the radial flow in thin (length (height)/diameter = 0.2) billets. Finally, in Task III the material flow in a full-scale production gear forging was investigated.

2.0. MODEL MATERIAL AND TOOLING

2.1. Model Materials

Wax, plasticene, lead and clay compositions have been used to obtain qualitative information about metal flow (1). No model material is known today which has non-elastic deformation behavior exactly like the material of the real process. Most materials have a temperature and rate zone in which the deformation resistance is

*Numbers in parentheses refer to references at the end of the appendix.

practically independent of the degree of deformation. This is the case with steel during hot working and with sodium and lead at room temperature when the deformation rate is sufficiently low (2).

2.1.1. Preliminary Investigation.

2.1.1.1. Plasticene. During a preliminary investigation, plasticene was used as a model material in a spur gear forging die using various lubricants. The plasticene was difficult to remove from the die without tearing and left a tedious cleanup job before a new sample could be deformed. This was the case no matter which lubricant was used (Note: the various lubricants used are discussed in the next section).

2.1.1.2. Lead. Lead billets were also used in the preliminary investigation. The deformation loads were higher and the deformed material required a higher push-out load as compared to the plasticene. However, there was virtually no die pickup and the formed part did not undergo any noticeable additional deformation during removal from the die. For these reasons it was decided to use lead as the model material.

2.1.2. Lead Processing. Prior to cutting the various lead specimens to size, the lead was processed to obtain a fine grain size with as little directionality as possible in the final product. A split mold for casting the lead (99.9 percent pure) was made from stainless steel pipe (0.25 in. wall thickness x 6 in. O.D. x 11 in. long) by sawing the pipe in half, longitudinally. Cast lead billets were made by first pouring about 20 pounds of lead into the mold, then continuously adding molten lead to this material by melting ingots over the mold with an oxygen-acetylene torch until a billet of approximately six in. in length had been cast.

This 5-1/2 in. diameter billet was then hammer forged to an outside diameter of about 3-1/4 in. The ends were trimmed and the diameter machined to 3 in. to remove surface defects and laps. Finally, this machined billet was extruded through a 2-1/8 in. diameter die. About 75 tons were required to initiate extrusion, after which the load decreased. A 700-ton hydraulic press was used for this work. A sketch of the extrusion tooling is shown in Figure G-1.

2.2. Tooling

The tooling used for the modeling studies is shown in Figures G-2 and G-3. The container, or die, consisted of a cylindrical piece of tool steel with the shape of a spur gear cut entirely through the center. The punch, also made of tool steel, was shaped to fit

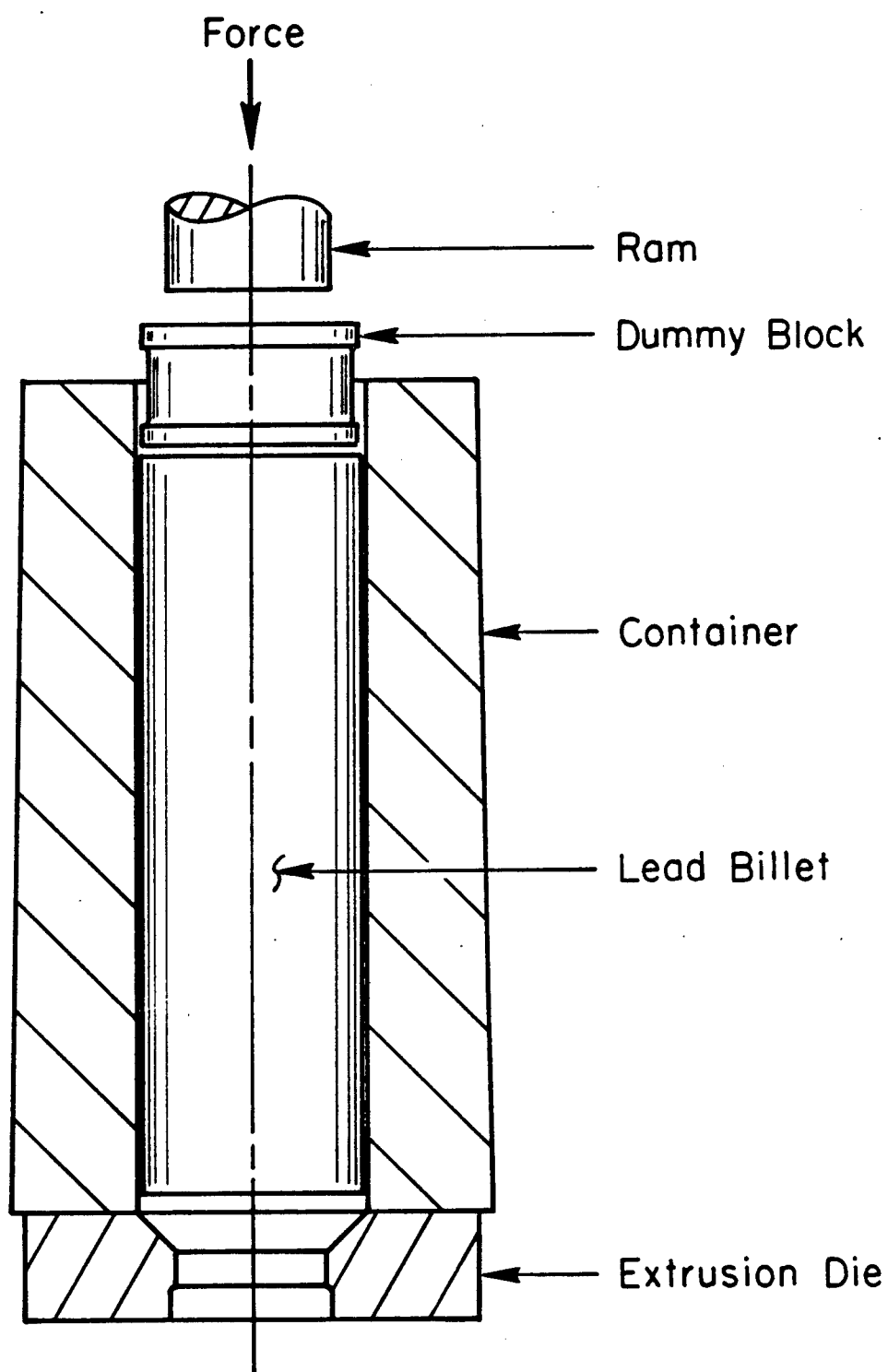


FIGURE G-1. Extrusion Setup Used for Preparing Lead Specimens

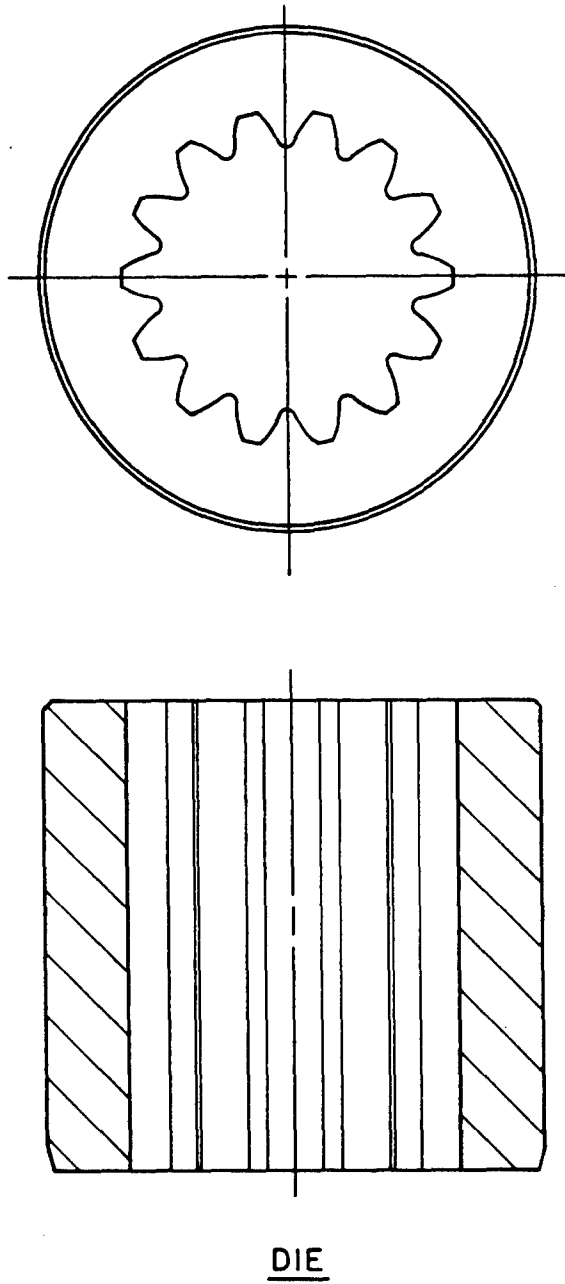
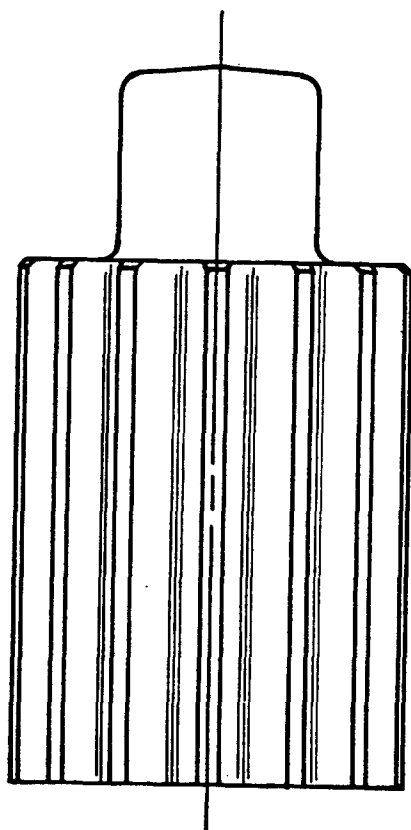
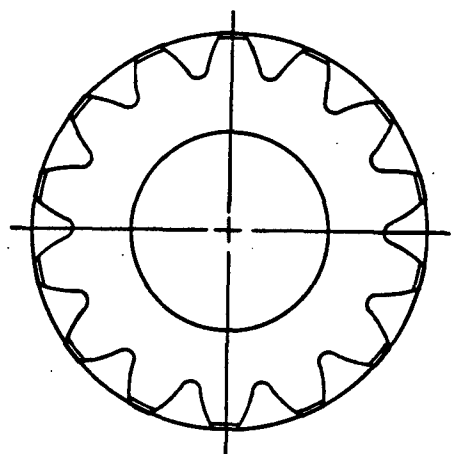
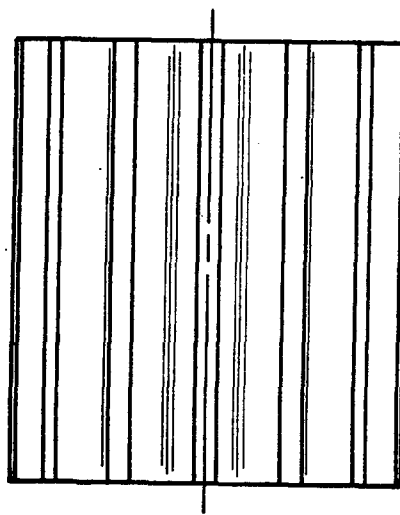
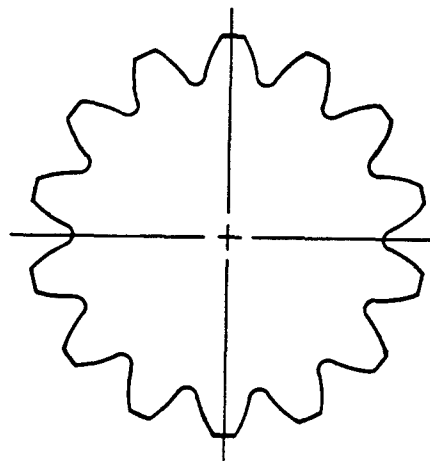


FIGURE G-2. Top and Section View of Die Used for Spur Gear Modeling Studies



PUNCH



COUNTER PUNCH

FIGURE G-3. Top and Side View of Punch and Counter Punch Used for Spur Gear Modeling Studies

inside the die with a minimum amount of clearance to allow for free axial movement. The final piece of tooling was a counter punch which had the same configuration as the punch except there was no projection on the counter punch.

3.0. LUBRICATION TESTS

The objective of lubrication tests was to determine the most suitable lubricant for later use in the modeling of radial flow. In the radial flow trials, it was desired to have as little friction as possible on the punch and insert so that a plain strain condition could be assumed, thus allowing better correlation with the finite element results discussed in Appendix C.

3.1. Ring Geometry

The lubrication trials were done using lead ring specimens and by conducting a simple upsetting in a Baldwin Universal Testing Machine. The rings had an overall O.D.:I.D.:Height ratio of 6:3:2. Four lubricants were investigated with a 25 percent and a 50 percent reduction being done for each. The lubricants studied were as follows;

- (1) Lead oxide (Pb), J. T. Baker Chemical Co.) & Mobil heavy duty 10W motor oil (PbO:oil = 1:1.25)
- (2) K-Y Lubricating Jelly, Johnson & Johnson,
- (3) Johnson's Baby Powder (talc), Johnson & Johnson, and
- (4) Dgf 123 Dry Graphite Film Lubricant, Miracle Power Products Corp.

3.2. Ring Tests

Several specimens were tested, some using no lubricant as a control. Table G-1 summarizes the ring test results. the effectiveness of each lubricant was determined by plotting the percent decrease in the inside diameter of each ring against the percent reduction in height. This is shown in Figure G-4. From this graph, the best lubricant was selected to be the lead oxide-motor oil combination (PbO) which had an m value (friction shear factor) of 0.2. This was the lubricant used in the radial flow trials and the production scale simulation.

4.0. RADIAL FLOW TESTS

Appendix C discusses the simulation conducted using a two-

TABLE G-1. Results of Lubrication Trials Using Lead Ring Specimens

Ring Specimen No.	Original Dimensions, inch		Lubricant	Top Surface		Final Dimensions, inch				Reduction in Height, percent	Maximum Deformation Load, lb	Average(h) Decrease in I.D., percent
	Height	I.D.		Max	Min	Mid/Bulge	Max	Min	Bottom Surface			
1	0.667	1.001	2.001	0.932	0.932	0.829	0.829	0.829	0.932	0.932	10,350	6.9
2	0.667	1.000	2.000	0.670	0.613	0.532	0.482	0.482	0.656	0.611	20,400	36.2
3	0.667	1.001	2.000	1.087	1.007	1.092	0.996	1.088	1.003	0.508	8,500	-4.5
4	0.667	1.001	2.000	1.019	0.928	1.012	0.916	1.025	0.964	0.339(a)	15,600	1.7
5	0.668	1.002	2.000	1.003	0.996	0.975	0.964	0.969	0.964	0.505	9,000	1.9
6	0.667	1.001	2.000	0.887	0.865	0.815	0.786	0.876	0.815	0.342	16,650	14.0
7	0.667	0.999	2.001	0.954	0.950	0.880	0.874	0.943	0.943	0.509	9,500	5.1
8	0.667	0.999	2.000	0.640	0.619	0.503	0.502	0.620	0.592	0.334	22,200	38.1
9	0.667	1.002	2.001	1.067	1.009	1.086	1.001	1.066	1.009	0.506(f)	9,100	-3.6
10	0.667	1.002	2.000	1.071	1.046	1.077	1.049	1.054	1.033	0.506	8,900	-4.9
11	0.667	1.000	2.000	1.104	0.971	1.123	0.960	1.092	0.926	0.353	14,000	-2.3
12	0.668	1.001	2.001	0.961	0.953	0.927	0.912	0.973	0.968	0.506	9,150	3.7
13	0.667	1.000	2.001	0.848	0.756	0.776	0.674	0.848	0.751	0.337	16,800	19.9
14	0.667	1.001	2.001	1.000	0.969	0.992	0.911	0.994	0.962	0.511	8,900	2.0
15	0.667	1.002	2.000	0.933	0.824	0.905	0.767	0.939	0.832	0.368(g)	14,900	12.0
16	0.667	1.000	2.000	0.937	0.934	0.836	0.830	0.937	0.934	0.504	9,800	6.4
17	0.667	1.000	2.000	0.699	0.686	0.542	0.539	0.681	0.679	0.370(f)	18,600	31.4

Note: Trials were done on a Baldwin-Universal Testing Machine; Crosshead speed, 0.3-inch per minute. Upsetting dies were flat-face hardened and ground. Their surface finish is estimated to be 16, based on experience. The specimens were cleaned with acetone damped tissue before testing dry or applying lubricant. Lubricant was applied to all surfaces of ring when used. Dies were not lubricated.

(a) Volume ratio of PbO to oil was approximately 1:1.25; the oil used was Mobil Heavy Duty 10W. Lead oxide (Litharge) powder, J. T. Baker Chemical Company.

(b) K-Y Lubricating Jelly, Johnson & Johnson.

(c) Talc, Johnson's Baby Powder, Johnson & Johnson.

(d) dgf 123, Dry Graphite Film Lubricant, Miracle Power Products Corporation.

(e) Slight flaw in O.D. of ring.

(f) Major flaw in O.D. of ring.

(g) Loaded off-center of swivel head, 0.068 taper across upset ring.

(h) Based on average I.D. at top and bottom surfaces only.

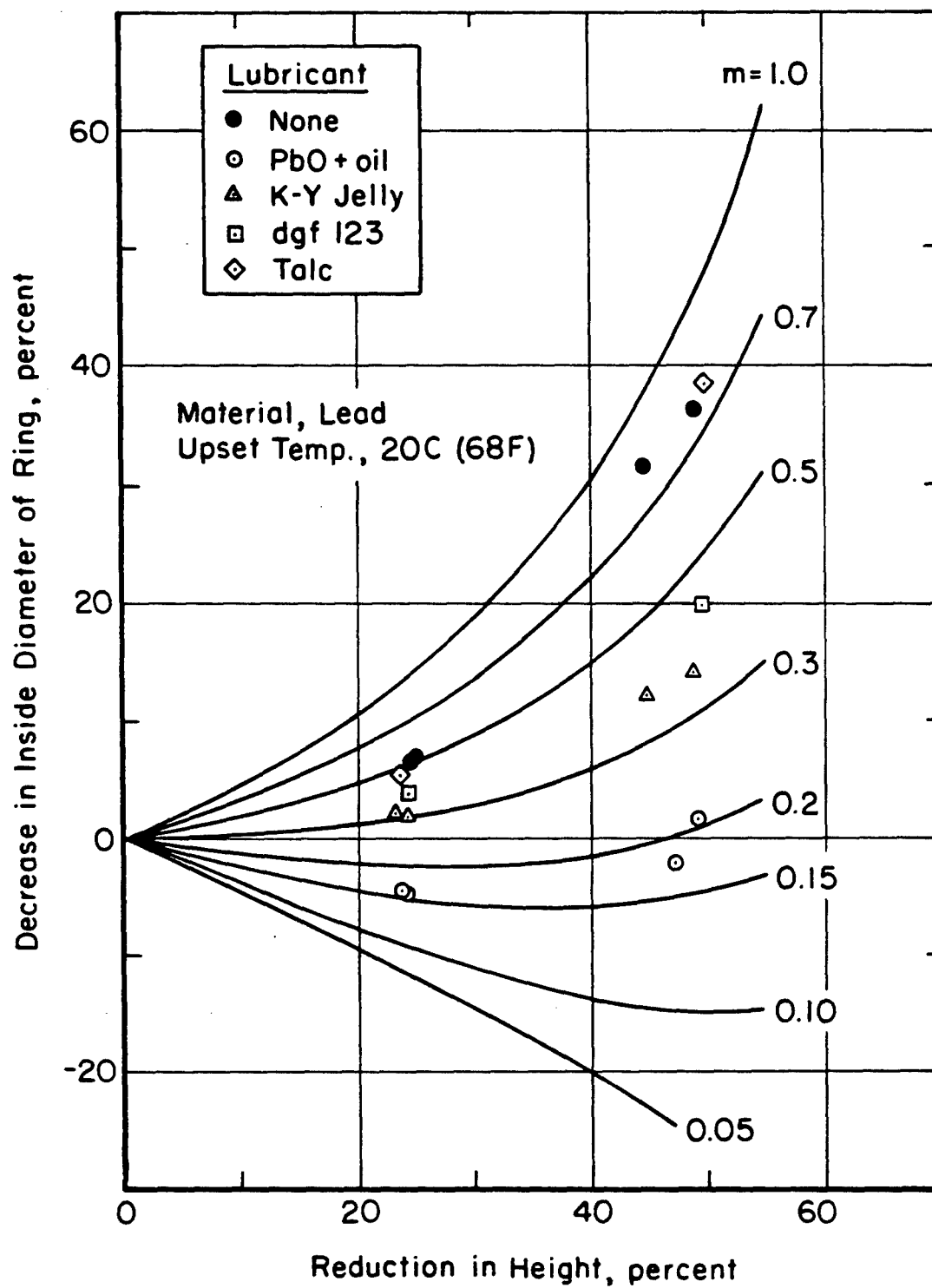


FIGURE G-4. Friction Factor Determination for Various Lubricants Applied to Lead Rings and Forged at Room Temperature

dimensional finite element method (FEM) program called ALPID (3) which predicted the ratio of the radial pressure to flow stress required to fill the corners of the gear teeth. In an effort to both correlate and validate the results of this FEM analysis, a series of radial forgings were done with lead as the model material. These forgings were made using thin sections of lead (O.D.:Height = 3) in a spur gear die and a flat punch.

4.1. Tool Setup

The tool setup for these tests is shown in Figure G-5. Based on experience, the finish on surface 'A' was estimated to be 8 micro-inches and the finish on surface 'B' was estimated at 16 micro-inches. The lubricant used for these trials was a lead-oxide and motor oil mixture as determined during the lubrication tests described earlier.

4.2. Test Procedure

The lubricant, when used, was only applied to surfaces 'A' and 'B'. By coating these surfaces, it was assumed that the flow would be purely radial and so permitted the use of a two-dimensional FEM simulation.

Prior to each trial, metal particles were removed from the tooling and then both the tooling and the new billet were cleaned with acetone dampened tissues. Whenever the PbO + oil lubricant was used, it was applied with a paint brush to surfaces 'A' and 'B' (see Figure G-5). After cleaning the tools and workpiece and, when appropriate, applying the lubricant, the assembly (Figure G-5) was placed on a Baldwin Universal Testing Machine. A cross-head speed of 0.3 inch per minute was used and a load vs. stroke curve was obtained while deforming the billet. A typical load-stroke curve is shown in Figure G-6. The first billet was deformed until the load increased at a rate which suggested that the die was completely filled. Subsequent tests were then run by loading to a specific point on the first load-stroke curve. These points were picked based both upon experience and the inflection points observed on the first load-stroke curve.

4.3. Results

The results of the radial flow tests are tabulated in Table G-2. Several photographs were taken of each specimen from several different angles. These photographs are shown in Figures G-7 through G-12. Specimens 101 through 109 were formed using the selected lubricant, yet the photographs show a noticeable amount of friction was still present between the part and the counter punch and between the part and the bottom plate. However, this friction was much less than when no lubricant was used (specimens

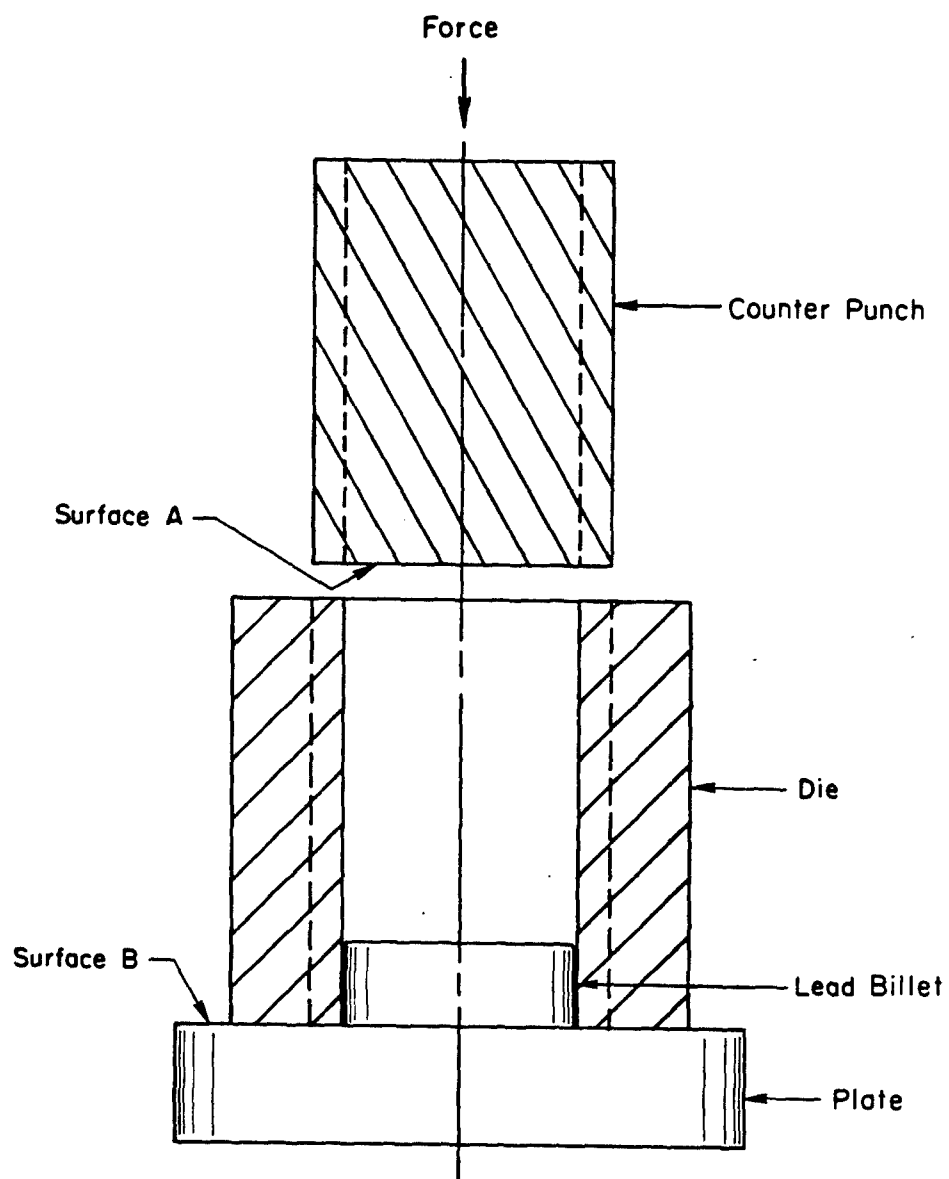


FIGURE G-5. Tooling for Radial Flow Trials

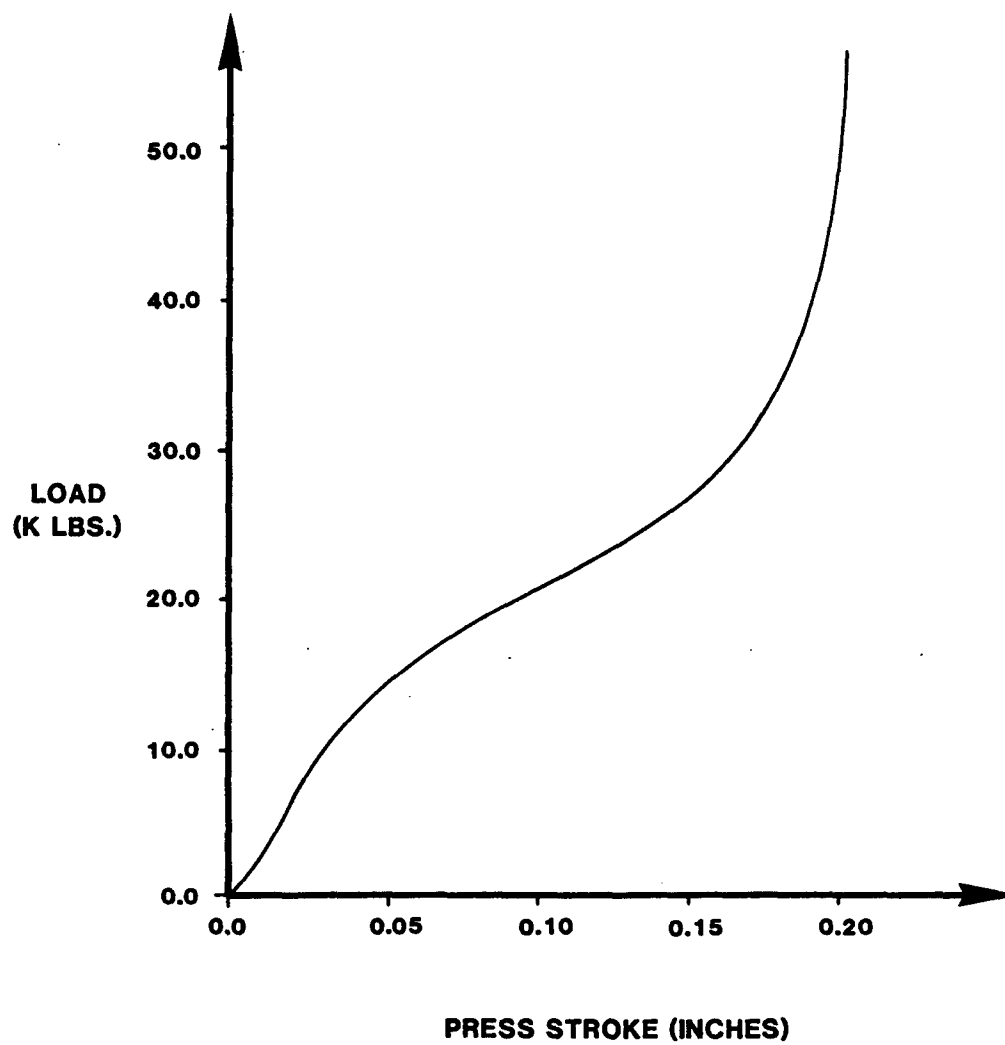


FIGURE G-6. Typical Load vs. Stroke Curve as Generated from a Radial Flow Trial with the Model Material Lead

TABLE G-2. Incremental Radial Flow Study Trials Using Thin Billets

Trial No.	Original Dimensions, in. Height	O.D.	Lubricant(a)	Deformation Load, lb	Final Height, inch	Stroke, inch	Comments
101	0.681	2.052	PbO + oil	53,700	0.494	0.187	
102	0.678	2.052	Ditto	152,000	0.495	0.183	Teeth not filled at die surface "B" (Dwg. p. 42), trapped lubricant
103	0.679	2.051	"	72,000	0.492	0.187	
104	0.680	2.050	"	31,500	0.517	0.163	
105	0.681	2.050	"	23,000	0.551	0.130	
106	0.681	2.051	"	35,000	0.508	0.173	
107	0.680	2.051	"	71,800	0.493	0.187	
108	0.682	2.051	"	40,200	0.502	0.180	
109	0.679	2.050	"	56,000	0.491	0.188	
110	0.681	2.051	None	176,000	0.494	0.187	Note: Flash was formed on all 17 specimens. It occurred between the moving punch and the die. The PbO + oil lubricant was applied by brush to the punch face (Surface "A") and the bottom plate (Surface "B") only. See Figure G-7 for details.
111	0.679	2.051	"	50,000	0.499	0.180	
112	0.681	2.052	"	30,250	0.544	0.137	
113	0.682	2.050	"	70,500	0.495	0.187	
114	0.682	2.049	"	60,600	0.4955	0.1865	
115	0.682	2.051	"	80,800	0.496	0.186	
116	0.682	2.048	"	100,000	0.492	0.190	
117	0.682	2.049	"	55,500	0.499	0.183	

(a) Volume ratio of PbO to oil was approximately 1:1.25; the oil used was Mobil Heavy Duty 10W; the lead oxide (Litharge) powder, J. T. Baker Chemical Company. Note: Trials were done on a Baldwin Universal Testing Machine; Crosshead speed, 0.3-inch per minute.

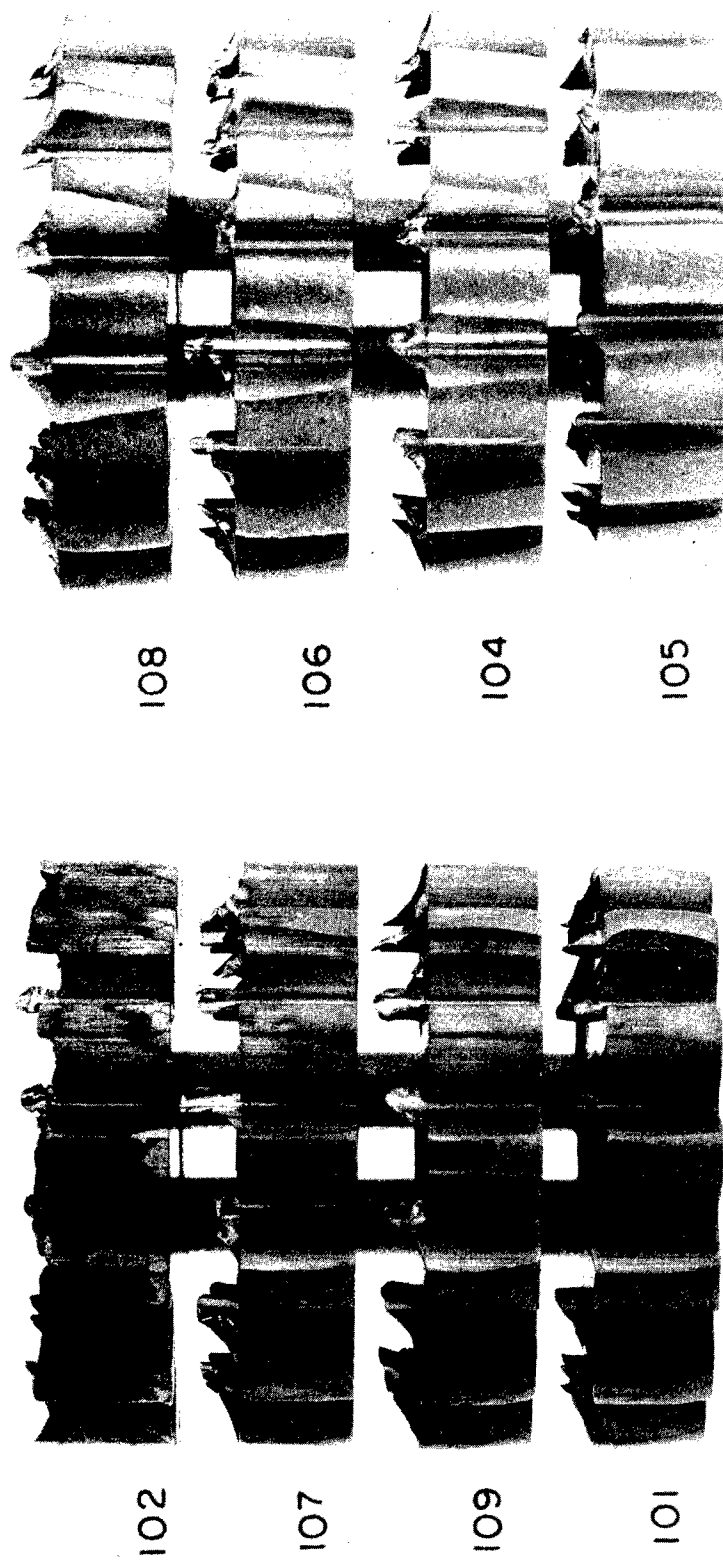


FIGURE G-7. Side View of Radial Flow Trial Specimen Numbers 101 Through 109 (PbO + oil lubricant; specimen No. 103 not shown)

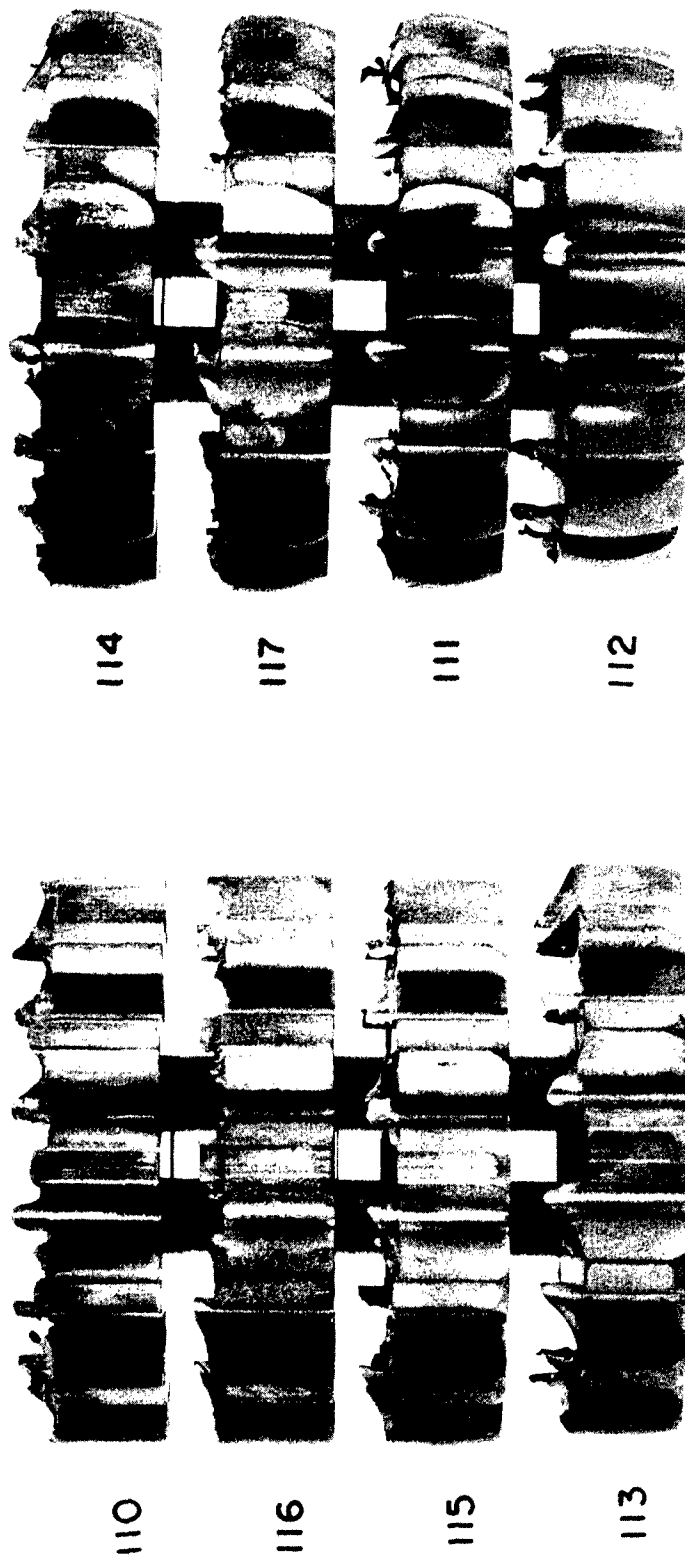


FIGURE G-8. Side View of Radial Flow Trial Specimen Numbers 110 Through 117 (no lubricant)

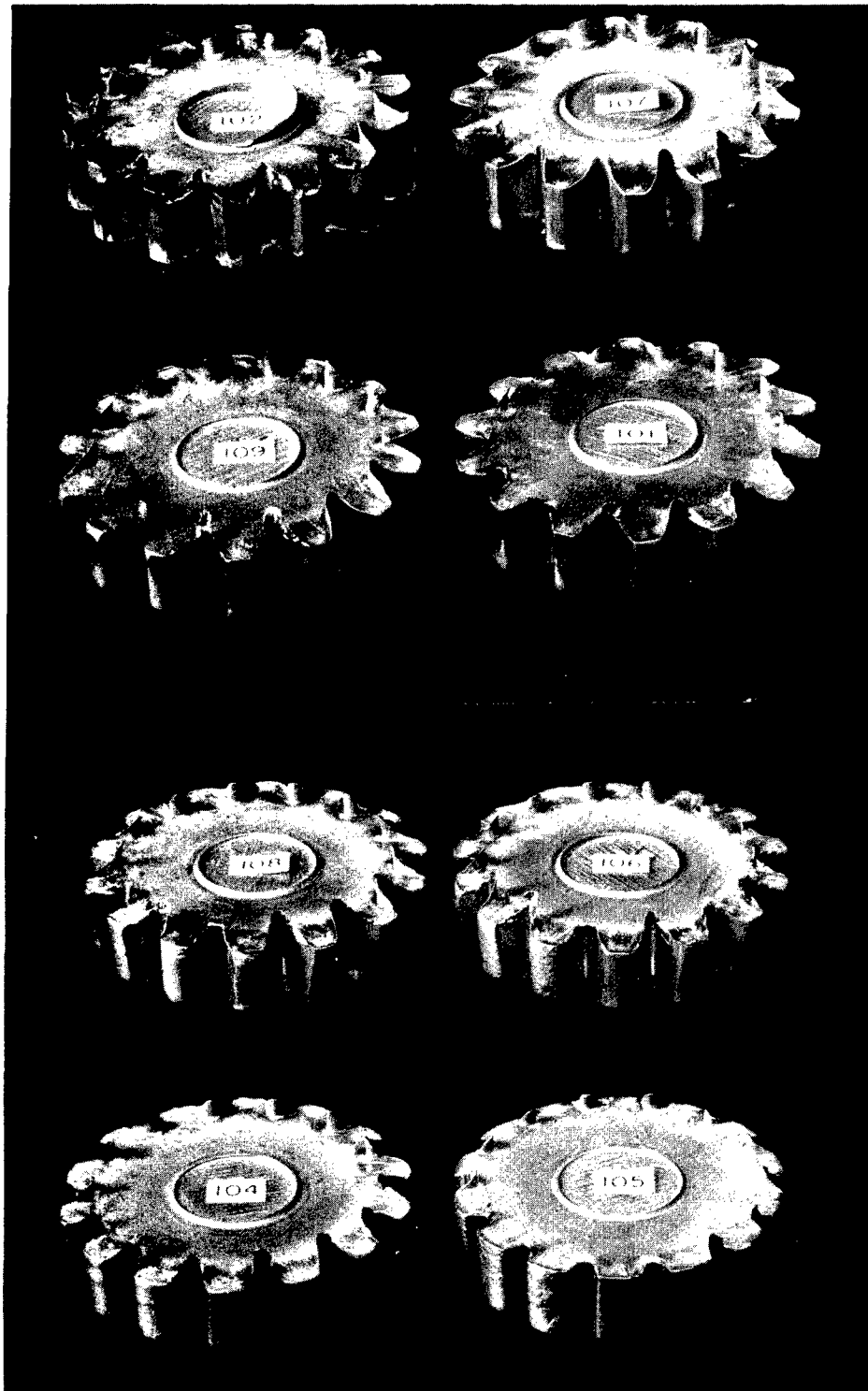


FIGURE G-9. Isometric View of Radial Flow Trial Specimen Numbers 101 Through 109 (PbO + oil lubricant; specimen No. 103 not shown)

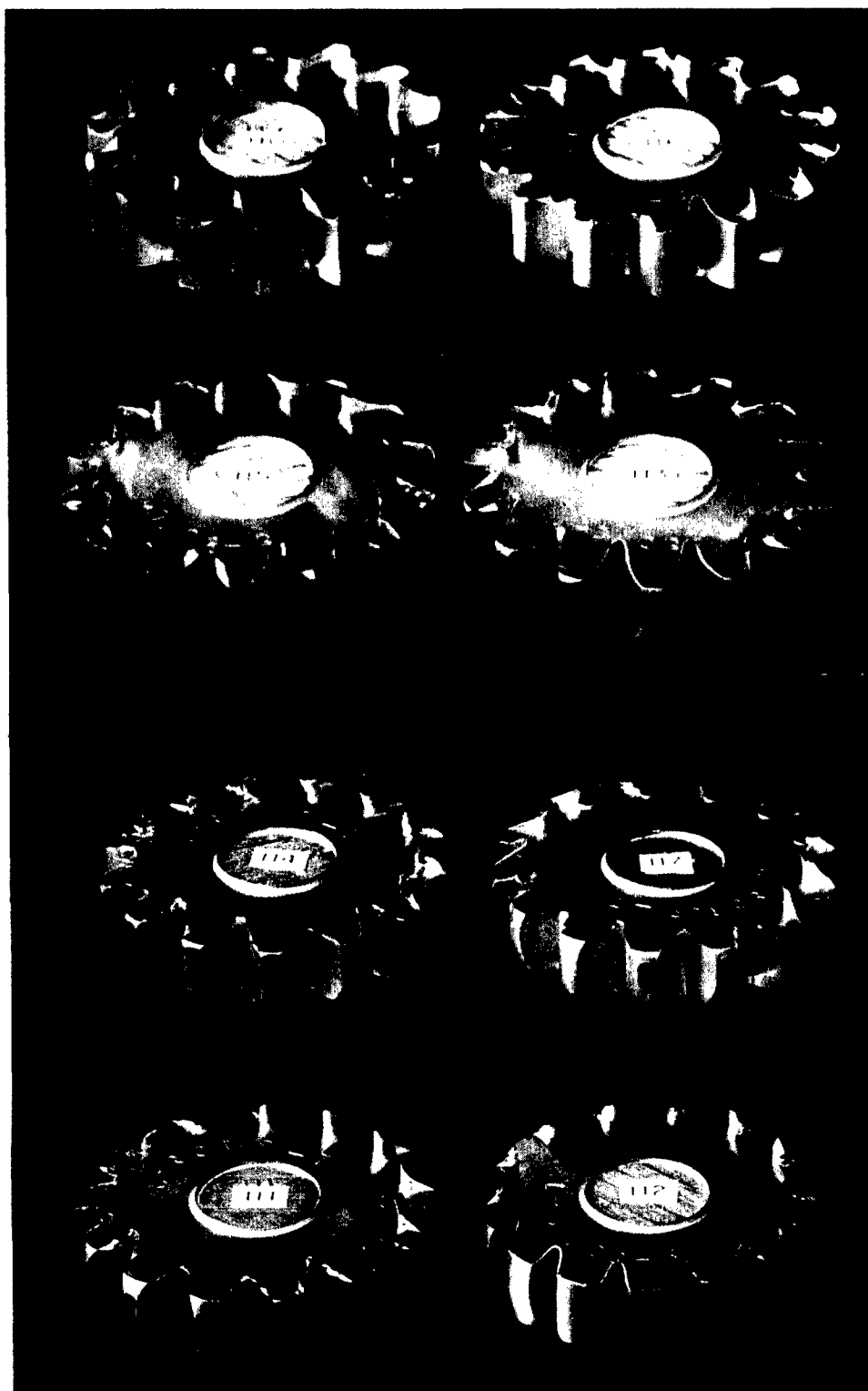


FIGURE G-10. Isometric View of Radial Flow Trial Specimen Numbers 110 Through 117 (no lubricant)

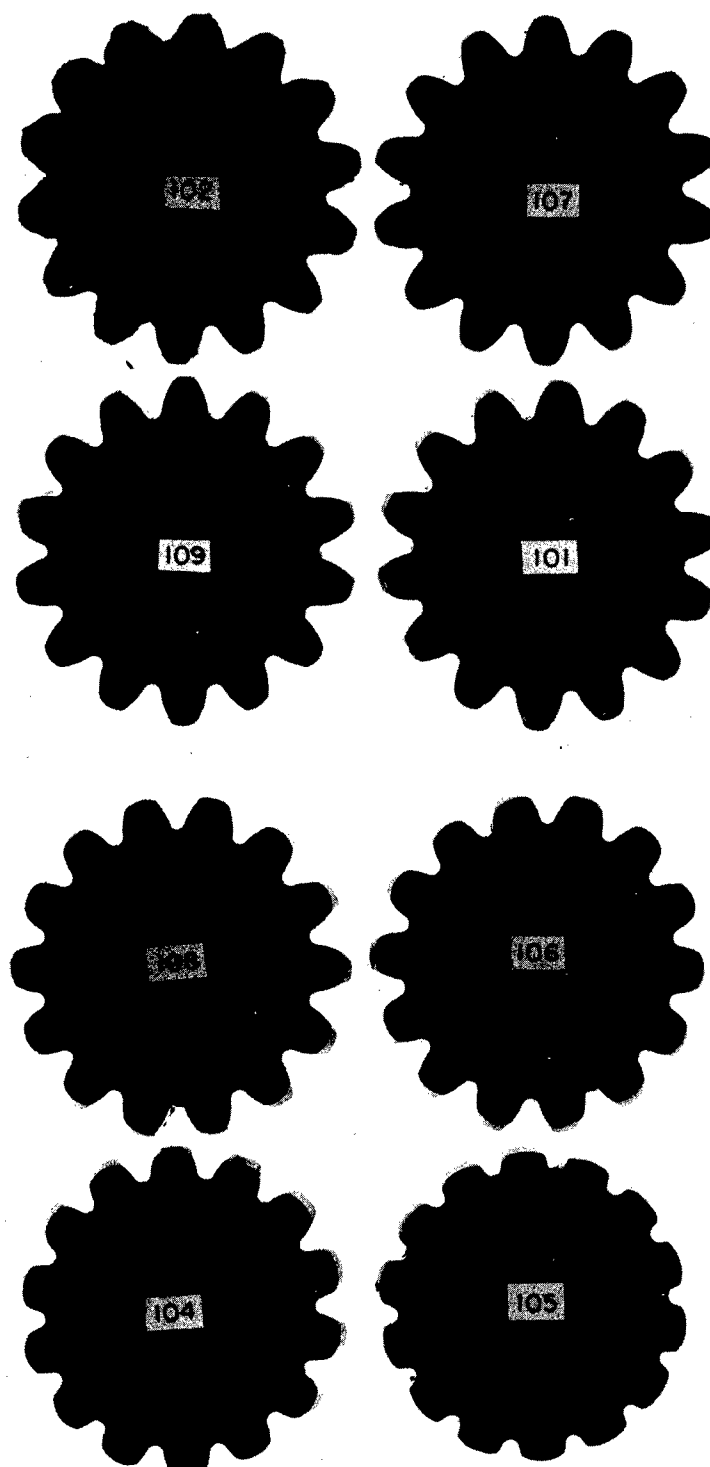


FIGURE G-11. Bottom View of Radial Flow Trial Specimen Numbers 101 Through 109 (PbO + oil lubricant; specimen No. 103 not shown)

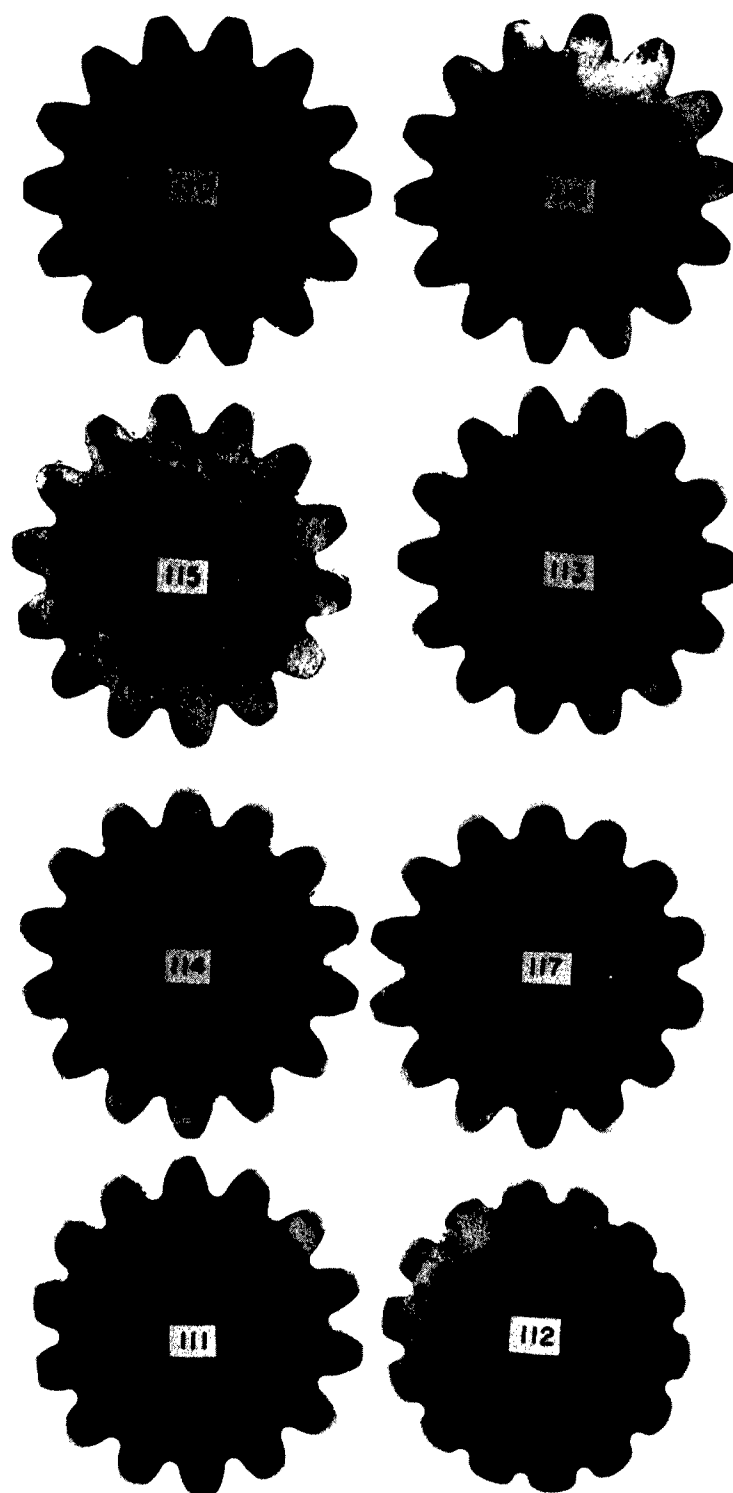


FIGURE G-12. Bottom View of Radial Flow Trial Specimen Numbers 110 Through 117 (no lubricant)

110 through 117). The most difficult areas to fill on the forging were the corners of the gear teeth at the tip of each tooth. These should be the most difficult areas to force the material into.

4.4. Comparison with FEM Results

As stated in Appendix C, the ratio of radial pressure to flow stress which is required for maximum die filling is 5.0 as predicted by the FEM program ALPID. In order to compute this ratio for the lead modeling trials, the flow stress of the lead had to be determined. Using a program called RINGFS, (4) each load-stroke curve from the lubrication tests was digitized and the data was manipulated to compute the flow stress curve for each ring used in the lubrication tests. All of these curves were similar, one of which is shown in Figure G-13. This curve indicates that the average flow stress and the maximum flow stress are both approximately equal to 2500 psi. Using this value for the maximum flow stress, the corresponding ratio of radial pressure to flow stress can be computed.

Assuming a hydrostatic state of stress, the radial pressure was determined by dividing the peak load by the area of the gear as determined in a gear die design program called GEARDI (GEAR Die design). Table G-3 summarizes this data. Specimen numbers 101, 107, and 109 most nearly represent the load at which the die was just filled (number 102 exhibited compacted lubricant in the corners which suggested the presence of a higher load than necessary to produce complete filling). The average value for the radial pressure to flow stress ratio ($p/\bar{\sigma}$) for these three specimens was approximately equal to 5.38 which agrees closely with the FEM result of ($p/\bar{\sigma}$) = 5.0.

In the GEARDI program, the user can specify the amount of corner-filling desired for a particular die design. The program then uses empirical formulas to compute the required punch pressure and flow stress for a given material. These values are tabulated in Table G-4. A comparison of the FEM and GEARDI results is plotted in Figure G-14. Notice that the plot of the GEARDI results shows a drop in the ($p/\bar{\sigma}$) ratio before an increase. The cause of this decrease is not known but is most likely due to the assumptions which were made in approximating the shape of the gear tooth cavity with a simple geometry for which load equations were derived. The similarity of the two curves in Figure G-14 supports the use of the equations in the GEARDI program which allows for much quicker evaluation of forging loads as compared to a lengthy finite element analysis.

The close agreement between the FEM, GEARDI, and lead modeling results suggests that to achieve complete filling of the die

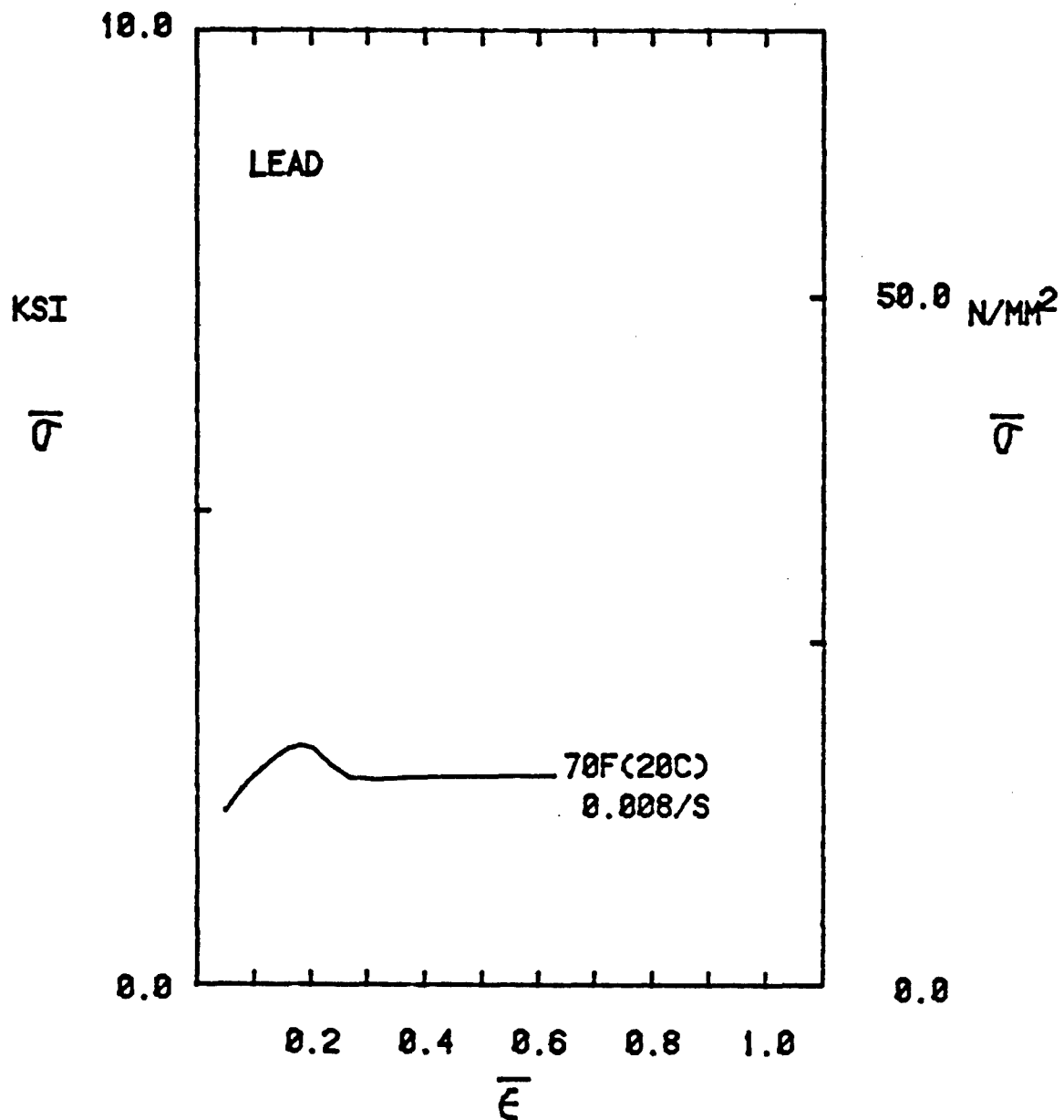


FIGURE G-13. Typical Flow Stress Curve for Lead Using Ring Test Data and the Computer Program RINGFS

TABLE G-3. Ratio of Radial Pressure to Flow Stress for Various Radial Flow Test Specimens

Trial No.	Deformation Pressure, P (ksi)	$P/\bar{\sigma}$
101	11.94	4.78
102	33.79	13.52
103	16.01	6.40
104	7.00	2.80
105	5.11	2.05
106	7.78	3.11
107	15.96	6.39
108	8.94	3.57
109	12.45	4.98

TABLE G-4. Radial pressure and flow stress values for lead at various stages of corner tooth filling as determined by the GEARDI program

<u>Percent Fill</u>	<u>Punch Pressure P (ksi)</u>	<u>Average Flow Stress, σ (ksi)</u>	<u>P / σ</u>
0	3.57	0.9938	3.58
10	3.60	0.9938	3.61
20	3.64	0.9938	3.65
30	3.70	0.9938	3.71
40	3.77	0.9938	3.78
50	3.87	0.9938	3.88
60	4.02	0.9938	4.03
70	4.27	0.9938	4.28
80	4.77	0.9938	4.78
90	6.27	0.9938	6.29

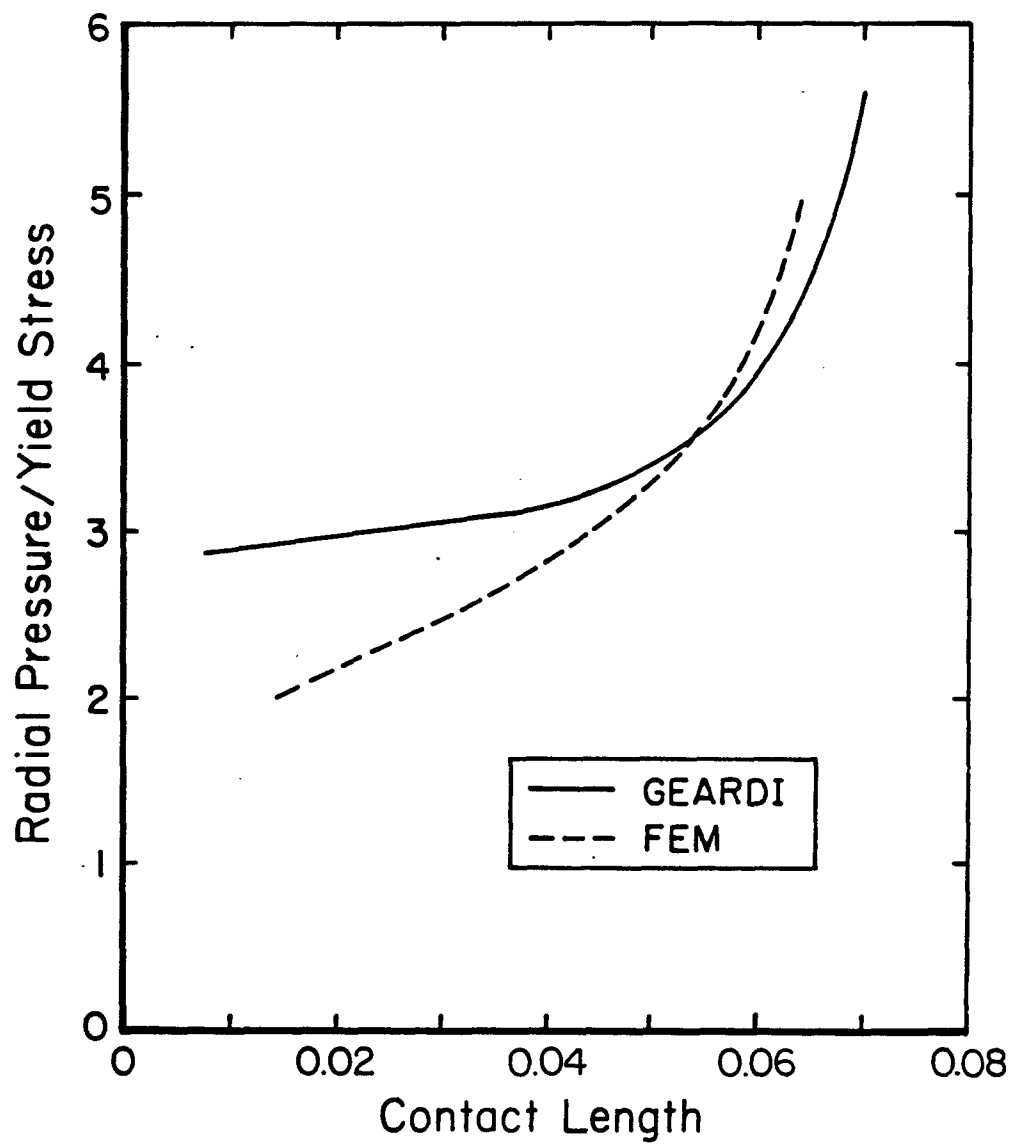


FIGURE G-14. Comparison of FEM and GEARDI Results for Corner Filling of the Tip of a Single Gear Tooth

cavity, the designer should not need a punch pressure greater than five times the flow stress of the material. Thus, if the flow stress of a particular material were 50 ksi, the maximum pressure required for complete filling of the gear teeth corners would be 250 ksi.

The results of these radial forging simulations have several assumptions preceding them and may not be representative of the actual forging process. In order to accurately predict the punch pressure required for forging gears, a final model study was done using actual production tooling and production-size billets.

5.0. PRODUCTION SCALE SIMULATION

5.1. Tool Setup

The tool setup for the simulation using production-size billets and production-size tooling is shown in Figure G-15. In addition to the configuration of Figure G-15, another orientation of the tools was used for a comparison of loads and degree of die filling. This is shown in Figure G-16. In this set of trials, lead specimen numbers 201 through 213 were lubricated on all surfaces using PbO and motor oil. No lubricant was applied to the die, the punch or the counter punch.

5.2. Test Procedure

Similar to the radial flow tests, initially a billet was completely deformed to determine the peak load. The load stroke curve was then divided into load segments and lead specimens were forged to a variety of final load values. A 200-ton Baldwin Universal Testing Machine was used for this series of tests. In some cases the punch was moving (Figure G-15). In other cases the punch was stationary and the counter punch was moving (Figure G-16). The billet dimensions, lubrication conditions, tool orientation and forging load are summarized in Table G-5. Figure G-17 shows a typical load vs. stroke curve for the production scale simulations.

5.3. Analysis of Forged Specimens

After forging the 16 samples, each lead specimen was sectioned through the center, parallel to the axis of the gear. The cut surfaces were then machined smooth and photographs were taken showing the section view and the partially formed gear teeth. These photographs are shown in Figures G-18 through G-23. Only those specimens which were formed using PbO and oil as a lubricant have been shown. In the partially-formed stage, each gear had a bulge somewhere between the two ends of the billet. The position

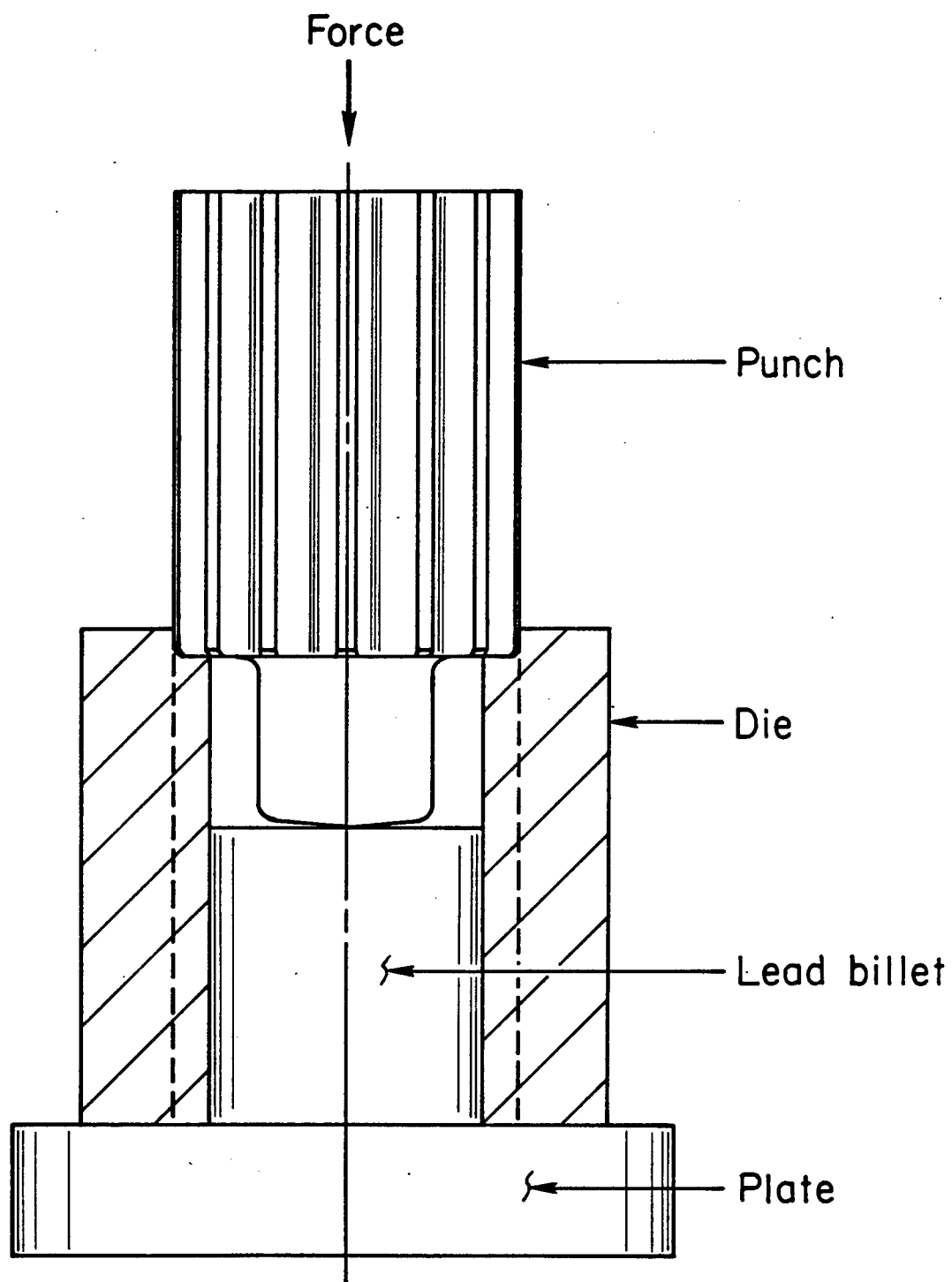


FIGURE G-15. Production Scale Tooling Setup; Moving Punch

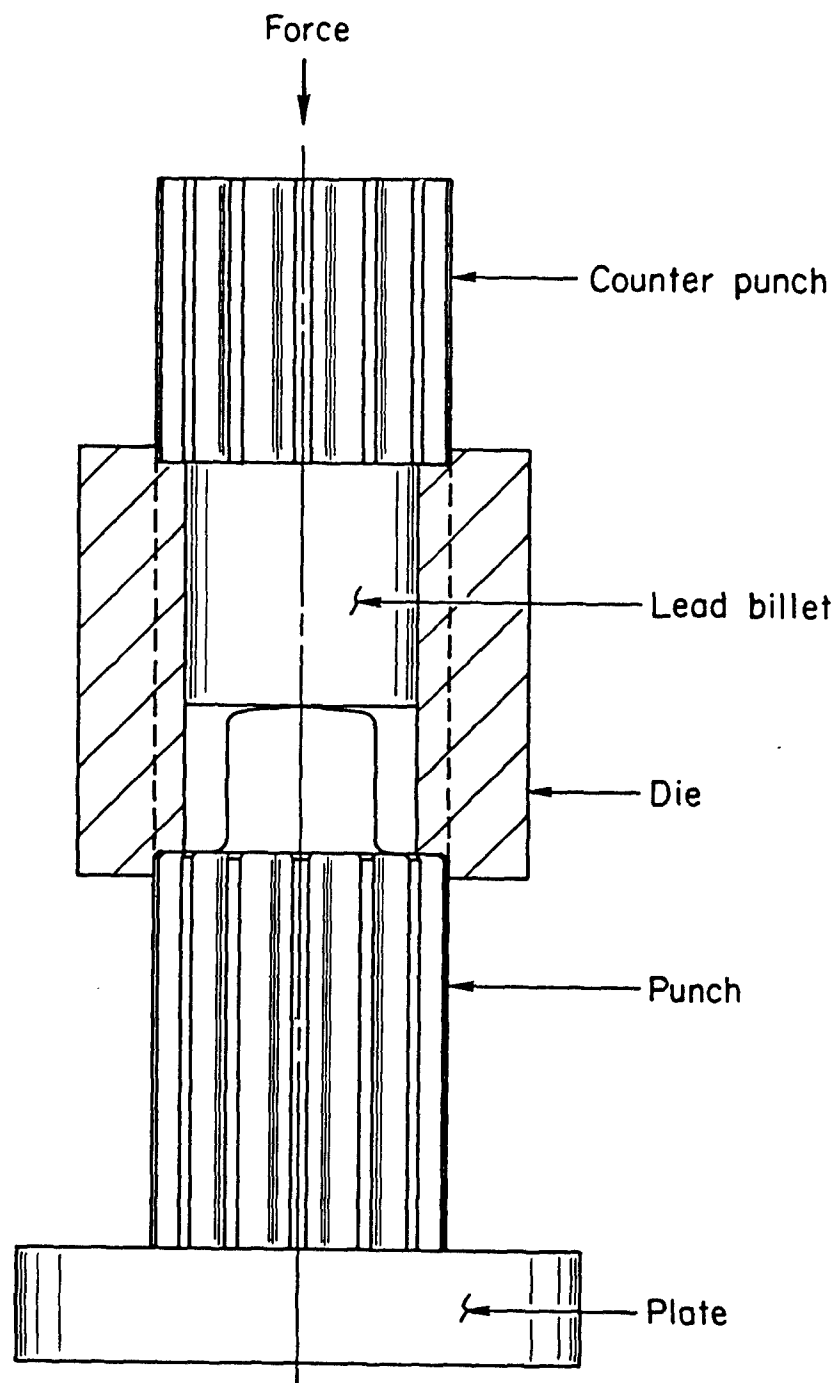


FIGURE G-16. Production Scale Tooling; Stationary Punch, Moving Counter Punch

TABLE G-5. Production Scale Simulation Forging Data

Trial No.	Diameter, inch	Lead Billet Height, inch	Lubricant	Die Lubricant	Punch, Stationary (S) Moving (M)	Deformation Load, k lb	Maximum Effect Load, k lb	Crosshead Speed, in./min
201	2.050	2.201	PbO + oil	None	S	43.0	—	0.3
202	2.050	1.906	Ditto	"	M	181.0	—	0.3
203	2.049	2.195	"	"	S	181.5	—	0.4
204	2.050	2.198	"	"	S	100.0	—	0.4
205	2.050	2.201	"	"	S	140.0	—	0.4
206	2.050	2.199	"	"	S	44.0	—	0.4
207	2.049	2.199	"	"	S	45.5	20.0	0.4
208	2.050	2.199	None	"	S	141.0	30.0	0.4
209	2.050	1.944	PbO + oil	"	M	36.0	—	0.4
210	2.050	1.952	Ditto	"	M	36.0	9.0	0.4
211	2.050	1.946	"	"	M	22.0	5.0	0.4
212	2.050	2.200	"	"	S	29.0	9.0	0.4
213	2.050	1.955	"	"	M	11.0	5.0	0.4
214	2.050	2.201	None	PbO + oil(a)	S	120.0	22.5	0.4
215	2.049	2.199	"	K-Y jelly(b)	S	150.6	29.5	0.4
216	2.050	2.204	K-Y jelly	K-Y jelly(c)	S	101.0	24.0	0.4

(a) Lubricant applied to punch and insert working faces only with brush.

(b) K-Y lubricant applied to punch and insert working faces only by rubbing.

(c) Lubricant applied to all working surfaces of tooling.

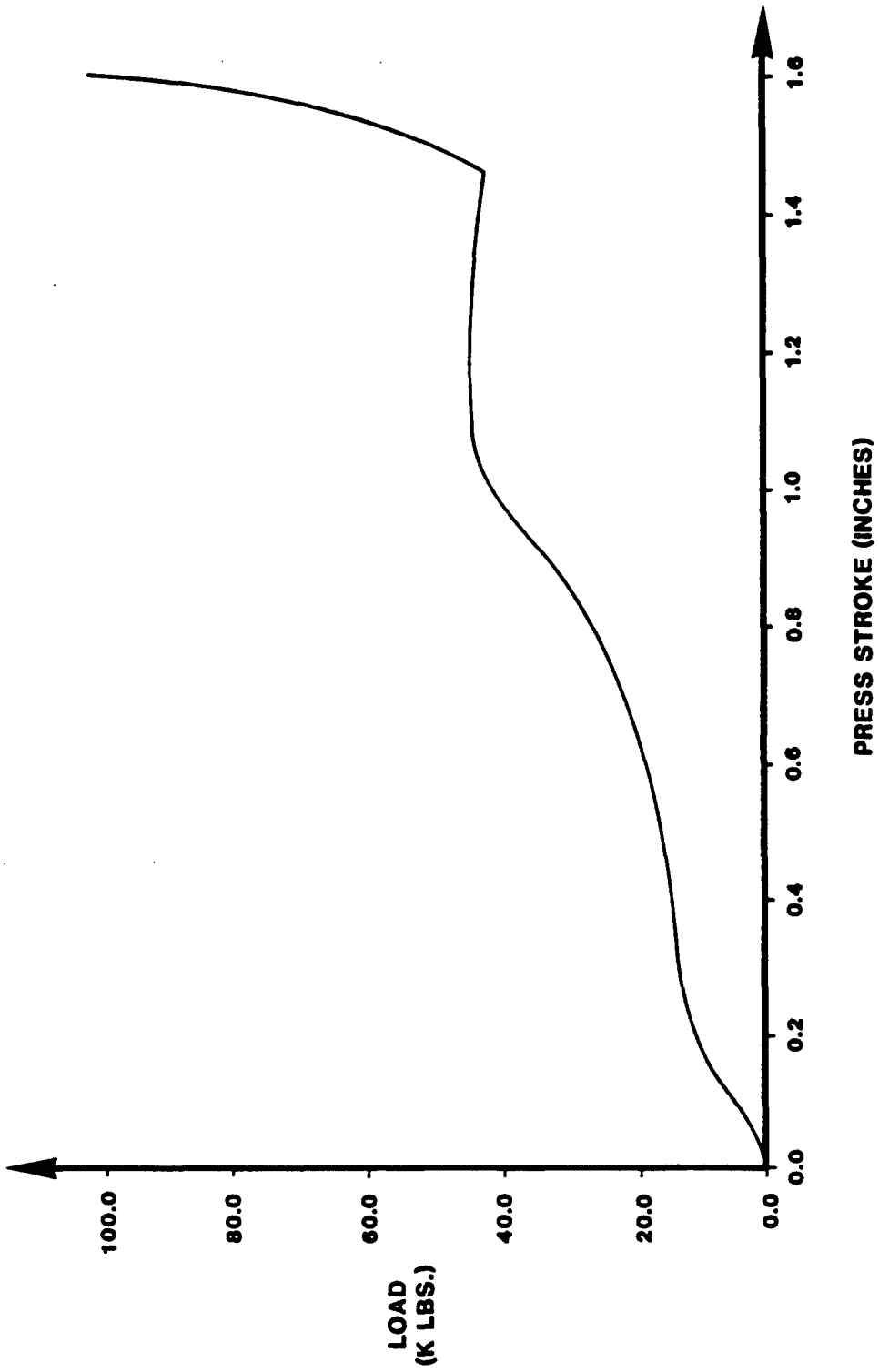


FIGURE G-17. Typical Load-stroke Curve for Production Scale Simulation

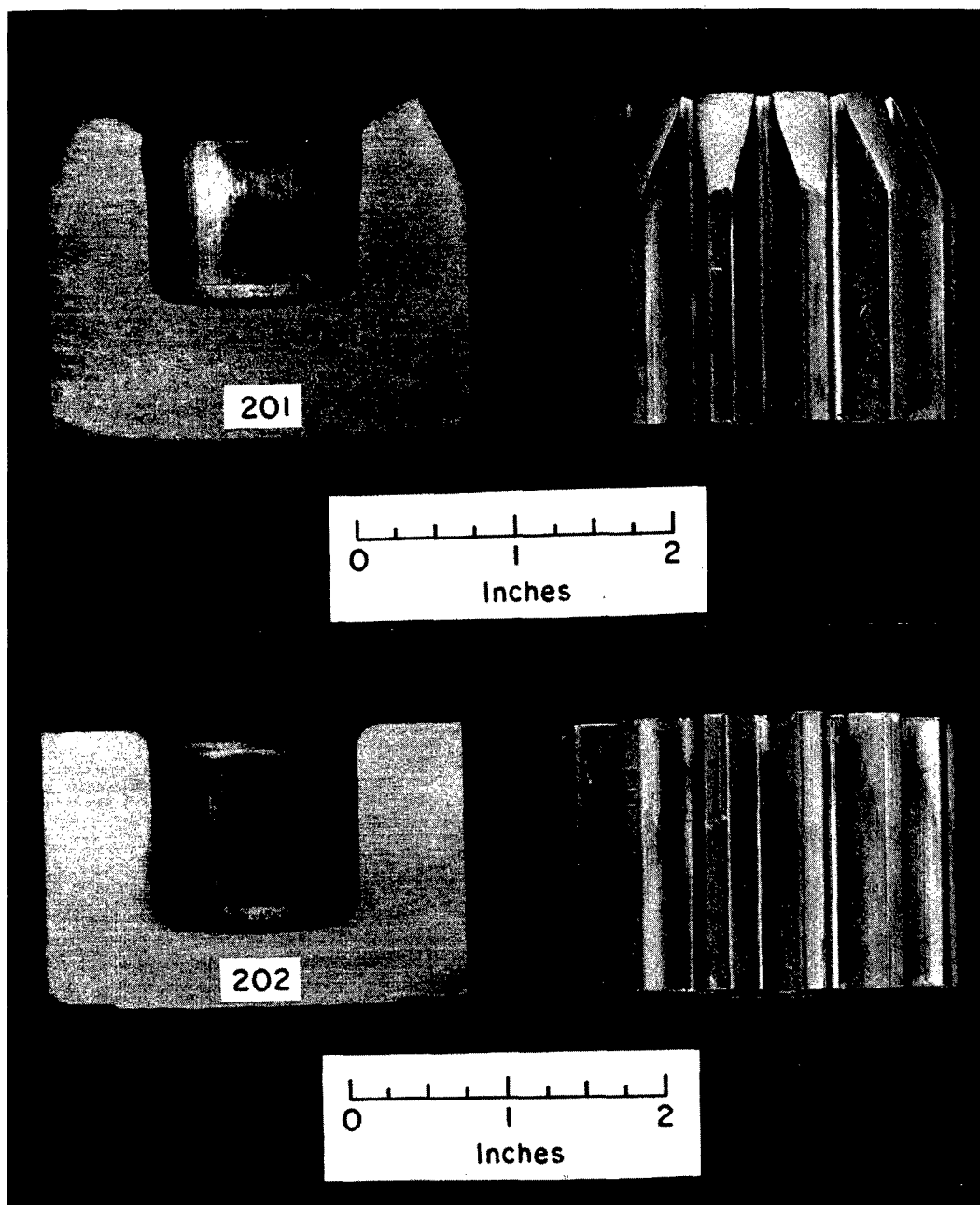


FIGURE G-18. Production Scale Simulation Specimen Numbers 201 and 202

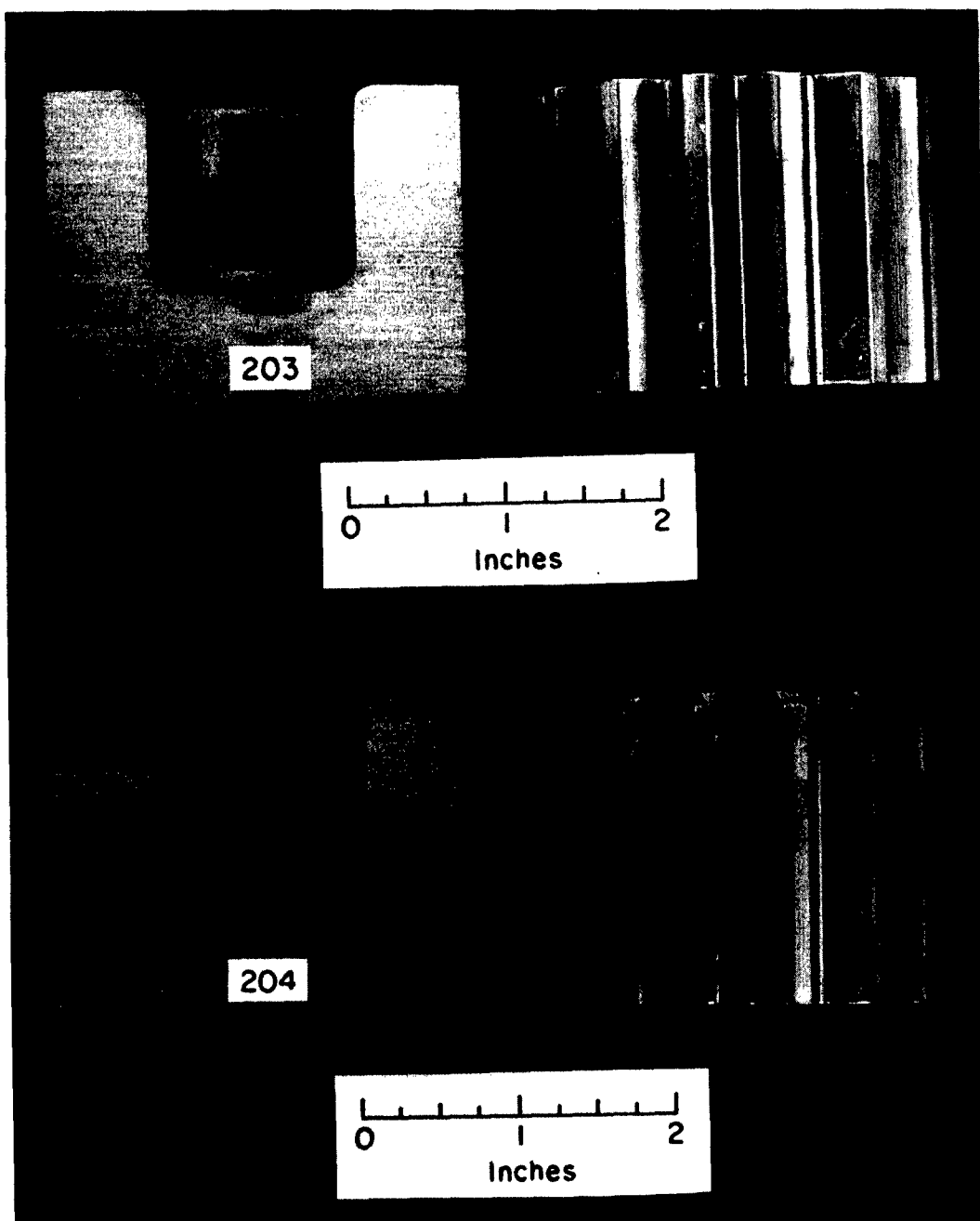


FIGURE G-19. Production Scale Simulation Specimen Numbers 203 and 204

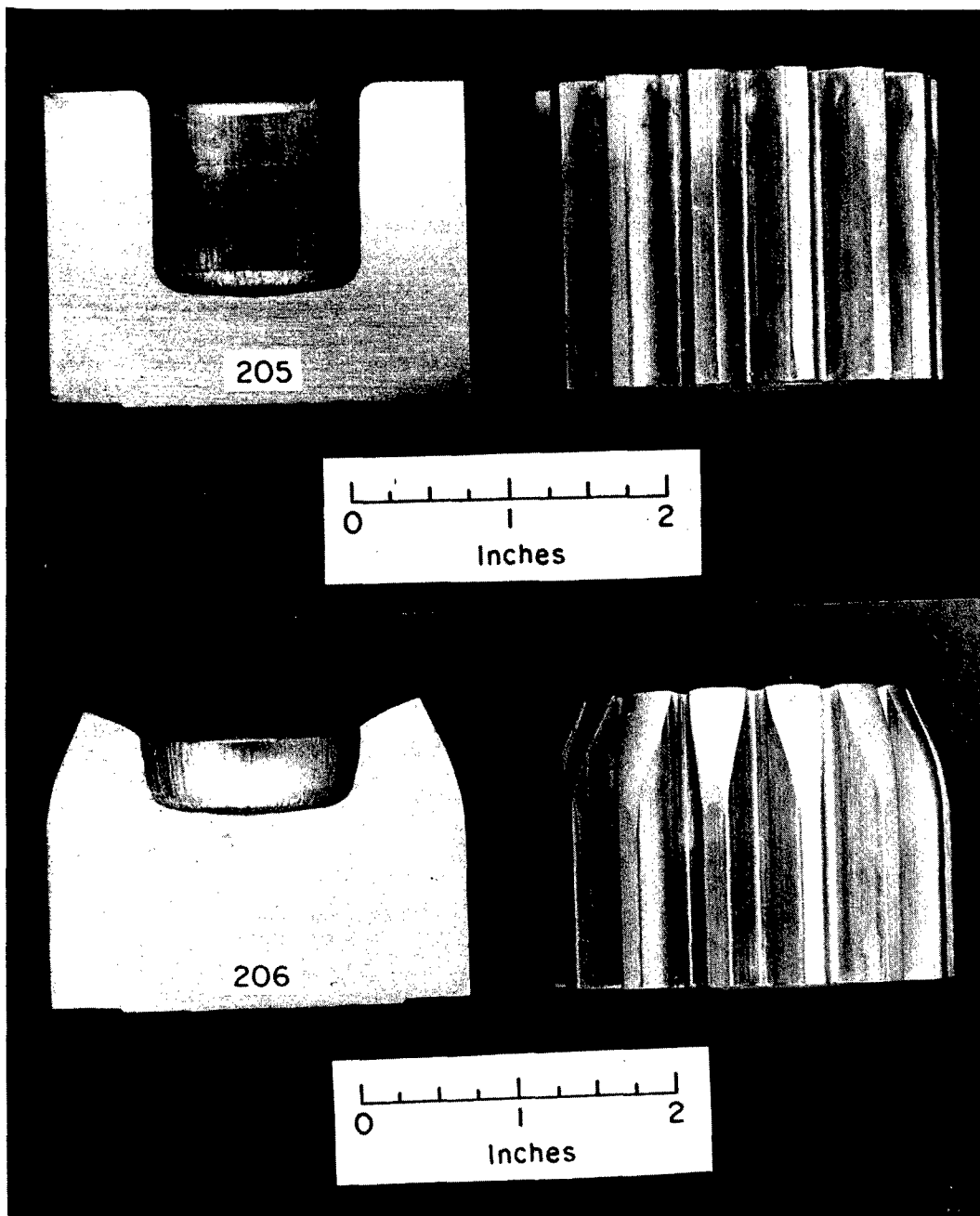


FIGURE G-20. Production Scale Simulation Specimen Numbers 205 and 206

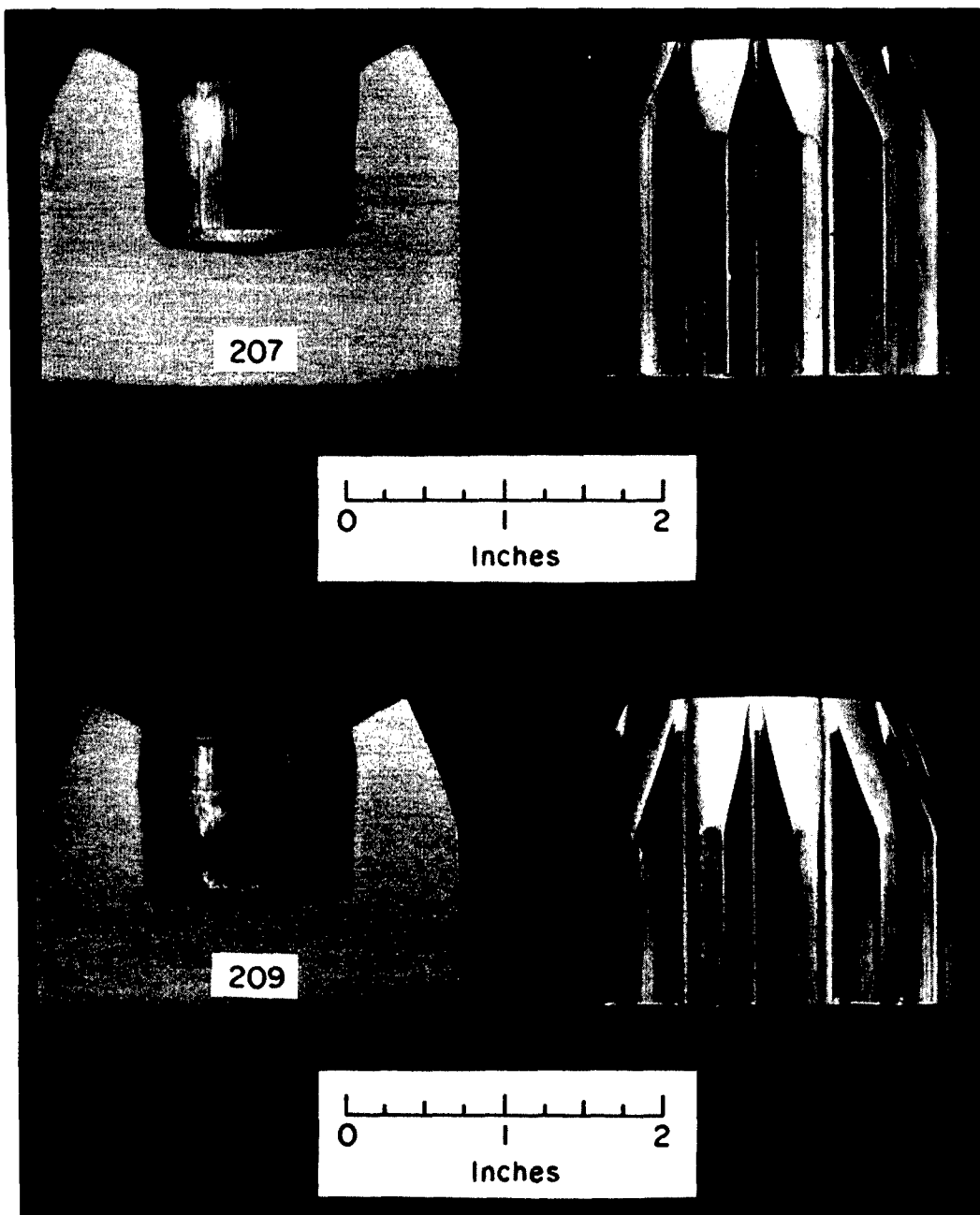


FIGURE G-21. Production Scale Simulation Specimen Numbers 207 and 209

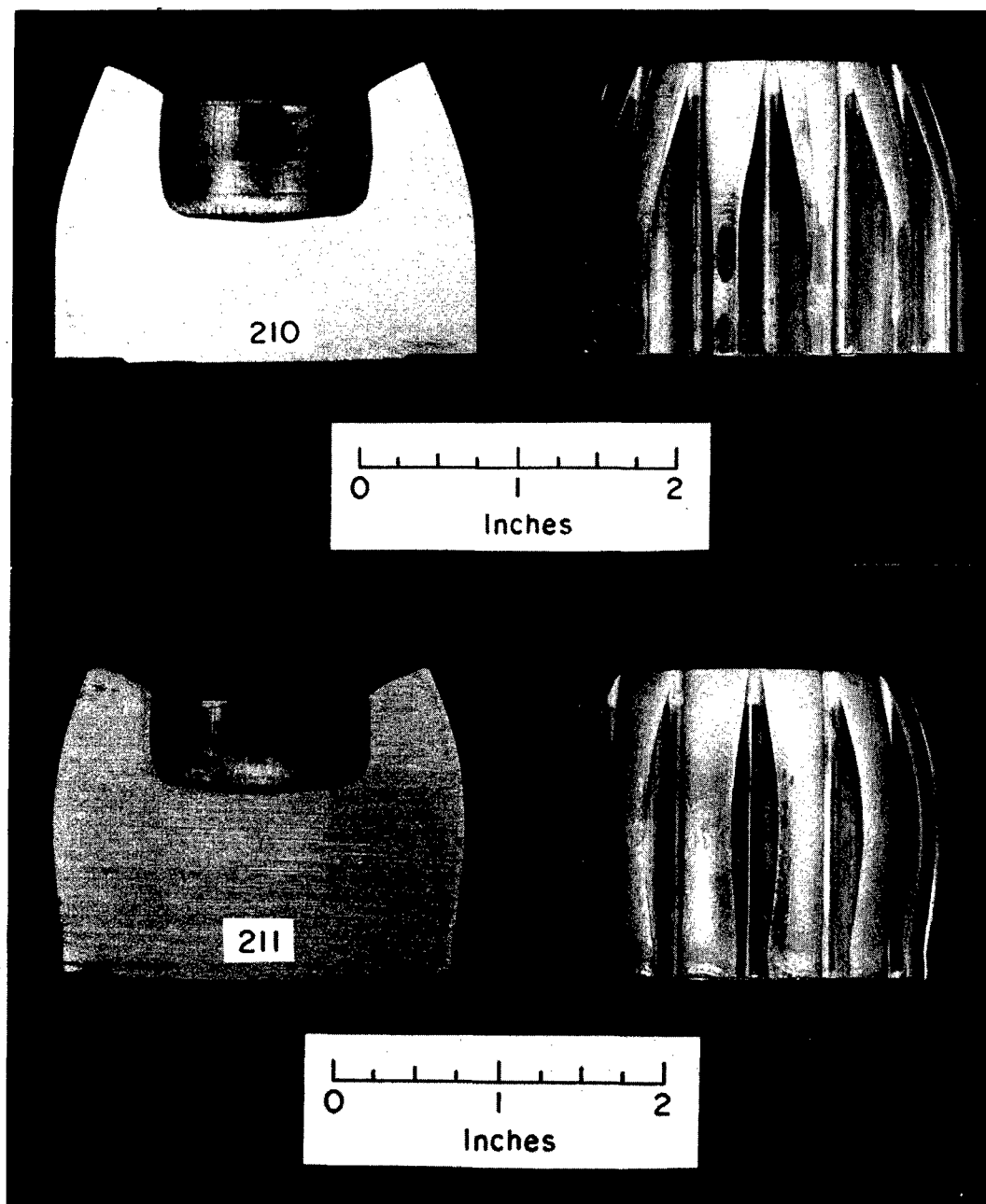


FIGURE G-22. Production Scale Simulation Specimen Numbers 210 and 211

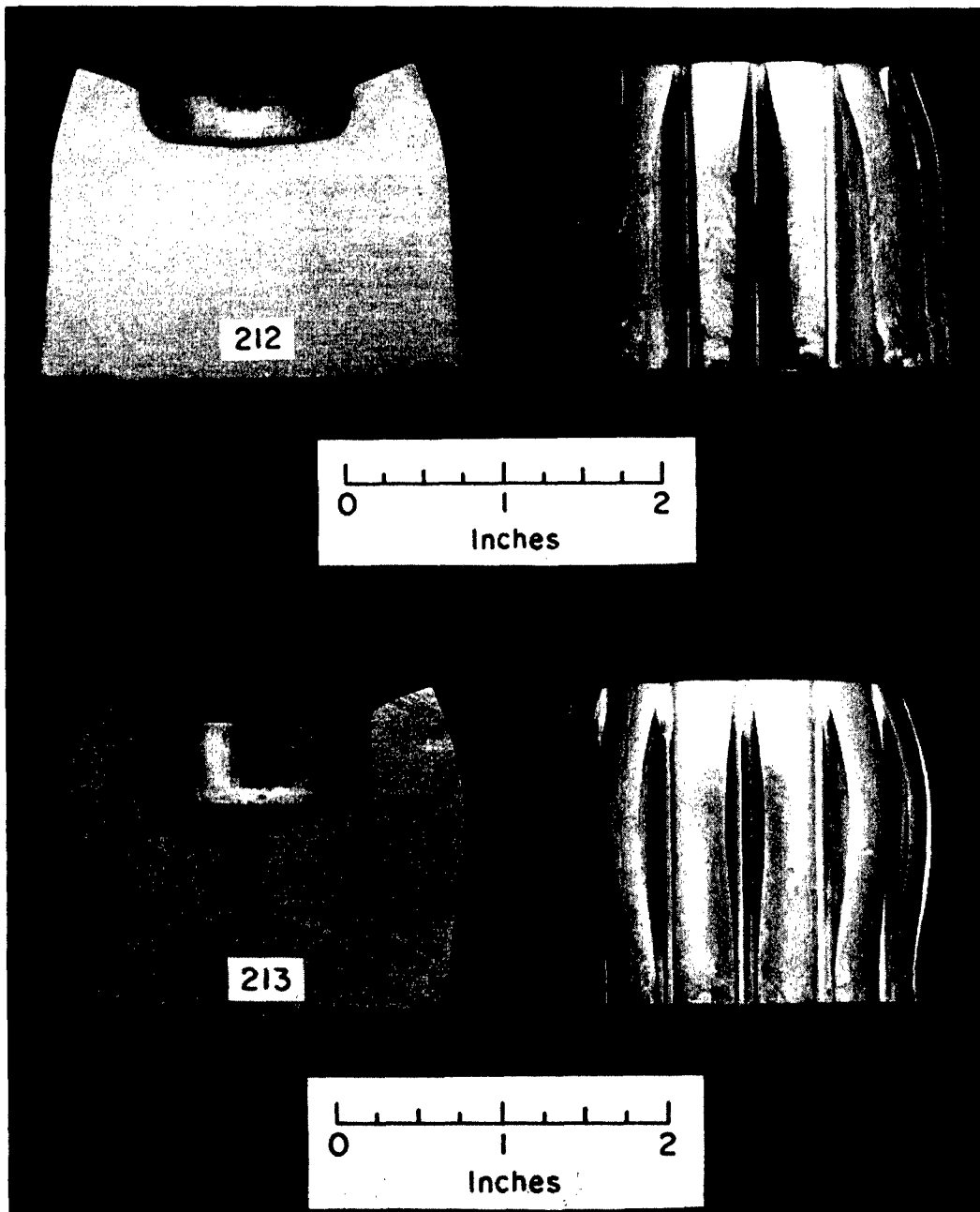


FIGURE G-23. Production Scale Simulation Specimen Numbers 212 and 213

of the bulge usually coincided with the location of the tip of the punch, which was to be expected.

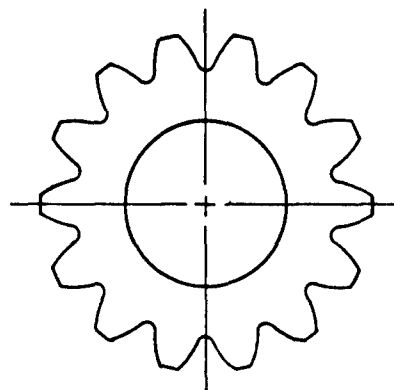
5.3.1. Geometry. Each partially-formed gear had a geometry similar to that shown in Figure G-24. The indicated dimensions in Figure G-24 were measured and are summarized in Table G-6 along with the ratios of several pairs of measurements. These ratios along with the dimension 'D' and the forging load have been plotted against the press stroke in Figure G-25 (punch moving) and Figure G-26 (punch stationary, moving counter punch).

5.3.1.1. Curve I. Referring to Figures G-25 and G-26, Curve I shows the change in the ratio between the final height of the specimen, 'A', and the original height. In Figure G-25 this ratio is virtually constant (1.0) up to the point on the curve which corresponds to the point in the simulation when the material completely filled the tooth cavity on a single plane (when dimension 'B' became non-zero). This is where Curves V and VI begin at stroke location 1 on Figure G-25. During the simulation, as 'B' increased, 'A' began to decrease and then increased again until the material touched the top of the punch, outside the center projection. At this point, the material flow was no longer backwards, but into the gear teeth. The value of 'A' decreased again (location 2) and then increased rapidly as the die filled completely.

Conversely, when the counter punch was moving and the punch was stationary (Figure G-26), the value of 'A' continuously decreased from the start of the process until the material filled the tooth cavity on a single plane. Similar to Figure G-25, Figure G-26 shows how 'A' decreased and then increased as the load peaked and the teeth filled completely.

5.3.1.2. Curve II. Curve II is a plot of the dimension 'D' vs. press stroke. Both Figures G-25 and G-26 show that 'D' increased from the start of the process up to location 2. At the point in the simulation corresponding to location 2 in Figures G-25 and G-26, the material contacted the top of the punch outside the center projection, and the value of 'D' remained constant as 'A' decreased and the teeth filled. The moving punch plot of 'D' shows much greater variation in the rate at which 'D' changed. At the beginning of the process, 'D' increased rapidly and then slowed down, almost to a stop, until location 1 was reached. At location 1, the load began to increase after the material touched the O.D. and the dimension again began to increase rapidly to location 2 due to a lower load requirement then for filling of the tooth cavity.

When the punch was stationary it appears that 'D' increased at a steady rate with no inflection point when location 1 was reached.



- A - Overall height
- B - Length of formed teeth
- C - Web thickness
- D - Cavity depth

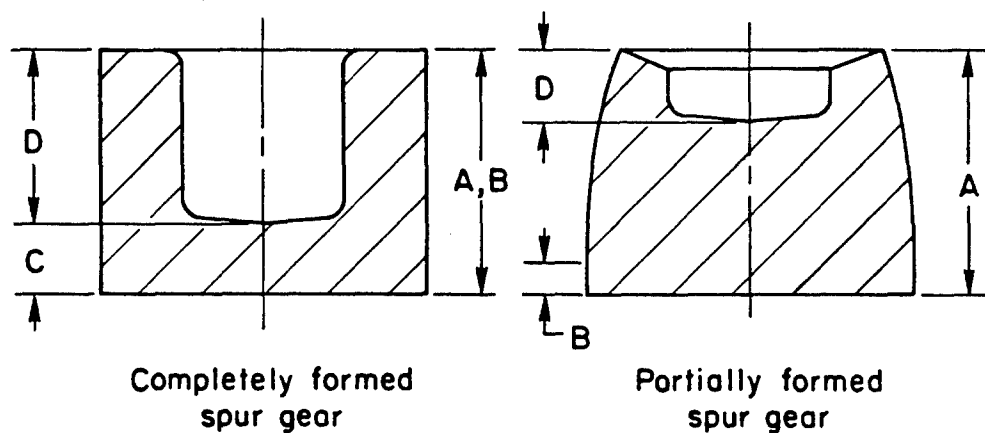


FIGURE G-24. Geometry of Partially and Completely Formed Spur Gears from Production Scale Simulation

TABLE G-6. Dimensions of Forged and Partially Forged Lead Spur Gears

Trial No.	"A"	"B"	Dimension, inches or unitless; refer to Figure G-7	B/A	D/A	A/H _{B,O} ^{††}	Final Load, k lb	Total Punch* Travel, in. [1]	Comments
			"C"						
			"D"***						
201	2.080	1.400	0.800	0.673	1.094	0.615	42.0	1.401	—
202	1.753	1.720	0.445	0.981	1.315	0.746	181.0	1.461	Fully formed gear, cavity depth 1.308 inches
203	1.962	1.929	0.654	0.983	1.475	0.667	181.5	1.541	Ditto
204	1.978	1.805	0.670	0.913	1.380	0.661	100.0	1.528	—
205	1.975	1.942	0.667	0.983	1.485	0.662	140.0	1.534	Fully formed gear, cavity depth 1.308 inches
206*	1.905	1.060	1.208	0.697	1.521	0.360	44.0	0.991	—
207†	2.085	1.430	0.790	1.295	1.104	0.621	44.0	1.409	—
208	1.960	1.927	0.652	—	—	—	141.0	1.547	Fully formed gear, cavity depth 1.308 inches
209	1.928	1.027	0.627	1.301	0.789	0.675	34.0	1.317	—
210	1.847	0.710	0.857	0.990	0.384	0.717	36.0	1.095	Some teeth not filled to corners
211	1.870	None	1.092	0.778	0.000	0.416	22.0	0.854	—
212	1.895	0.064	1.393	0.502	0.034	0.265	29.0	0.807	[2]
213	1.934	None	1.186	0.748	0.000	0.387	11.0	0.769	—

* Average backflash height = 0.5".

† Average backflash height = 0.8".

***"D" = total stroke — (original billet height — "A").

††H_{B,O} = original billet height.

[1] Total punch travel refers to the total distance the moving part of the setup travelled. In Trials 202, 209-211, and 213, the moving part is the piece used as the punch in a production setup. The remaining cases used an inverted production setup with a stationary punch and the counter punch was the moving part.

[2] Seven teeth show some complete filling to height of tooth, seven not filled. Dimension "B" (Figure G-7) represents average height.

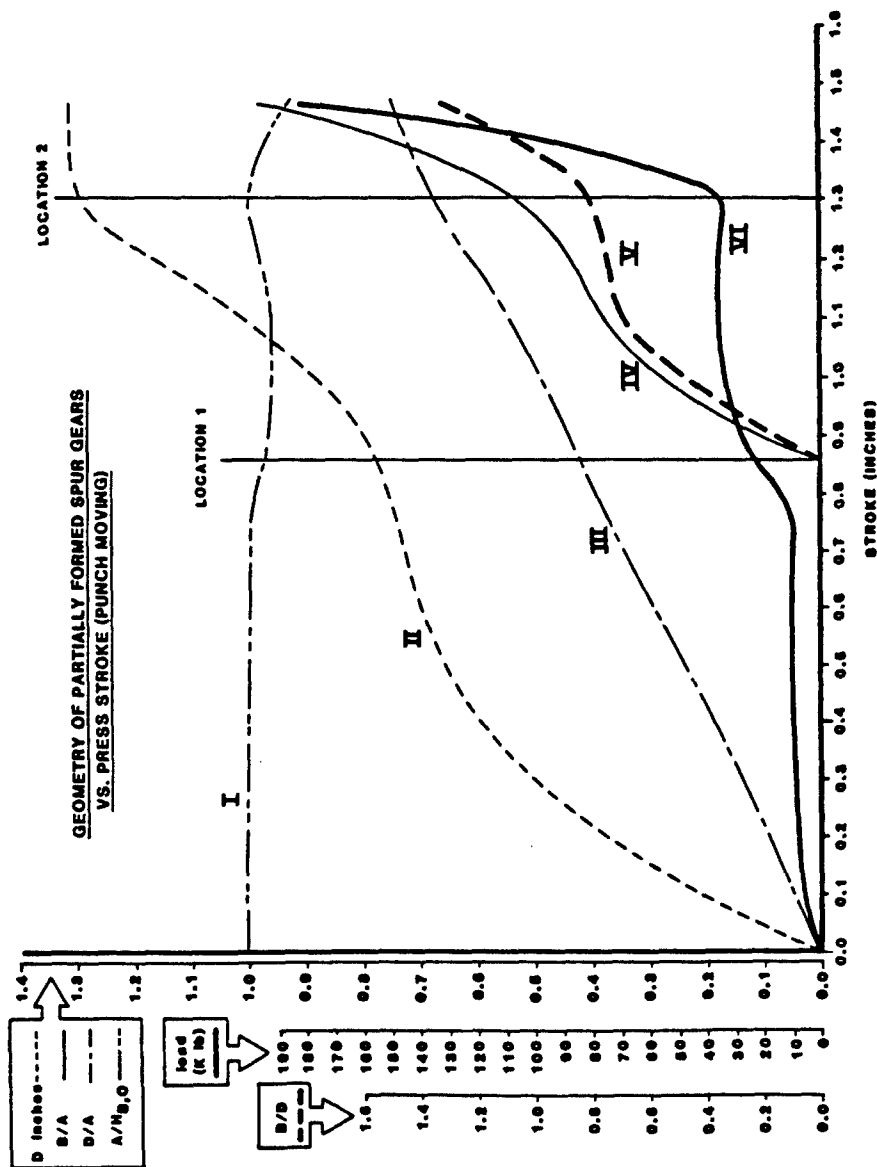


FIGURE G-25. Variations in Gear Dimensions with Respect to Moving Punch Position

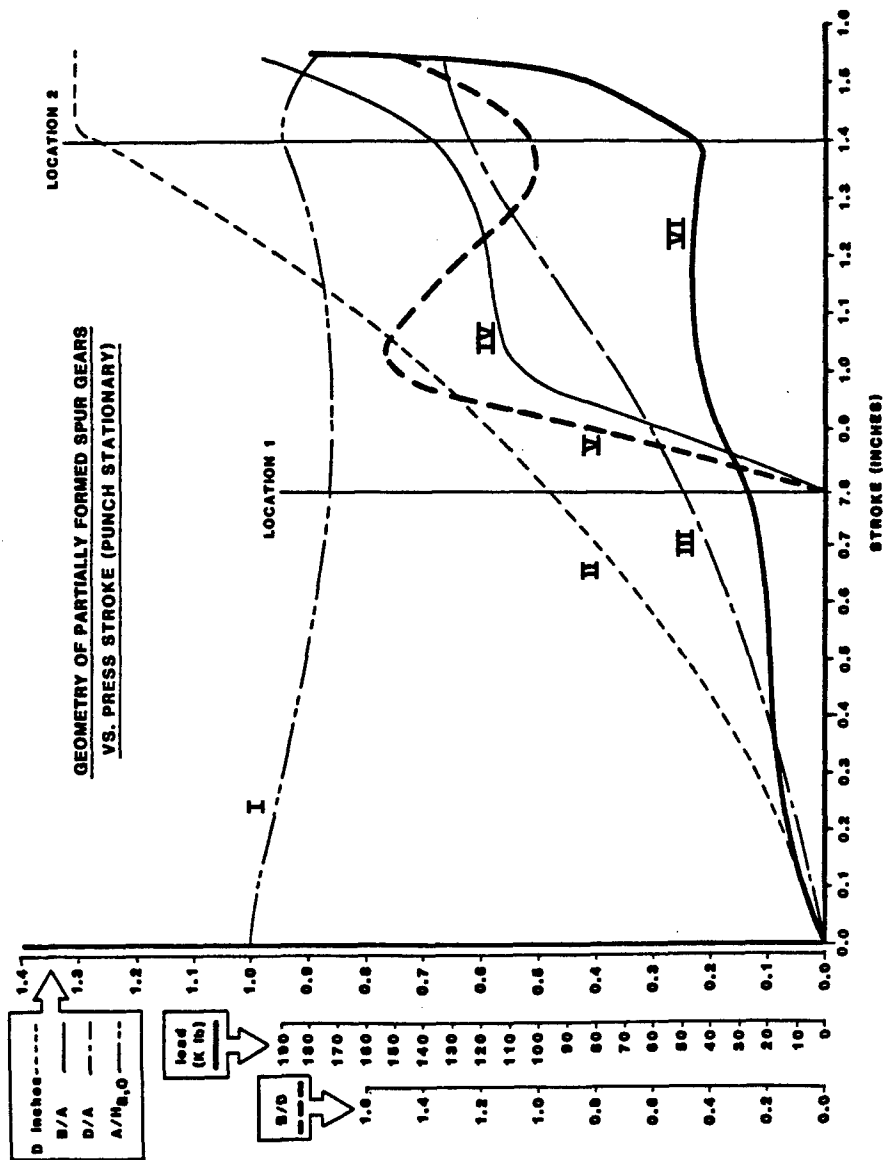


FIGURE G-26. Variations in Gear Dimensions with Respect to Moving Counter Punch Position (punch is inverted and stationary)

The source of this phenomenon is difficult to determine. It is likely that the dimensions 'A' and 'D' were closely related and in such a way that even though 'D' was increasing in length, material may not really have been flowing into this region at all since 'A' was decreasing. It could be that 'D' was increasing because the center projection was pushing material out of the center of the billet and into the tooth cavities, thus giving the impression that the material was flowing from the billet into the region where 'D' was measured.

5.3.1.3. Curve II. The variation of the ratio of 'D' to 'A', shown as curve III in both Figures G-25 and G-26, was basically the same for the moving punch and the moving counter punch, increasing at a constant rate. This plot does not give any further indication of where the material moved in relation to the dimension 'D'. In Figure G-25, even though Curves I and II have multiple inflection points, Curve III which is based on Curves I and II, shows no such inflection points.

5.3.1.4. Curve IV. Curve IV is also shaped the same in both Figures G-25 and G-26. Each curve shows the length of completely formed teeth 'B' as zero up to a certain point (location 1), and then a sudden and rapid increase in the formed length. The curve then levels off somewhat until location 2 in the simulation was reached, at which point the value of 'B'/'A' again increased rapidly with the load as the tooth cavity was completely filled. It appears that the leveling-off point occurred at the point where Curve I increases after the initial decline. The explanation is that at this point, the load required to change the dimension in Curve I was lower than the load required to continue to completely form the gear tooth in the die cavity.

Since materials tend to plastically deform in the region of least resistance, the ratio of 'A' to the original height (Curve I) changed for a period and the ratio of 'B'/'A' remained unchanged. Then at location 2, the material reached the top of the punch outside the center projection and no longer flowed at the current load. Hence, the tooth cavities resumed filling.

5.3.1.5. Curve V. Curve V reinforces the finding in Curve IV that the completely formed teeth were not continuously developed from beginning to end but rather leveled off for a while before starting to fill again. The trend of Curve V in Figure G-26 shows this particularly well as the value of 'B'/'D' began to drop as the length of 'B' virtually remained unchanged while the value of 'D' (Curve II) continued to increase.

5.3.1.6. Curve VI. The load vs. stroke curve (Curve VI) is basically the same in Figures G-25 and G-26. All of the information gathered does not seem to suggest which configuration

of the tooling was most advantageous for forming of the gear. There were noticeable differences in the way the gear was formed in each arrangement, but there was no indication as to the efficiency of either process or the physical property differences, if any, of the gears forged in either tool setup.

6.0. CONCLUSION

The three-phase modeling study summarized in this appendix has been a useful tool in understanding the principles of forging spur gears. The results support the use of the assumptions utilized in the GEARDI computer program and also agree closely with the FEM analysis described in Appendix C. The full-scale modeling trials have revealed several facts concerning the way in which the material flows to fill the die cavity and the gear teeth. However, the usefulness of this information seems to be limited at this time. In order to take full advantage of the full-scale modeling results, more real forging trials need to be done in more detail.

THIS PAGE LEFT BLANK INTENTIONALLY

LIST OF REFERENCES

- (1) Altan, T., Henning, H. J., and Sabroff, A. M., "The Use of Model Materials in Predicting Forming Loads in Metalworking," ASME Paper No. 69-WA/Prod-9, November, 1969.
- (2) Brill, K., "Use of Model Materials For Determination of Geometrical and Dynamic Factors in Drop Forging," Report from the Drop Forging Research Center, Hanover, West Germany.
- (3) Oh, S. I., Lahoti, G. D., and Altan, T., "ALPID - A General Purpose FEM Program for Metal Forging," NAMRC IX, University Park, 1981.
- (4) Lee, C. H., and Altan, T., "Influence of Flow Stress and Friction Upon Metal Flow in Upset Forging of Rings and Cylinders," J. Engrg. Ind., Trans. ASME, Series B, Vol 94, No. 3, August 1972.

THIS PAGE LEFT BLANK INTENTIONALLY

APPENDIX H

TOOL DESIGN CONCEPTS FOR FORMING SPUR AND HELICAL GEARS

THIS PAGE LEFT BLANK INTENTIONALLY

1.0. INTRODUCTION

The success of forming both spur and helical gears depends to a great extent on the design and manufacture of the tooling. Several forming processes can be theoretically used for forming a gear tooth. The most important processes are rolling, forging and extrusion. Table H-1 (1)* shows a schematic representation of various forming processes for manufacturing gears. Some of the tooling concepts from Table H-1 will be briefly discussed in this appendix.

2.0. ROLLING PROCESSES

2.1. Crossrolling

For spur gears, the crossrolling (5-1 and 5-3 in Table H-1) and the longitudinal rolling with a rotating head (6-1 in Table H-1) processes hold much promise. The ROTO-FLO process (Figure H-1) corresponding to 5-3 in Table H-1 and the GROB planetary rolling process (2) (Figure H-2) corresponding to 6-1 in Table H-1 are two commercial versions of the above processes. The ROTO-FLO process has been highly successful in forming splines. The GROB process is widely used in Europe for making both spur gears and splines. The application of this method is basically confined to cold-forming and straight tooth shapes (spur gears and splines). The GROB process can be used to make spur gears by forming involute teeth on long shafts and parting them to size. There have been reports of some successful commercial applications of this process.

2.2. Polish Process

A recently-developed process in Poland (3), schematically represented in Figure H-3, is claimed to be superior to the two rolling methods mentioned earlier. The tooling is, however, expensive, especially for large (greater than 3 in; 75 mm) gears/splines.

3.0. FORGING PROCESSES

The concept of a spur gear forging process is shown in Figure H-4 (similar to 1.2 in Table H-1). The process (for spur gears)

*Numbers in parentheses refer to references at the end of the appendix

TABLE H-1. Summary of Major Forming Methods for Manufacturing Splines and Gears

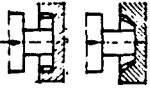




Type of Process	Process Description	Schematic Sketch	Type of Gear Teeth	Achievable Quality Level ISO Class*
Die Forging (Warm/Hot)	1.1 Upsetting with a flat upper die - the upper die does not enter lower die		a) Spur gear and b) bevel gear with a flash at the top surface	a) 10 to 11 b) 9 to 10
	1.2 Upsetting with a flat upper die - the upper die enters the lower die		Spur gear	10 to 11
	1.3 Upsetting between two different die-halves		Gears with two sets of teeth with a flash between the separating surface	10 to 11
	1.4 Upsetting in a rotating die		Bevel gears with flash on the top surface	10 to 11
	1.5 Upsetting in a die with teeth at the bottom surface		Planetary gear	10 to 11

TABLE H-1. Summary of Major Forming Methods for Manufacturing Splines and Gears (continued)



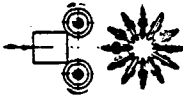
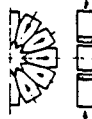
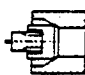
Type of Process	Process Description	Schematic Sketch	Type of Gear Teeth	Achievable Quality Level ISO Class*
Extrusion	2.1 Cold extrusion with toothed punch		Straight/inner toothed components	9 to 10
	2.2 Cold extrusion open die extrusion		Spur gears, splines	9 to 10
	2.3 Pressing the work-piece in a multiroll workhead		Spur gears, splines	10 to 11
Swaging/Side Extrusion	3.1 Swaging with a number of radially moving punches		Splines, planetary gears, chain shafts	9 to 10
	3.2 Side extrusion in a conical die with toothed punch		Internal toothed components, sprocketed boss	9 to 10

TABLE H-1. Summary of Major Forming Methods for Manufacturing Splines and Gears (continued)



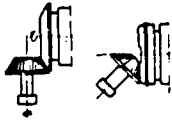



Type of Process	Process Description	Schematic Sketch	Type of Gear Teeth	Achievable Quality Level ISO Class*
Combined Swaging and Extrusion	4.1 Radial Swaging with a number of punches with simultaneous upsetting and piercing		Spur gears with central bore, chain shafts	9 to 10
Crossrolling	5.1 Crossrolling with radial feed of the tool (roll)		Spur gears with straight and inclined teeth	8 to 9
	5.2 Conical rolling		Bevel gears with straight and inclined teeth	9 to 10
	5.3 Rolling between toothed racks		Spur gears, splines	10 to 11

TABLE H-1. Summary of Major Forming Methods for Manufacturing Splines and Gears (continued)

Type of Process	Process Description	Schematic Sketch	Type of Gear Teeth	Achievable Quality Level ISO Class*
Longitudinal Rolling	6.1 Rolling with rotating tool head		Spur gears, splines	8 to 9
	6.2 Rolling with two circular tools arranged perpendicular to the component axis		Spur gears, splines	10 to 11

* The quality level denoted is on the high side of the range for the forging processes and on the low side of the range for the rolling processes. This quality level determines the tolerance of the major important dimension as per ISO. The basic tolerance level is given by

$$i = 0.45 \sqrt[3]{d} + 0.001 \quad d \text{ (}\mu\text{m)}$$

where

i = base tolerance, μm

d = nominal dimension, mm

The tolerance levels for the various classes are obtained by multiplying this base value i by a factor given in the table below:

Class	7	8	9	10	11
Factor	16	25	40	63	100

Lower ISO class numbers indicate closer tolerances and higher class number wider tolerances.

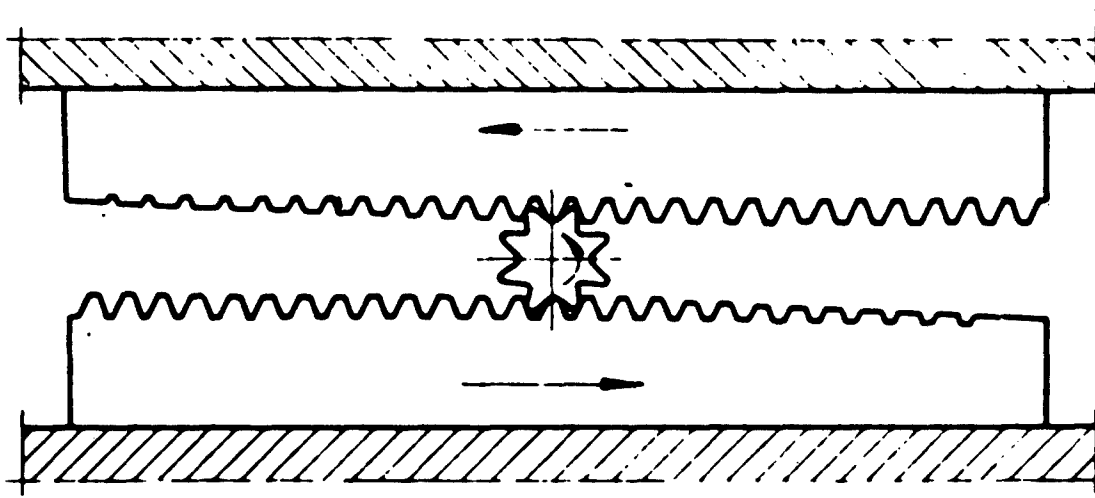


FIGURE H-1. Schematic of a Spline Rolling Operation with Racks (ROTO-FLO proces)

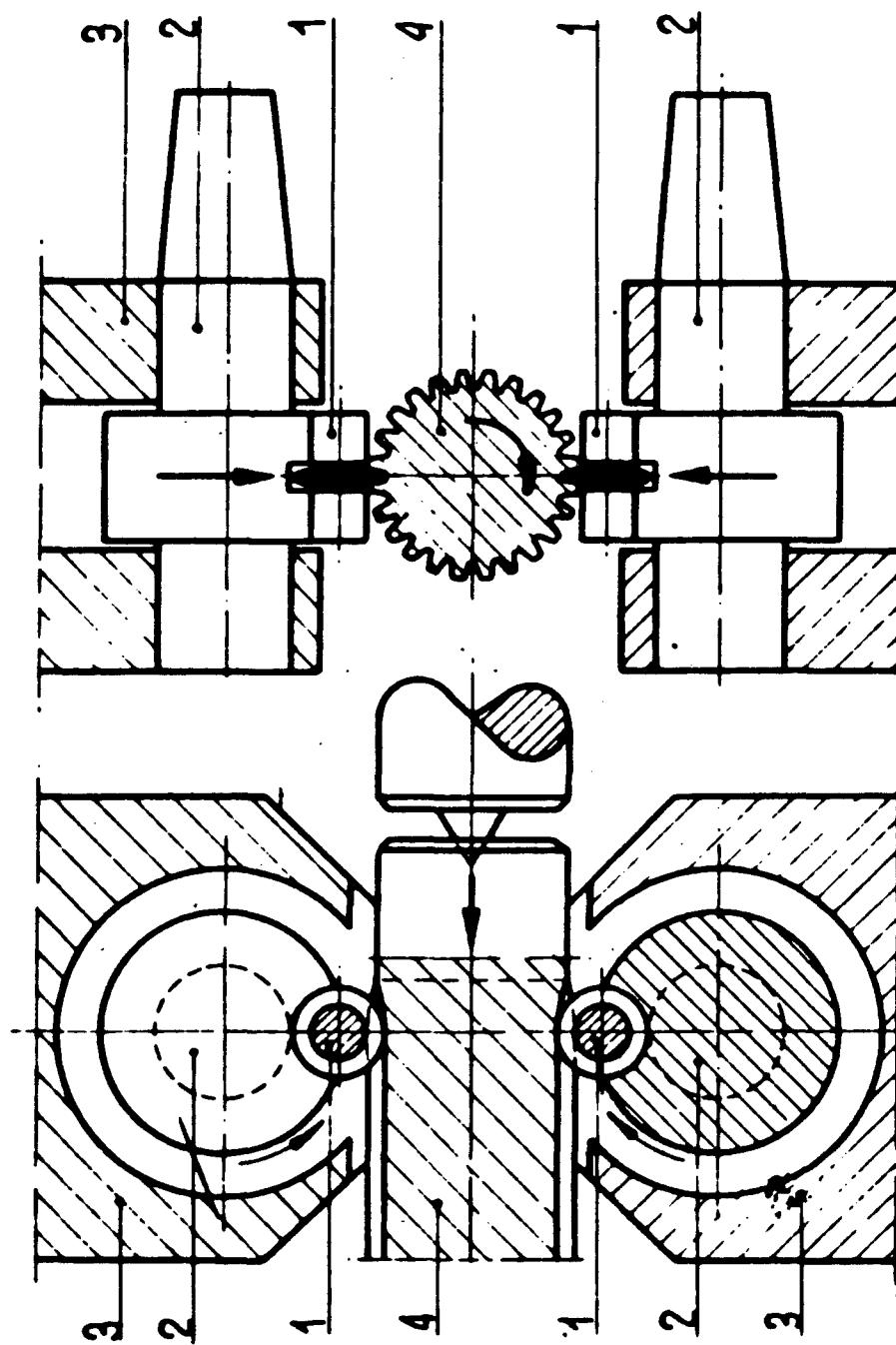


FIGURE H-2. Planetary Rolling - GROB Process

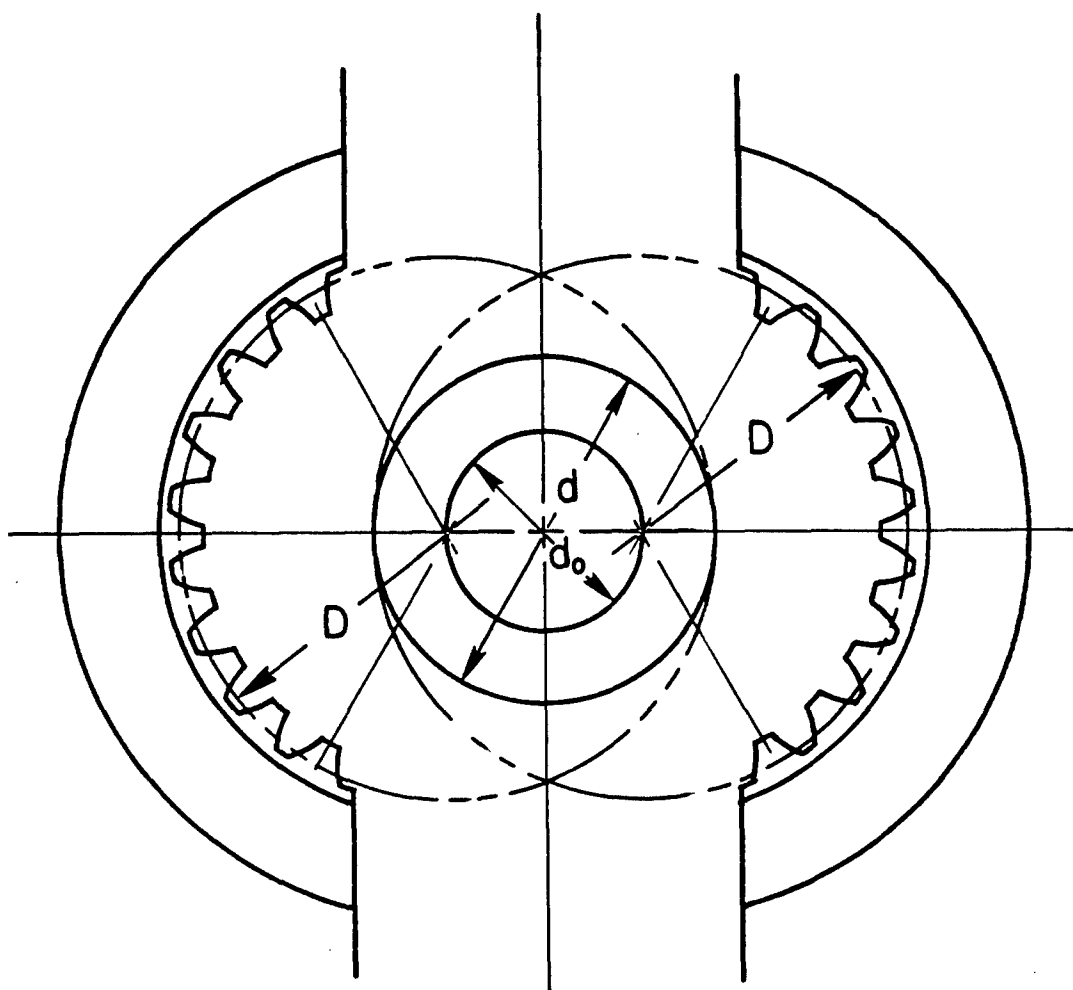


FIGURE H-3. Schematic Representation of the Oscillating Rolling Method

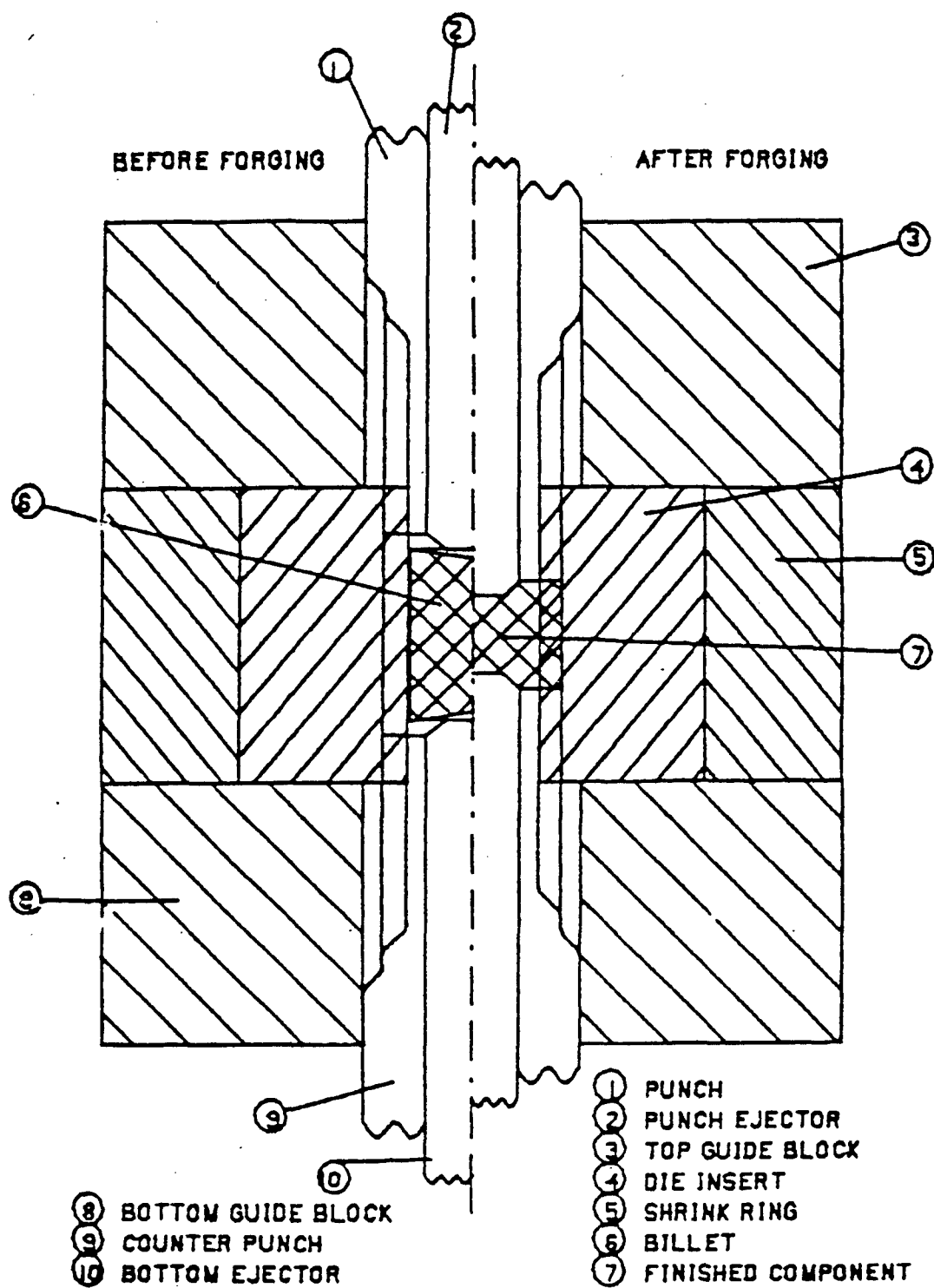


FIGURE H-4. Suggested Tool Design for Cold Forging of Spur Gears

involves inserting a billet whose outer diameter is slightly smaller than the root of the gear into a die cavity. The material flows radially into the die cavity to form the gear. The word "forging" is used for this process to differentiate radial extrusion of the metal in this process from the axial extrusion process (discussed later).

Another variation of the radial extrusion or forging process is schematically represented in Figure H-5 (similar to 1.1 in Table H-1) (4). The outer punch and the inner punch should be capable of independent motions in this tooling arrangement. With the movement of the ejector, either a triple action press or a special tooling is required for this type of operation. The advantage of this process is the simplified tooling; except for the die, none of the other parts need to have the configuration of the gear teeth.

4.0. EXTRUSION PROCESSES

The process of extruding a spur or helical gear is shown schematically in Figure H-6 (similar to 2.2 in Table H-1). The billet has a diameter equal to the outside diameter of the gear and is extruded through the die. A push-through operation (pushing a billet on top of a partially extruded gear) will produce a part with the gear teeth on the entire length. If a part with a flange portion is required, the partially extruded gear with the flange must be ejected. This may require;

- proper lubricant selection as the ejection is also required, and
- a turning motion for the part in the case of helical gears with large helix angles during ejection.

The outer diameter in the above method of extrusion does not undergo any deformation. This may result in an undesirable residual stress distribution. The concept of tooling shown in Figure H-7 (4) allows the outer diameter to be deformed also. Streamlined die concepts can be used in such designs to obtain nearly uniform deformation.

6.0. CONCLUDING REMARKS

From the few concepts presented in this section, the processes of forging (radial extrusion) and extrusion have not been systematically studied and developed for spur and helical gears. Rolling processes have been successfully applied especially in the forming of spur gears and splines. However, their commercial viability, especially for spur gears, is not yet known. If any of

- | | | |
|------------------|--------------------|------------|
| 1 Inner Punch | 5 Support Insert | 9 Billet |
| 2 Outer Punch | 6 Stationary Ring | 10 Forging |
| 3 Top Insert | 7 Reinforcing Ring | |
| 4 Helical Insert | 8 Ejector | |

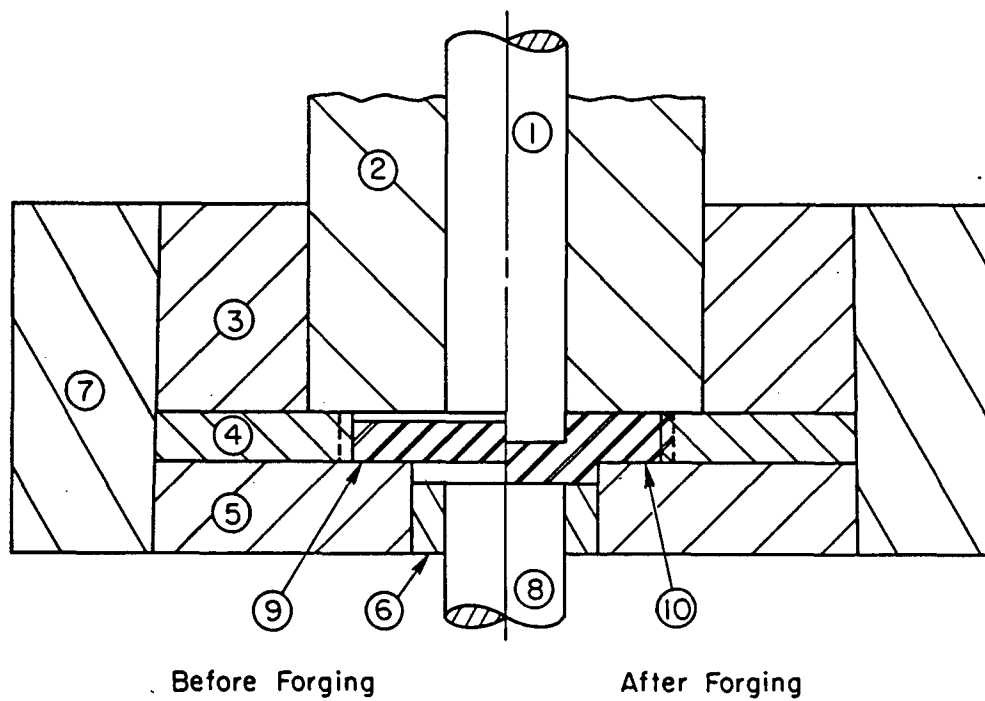


FIGURE H-5. Double-action Tooling for Forging of Spur Gears

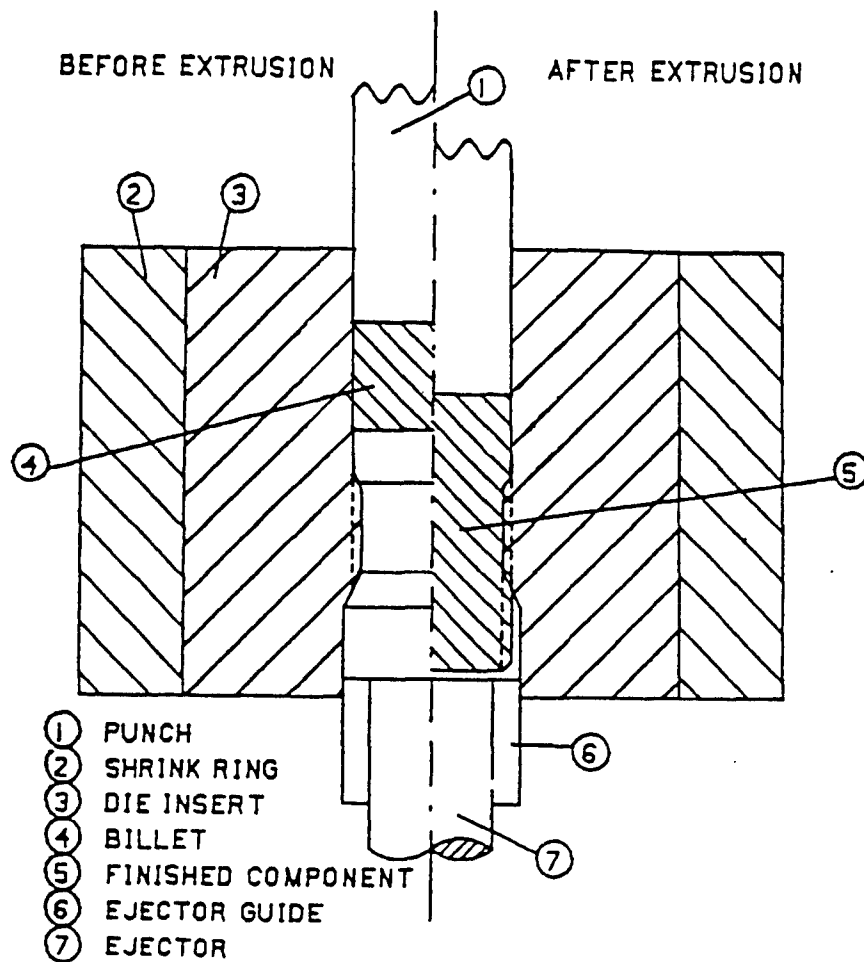


FIGURE H-6. Typical Tool Setup for Extruding Helical Gears

- | | |
|---------------------------------|--------------------|
| 1 Punch | 5 Support Insert |
| 2 Top Insert | 6 Reinforcing Ring |
| 3 Conical or Streamlined Insert | 7 Billet |
| 4 Gear Insert | 8 Extrusion |

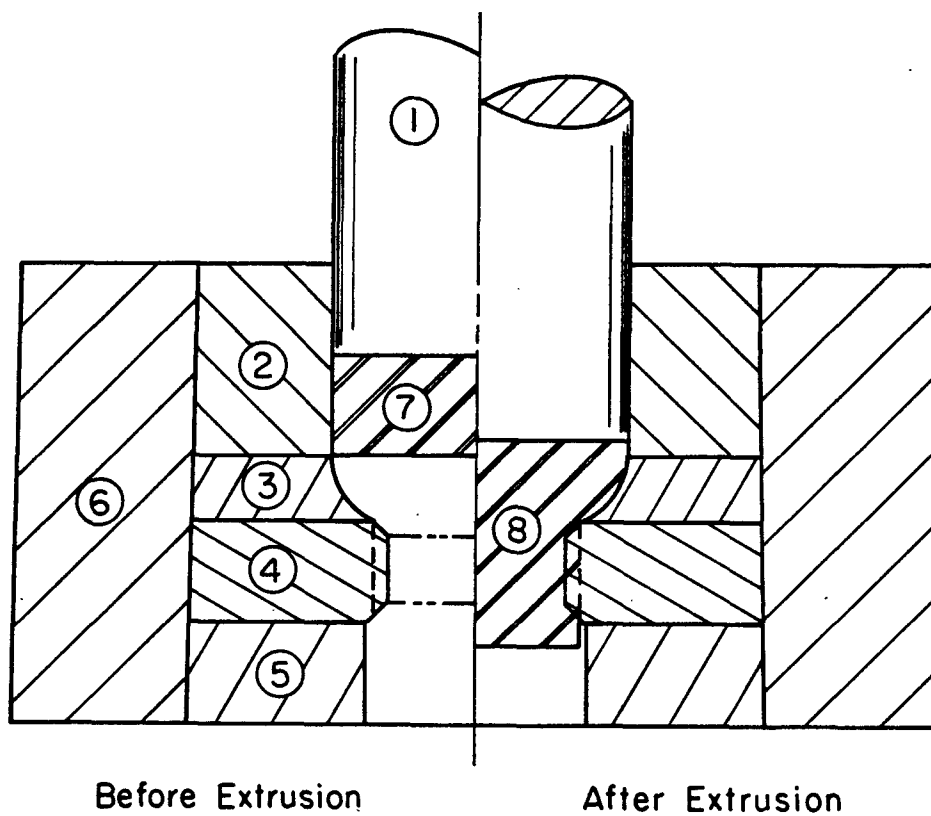


FIGURE H-7. Extrusion Process for Helical Gears Using a Streamlined Die

of the extrusion or forging processes detailed in this appendix can be developed to guarantee a reasonable degree of success in the current program, many end users in the industry will benefit because;

- they may already have presses with adequate capacity in their production line, and
- the technology of proper tooling and its manufacture will be made available to them through this program and hence their development costs will be much less than in new investments such as rolling, for example.

LIST OF REFERENCES

- (1) Turno, A., Romanowski, and Olszweski, M., "Chipless Manufacturing of Gears," (in German), Vol. 1 and 2, VDI Verlag, Duesseeldorf, 1971.
- (2) Krapfenbauer, H., "Cold Rolling of Precision Gears from the Solid," (in German), Werkstattblatt 618, D K pp. 612-833, Vol. 621, pp. 824-844.
- (3) Kopacz, Z., "Cold Forming of Involute Splines by WMP Method," International Cold Forging Group, IX Plenary Meeting, Paris, 1976.
- (4) Kuhlmann, D. J., and Raghupathi, P. S., "Internal Notes - Battelle Memorial Institute," Columbus, Ohio, 1983.

REPORT DISTRIBUTION

	Copies
Commander	
U.S. Army Tank-Automotive Command	
Warren, Michigan 48090	
ATTN: DRSTA-RCK	30
DRSTA-RCKM	1
DRSTA-IR	1
DRSTA-TS	1
ACO	1
Defense Technical Information Center	
Cameron Station	
Alexandria, Virginia 22314	1
Eaton Corporation	25
Manufacturing Services Center	
32500 Chardon Road	
Willoughby Hills, Ohio 44094	